RCRA Facility Investigation Report
Pawtuxet River

Former CIBA Site
Cranston, Rhode Island

Volume 2:
Contaminant Transport and Fate Modeling

Submitted by:

CIBA Corporation
Route 37 West
Toms River, New Jersey 08754

31 March 1996

Ciba Corporation
Toms River, New Jersey

CONTAMINANT TRANSPORT AND FATE MODELING OF THE PAWTUXET RIVER, RHODE ISLAND

Job Number: CIBA0012

Prepared by:

HydroQual, Inc.
1 Lethbridge Plaza
Mahwah, New Jersey 07430

March 26, 1996

Ciba Corporation
Toms River, New Jersey

CONTAMINANT TRANSPORT AND FATE MODELING OF THE PAWTUXET RIVER, RHODE ISLAND

Job Number: CIBA0012

Prepared by:

HydroQual, Inc.
1 Lethbridge Plaza
Mahwah, New Jersey 07430

March 26, 1996

CONTENTS

CONTENTS (cont.)

FIGURES

FIGURES

TABLES

Executive Summary

EXECUTIVE SUMMARY

Ciba is conducting a RCRA Corrective Action Study for their Cranston, Rhode Island site (Figure E-1). Between 1930 and 1986 the Cranston site was used for chemical manufacturing, initially by the Alrose Chemical Company, followed by the Geigy Chemical Company, and most recently by the Ciba Geigy Corporation. As part of this study an investigation of the adjacent Pawtuxet River was conducted. The Pawtuxet River portion of the study included collection of water column and sediment contaminant data and development of a mathematical modeling framework to evaluate the fate and transport of contaminants in the river. The modeling framework provides a quantitative basis for evaluating the effects of various remediation alternatives on contaminant levels in the Pawtuxet River.

E.1   Brief Overview of the Model

The modeling framework used in this study represents the state-of-the-art in scientific understanding of the relevant environmental mechanisms influencing the transport and fate of contaminants in surface waters. The model is a mathematical representation of the transport and transfer processes that control the temporal and spatial distributions of a chemical in the environment. The framework is comprised of three sub-models, as depicted in Figure E-2: the 1) hydrodynamic, 2) sediment transport, and 3) chemical fate components.

The hydrodynamic sub-model calculates spatial and temporal velocity (and flow) distributions, water depths, advective and dispersive mixing processes, and bottom shear stresses. The two dimensional, vertically integrated hydrodynamic model properly accounts for lateral variations in shear stress at the sediment-water interface, which strongly influences the transport and fate of sorbed chemicals due to cohesive sediment transport.

The sediment transport sub-model simulates the resuspension and settling of particulate material in the system and the concurrent transport of solids downstream. Because hydrophobic chemicals preferentially adsorb onto fine grained, cohesive sediments, the resuspension, deposition, and transport of cohesive sediments plays a critical role in the fate of hydrophobic chemicals in an aquatic system. Non-cohesive solids are generally less important as a sorptive phase for hydrophobic contaminants, but deposition of non-cohesive solids can provide a dilution of in-place contaminated sediments. The formulations used to describe non-cohesive sediment transport have been developed over a longer period of time, compared to the more recent advances in cohesive sediment transport. Both non-cohesive and state-of-the-art cohesive particle transport formulations are included in the sediment transport model applied to the Pawtuxet River, producing realistic simulations of suspended sediment transport processes. The results of the sediment transport sub-model provide input to the contaminant fate sub-model.

The contaminant fate sub-model uses the information generated by the hydrodynamic and sediment transport sub-models to define contaminant transport within the system. The fate sub-model is based on a mechanistic framework for the transport and transfer of contaminants in the aqueous environment. This sub-model includes such processes as dissolved-particulate partitioning, volatilization, settling, resuspension, and diffusion. The results of the contaminant fate model are estimates of future concentrations which vary in response to alternate remediation activities.

The general approach in the development of mathematical models of the fate and transport of chemicals in the environment is to: 1) collect and analyze relevant environmental data, 2) select and develop a model framework, 3) calibrate the model with ambient data, and 4) project future environmental conditions. These four steps have been followed in this study to produce a comprehensive model for determining the fate and transport of chemicals in the Pawtuxet River.

E.2 Application of the Model Framework to the Pawtuxet River

Contaminant data from surface water and sediments of the Pawtuxet River were analyzed to select a limited number of chemicals for modeling. Contaminants detected in the Phase I Release Characterization were ranked based on the toxicological significance of measured concentrations and/or evidence that the chemical was used or produced at the facility. A subset of five chemicals were selected based on their ranking and the objective to have calibrated models for all of the major chemical classes. The five chemicals that were modeled are:

- Chlorobenzene
- Naphthalene .
- PCBs
- Tinuvin 328
- Zinc.

Examples of calibration of the three submodels are shown on Figure E-3. The hydrodynamic sub-model reproduces water surface elevations through two high flow events measured at Cranston in March 1992. The sediment transport model reproduces suspended solids data near the Ciba facility from the same time period. Water column chlorobenzene concentrations computed by the contaminant fate sub-model reproduce the decrease in concentration between the USGS flow gage at Cranston and the Facility, and the increase in concentration observed in the facility reach. Chlorobenzene concentrations in the sediment, computed during a two year period, indicate fairly constant sediment concentrations.

E.3 Summary of Results

The primary objective in developing a contaminant fate and transport model of the Pawtuxet River is to provide a tool for the evaluation of the effect of alternate remedial measures on contaminant concentrations in the river. Sediment contaminant

concentrations computed in projections for no action (base case) or alternate remediation scenarios are strongly influenced by sediment resuspension and deposition patterns within the study area. Resuspension within the study area can transport sorbed sediment contaminants to the overlying water. Re-deposition of sediments resuspended from within the study area is not a significant component in the depositional processes in this portion of the Pawtuxet River. Depositional patterns control how upstream sources of sorbed contaminants are distributed within the study area.

Results of the sediment transport sub-model are summarized on Figure E-4. Net resuspension, indicated by negative bed elevation changes, is calculated in only limited areas. Net depositional rates are generally low, less than 0.5 cm/yr, in the majority of the study area. Overall, the center channel is more stable than the more shallow areas along the north and south banks. Higher deposition rates, beginning near km 2.8 (~0.5km upstream of the facility), are due to a decrease in the bed slope in that area. The highest deposition rates are computed upstream of the Pawtuxet Cove Dam (downstream boundary) in response to backwater effects of the dam. In depositional areas, upstream sediments will gradually cover present surface sediments. Changes in sediment contaminant concentrations depend on deposition rates and contaminant concentrations on the depositing solids, relative to in-place sediment contaminant concentrations.

The contaminant fate sub-model was used to evaluate the response to two remedial measures: 1) operation of a groundwater capture system along the production area bulkhead and 2) excavation of a limited portion of the sediments from the location of a former coffer dam, adjacent to the production area. Results from these 2 simulations are compared to results from a base case simulation representing no remedial action.

Figures E-5a-c summarize projection results for three locations: 1) the former coffer dam area, where peak concentration of chlorobenzene, naphthalene, PCBs and Tinuvin 328 are presently observed, 2) on the south bank just upstream of the sharp bend in the river near km 1.25, and 3) on the south bank of the river immediately upstream of the Pawtuxet Cove dam. The latter two locations represent areas where peak concentrations of some

of the 5 chemicals are calculated at the end of the projections. Zinc concentrations are presented for a forth location, along the bulkhead of the production area upstream of the former coffer dam area. Peak concentrations of zinc are currently observed at this location.

No Action-Base Case

If no remedial actions are taken, the model indicates that natural attenuation will cause a reduction of contaminant levels in the area of the former coffer dam. This reduction occurs largely through burial of sediments by less contaminated solids. The rate and extent of the reductions are dependent on the sedimentation rate and the contaminant concentrations on the water column solids. The concentrations of chlorobenzene, naphthalene, PCBs and Tinuvin 328 on water column solids are several orders of magnitude lower than in the surface sediment at the location of the former coffer dam. Thus, the contaminated sediments are being buried by essentially clean solids. Reductions of about 70 percent are predicted at the location of the former coffer dam for each of these chemicals after 10.6 years. In contrast, surficial sediment zinc concentration declines by less than 25 percent as a result of relatively high zinc concentrations on water column solids which enter the upstream boundary at Cranston and settle onto the sediment.

Concentrations in the former coffer dam area subsurface sediments are also affected by deposition. Concentrations in the 5-10cm layer decline to a lesser extent than the surficial sediments (0-5 cm), reflecting the transport of contaminated sediments from the surface layer to the subsurface layer. The reductions vary depending on the initial concentration gradient in the sediments. The net decline of PCBs is near zero. For all the other contaminants a decline of about 20 to 40 percent occurs after 10.6 years.

Outside the former coffer dam area, concentration changes are less dramatic. In general, the surficial sediments appear to be at or near steady-state with the water column and little change occurs. The greatest change occurs with zinc: concentrations increase

by about a factor of two in most of the study area over the 10.6 year projection due to zinc entering the upstream boundary at Cranston.

Groundwater Capture at the Production Area

Ciba is implementing a groundwater capture system to block the migration of contaminants beneath the production area. This system will reverse the hydraulic gradient and draw approximately 0.1 cfs of river water through the sediments adjacent to the production area bulkhead. The groundwater capture is effective in reducing peak concentrations of chlorobenzene and naphthalene near the former coffer dam area, and would be expected to be equally effective in reducing concentrations of other chemicals with similar partition coefficients. During the first three years of operation, chlorobenzene and naphthalene concentrations in the top 10 cm at this location are reduced to less than 0.1 mg/kg, which can be compared to final concentrations from the base case (no action) simulation for chlorobenzene of about 1000 mg/kg and 40 mg/kg of naphthalene. The groundwater capture system also produces approximately a 40 percent reduction in the peak zinc concentration. The groundwater capture system does not significantly affect sediment PCB or Tinuvin 328 concentrations.

Excavation of Sediments from the Former Coffer Dam Area

Ciba excavated sediments from the location of the former coffer dam in the fall of 1995. The concentration of PCBs and Tinuvin in the former coffer dam area was significantly reduced by the excavation of sediments in that area. Ten years after excavation, PCB concentrations in the former coffer dam area are calculated at 0.6 and 1.6 mg/kg in the top 5cm and 5-10 cm layers, respectively. These concentrations represent approximately a factor of 30 reduction compared to the concentrations calculated at the end of the base case run (22 and 45 mg/kg in the same two layers).

Sediment contaminant concentrations in areas away from Ciba's production area are not significantly affected by either remedial action, because current mass fluxes out

of the production area reach do not significantly affect downstream sediment concentrations. Peak concentrations of each of the chemicals modeled, measured near the Ciba facility, are significantly reduced by the combination of the two remedial actions.

E.4   Summary and Conclusions

The significant findings of these analyses are:

- The lower 2.8 km of the study area (from approximately 0.5 km upstream of the Facility to the Pawtuxet Cove Dam) is, in general, a depositional area. Net resuspension is calculated in only very limited areas. Net deposition begins roughly 0.5 km upstream of the facility in response to a reduction in the slope of the river bed.

- Re-deposition of sediments resuspended from within the study area is not a significant component in the depositional processes in the study area. Therefore, sediment contaminant concentrations in downstream areas are not significantly affected by resuspension of contaminated sediment from locations within the study area.

- Deposition in the lower 2.8 km of the study area results in gradual burial of surficial sediments with upstream water column solids. The change in contaminant concentrations due to this burial is a function of the local deposition rate and the relative concentration of contaminants in the sediment and on the depositing solids.

- Sediment concentrations of chlorobenzene, naphthalene and PCBs are fairly constant in locations away from the former cofferdam area, indicating that sediment - water column exchanges of these chemicals are near equilibrium. Most locations in the lower 2.8 kilometers of the study area experienced an increase in zinc concentrations in the sediment due to deposition of zinc contaminated solids.

The zinc contaminated water column solids are associated with zinc entering the study area at the upstream boundary. Tinuvin 328 concentrations in most of the lower 2.8 km of the study area decreased in response to deposition of uncontaminated solids.

- Contaminant concentrations in sediments of areas away from Ciba's production area are not significantly affected by either remedial action (groundwater capture or excavation of sediment from the former coffer dam area) because current mass fluxes out of the sediments adjacent to the production area do not significantly affect the sediments in the downstream Pawtuxet River.

- Operation of the groundwater capture system along the production area bulkhead is effective in reducing peak concentrations of chlorobenzene and naphthalene. This remedial action should be equally effective in reducing the concentrations of other chemicals with similar partition coefficients. Chlorobenzene concentrations in the top 10 cm of the sediment of the former coffer dam area decrease from over 3000 mg/kg to less than 0.1 mg/kg in the first two years of the simulation of the groundwater capture system. Naphthalene concentrations in the same area decrease from over 100 mg/kg to less than 0.1 mg/kg in the first three years of the simulation.

- Excavation of sediment from the former coffer dam area is effective in reducing concentrations of PCB, Tinuvin 328, and zinc at that location. Ten years after excavation, PCB concentrations in the top 5 cm and 5-10 cm layers are calculated at 0.6 and 1.6 mg/kg, respectively. These represent substantial reductions compared to concentrations calculated in the base case (no remedial action), which were 22 and 45 mg/kg in the top 5 cm and 5-10 cm layers, respectively. Tinuvin concentrations of 0.3 mg/kg, or less, in the top 10 cm, calculated ten years after excavation, are significantly lower than concentrations of several hundred mg/kg, calculated at the end of the no action simulation. Zinc concentrations in the 0-5 and 5-10 cm layers are initially reduced from between 1000 and 3000 mg/kg to

approximately 200 mg/kg as a result of the excavation. Deposition of contaminated solids from upstream gradually increases the sediment concentrations of zinc to approximately 550 and 330 mg/kg in the two layers, during the 10.6 year simulation.

- The combination of the two remedial actions produces substantial reductions in the peak concentrations of each of the five chemicals modeled. Table E-1 summarizes the reduction in contaminant concentration in sediments near the production area, calculated over the course of the 10.6 year projection analyses. The indicated reductions of chlorobenzene and naphthalene concentrations are achieved in the first 2 and 3 years, respectively.

Table

Table E-1. Effect of Remedial Actions on Contaminant Concentrations in Sediments Adjacent to the Ciba Production Area over 10.6 Year Projection			
Chemical	Effective Action	Concentration at Production Area (mg/kg)	
		Initial	Final
Chlorobenzene	Groundwater Capture	3700	0.06[1]
Naphthalene	Groundwater Capture	150	0.05[2]
PCBs	Excavation	66	1.6
Tinuvin 328	Excavation	640	0.3
Zinc	Excavation	2800	330

Note:
[1] Achieved after 2 years
[2] Achieved after 3 years

Figures

FIGURE E-1. Study Area Map

MODEL 1:

HYDRODYNAMIC
MODEL

MODEL 3:

FATE &
TRANSPORT
MODEL
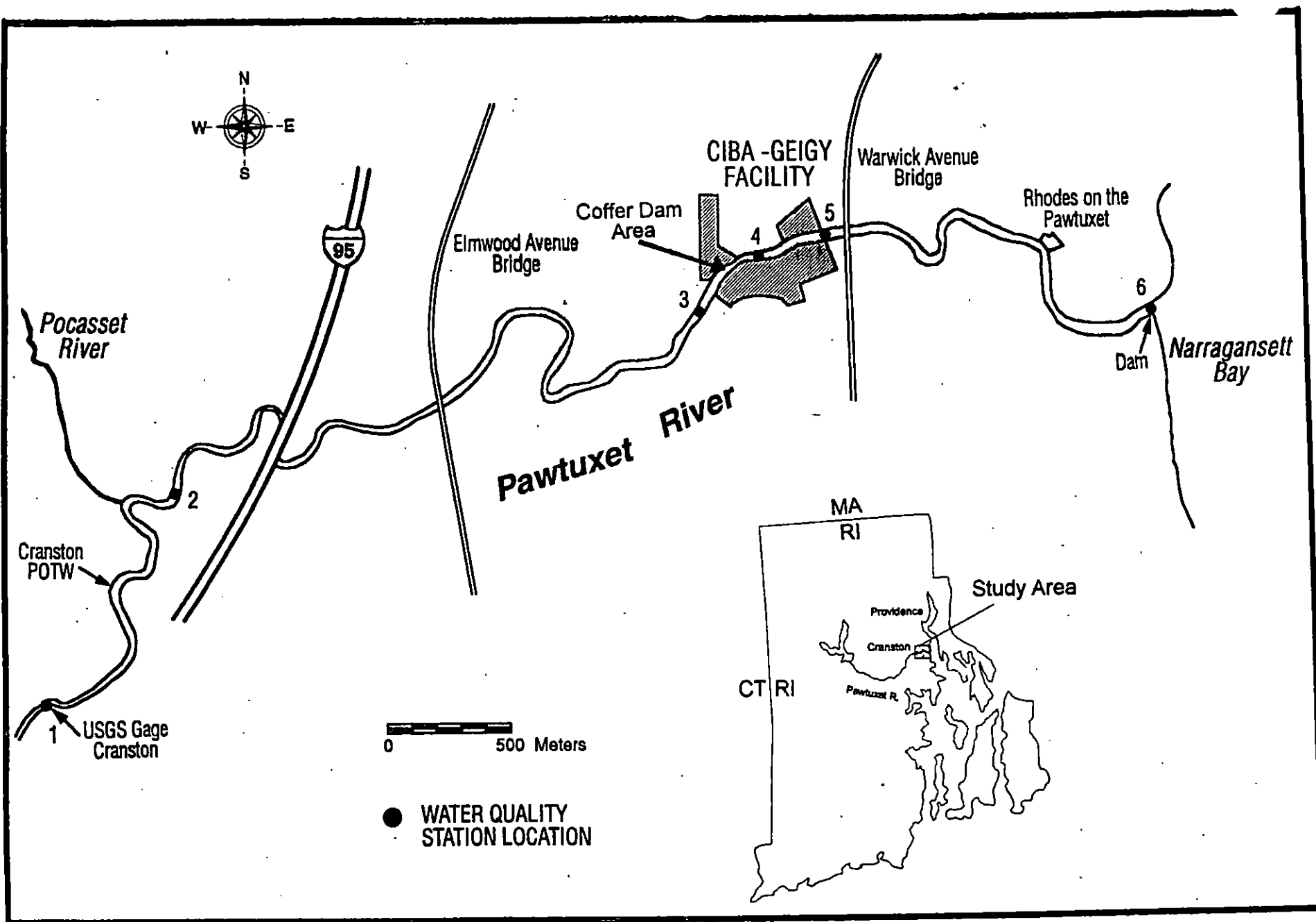
MODEL 2:

SEDIMENT
TRANSPORT
MODEL
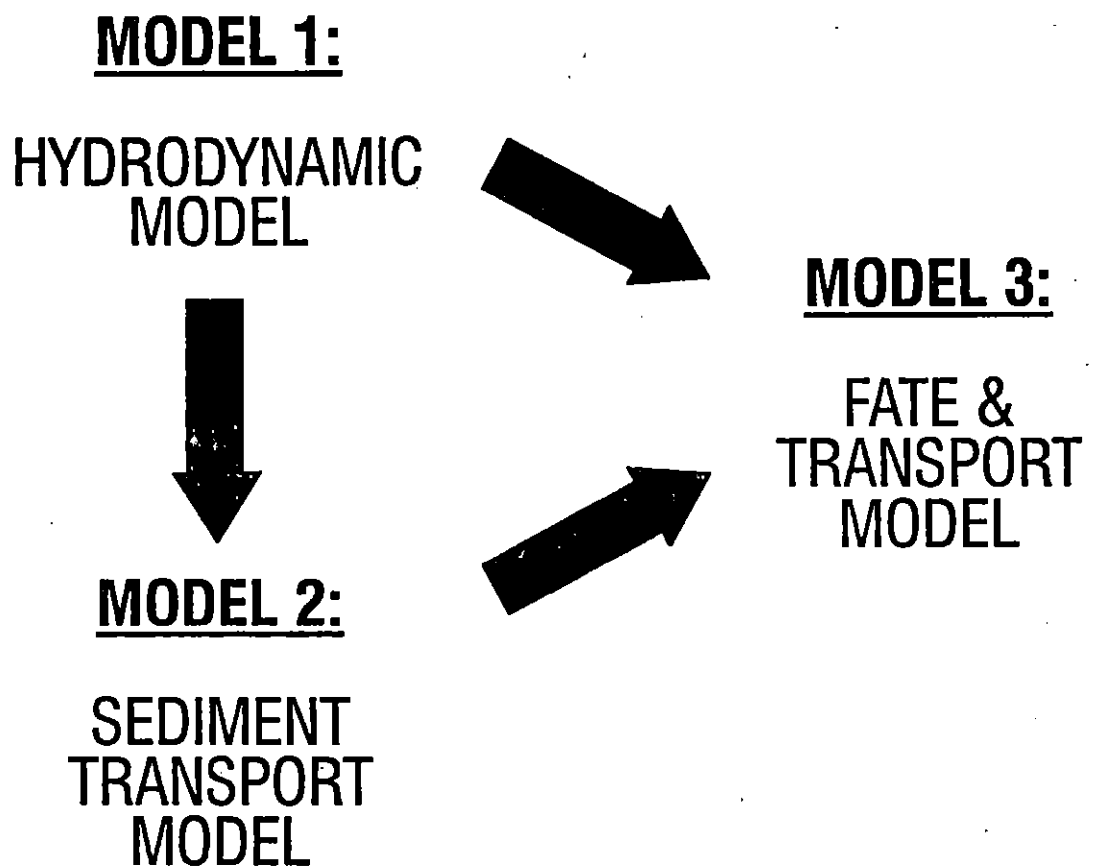
FIGURE E-2.   Model Components

HYDRODYNAMICS

SEDIMENT TRANSPORT

CONTAMINANT FATE MODEL

WATER COLUMNN

SEDIMENT (0-5cm)
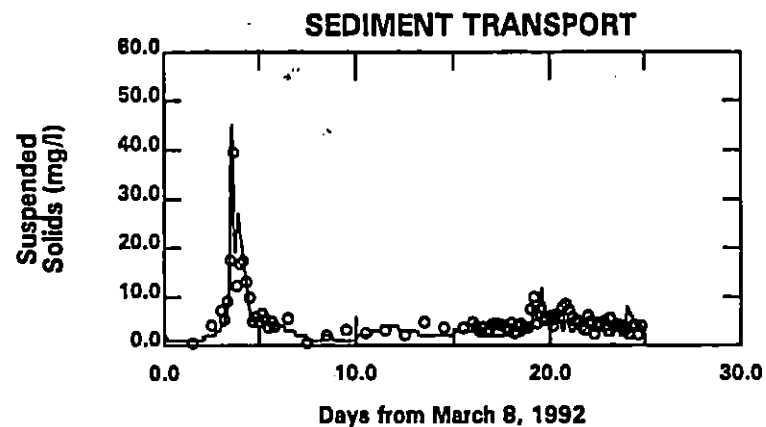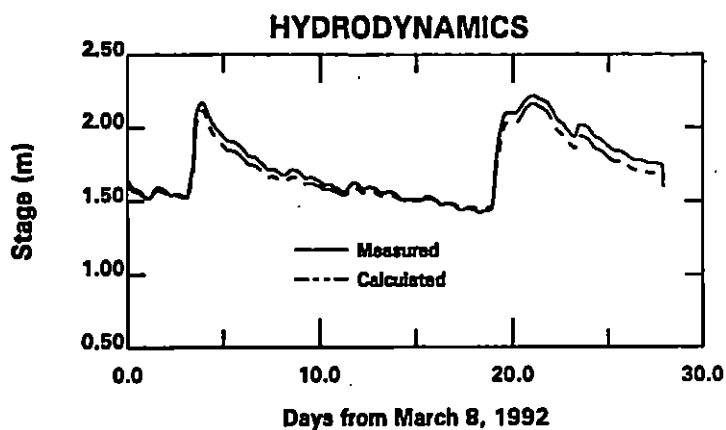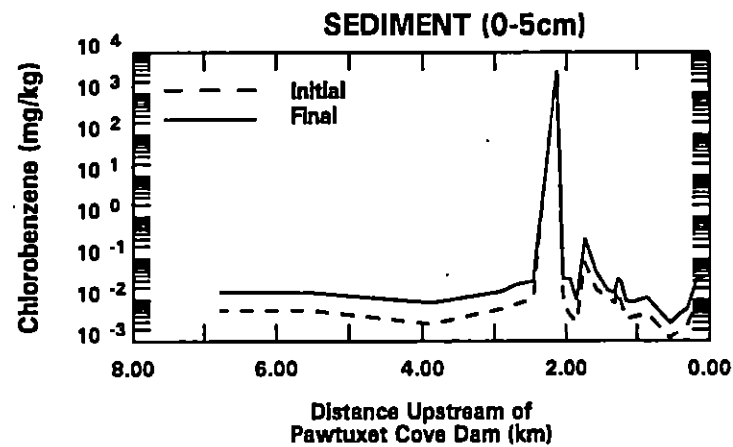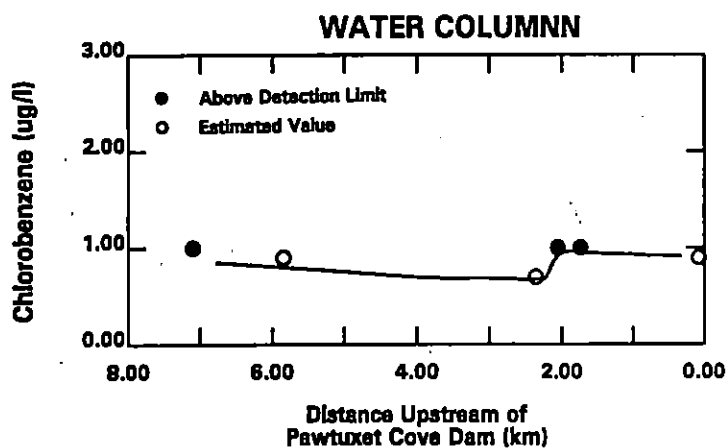
FIGURE E-3.   Example of Model Calibration
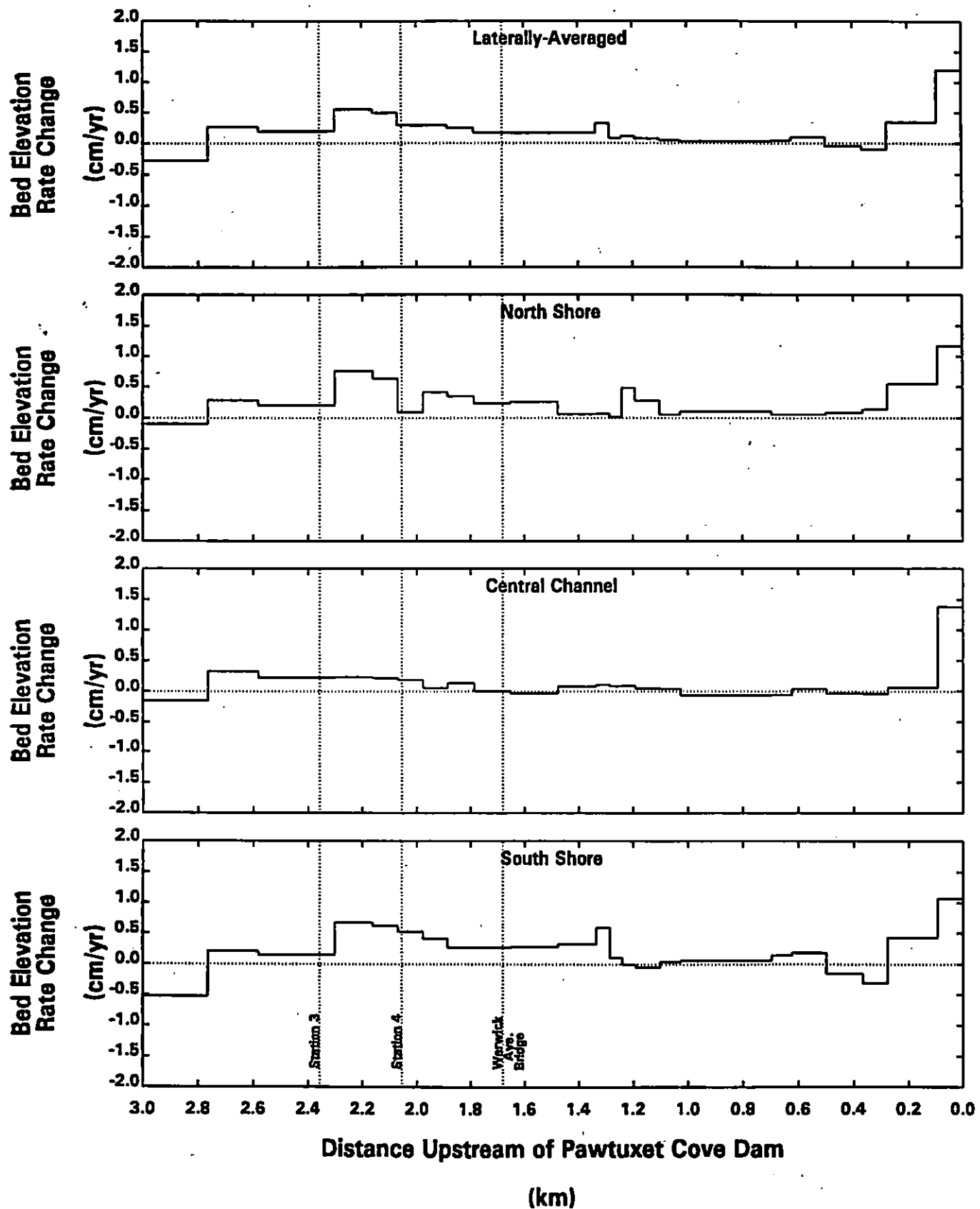
FIGURE E-4.   Predicted Change in Sediment Bed Elevation for Projection Period
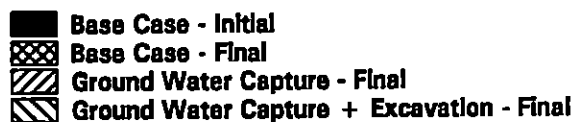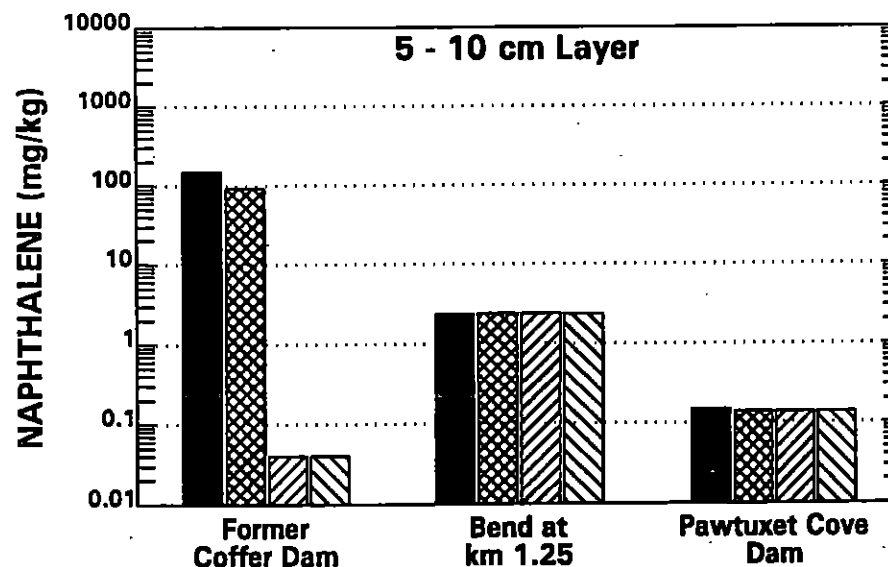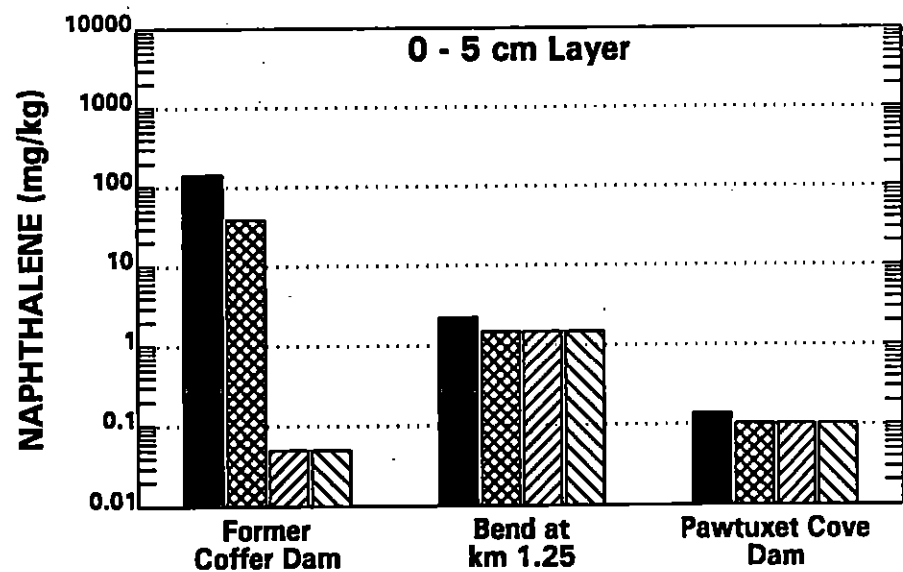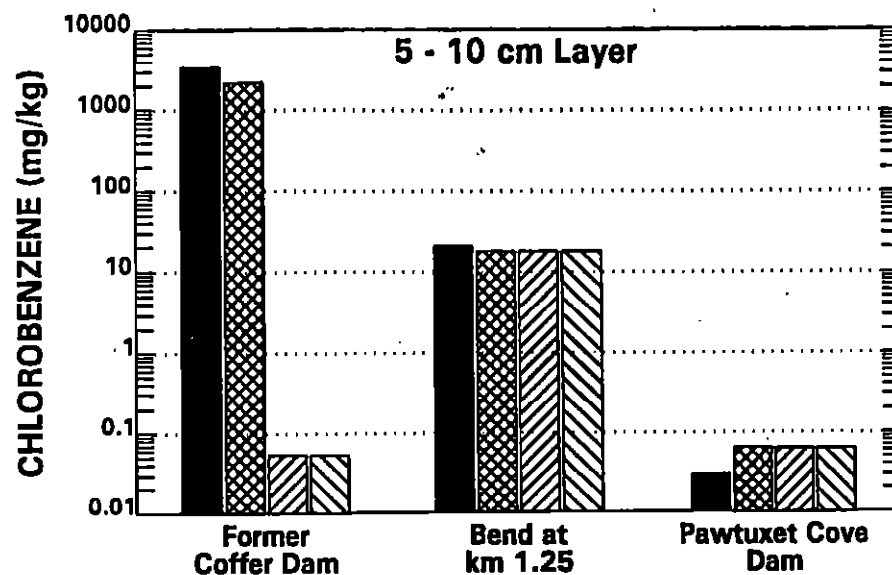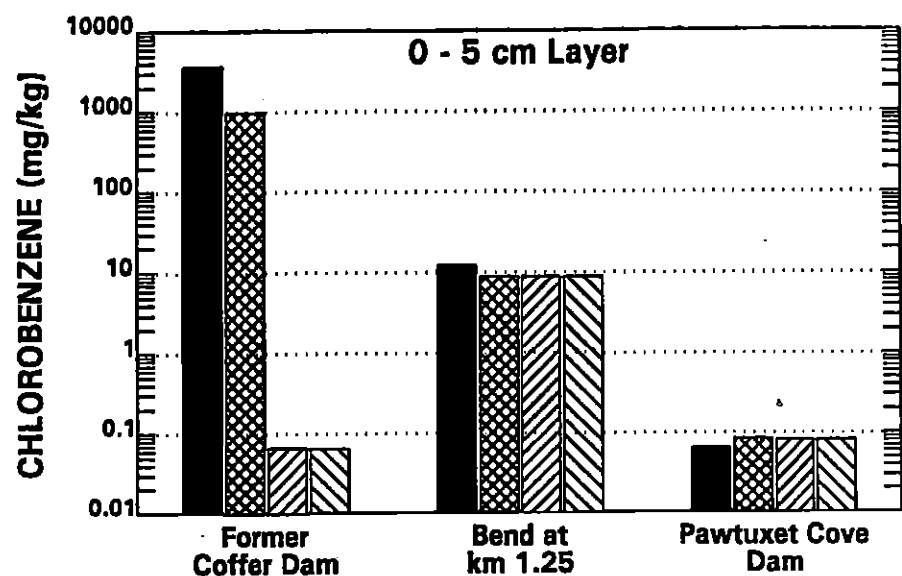
FIGURE E-5a.   Comparison of Present and Future Contaninant Concentrations for Base Case and Alternate Projections - Chlorobenzene & Naphthalene
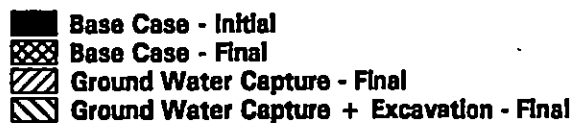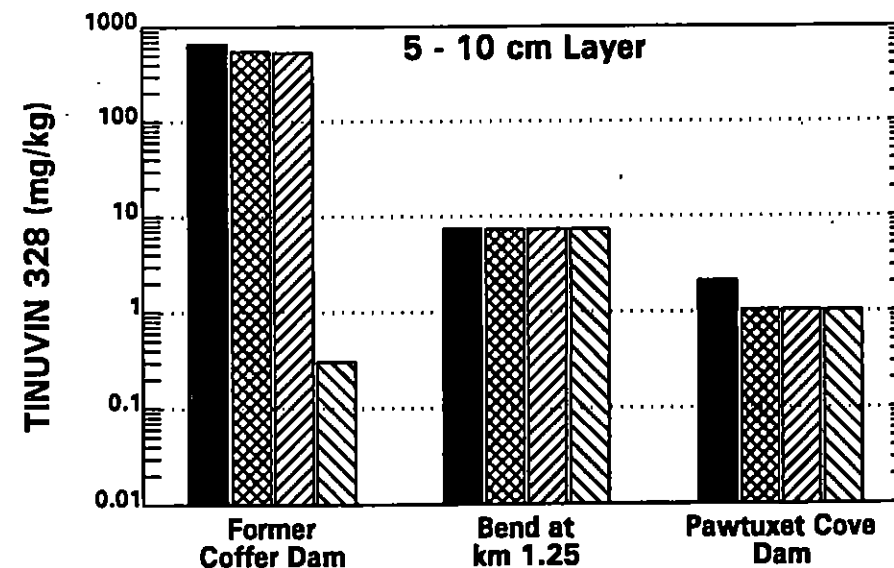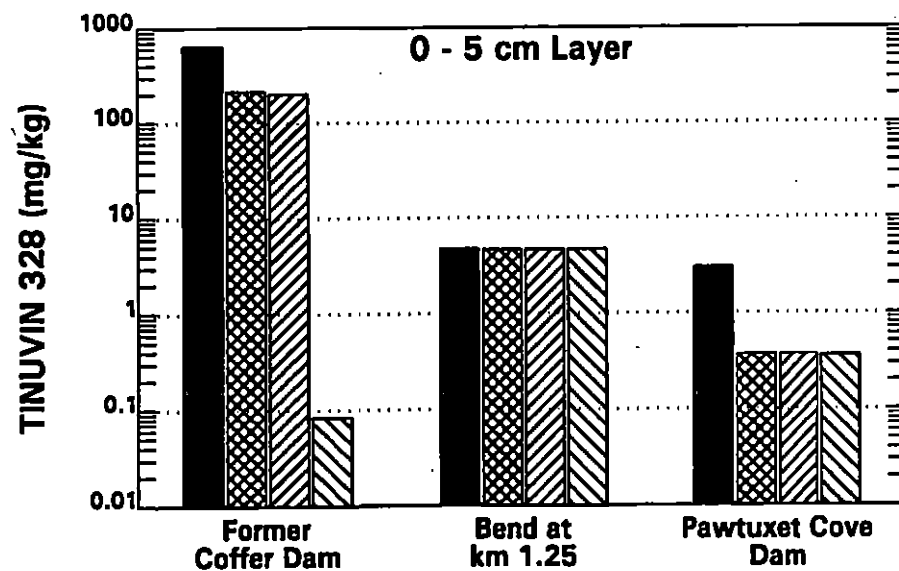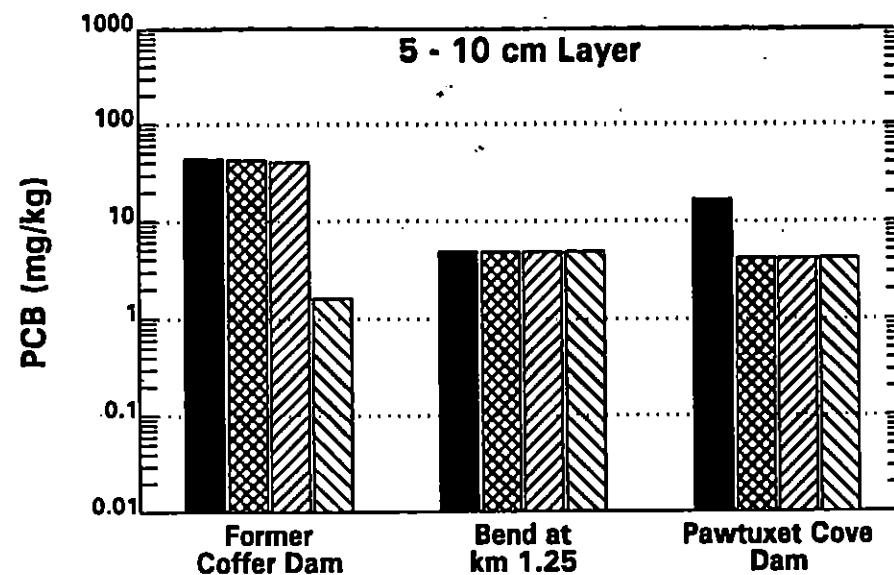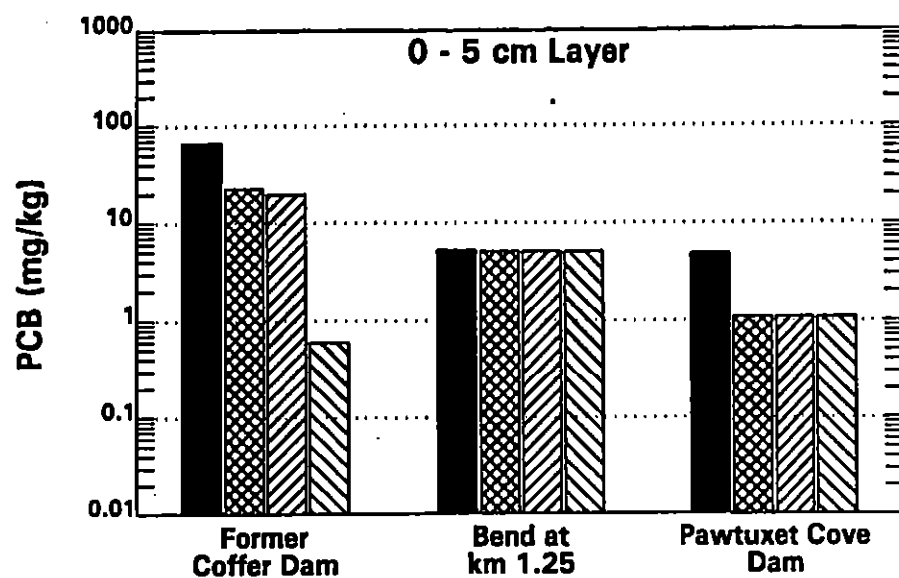
FIGURE E-5b.   Comparison of Present and Future Contaninant Concentrations
for Base Case and Alternate Projections - PCBs and Tinuvin 328
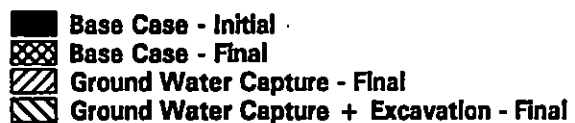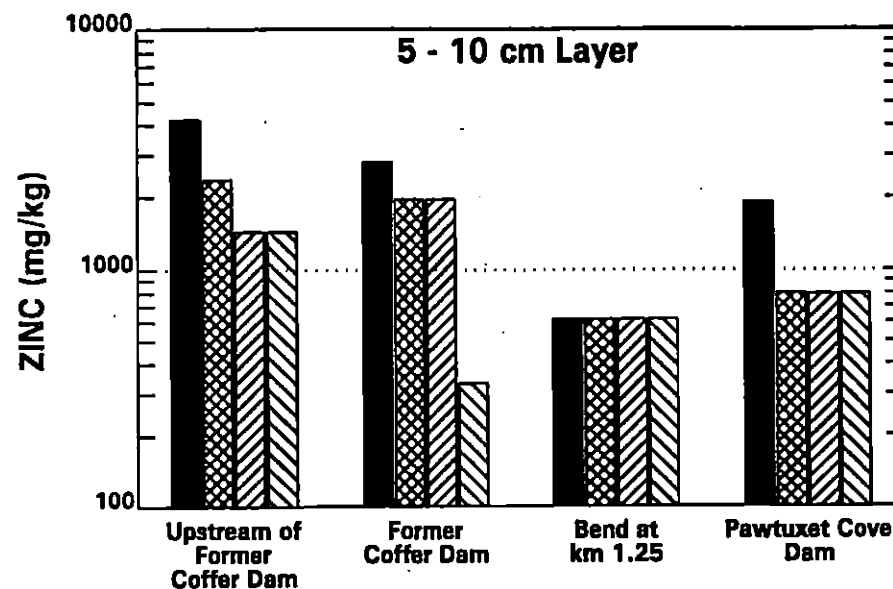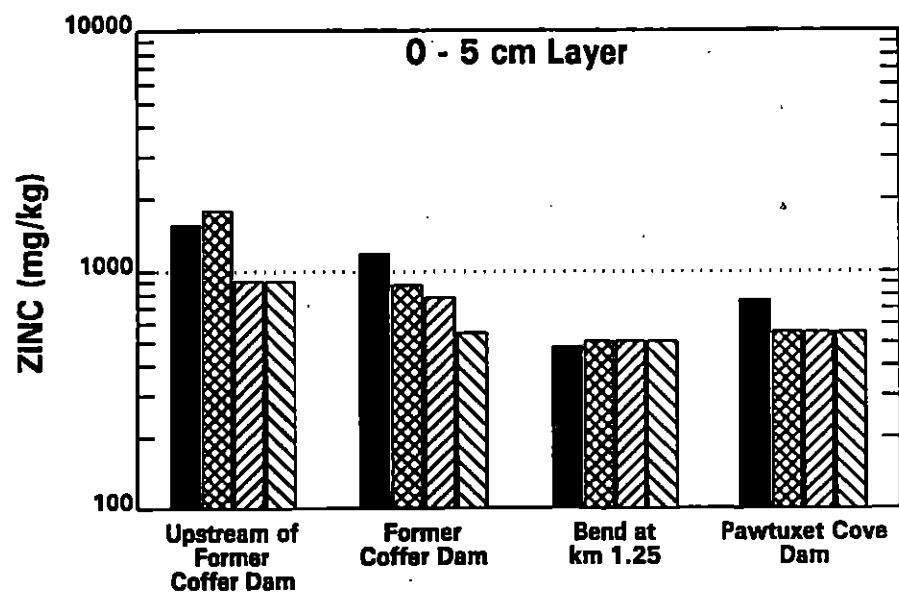
FIGURE E-5c. Comparison of Present and Future Contaninant Concentrations for Base Case and Alternate Projections - Zinc

SECTION 1

INTRODUCTION

1.1 GENERAL PURPOSE OF REPORT

A comprehensive modeling framework for determining the transport and fate of contaminants in the Pawtuxet River has been developed for use as a tool to rationally evaluate the effects of various remedial measures. This report summarizes the development, calibration and application of the overall model, which is comprised of three distinct sub-models that have been linked together. The three sub-models, i.e., hydrodynamic, sediment transport, and physical-chemical, have each been calibrated for the period from March 1991 to May 1992. The models are used to evaluate the effectiveness of different remediation measures.

1.2 BACKGROUND

Chemical manufacturing operations at Ciba Geigy's Cranston, Rhode Island site (Figure 1-1) began in 1930, under the ownership of the Alrose Chemical Company. The Geigy Chemical Company acquired the facility in 1954 and merged with the Ciba corporation in 1970. Manufacturing was discontinued at this location in 1986. Manufacturing operations included agricultural products, leather and textile auxiliaries, plastics additives, optical brighteners, and pharmaceuticals.

Ciba Geigy entered into an Administrative Order of Consent in 1989, which required them to conduct a RCRA Corrective Actions Study. The RCRA Corrective Actions Study includes investigations of Ciba's property as well as the Pawtuxet River which is adjacent to the facility. The subject of this report is limited to investigation of the Pawtuxet River.

1.3   DESCRIPTION OF STUDY AREA

The Pawtuxet River drainage basin includes an area of approximately 600 km^2 (230 mi^2) south and west of Providence, Rhode Island (Figure 1-1). This study is limited to the lower 7 km (4.3 mi) of the river, between the USGS gage at Cranston and the Pawtuxet Cove Dam. At the downstream end of the study area the Pawtuxet River flows over a low head dam (~1m) into Narragansett Bay. The annual average flow of the Pawtuxet River, at Cranston, is approximately 350 cfs. Within the study area the river is generally 1 to 3 meters deep and approximately 30 m wide.

1.4   SPECIFIC GOALS AND OBJECTIVES OF THE CURRENT WORK

The primary objective of this modeling effort is the development of a tool to evaluate the effect of different remediation alternatives on contaminant levels in the Pawtuxet River. To achieve this goal a modeling framework is constructed to develop a quantitative understanding of the fate of in-place contaminants and a quantitative means of forecasting the spatial and temporal response of water column and bed contaminants to specific remedial measures.

Development of such a forecasting tool implies an inherent knowledge of the scientific principles and physical processes involved in the problem. Contaminant concentrations observed in the water column and sediment are dependent on complex interactions between sources, transport, transfer and decay processes. Identifying each of the major physical, chemical, and biological processes affecting contaminant concentrations represents a scientific approach toward the study objectives. Quantifying each process with mathematical expressions represents the development of a holistic modeling approach.

Figure
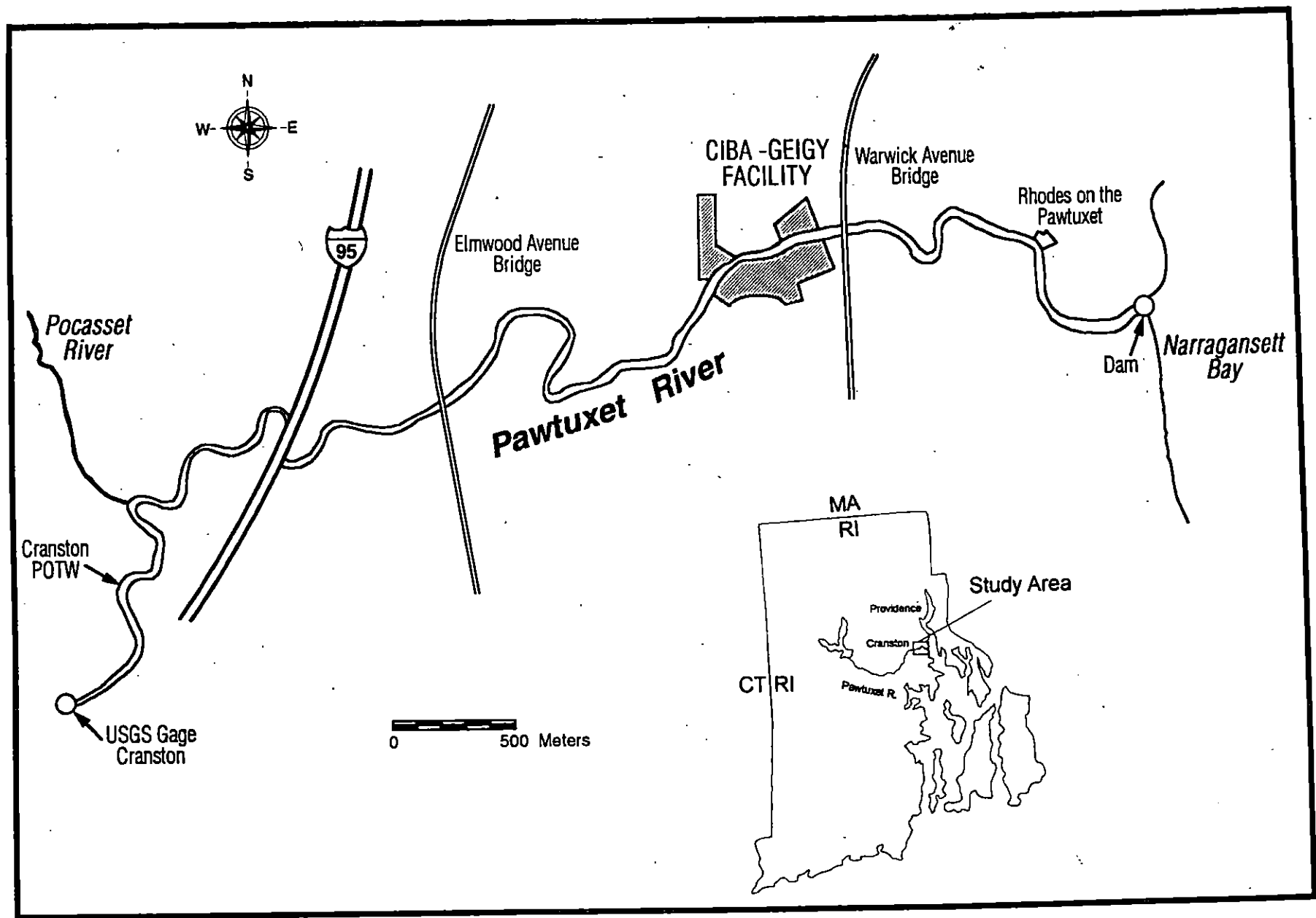
FIGURE 1-1.   Study Area Map

SECTION 2

GENERAL APPROACH

The general approach typically followed when using a mathematical model to evaluate an environmental problem consists of the following tasks: (1) analysis of data; (2) selection/development of a model framework (conceptual model); (3) calibration of the model and (4) forecasting future conditions. This section describes briefly, in general terms, each of these tasks as they pertain to the evaluation of contaminant fate in the Pawtuxet River. Subsequent sections describe the specific analyses performed in the process of developing and applying the hydrodynamic, sediment transport, and contaminant transport and fate models.

2.1 ANALYSIS OF DATA

Analyses of contaminant data from surface water and sediments of the Pawtuxet River were performed to evaluate the toxicological significance of the concentrations measured in Phase 1 of the RCRA release characterization. The approach that was followed for developing contaminant fate models of the Pawtuxet River was to calibrate models with data for a limited number of chemicals. Contaminants detected in the Phase 1 release characterization were ranked using the following criteria: 1) toxicological significance of the measured concentrations, and 2) evidence that the chemical was used or produced at the facility. A subset of five chemicals were modeled based on their ranking and the desire to have calibrated models for all the major chemical classes. The goal was to have calibrated models that could be applied to other compounds, if the need arises. The five chemicals that were modeled are:

- Chlorobenzene
- Naphthalene
- PCBs
- Zinc
- Tinuvin 328

The toxicological significance of measured concentrations was evaluated by comparing available data to selected criteria. Evaluation of surface water concentrations consisted of comparing Phase I data to USEPA and Rhode Island Department of Environmental Management chronic criteria for freshwater aquatic organisms. Silver was the only chemical considered for modeling based on water column data. Because Phase I silver water column data were inconclusive, additional data collection was recommended. As will be discussed in more detail in Section 3, additional data indicated upstream sources of silver, and with concurrence from EPA, silver was not included in the list of chemicals that would be modeled.

Evaluation of sediment data for nonionic organic chemicals involved the application of the approach being used by USEPA to develop sediment quality criteria (USEPA, 1993). USEPA is using an Equilibrium Partitioning (EqP) approach and Final Chronic Values (FCV) from water quality criteria to develop sediment quality criteria. Sediment quality criteria are expressed as mass of chemical per mass of organic carbon, and are calculated as:

$$SQCoc = Koc \; FCV$$

where:

$SQCoc$ = sediment quality criteria (M chem/ M organic carbon)

Koc = organic carbon partition coefficient (L^3/M organic carbon)

FCV = Final Chronic Value from water quality criteria (M chem/L^3)

The organic carbon partition coefficient (Koc) is approximately equal to the octonal water partition (Kow), for which estimates are available. USEPA has published draft criteria for acenadhthene, fluoranthene, phenanthrene, dieldrin and endrin. For the remainder of the chemicals evaluated in this study, the EqP method was used to calculate a screening value (EqPSV):

$$EqPSV = Koc \; FCV$$

where:

    EqPSV = sediment screening value (M chem/ M organic carbon)

While the screening values and criteria are calculated by the same equation, different terminology is used to differentiate criteria published by USEPA from screening values that have not been through the same review process. An example of the evaluation of sediment concentrations of chlorobenzene (which was selected for modeling) is shown on Figure 2-1. The top panel shows bulk sediment chlorobenzene concentrations (mass Chlorobenzene per mass sediment solids) plotted versus distance upstream of the Pawtuxet Cove Dam. Peak concentrations of several hundred mg/Kg are seen near the Ciba Facility. In the middle panel of Figure 2-1, chlorobenzene concentrations are normalized by sediment foc, and compared to the horizontal line drawn at the EqP screening value. Much of the apparent variability introduced by the carbon normalization is due to the non-detected concentrations (triangles) divided by varying foc values. The ratio of the carbon normalized concentrations to the EqP screening values, (bottom panel) indicates the peak concentrations are more than two orders of magnitude above the screening value. Evaluations of Naphthalene and PCB (aroclor 1248 shown) are presented on Figures 2-2 and 2-3. Both of these figures indicate concentrations significantly above the EqP screening value and provided the basis for selecting these chemicals for modeling.

In addition to these organic chemicals, zinc was selected so that a calibrated model for a metal would be available, and Tinuvin 328 was selected because it represents a fingerprint compound for the Ciba Facility. Additional data that were collected to support contaminant fate modeling for these five chemicals are presented in Section 3.

2.2 MODEL FRAMEWORK

The model of contaminants in the Pawtuxet River is comprised of three sub-models, as illustrated by Figure 2-4. The hydrodynamic model describes the processes that control advection and dispersive mixing in the water column as surface runoff flows through the Pawtuxet River and it also quantifies the shear stresses at the sediment-water interface.

As shown, these results serve as inputs to the sediment transport model. The sediment transport model simulates the resuspension and settling of particulate material in the system and the concurrent downstream transport of solids. Results from both of these sub-models feed forward to the contaminant fate and transport model. This model utilizes the fluid and particulate transport results, in conjunction with partitioning, reaction and transfer mechanisms, to define the movement of contaminants in the system. A more detailed description of the model frameworks used in each of these sub-models is described below.

2.2.1 Model 1: Hydrodynamic Model

The sediment transport and physical-chemical models both require hydrodynamic information, e.g., velocities and water depth, to determine the transport and fate of sediment and contaminants in the Pawtuxet River. A two-dimensional, vertically-integrated hydrodynamic model was developed to define velocities, depths and the distribution of shear stresses at the water-bed interface that control the transport of fine-grained, cohesive sediments in the Pawtuxet River.

2.2.2 Model 2: Sediment Transport Model

Hydrophobic chemicals, such as PCBs and tinuvin, readily adsorb onto fine-grained, cohesive sediments, i.e., clays and silts. The resuspension, deposition and transport of cohesive sediments, therefore, play a crucial role in the fate of hydrophobic chemicals in an aquatic system. A sediment transport model of the Pawtuxet River has been developed and calibrated. This model uses the results of laboratory and field studies to describe the resuspension and deposition processes of fine-grained sediments. Results of the sediment transport model, in the form of resuspension and deposition velocities, are used directly by the physical-chemical model, yielding an accurate representation of the effects of sediment transport on contaminant transport processes in the Pawtuxet River.

2.2.3 Model 3: Contaminant Transport and Fate Model

The model of contaminants in the water column and sediment of the Pawtuxet River is based on mechanistic descriptions of the transport, transfer and reaction processes occurring in the river. Figure 2-5 is a schematic diagram which shows the mechanisms included in the model. The diagram represents the water column in a receiving water bounded by a sediment bed and the atmosphere. Chemical is added to the water column as a result of direct inputs from point sources and/or diffuse, non-point sources. Partitioning of the chemical between the dissolved and particulate phases, is assumed to be sufficiently rapid to justify an equilibrium description of the partitioning process.

Dissolved chemical maybe transferred from the water column to the atmosphere by volatilization through the air-water interface. Particulate chemical settles from the water column to the sediment bed, and is resuspended from the sediment bed into the water column. Dissolved chemical is exchanged between the water column and sediment bed in accordance with the laws of diffusion, that is, from a region of greater concentration to one of lesser concentration, with the rate of transfer controlled by a mass transfer coefficient.

In general, dissolved and particulate chemical forms may undergo various decay transformations in the water column and bottom sediment, depending on the nature of the compound. In the case of the Pawtuxet River, it was assumed that decay processes did not significantly affect the contaminants modeled.

2.3 MODEL CALIBRATION

The utility of the model is dependent upon the ease with which the parameters describing individual processes may be properly defined using information obtained from previous studies or from laboratory and field investigations conducted as part of this project. Once preliminary estimates of the requisite parameters are assigned on the basis of previous experience, available correlations, or the like, the model is run and the

computed results are compared to field data. The data types summarized in Table 2-1 have been used to check the capability of the three sub-models to accurately represent conditions in the Pawtuxet River. The comparisons between model and field data will be reviewed in detail in Sections 4, 5 and 7 of this report. The subsequent adjustment of the parameter estimates, within the limits of experience and the uncertainty of the correlations on which the estimates have been based, to obtain improved agreement between the model and field data, is referred to as the model calibration phase of the analysis.

TABLE 2-1. COMPARISONS OF MODEL AND DATA

Model	Data Sets Used for Comparison
Hydrodynamic	Water surface elevation
Sediment Transport	Total suspended solids concentration
Contaminant Fate	Water column contaminant concentration Sediment bed contaminant concentration

Figures
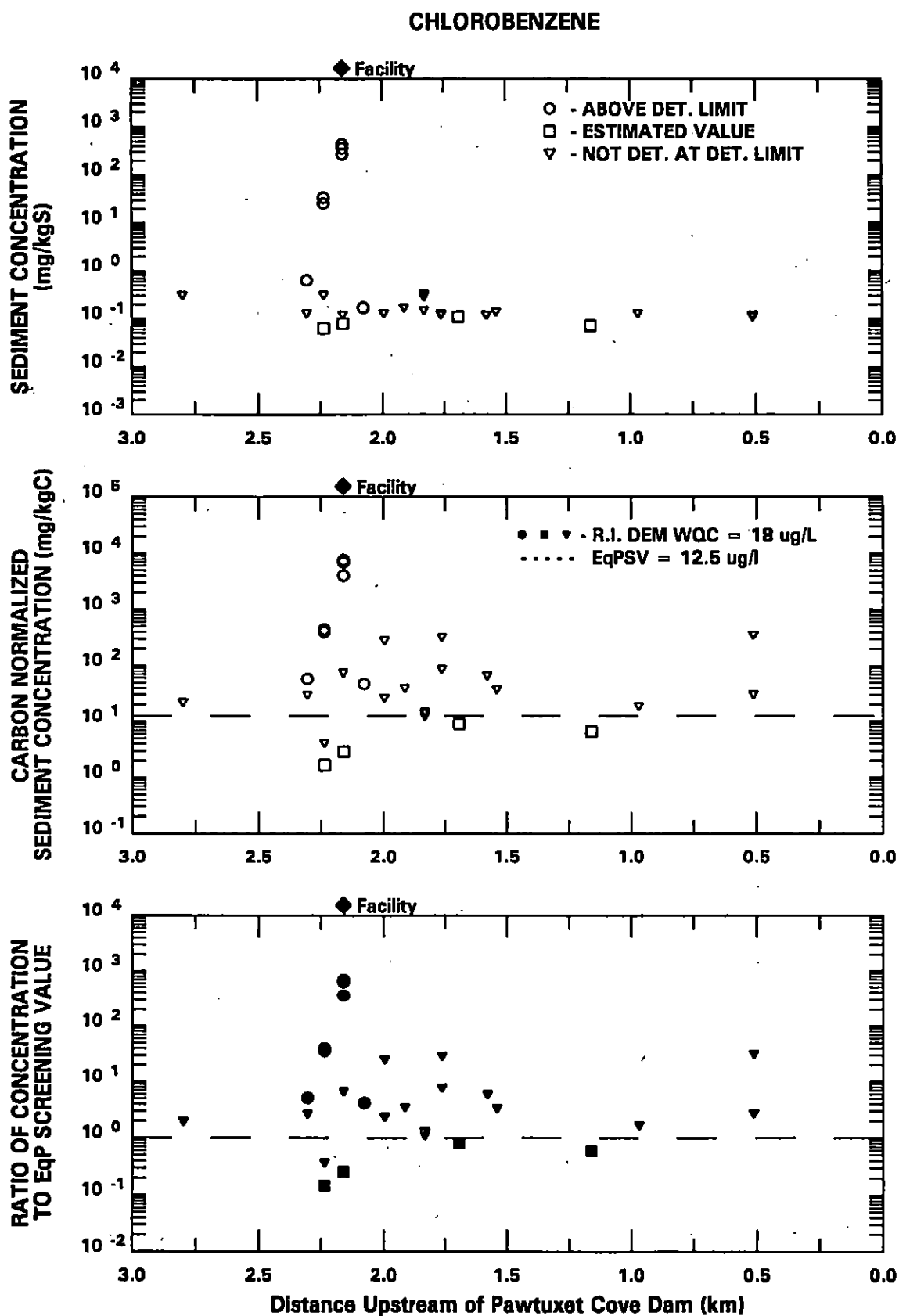
CHLOROBENZENE

FIGURE 2-1.　　Comparison of Phase I Sediment Chlorobenzene Data to Equilibrium
Partitioning Screening Value
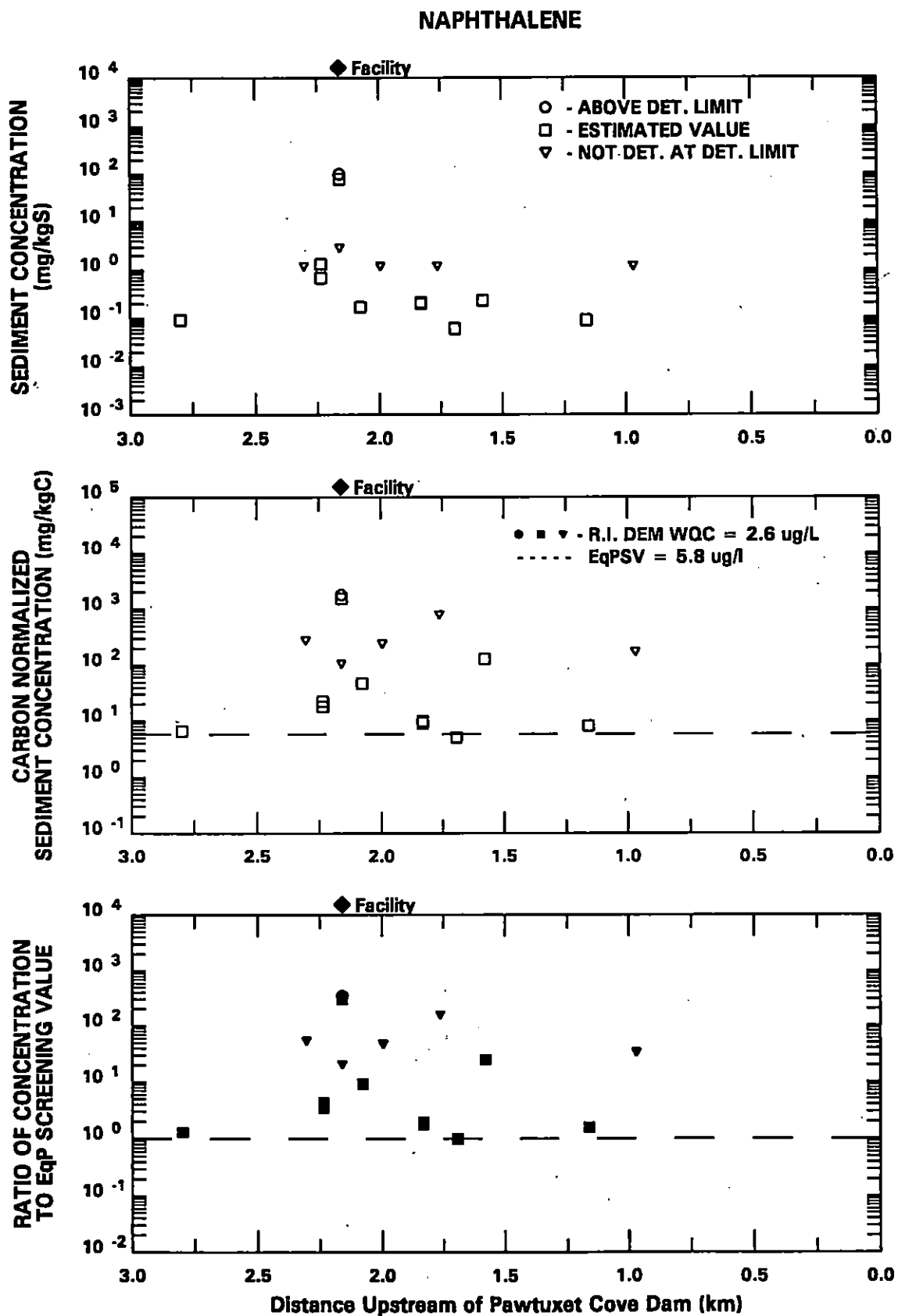
NAPHTHALENE

FIGURE 2-2. Comparison of Phase I Sediment Naphthalene Data to Equilibrium Partitioning Screening Value
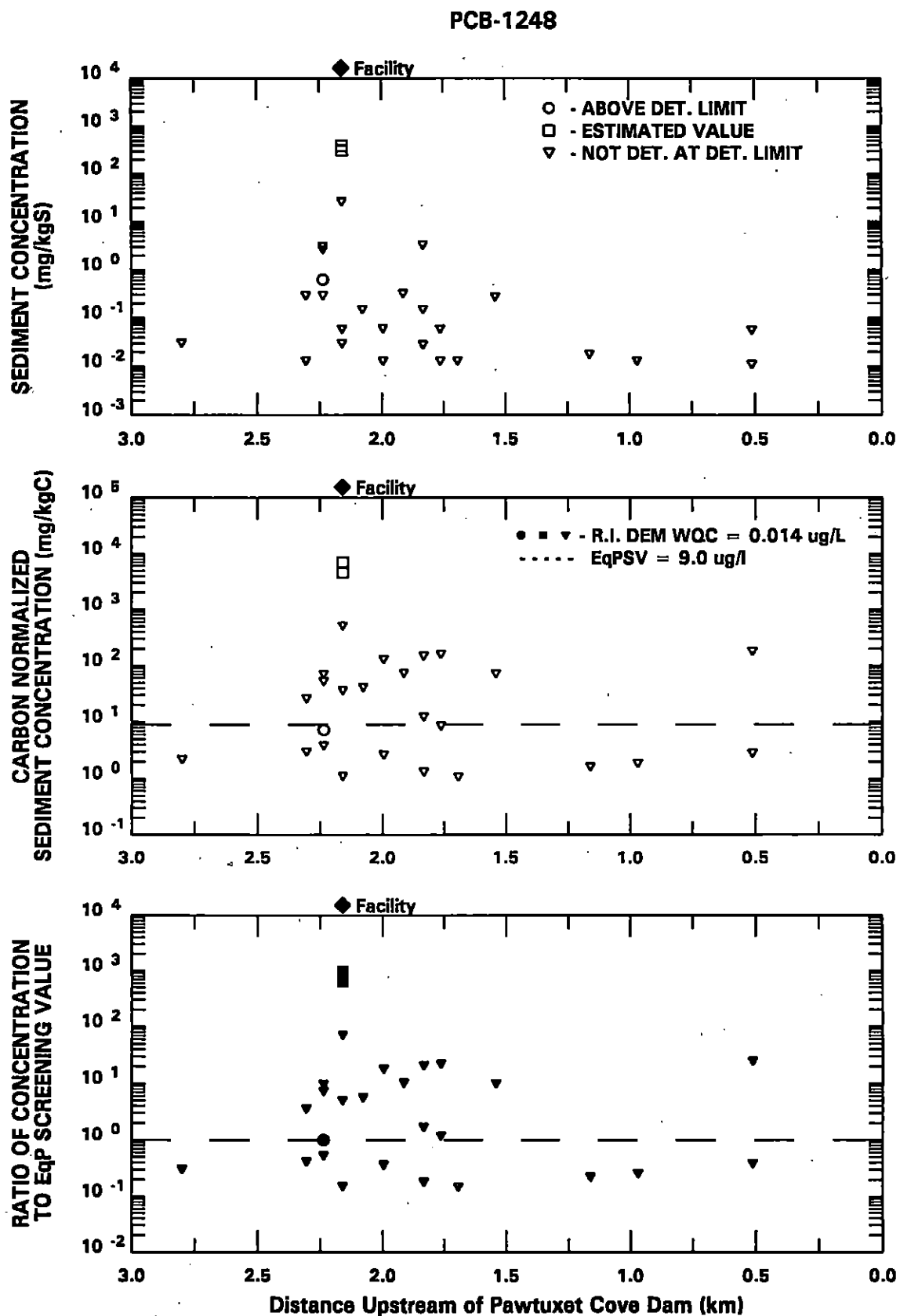
PCB-1248

FIGURE 2-3. Comparison of Phase I Sediment PCB-1248 Data to Equilibrium Partitioning Screening Value

MODEL 1:

HYDRODYNAMIC MODEL

MODEL 3:

FATE & TRANSPORT MODEL

MODEL 2:

SEDIMENT TRANSPORT MODEL
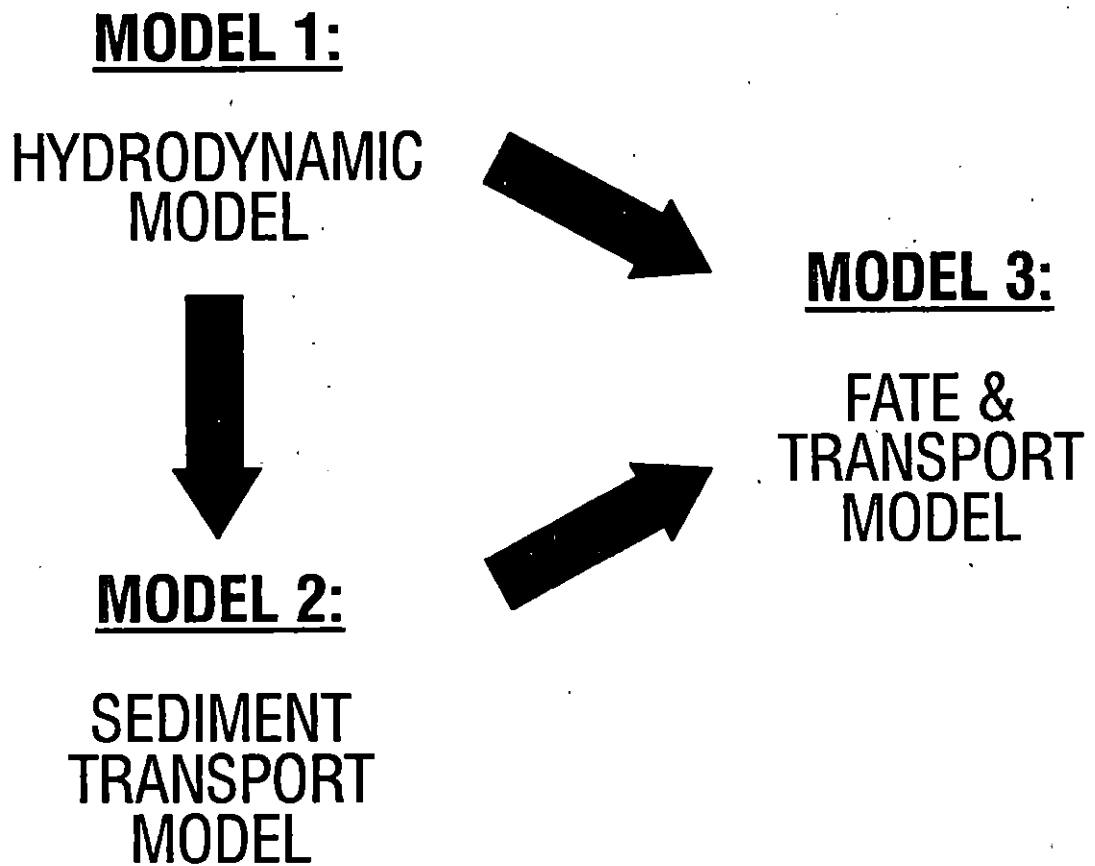
FIGURE 2-4.   **Model Components**

FIGURE 2-5.   Schematic Diagram of Models, State Variables, and Kinetic Processes

SECTION 3

CONTAMINANTS IN THE PAWTUXET RIVER

Historical data from the Pawtuxet River are fairly limited for the 5 chemicals selected for modeling (STORET; Quinn, 1985). The data for zinc and PCBs indicate higher concentrations during the late 1970's and early 1980s, compared to data from the late 1980's and early 1990's. As part of this modeling effort, sampling plans were designed to collect water column and sediment contaminant data to support transport and fate modeling of chlorobenzene, naphthalene, PCBs, zinc, and Tinuvin 328.

3.1 WATER COLUMN DATA

Surface water samples were collected from six stations on the Pawtuxet River, between Cranston and the Pawtuxet Cove Dam (Figure 3-1). The station locations were designed to provide a description of concentrations entering the upstream boundary of this study area, as well as any change in concentration due to tributary or point source inputs. Weekly sampling was conducted between May and July 1992 and again during May 1994. Samples were obtained by positioning a boat at the mid-point of the cross section and collecting a water sample from mid depth.

3.1.1 Temporal Profiles

Temporal patterns of data collected at station 1, near the USGS gage at Cranston, are presented on Figure 3-2. Note that in addition to the five chemicals being modeled, data are also presented for total organic carbon (TOC), total suspended solids (TSS), toluene (obtained in the same analysis as chlorobenzene) and silver. The three symbols, circles, squares, and triangles, indicate analytical results that are above detection limits (without a qualifier), estimated values, and not detected (plotted at the detection limit), respectively. In cases where standards and/or criteria exist they are indicated by the horizontal lines. Except for silver and PCBs, no concentrations were detected above the water quality standard or criteria. Only one PCB measurement was above the PCB

standard of 14 ng/l, while 8 of the 9 silver measurements in 1992 were above the RIDEM standard of 0.09 ug/l (5 of 9 were above the USEPA criteria of 0.12 ug/l). Zinc concentrations measured in 1994 were somewhat higher than measurements in 1992, however, a similar evaluation can not be made for chlorobenzene, naphthalene, and toluene because of changes in detection limits between 1992 and 1994 for these constituents. River flow varied between approximately 125 and 325 cfs on the days that these samples were collected.

Figure 3-3 presents water column data collected at station 2, downstream of the Cranston POTW and Pocasset River. Samples were collected only in 1992 as this station (as is also the case for stations 4 and 5). A small increase in TOC and TSS concentrations is noted between stations 1 and 2. More significant increases in silver concentrations are noted along with an increase in the one PCB concentration above the detection limit. Water column silver concentrations were consistently above the state water quality standard. However, the lack of an increase downstream of this station, in conjunction with Phase II Release Characterization sediment data, provided the basis for the decision not to add silver to the list of chemicals to be modeled. The remainder of the chemicals were not measured above the applicable water quality standards. Data from the remaining stations, 3 to 6, are presented on Figures 3-4 to 3-7. Water column data at these locations are not significantly different (P > .05) than data from station 2. In some cases, concentrations increase or decrease between stations, but these observations are more easily made with plots of concentration versus distance (for a specific date), which follow.

3.1.2 Spatial Profiles

Results of the 1992 water column monitoring have been plotted versus distance. The 1994 monitoring was conducted at stations 1,3, and 6, and yielded very few results above detection limits, and therefore, spatial plots of these data are not presented. Spatial plots of a subset of the surveys are presented in this section. Plots of the remaining surveys are included in Appendix B. The surveys presented in this section are selected to highlight patterns observed over the range of flows experienced during the 1992 sampling

program. These plots are ordered from lowest to highest flow (129 cfs - 325 cfs) on Figures 3-8 to 3-13.

Several observations are made on the basis of these spatial patterns:

1)   In general, an increase in TOC and TSS concentrations occurs between the two upstream stations (at Cranston and downstream of the Pocasset River). No consistent trends exist between km. 5.6 (station 2) and km. 2.4 (station 3). Between the end of the Facility Reach (km 1.8) and the most downstream station (km. 0.2) near the Pawtuxet Cove Dam , TSS concentrations often decreased, sometimes slightly (Figure 3-9, 3-10, 3-13) and sometimes more significantly (Figure 3-11, 3-12), however, on some days, similar TSS concentrations were measured at these two locations (Figure 3-8).

2)   PCB concentrations were measured above the detection limit of approximately 11 ng/l on only two days and above the water quality criteria of 14 ng/l on only one day, May 28, 1992 (Figure 3-9). On this day, the PCB concentration measured at Cranston was 17 ng/l and downstream of the Pocasset River (km 5.6) and upstream of the Ciba Facility (km 2.4) concentrations of 68 and 101 ng/l were measured. Downstream of the Ciba Facility two non-detected results and a measurement of 39 ng/l were obtained. The suspended solids concentrations on this day, near 10 mg/l, were at the high end of values measured during the routine monitoring, even though the river flow was only 136 cfs.

3)   The chlorobenzene data generally indicate a pattern of declining concentration from Cranston to the facility. This decline is consistently observed between Stations 1 and 2. A decrease from Station 2 to 3 is observed in some data sets (Figure 3-8, 3-10, 3-12) while in others little or no change in concentration is observed between km 5.6 and 2.4. Within the Facility Reach, increases in chlorobenzene concentrations are noted in several data sets (Figure 3-8, 3-10, 3-12, and 3-13). while others show little or no increase (Figure 3-9, 3-11).

4) Naphthalene profiles are more erratic than chlorobenzene profiles. No increasing or decreasing pattern is consistently observed between the six stations.

5) Tinuvin 328 was not measured above the detection limit in any of the samples collected in this monitoring effort.

6) Zinc concentration profiles do not indicate any consistent spatial trends. There is an indication of a small increase in zinc concentrations between the two upstream stations in some surveys, although, not all. Likewise, in some data sets a small decrease in zinc concentrations is noted in the Facility Reach, between km 2.4 and 1.8 (Figure 3-10, 3-11, 3-12) while in other surveys, an increasing or erratic pattern is seen.

3.2   SEDIMENT CONTAMINANT DATA

A sampling plan was developed to measure sediment concentrations of the chemicals selected for modeling. The objective of the sampling effort was to define longitudinal, lateral, and vertical contaminant concentration patterns within the study area. Sampling locations were selected with consideration of concentration gradients indicated by the Phase I Release Characterization data and sediment composition information obtained from the Phase II Sediment Physical Characterization.

The sediment bed between Cranston and the Pawtuxet Cove Dam was divided into a grid of 360 elements, with 6 elements across the river and 60 elements in the direction of flow. Based on the physical characterization data, each element was given one of three classifications: cohesive, high TOC non-cohesive, or low TOC non-cohesive. Of the 360 grid elements, 51 elements were selected for sampling. Because cohesive organic sediments have a greater ability to sorb the chemicals selected for modeling, all of the sediment areas classified as cohesive were selected for sampling. Likewise, because the highest concentrations and most significant concentration gradients were observed in the vicinity of the Ciba Facility, 27 of the 51 sampling areas were located in the Facility Reach.

In order to estimate an average chemical concentration within each sampling grid element, five sediment cores were collected, sectioned vertically, and composited. Three vertical sections were obtained from each core, separated into 0 - 5, 5 - 10, and 10 - 20 cm intervals. A map showing the sampling locations in the lower 3 km section of the river is presented on Figure 3-14. Samples were collected from each sampling area, however, analyses for chlorobenzene and naphthalene were only performed on samples from the Facility Reach and one area upstream of the sharp bend near km 1.3. The sampling plan modification to limit the stations for which chlorobenzene and naphthalene analyses would be performed was based on Phase I and Phase II Release Characterization data that indicated low concentrations outside of these areas. This modification was approved by EPA.

3.2.1 Sediment Concentration Spatial Profiles

Chlorobenzene concentrations measured in the sediment sampling program are plotted versus distance on Figures 3-15a-c (3 depth intervals). These figures and subsequent spatial plots include analytical results that were above detection limits (no qualifier) and estimated values. Results reported as not detected are not included on these figures. The detection limits for Chlorobenzene range from approximately 0.005 to 0.010 mg/kg. Although the sampling grid was developed with 6 elements across the river, the results here are aggregated into the divisions north, center or south side of the river. In cases where samples were collected from the two nearshore grid elements, the average of the results are plotted.

Most notable are the hundreds and thousands of mg/kg concentrations measured along the Production Area. Concentrations near 1 mg/kg are noted in several other areas, including just upstream of the Warwick Avenue Bridge and on the south bank at km 1.3, near the sharp bend in the river. At other locations, especially in the center channel, concentrations were between 0.001 and 0.1 mg/kg.

Spatial patterns of organic chemical concentrations in sediment are influenced by many factors, including distance from sources, erosional and depositional patterns, chemical partitioning characteristics, and sediment characteristics. With the sampling conducted in the Pawtuxet River, data are available to normalize sediment chemical concentrations by organic carbon concentrations in the sediment, and thereby remove some of the variability introduced by variations in sediment composition. Figures 3-16a-c show the chlorobenzene data previously presented divided by sediment organic carbon concentrations. Because sediment chlorobenzene concentrations maybe influenced by active groundwater sources the normalization by organic carbon does not significantly change the spatial patterns. However, anticipating the influence of partitioning on the distribution of the other chemicals (e.g. PCB's or Tinuvin 328) subsequent spatial plots of sediment concentrations are presented with the normalization by organic carbon. A complete set of spatial plots presented on a bulk sediment basis is included in Appendix B.

Naphthalene sediment concentrations are plotted versus distance on Figures 3-17a-c. Naphthalene concentration profiles are similar to chlorobenzene, although absolute concentrations are much lower. The greatest difference occurs along the production area, where the highest concentrations of both naphthalene and chlorobenzene are observed. In this area, napthalene levels are 1 to 2 orders of magnitude less than chlorobenzene concentrations.

Spatial patterns of sediment PCB concentrations are presented on Figures 3-18a-c. Concentrations peak along the production area, however, contamination appears to be more widely dispersed than for chlorobenzene or naphthalene. Most values are in the range of 10 to 100 mg/kgOC. In addition to the peak along the production area, comparatively high concentrations are observed on the south bank of the river upstream of the Warwick Avenue Bridge and upstream of the Pawtuxet Cove Dam.

Carbon normalized sediment concentrations of Tinuvin 328 are plotted versus distance on Figures 3-19a-c. Tinuvin concentrations are highest near the Production area

and vary by approximately an order of magnitude downstream of the Production Area. Carbon normalized concentrations in the center channel tend to be somewhat higher than concentration along the North and South banks downstream of the production area.

Spatial profiles of carbon normalized zinc concentrations are presented on Figures 3-20a-c. While characteristics other than organic carbon, most notably, sulfide, can significantly affect partitioning, the normalization by organic carbon in this case does eliminate some of the variability in the spatial patterns. Zinc concentrations are highest along the production area, although the peak concentration was obtained from an area upstream of the peak chlorobenzene, naphthalene, and PCB concentrations. The range of carbon normalized zinc concentrations is fairly small compared to the other chemicals previously presented. Almost all of the measurements are within a factor of 2 above or below the 10,000 mg/kgOC level. Exceptions include the north bank along the production area, and on the south bank upstream of the Warwick Avenue Bridge and upstream of the Pawtuxet Cove Dam.

No clear patterns were identified in vertical profiles of the sediment chemical concentrations.
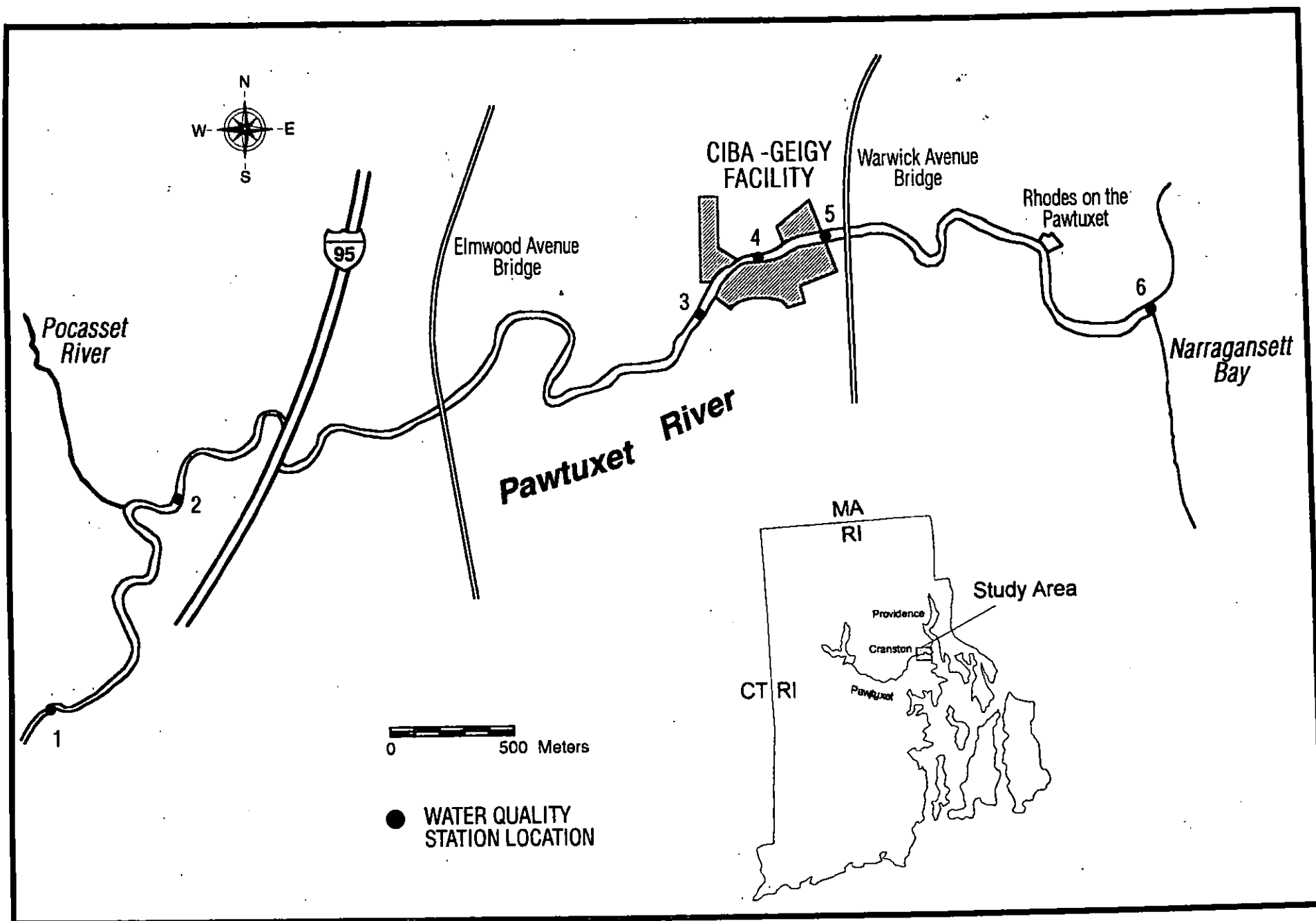
Figures

WATER QUALITY STATIONS

FIGURE 3-1.   Location of Water Column Sampling Stations

(LEGEND: ● ABOVE DET. LIMIT, ■ ESTIMATED VALUE ▼ NOT DETECTED - PLOTTED AT DET. LIMIT)
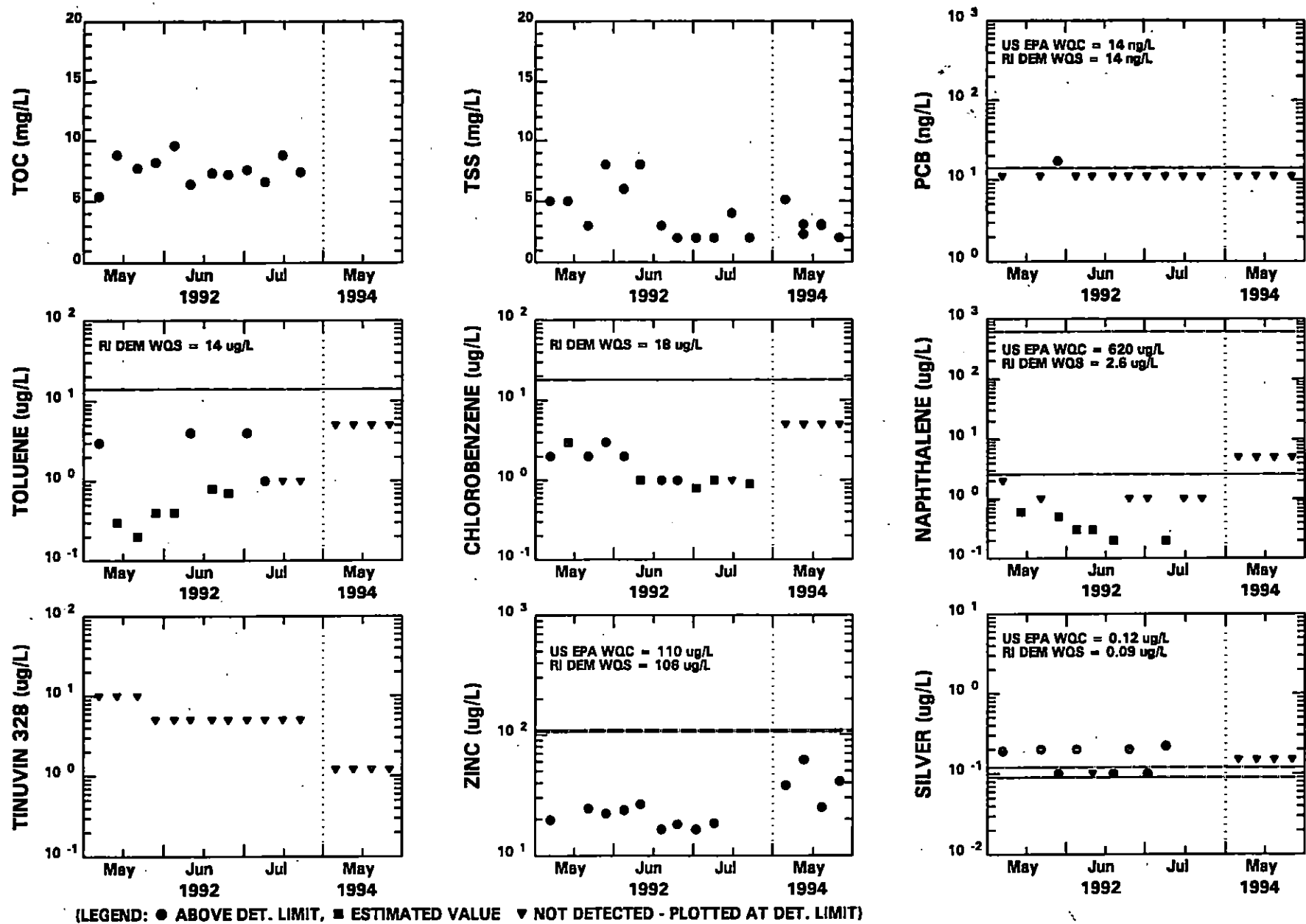
WATER COLUMN SAMPLING FOR FATE MODELING - DATA FROM STATION 1

FIGURE 3-2.   Water Column Sampling for Fate Modeling - Data for Station 1
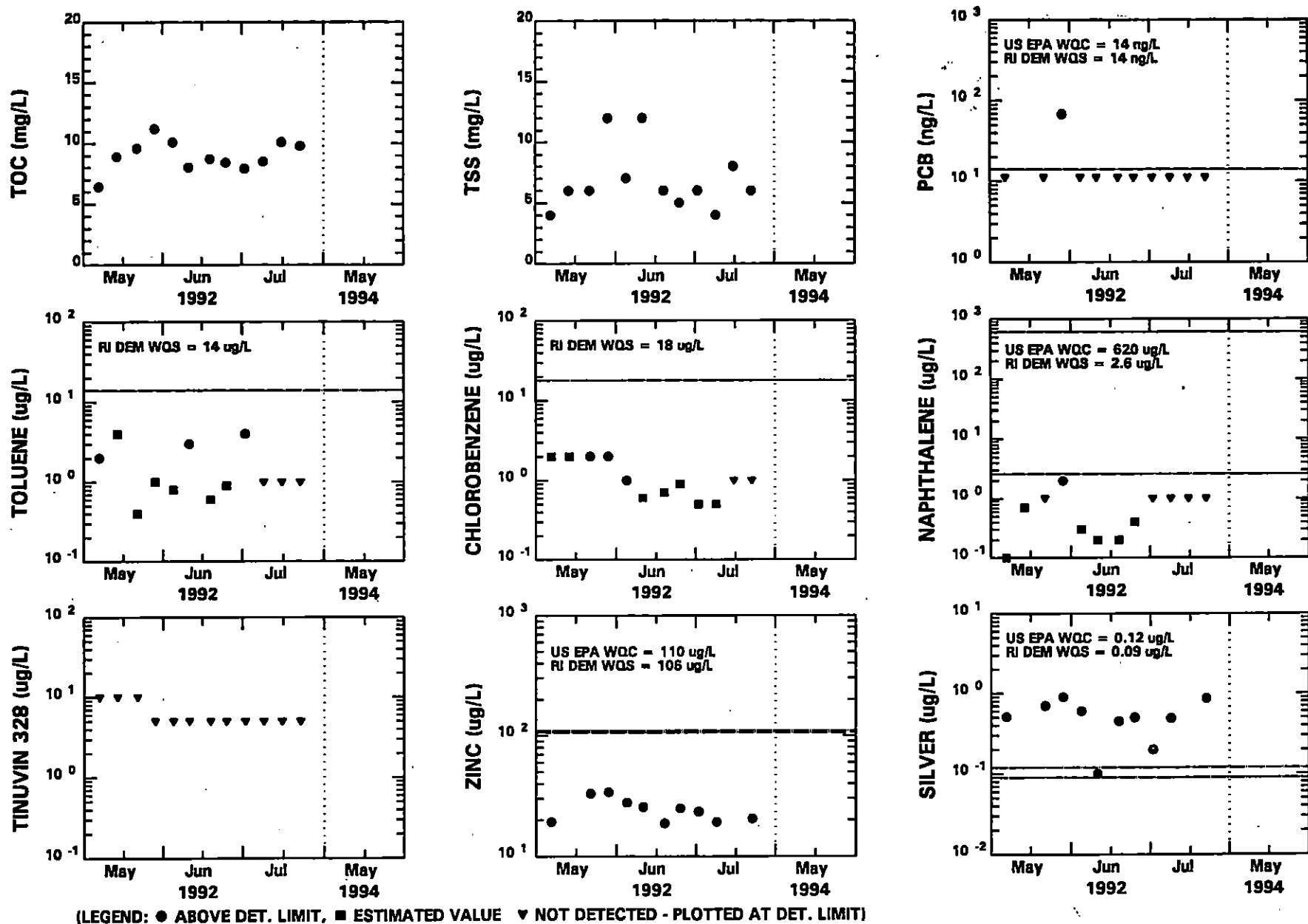
WATER COLUMN SAMPLING FOR FATE MODELING - DATA FROM STATION 2

FIGURE 3-3.   Water Column Sampling for Fate Modeling - Data for Station 2

(LEGEND: ● ABOVE DET. LIMIT, ■ ESTIMATED VALUE ▼ NOT DETECTED - PLOTTED AT DET. LIMIT)
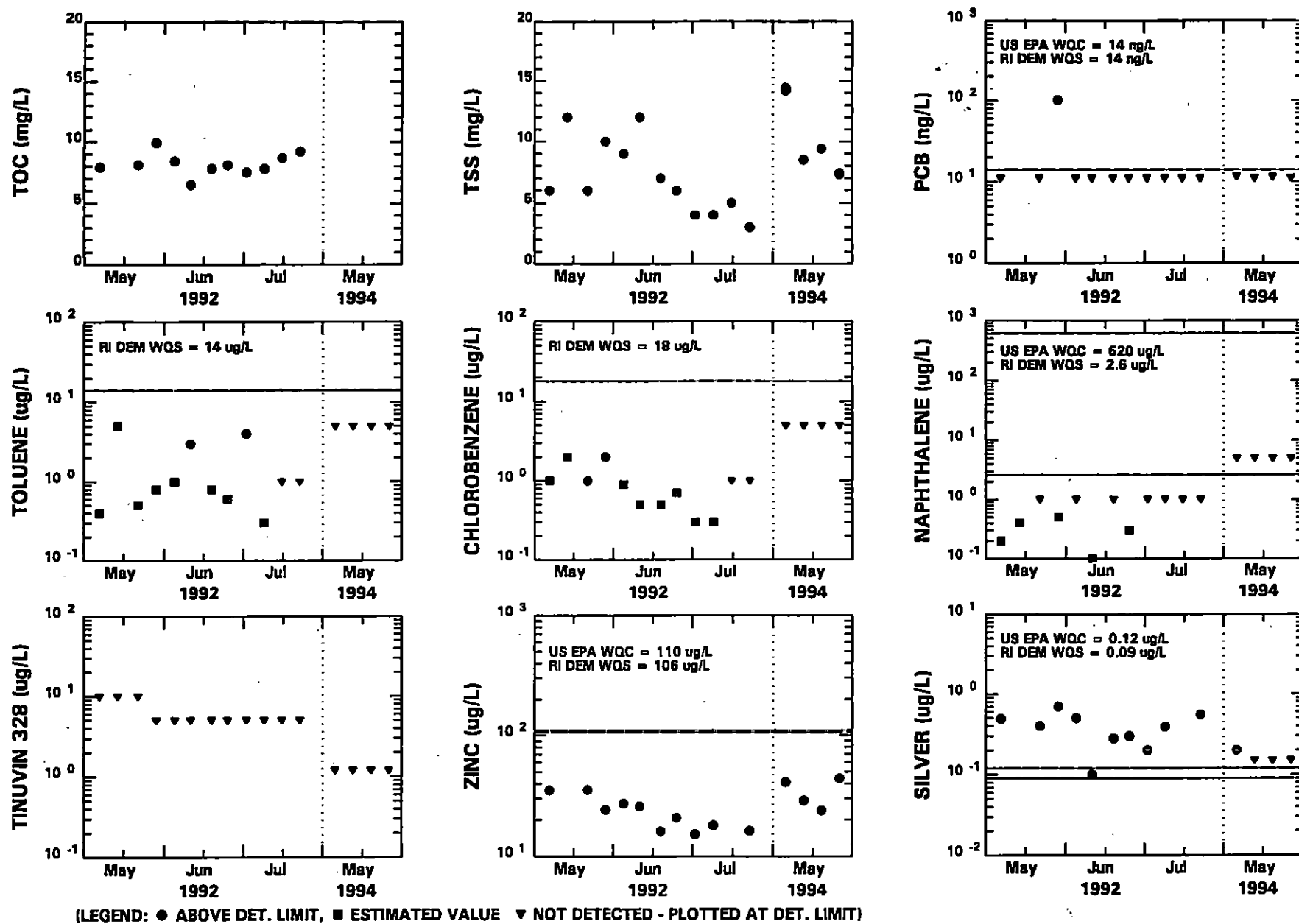
WATER COLUMN SAMPLING FOR FATE MODELING - DATA FROM STATION 3

FIGURE 3-4.   Water Column Sampling for Fate Modeling - Data for Station 3
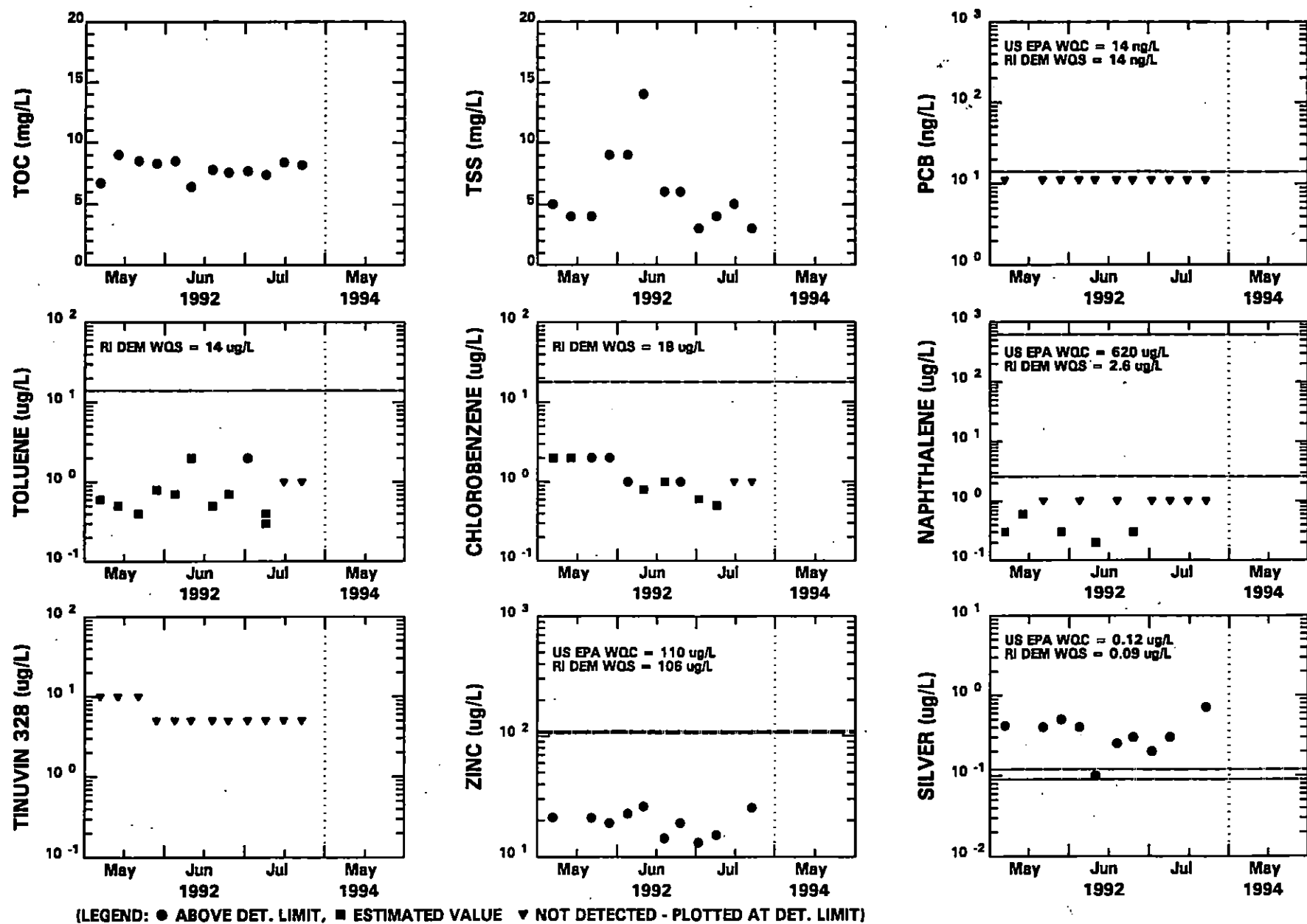
WATER COLUMN SAMPLING FOR FATE MODELING - DATA FROM STATION 4

FIGURE 3-5.   Water Column Sampling for Fate Modeling - Data for Station 4

(LEGEND: ● ABOVE DET. LIMIT, ■ ESTIMATED VALUE ▼ NOT DETECTED - PLOTTED AT DET. LIMIT)
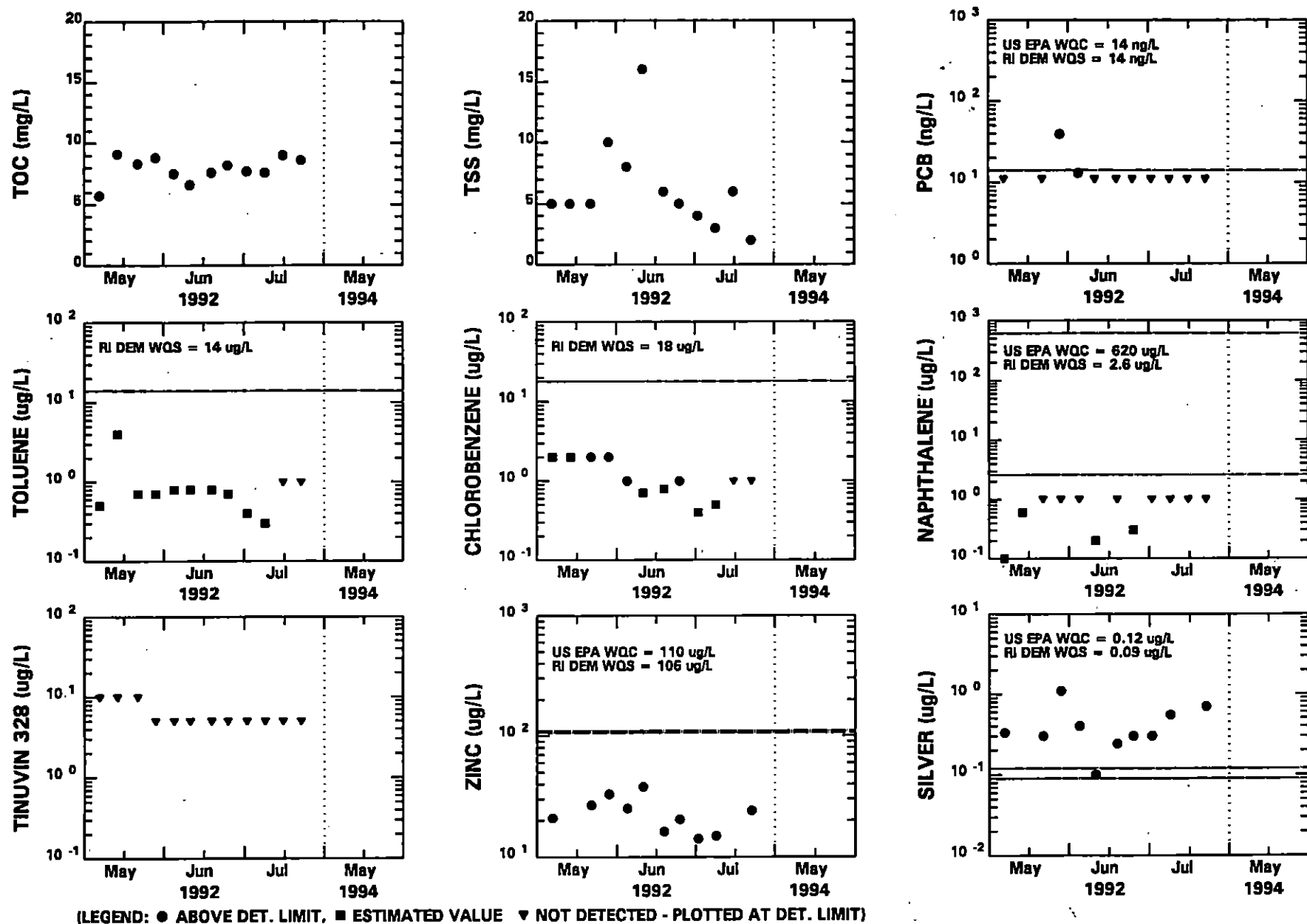
WATER COLUMN SAMPLING FOR FATE MODELING - DATA FROM STATION 5

FIGURE 3-6. Water Column Sampling for Fate Modeling - Data for Station 5

(LEGEND: ● ABOVE DET. LIMIT, ■ ESTIMATED VALUE ▼ NOT DETECTED - PLOTTED AT DET. LIMIT)
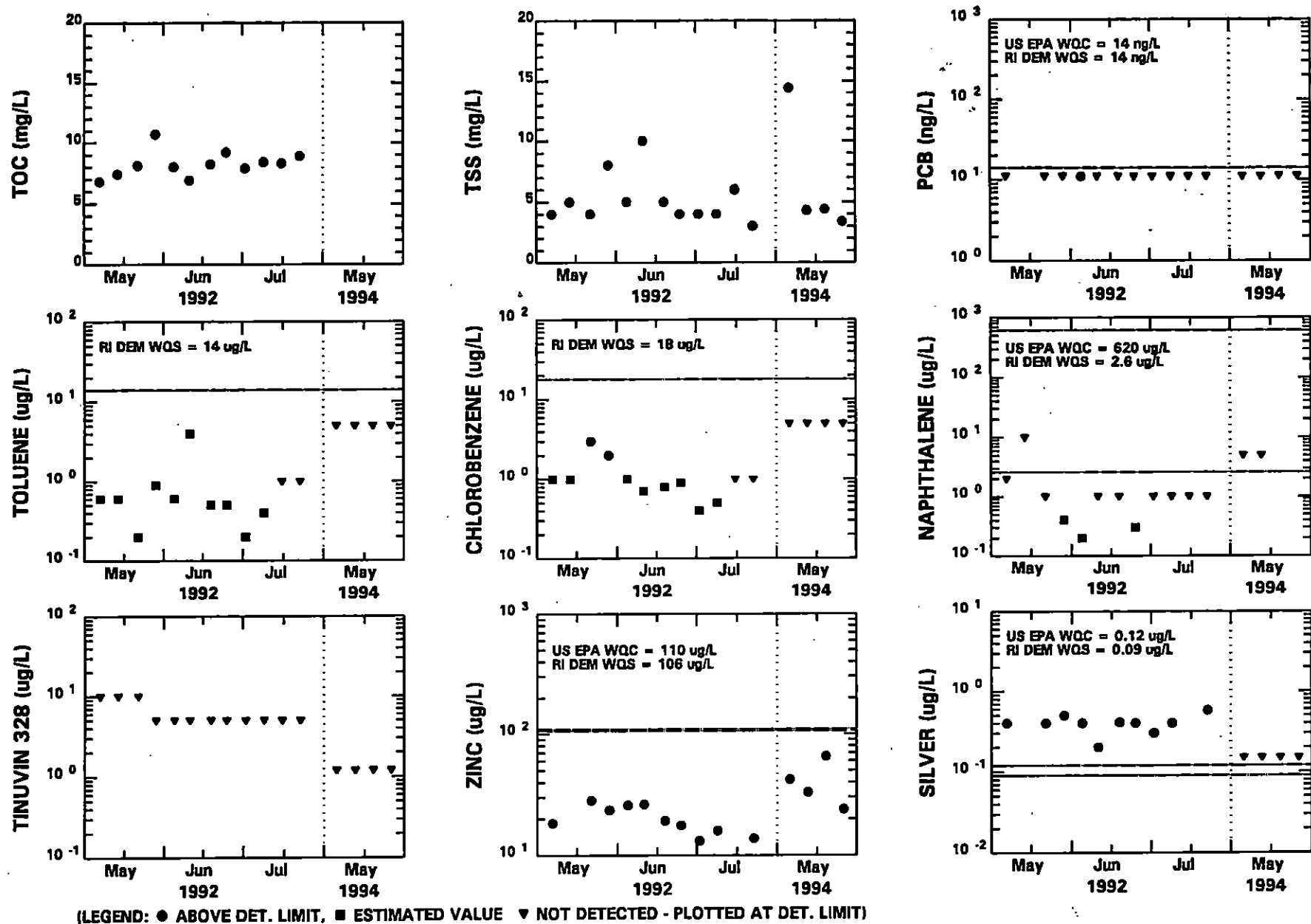
WATER COLUMN SAMPLING FOR FATE MODELING - DATA FROM STATION 6

FIGURE 3-7.   Water Column Sampling for Fate Modeling - Data for Station 6

(LEGEND: ● ABOVE DET. LIMIT, ■ ESTIMATED VALUE ▼ NOT DETECTED - PLOTTED AT DET. LIMIT)
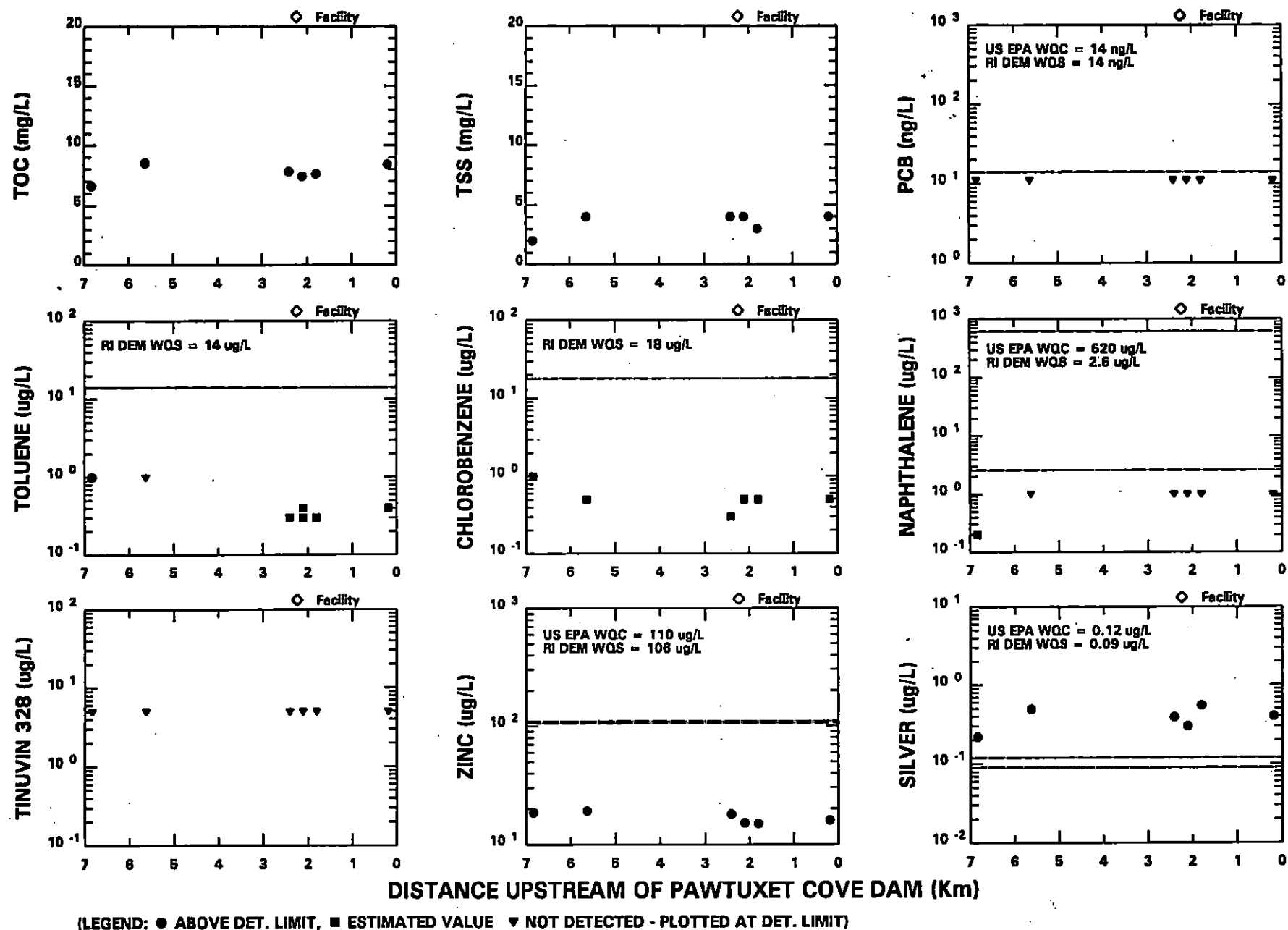
WATER COLUMN SAMPLING FOR FATE MODELING - JULY 8, 1992 DATA (RIVER FLOW = 129 cfs)

FIGURE 3-8.

(LEGEND: ● ABOVE DET. LIMIT, ■ ESTIMATED VALUE ▼ NOT DETECTED - PLOTTED AT DET. LIMIT)
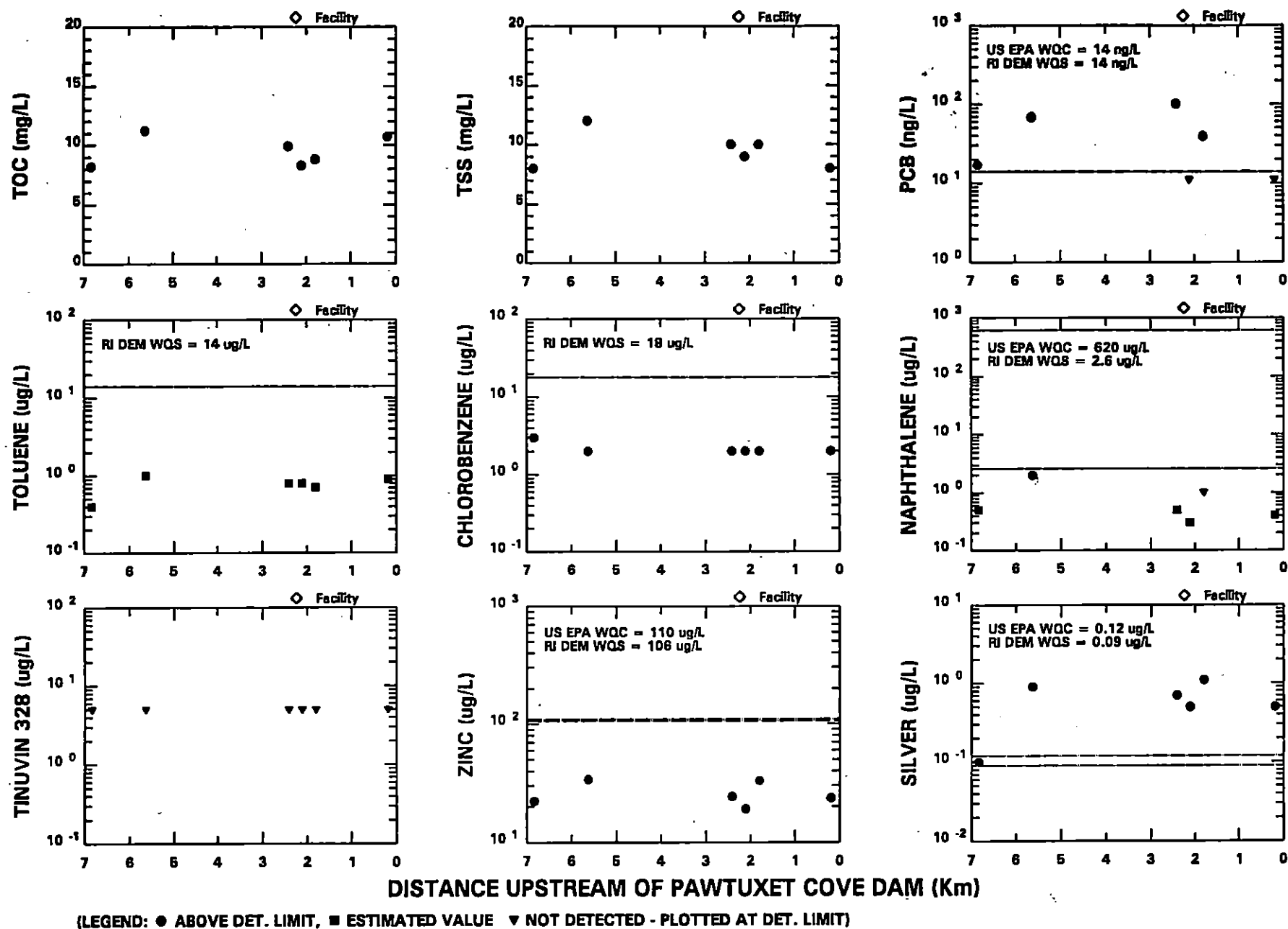
WATER COLUMN SAMPLING FOR FATE MODELING - MAY 28, 1992 DATA (RIVER FLOW = 136 cfs)

FIGURE 3-9.

(LEGEND: ● ABOVE DET. LIMIT, ■ ESTIMATED VALUE ▼ NOT DETECTED - PLOTTED AT DET. LIMIT)
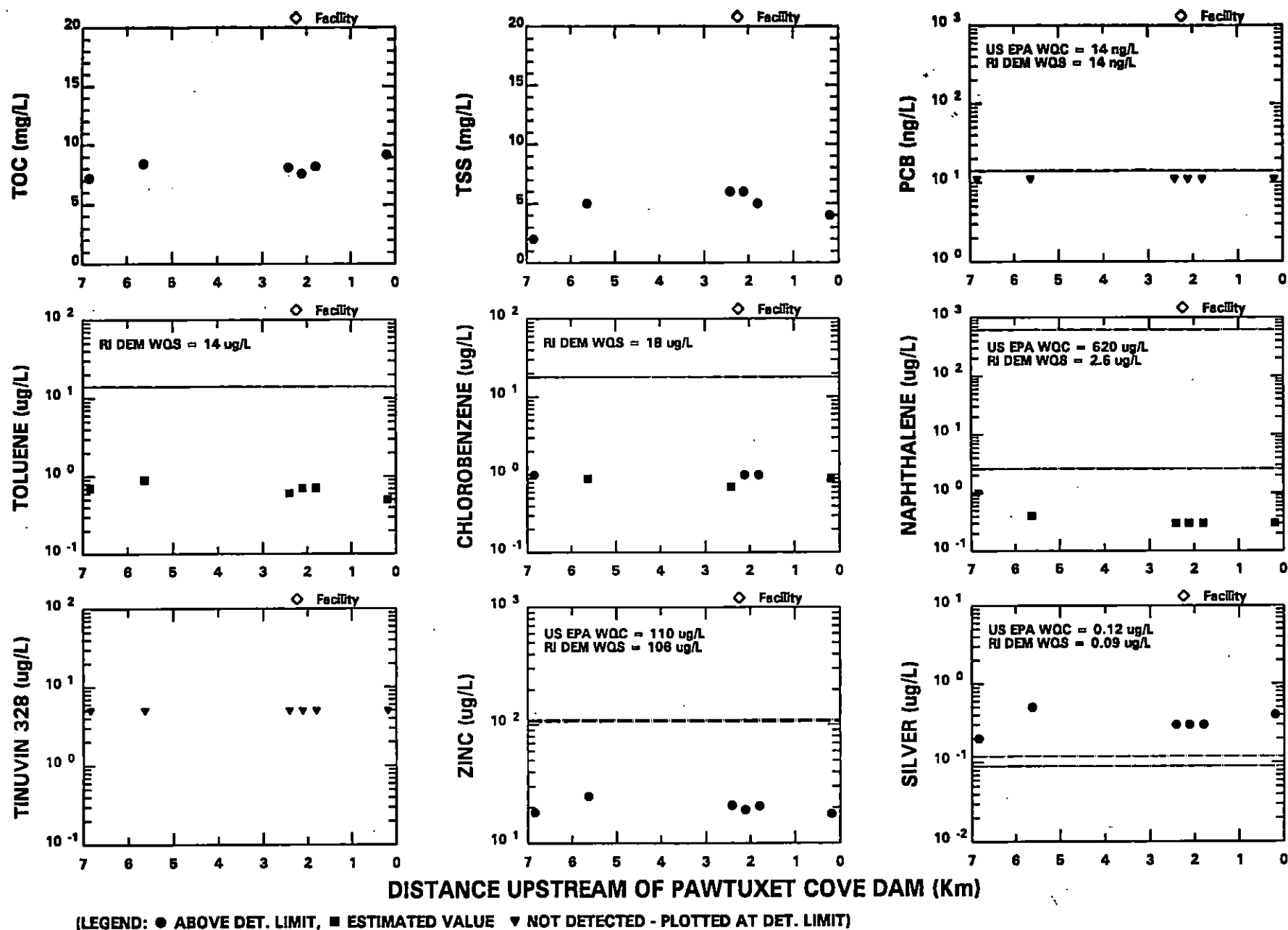
WATER COLUMN SAMPLING FOR FATE MODELING - JUNE 24, 1992 DATA (RIVER FLOW = 175 cfs)

FIGURE 3-10.

(LEGEND: ● ABOVE DET. LIMIT, ■ ESTIMATED VALUE ▼ NOT DETECTED - PLOTTED AT DET. LIMIT)
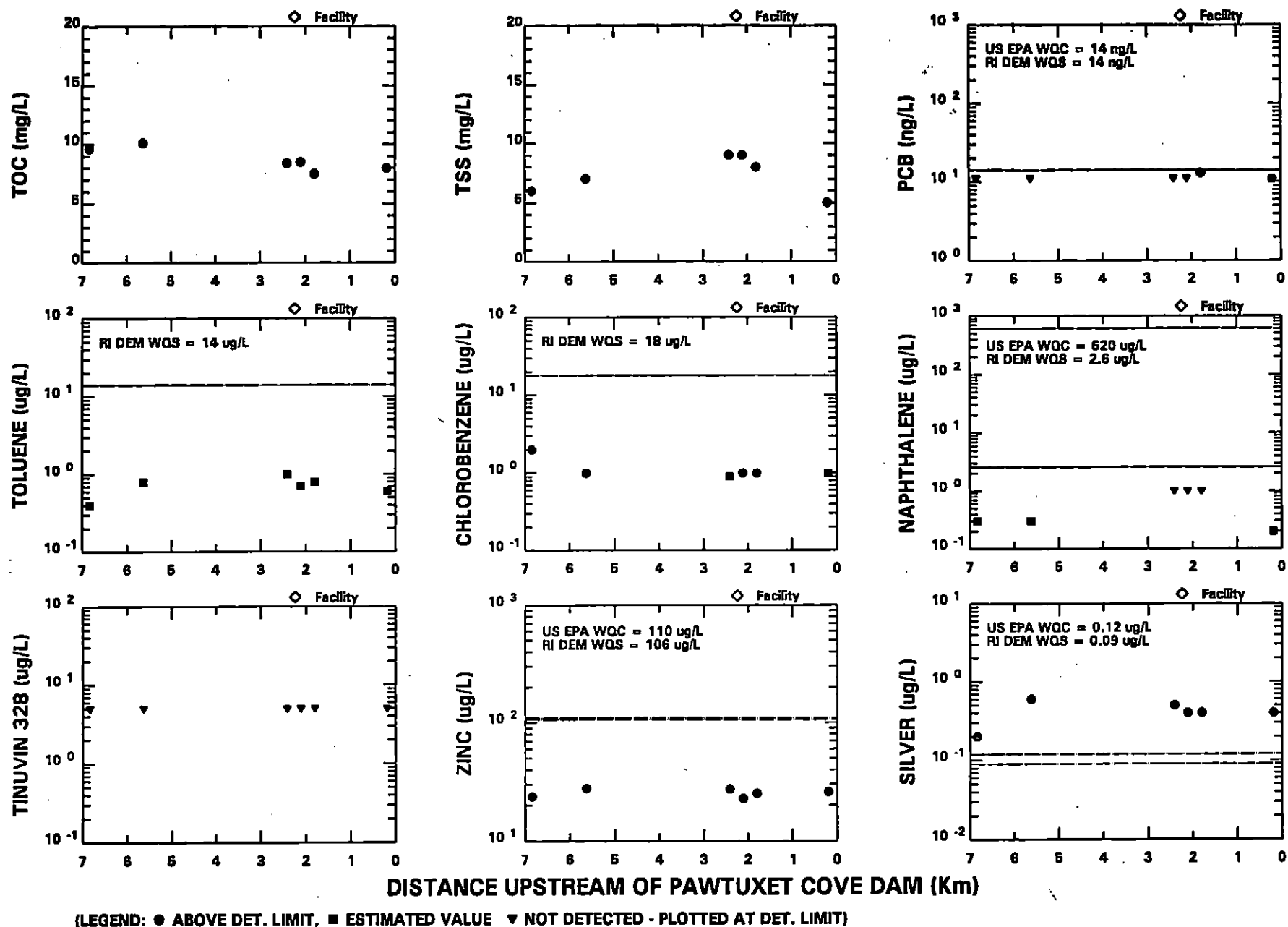
WATER COLUMN SAMPLING FOR FATE MODELING - JUNE 4, 1992 DATA (RIVER FLOW = 189 cfs)

FIGURE 3-11.

(LEGEND: ● ABOVE DET. LIMIT, ■ ESTIMATED VALUE ▼ NOT DETECTED - PLOTTED AT DET. LIMIT)
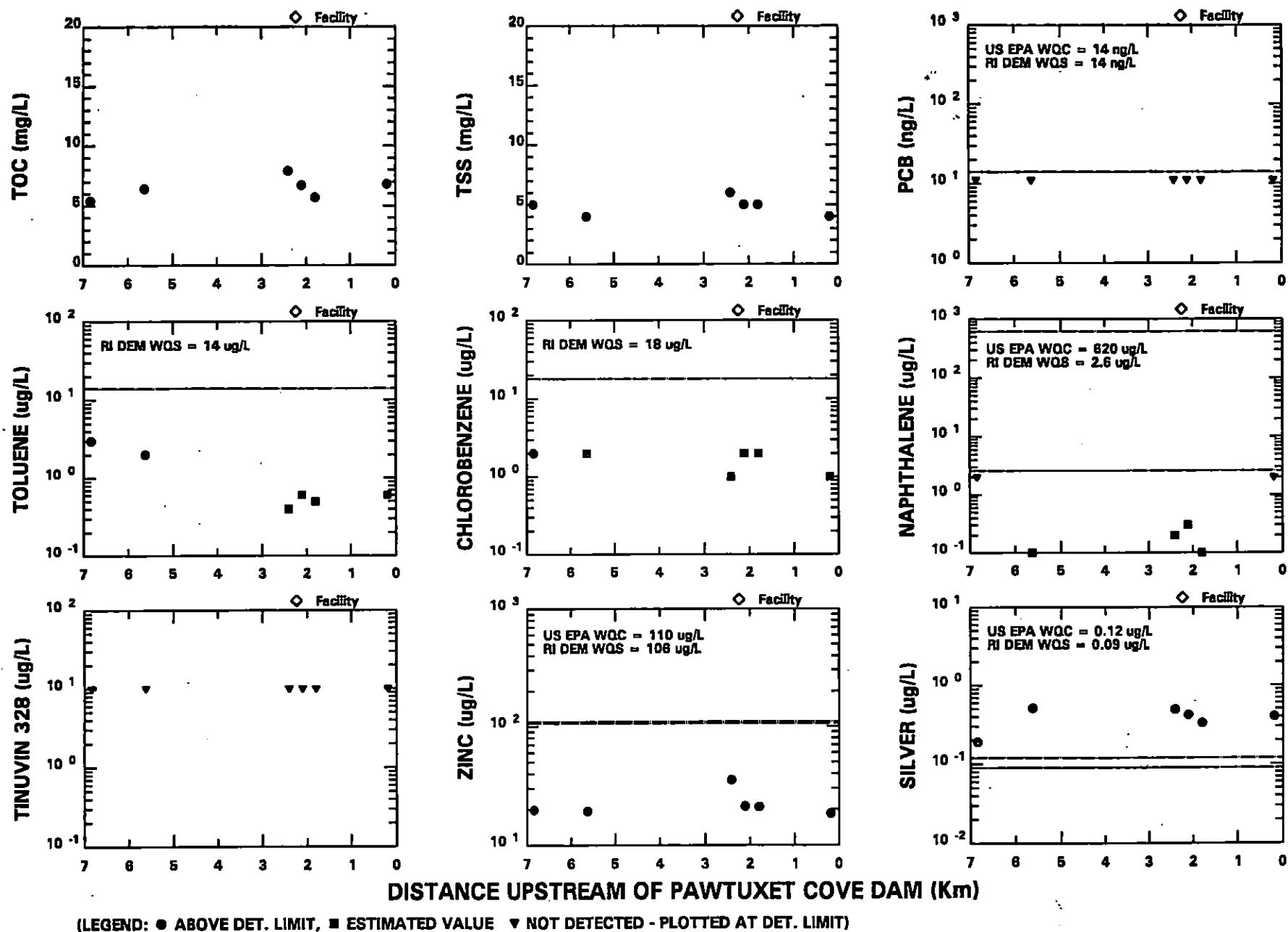
WATER COLUMN SAMPLING FOR FATE MODELING - MAY 6, 1992 DATA (RIVER FLOW = 216 cfs)

FIGURE 3-12.

(LEGEND: ● ABOVE DET. LIMIT, ■ ESTIMATED VALUE ▼ NOT DETECTED - PLOTTED AT DET. LIMIT)
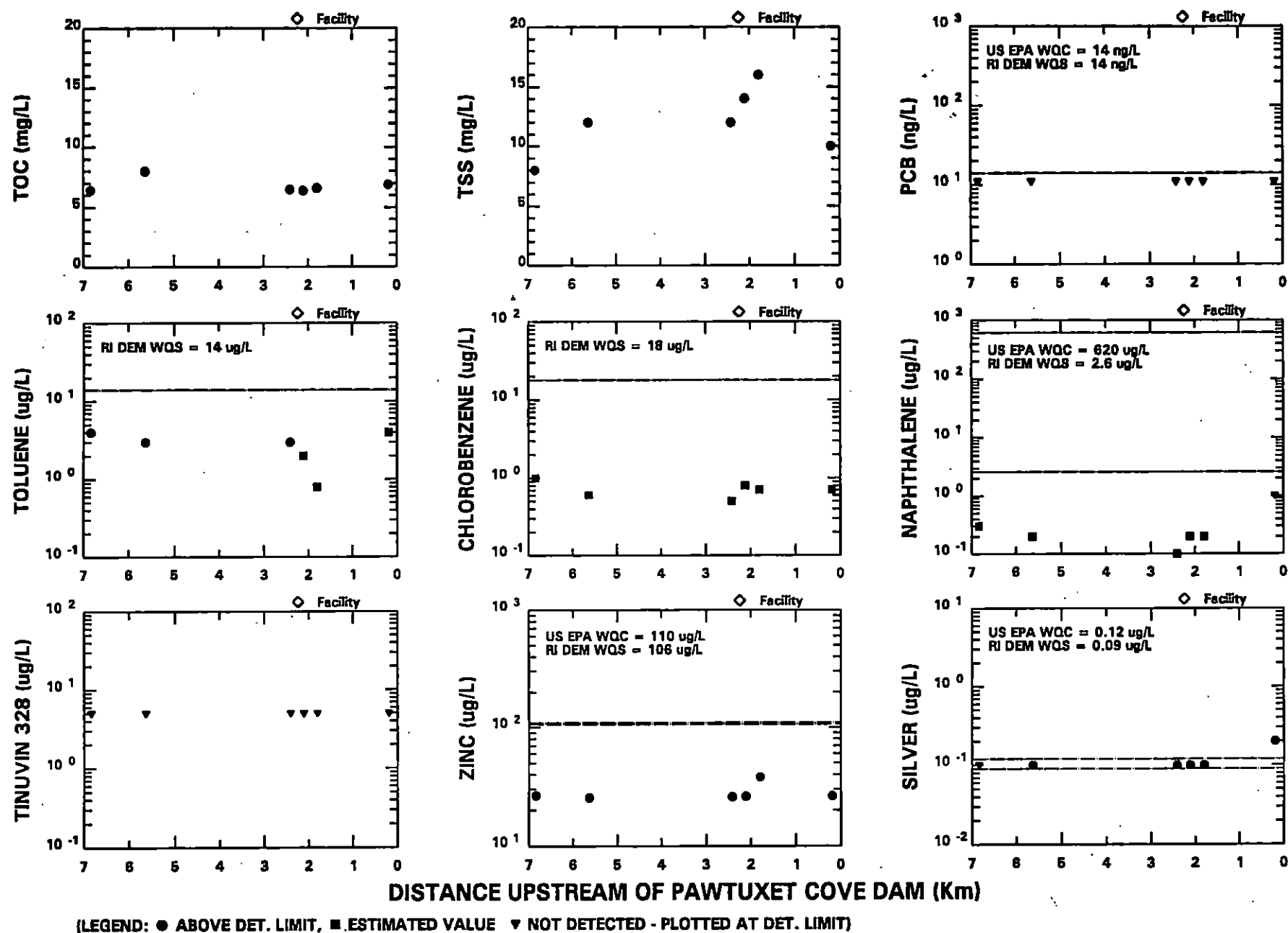
WATER COLUMN SAMPLING FOR FATE MODELING - JUNE 10, 1992 DATA (RIVER FLOW = 325 cfs)

FIGURE 3-13.
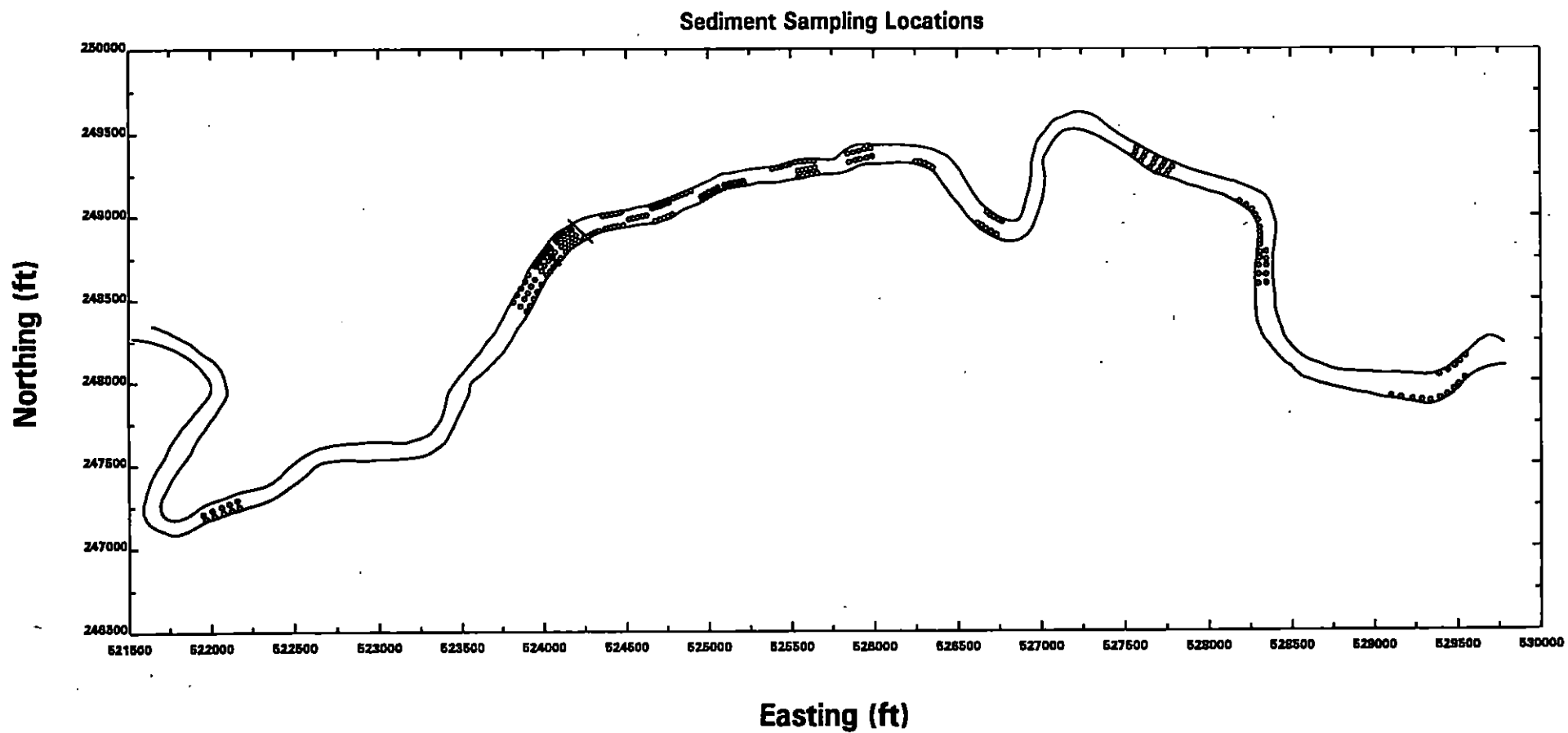
FIGURE 3-14. Location of Sediment Sampling Stations

Pawtuxet River
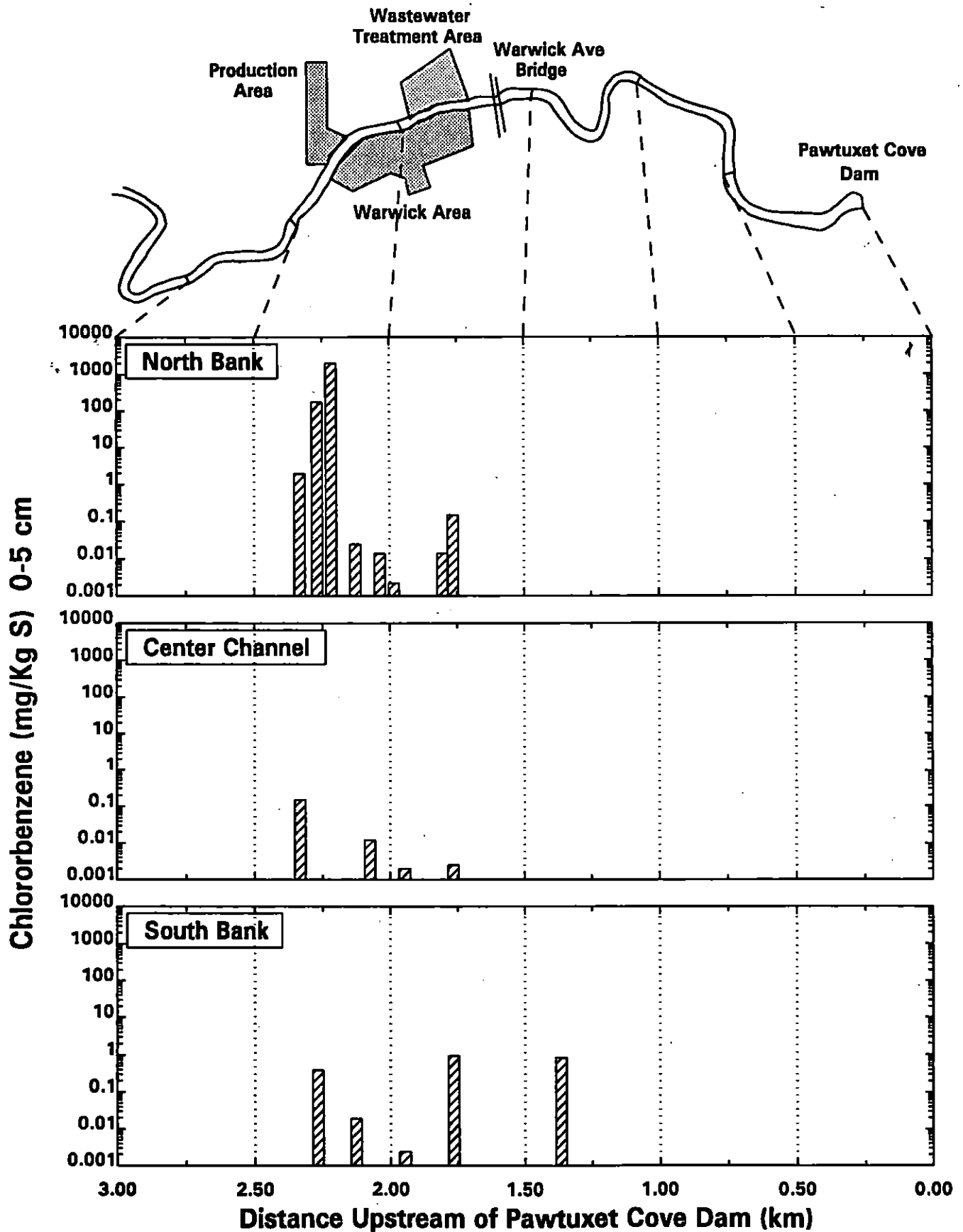
FIGURE 3-15a. Sediment Sampling for Fate Modeling - Chlorobenzene Data - 0-5 cm Layer
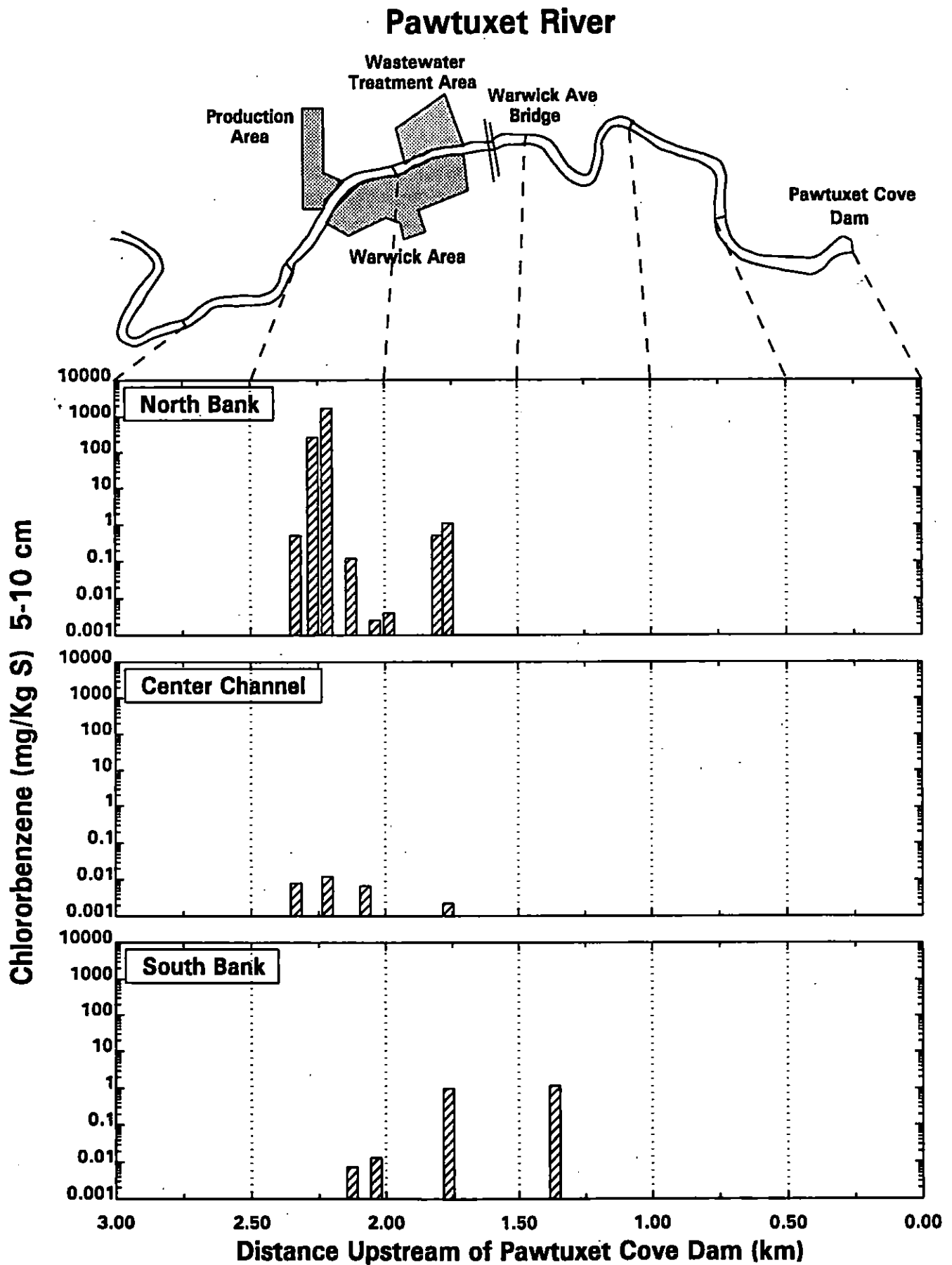
Pawtuxet River

FIGURE 3-15b.   Sediment Sampling for Fate Modeling - Chlorobenzene Data - 5-10 cm Layer
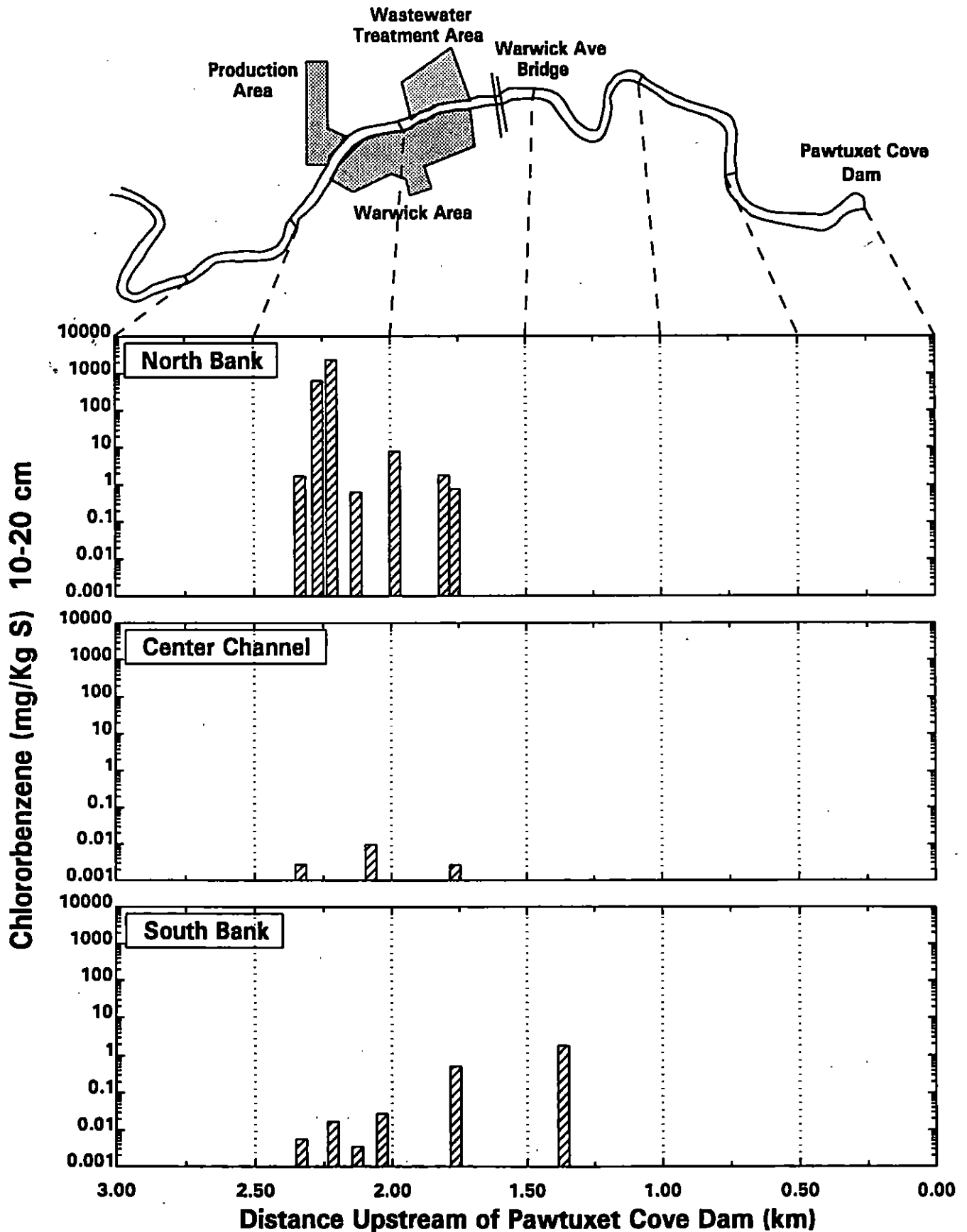
FIGURE 3-15c.   Sediment Sampling for Fate Modeling - Chlorobenzene Data - 10-20 cm Layer
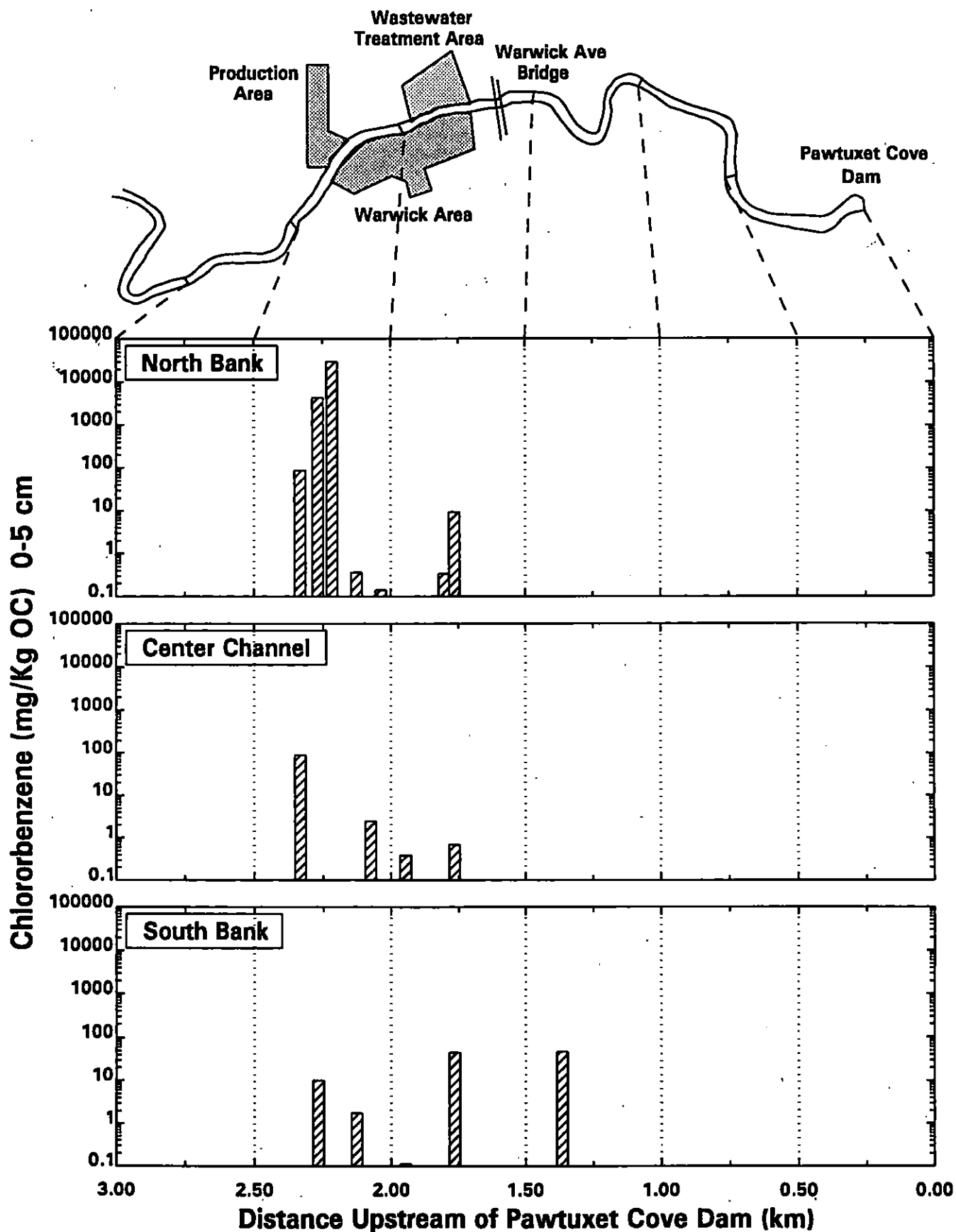
Pawtuxet River

FIGURE 3-16a.   Sediment Sampling for Fate Modeling - Carbon Normalized
Chlorobenzene Data - 0-5 cm Layer
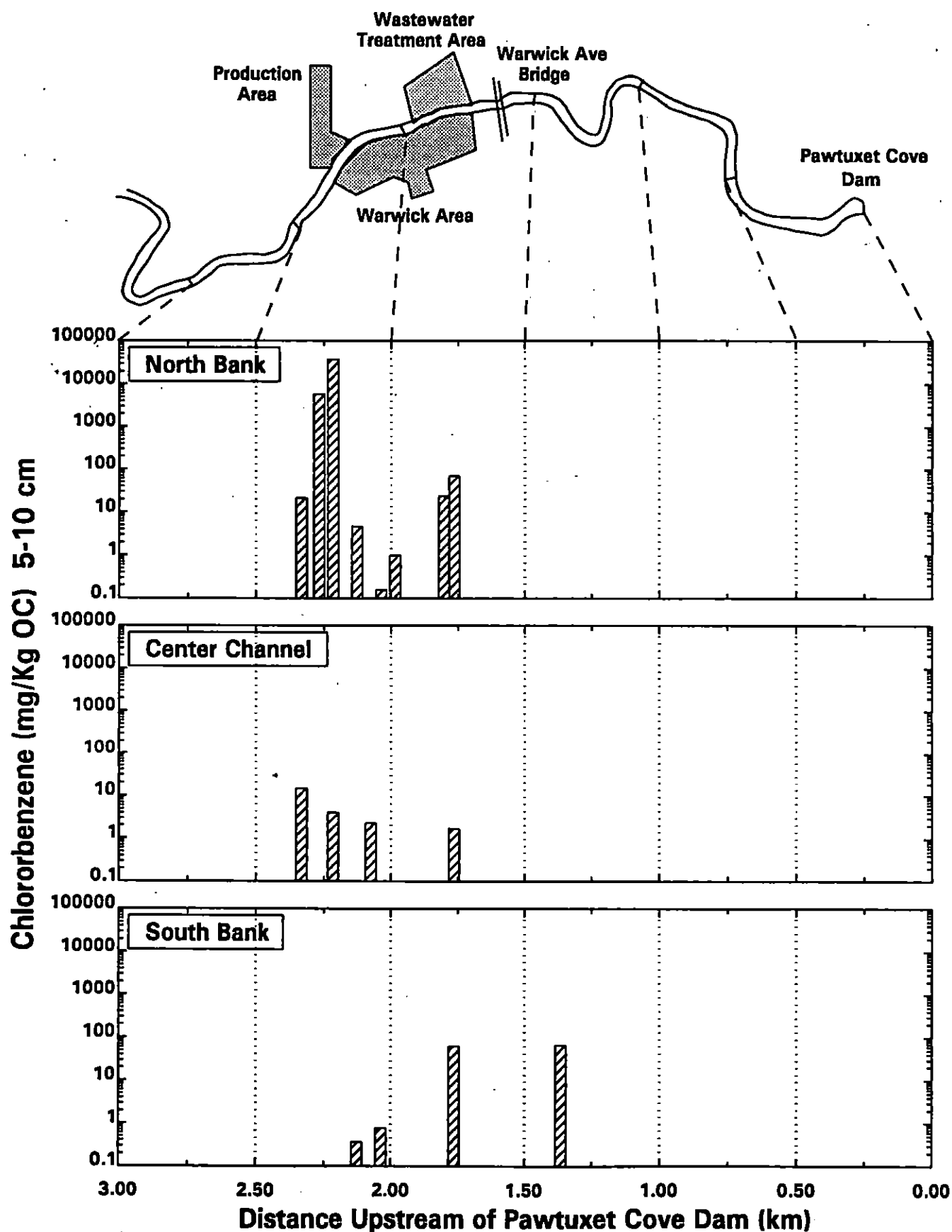
FIGURE 3-16b. Sediment Sampling for Fate Modeling - Carbon Normalized Chlorobenzene Data - 5-10 cm Layer
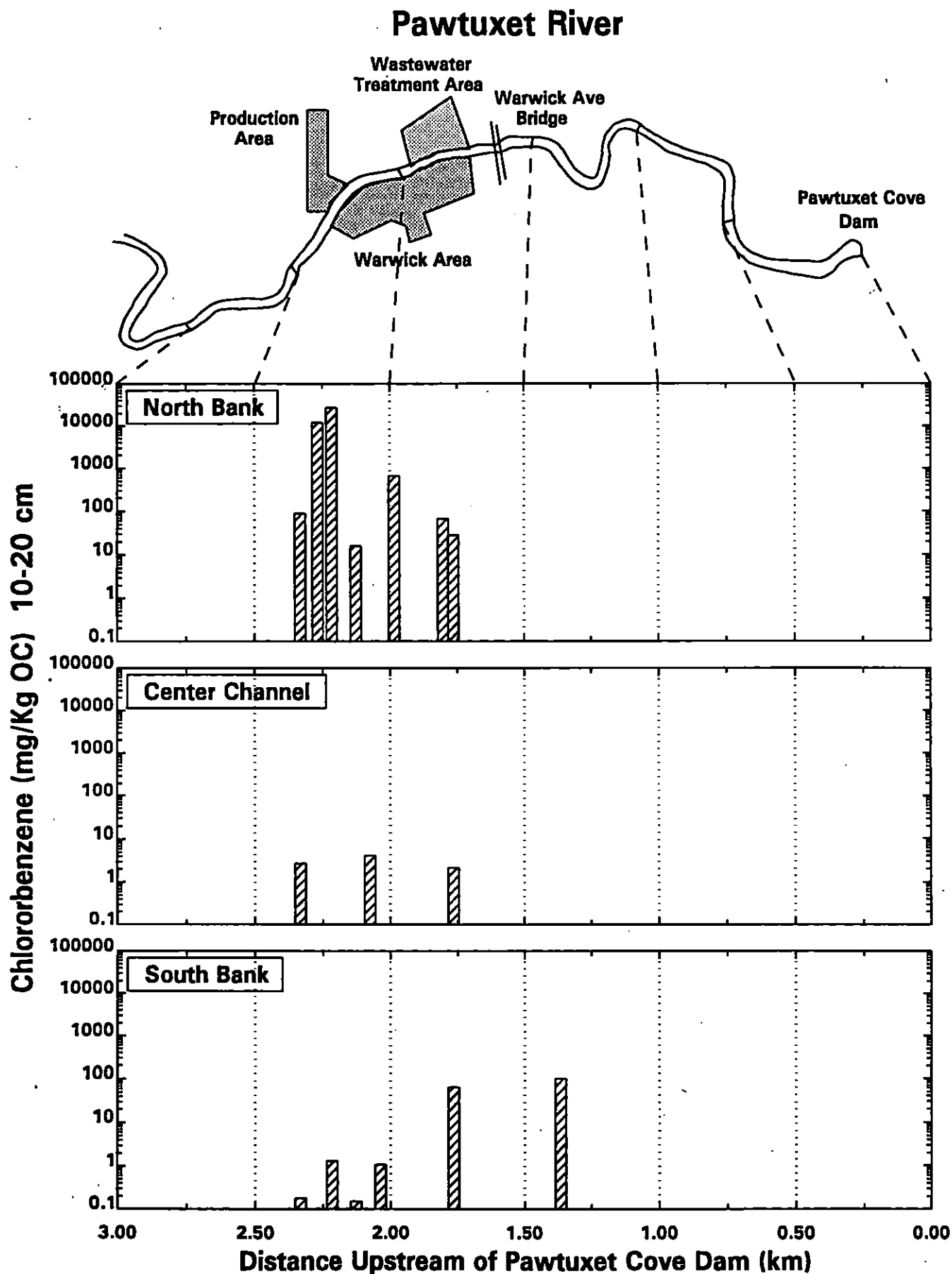
FIGURE 3-16c.   Sediment Sampling for Fate Modeling - Carbon Normalized
                Chlorobenzene Data - 10-20 cm Layer
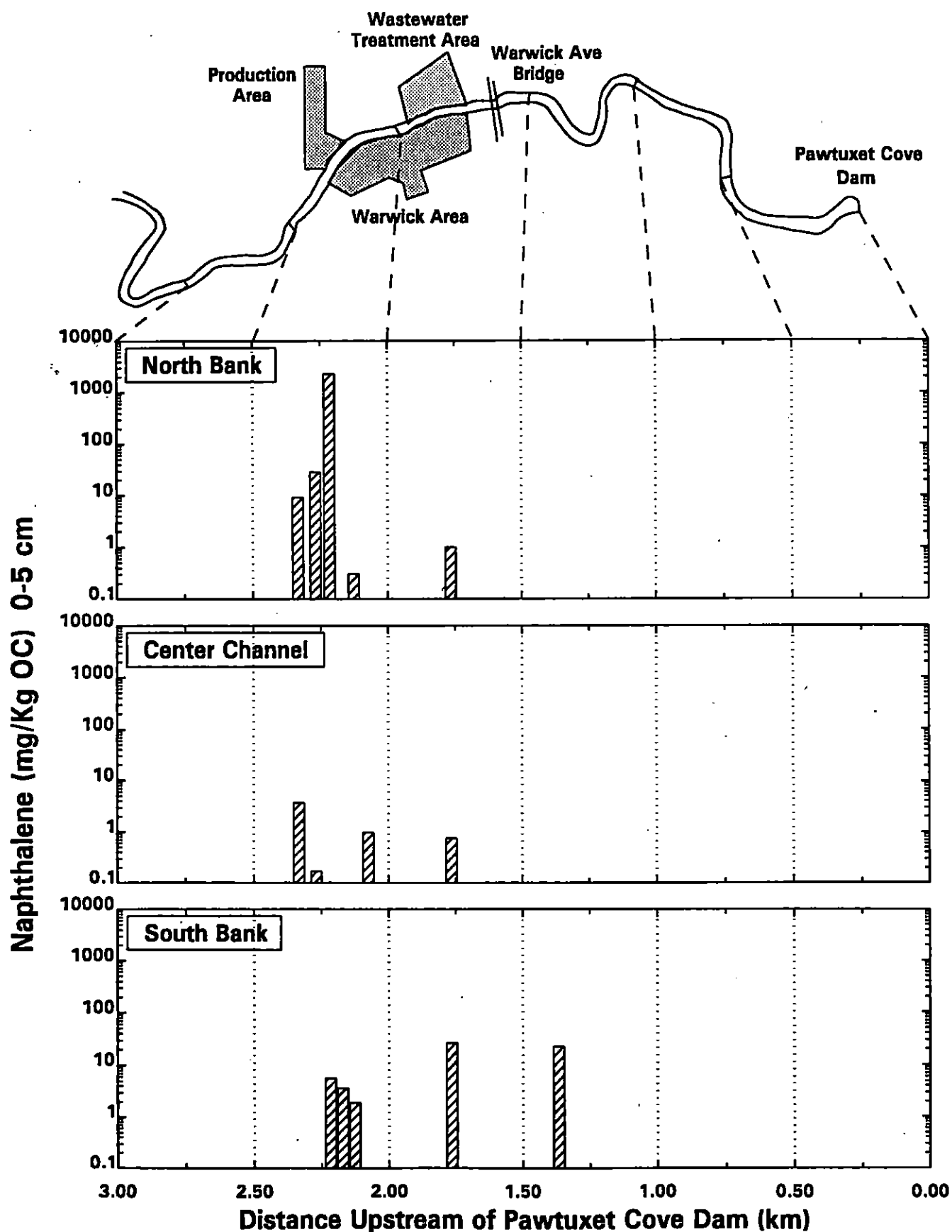
FIGURE 3-17a.   Sediment Sampling for Fate Modeling - Carbon Normalized
Naphthalene Data - 0-5 cm Layer
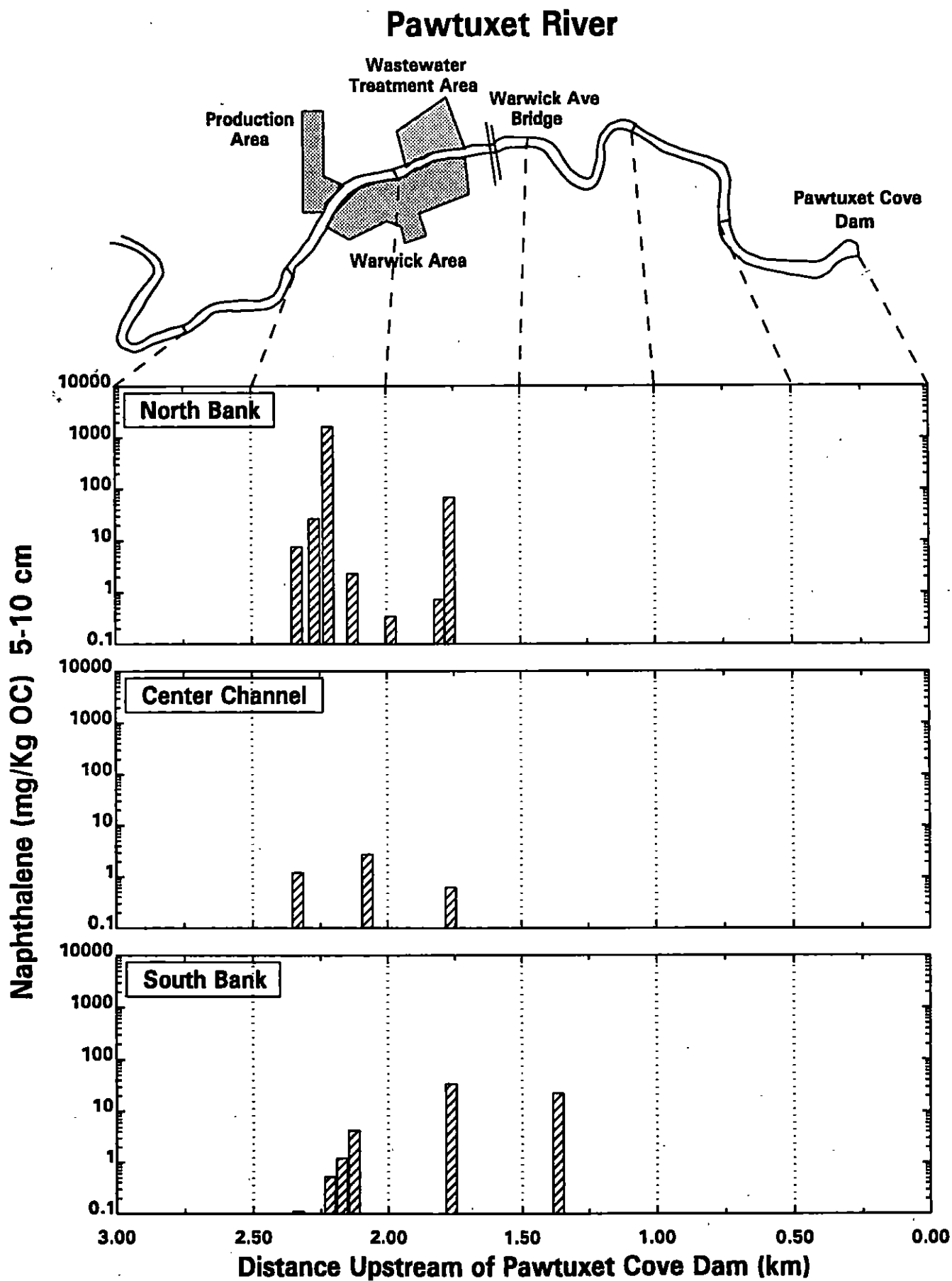
Pawtuxet River

FIGURE 3-17b. Sediment Sampling for Fate Modeling - Carbon Normalized Naphthalene Data - 5-10 cm Layer
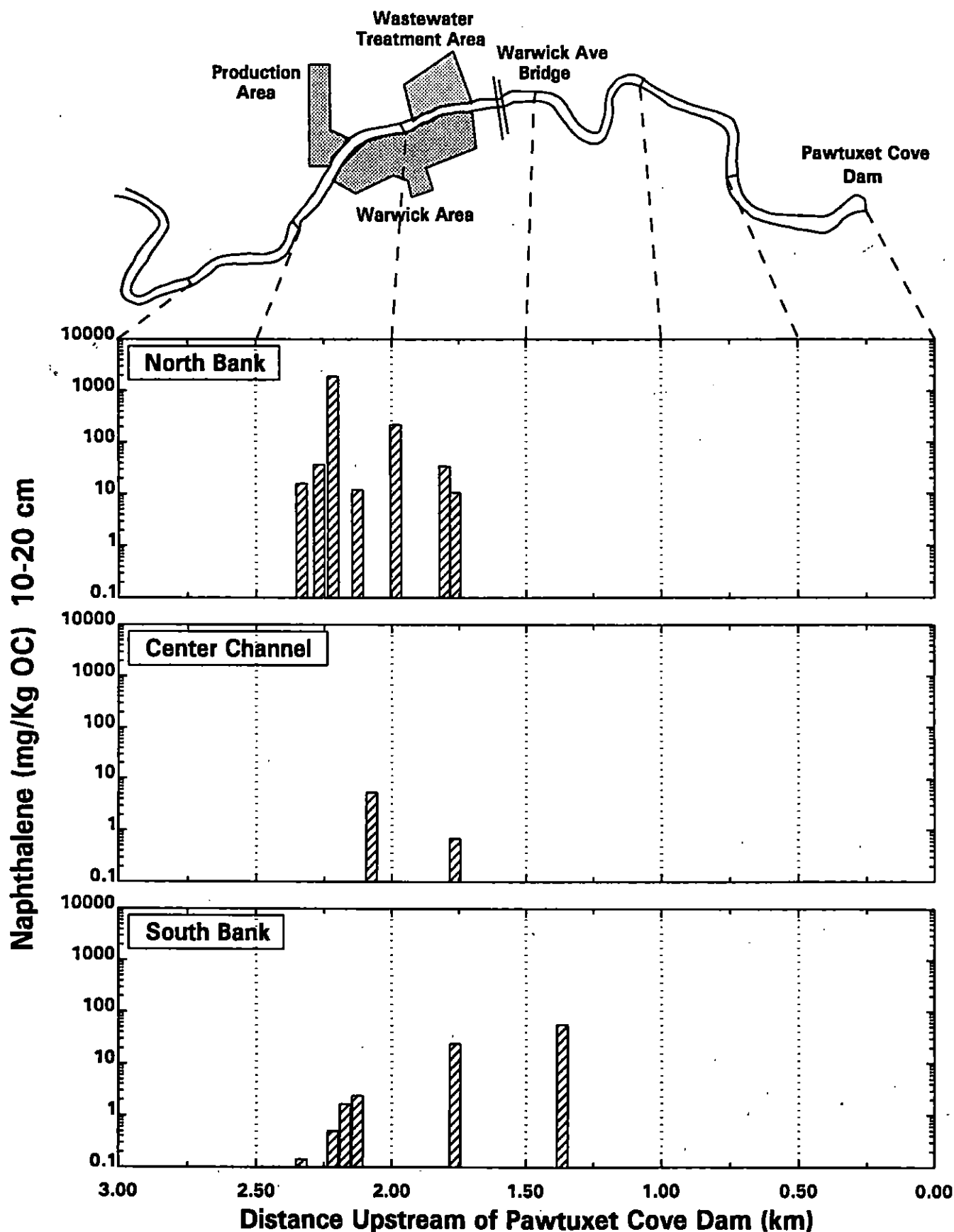
FIGURE 3-17c.   Sediment Sampling for Fate Modeling - Carbon Normalized Naphthalene Data - 10-20 cm Layer
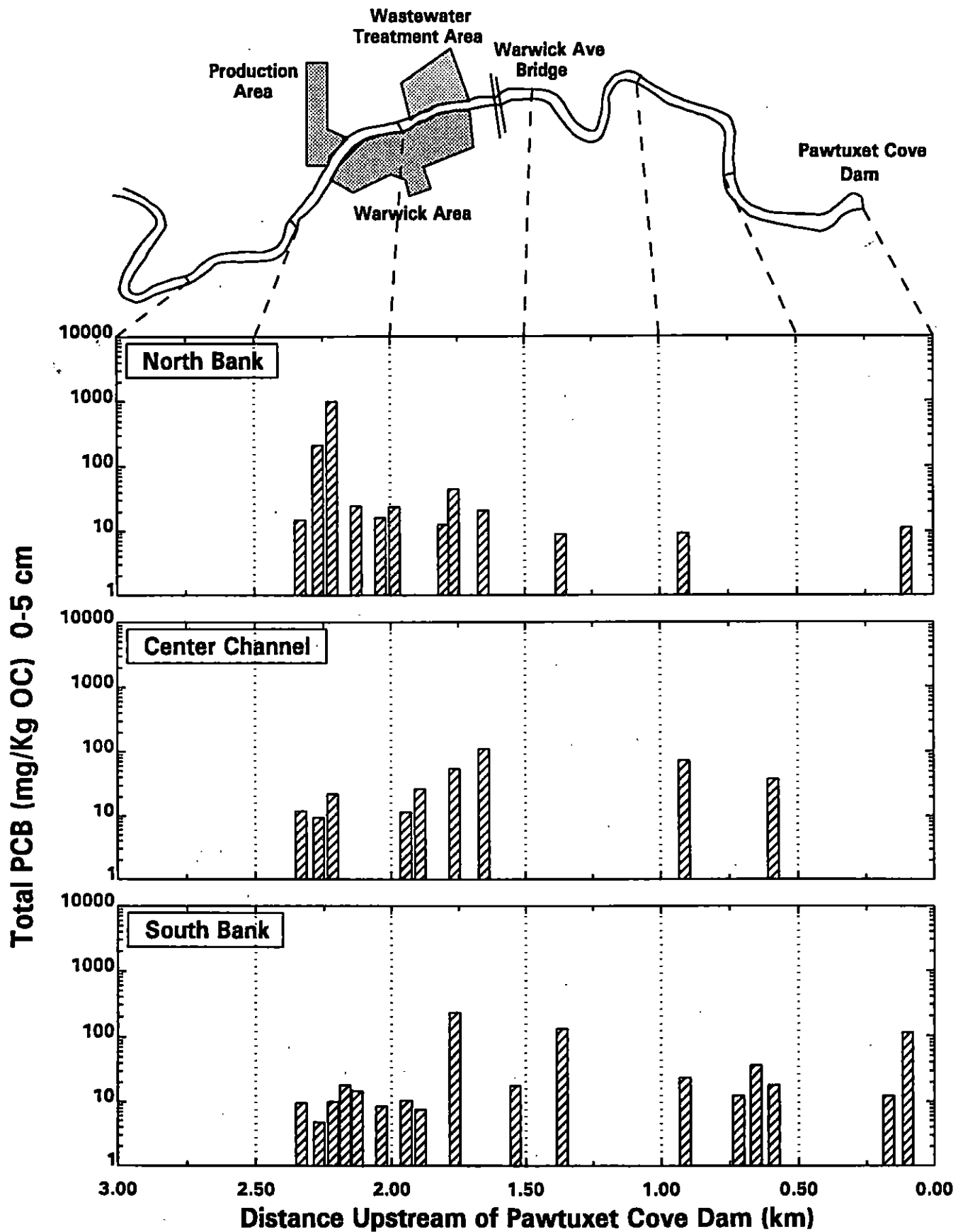
Pawtuxet River

FIGURE 3-18a.   Sediment Sampling for Fate Modeling - Carbon Normalized Total
PCB Data - 0-5 cm Layer

Pawtuxet River
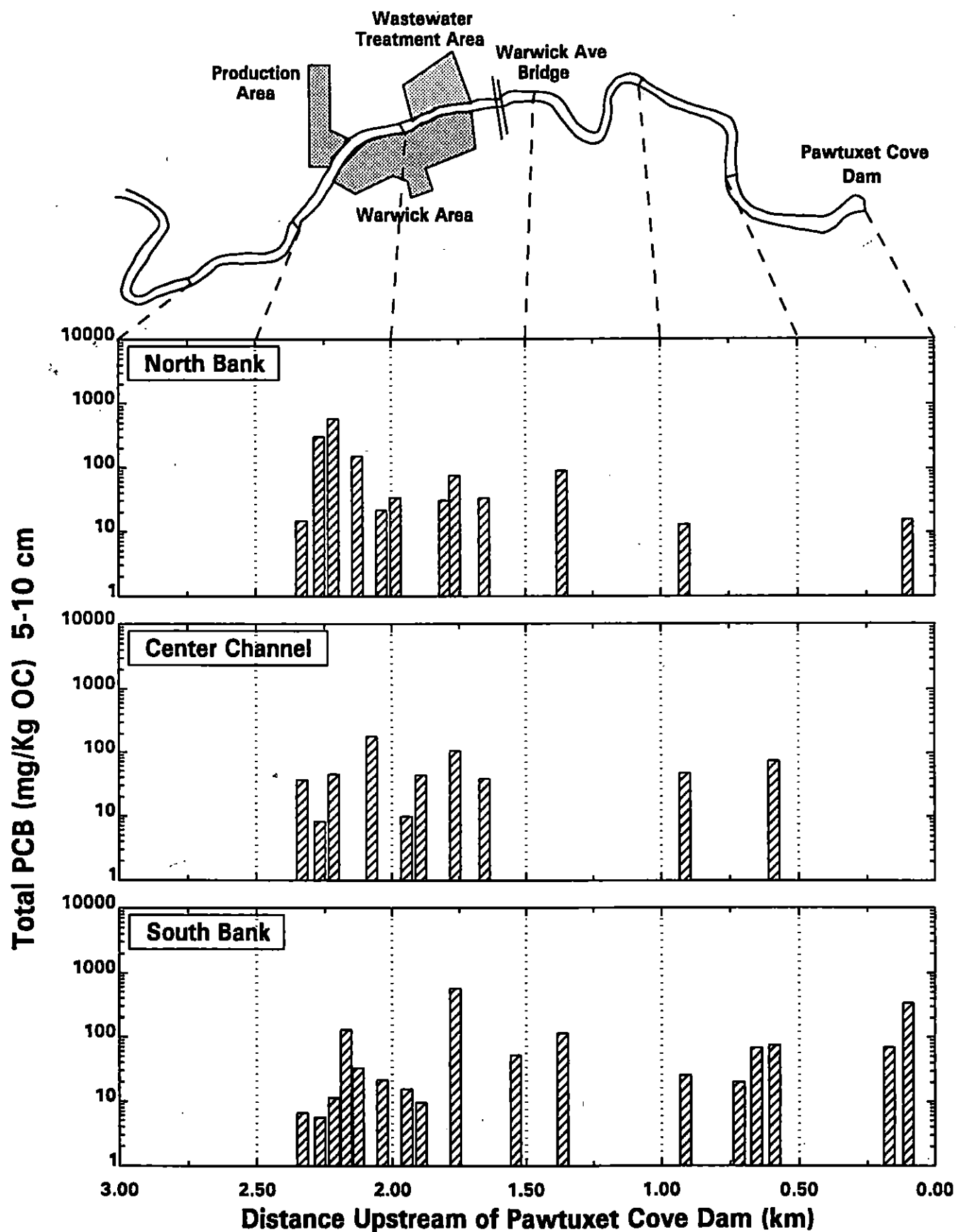
FIGURE 3-18b.   Sediment Sampling for Fate Modeling - Carbon Normalized Total
PCB Data - 5-10 cm Layer
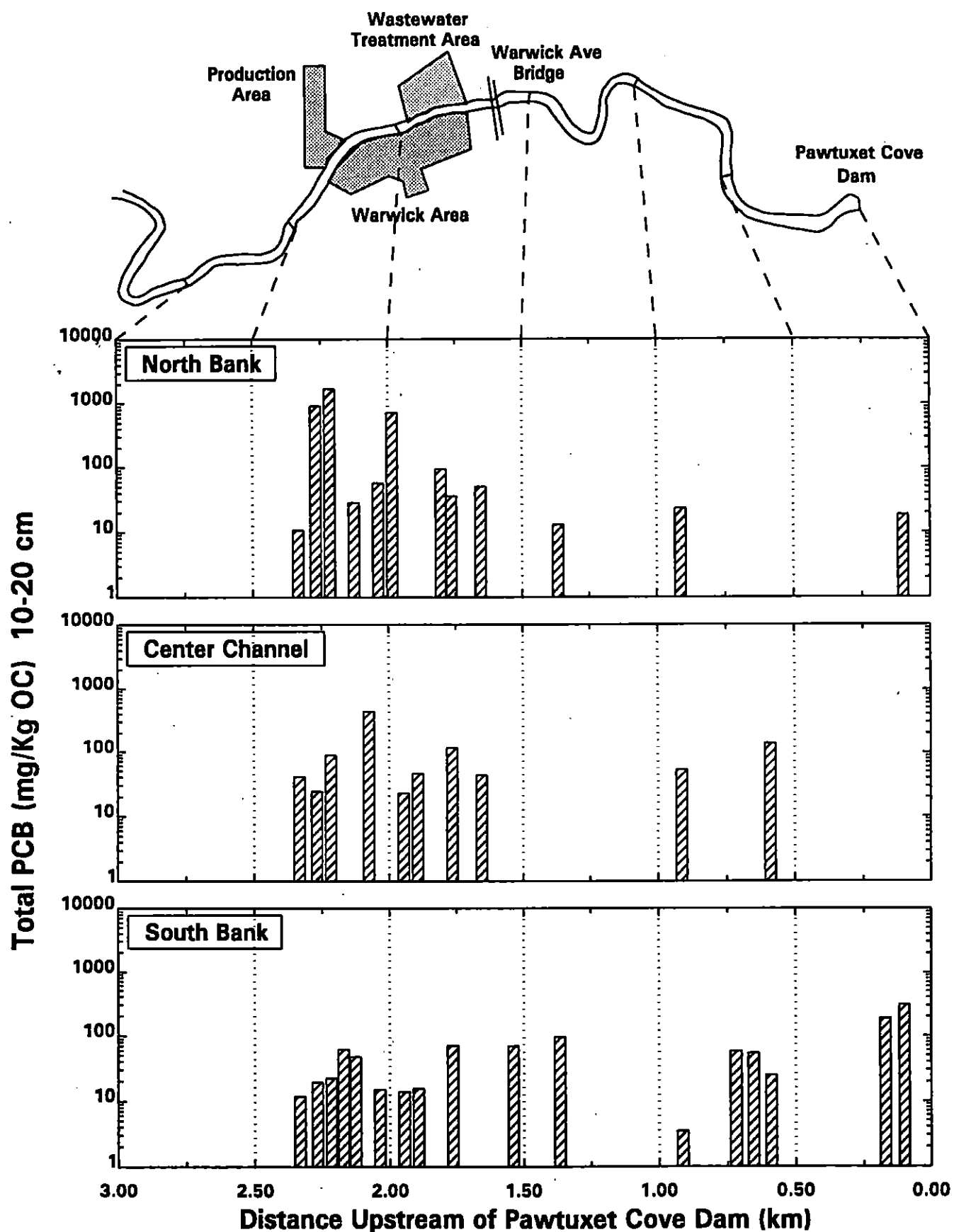
FIGURE 3-18c. Sediment Sampling for Fate Modeling - Carbon Normalized Total PCB Data - 10-20 cm Layer
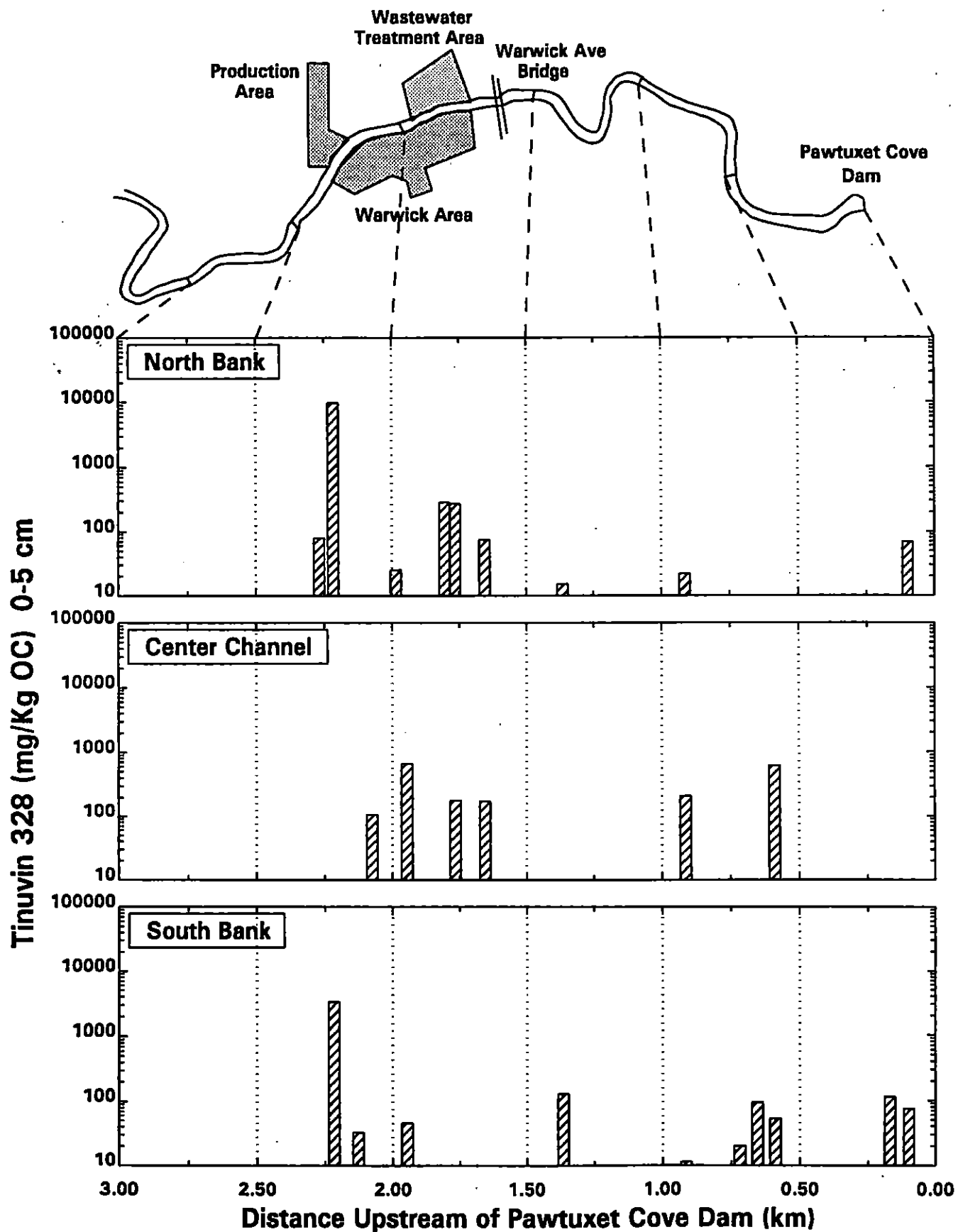
Pawtuxet River

FIGURE 3-19a.   Sediment Sampling for Fate Modeling - Carbon Normalized
Tinuvin 328 Data - 0-5 cm Layer
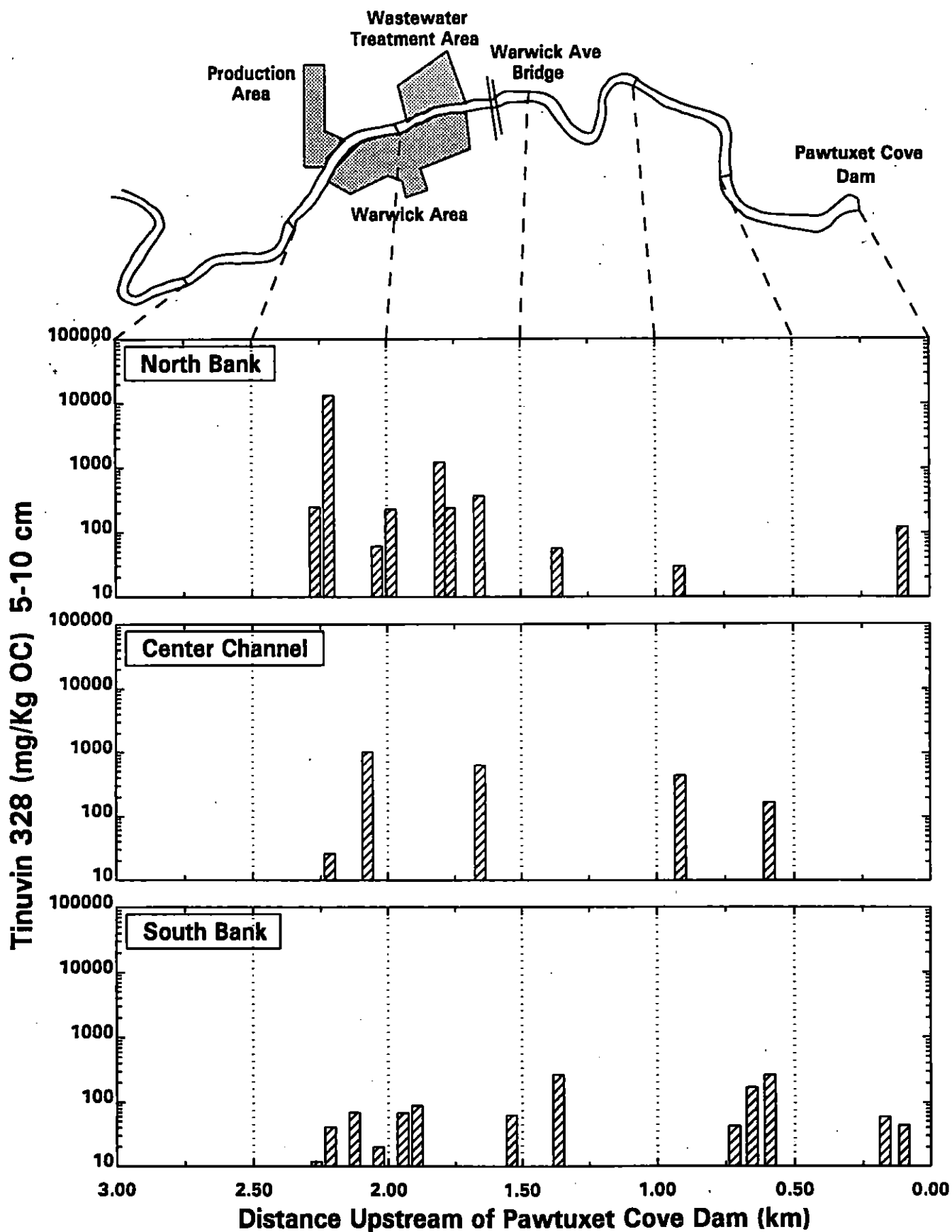
FIGURE 3-19b. Sediment Sampling for Fate Modeling - Carbon Normalized Tinuvin 328 Data - 5-10 cm Layer

Pawtuxet River
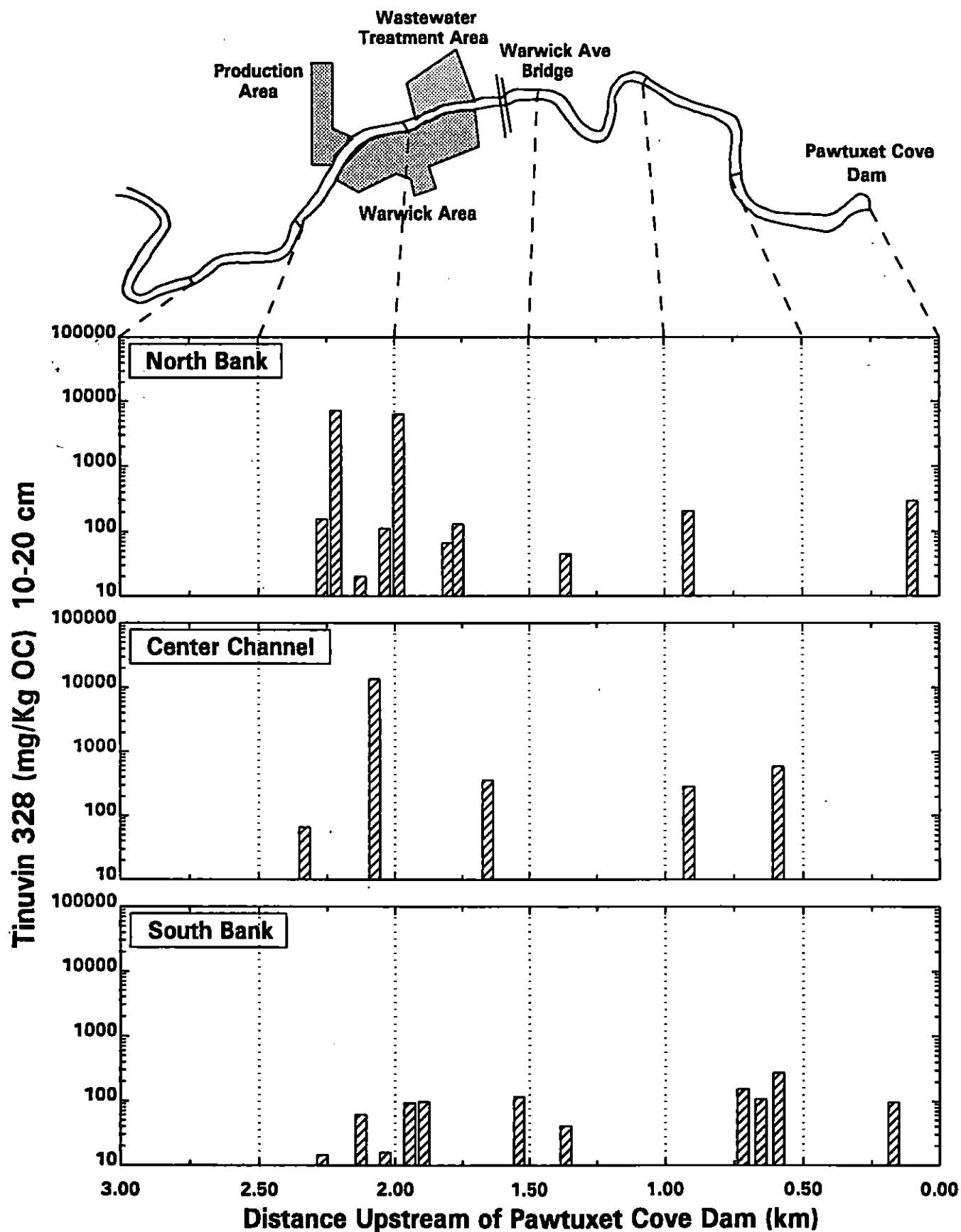
FIGURE 3-19c.   Sediment Sampling for Fate Modeling - Carbon Normalized
Tinuvin 328 Data - 10-20 cm Layer
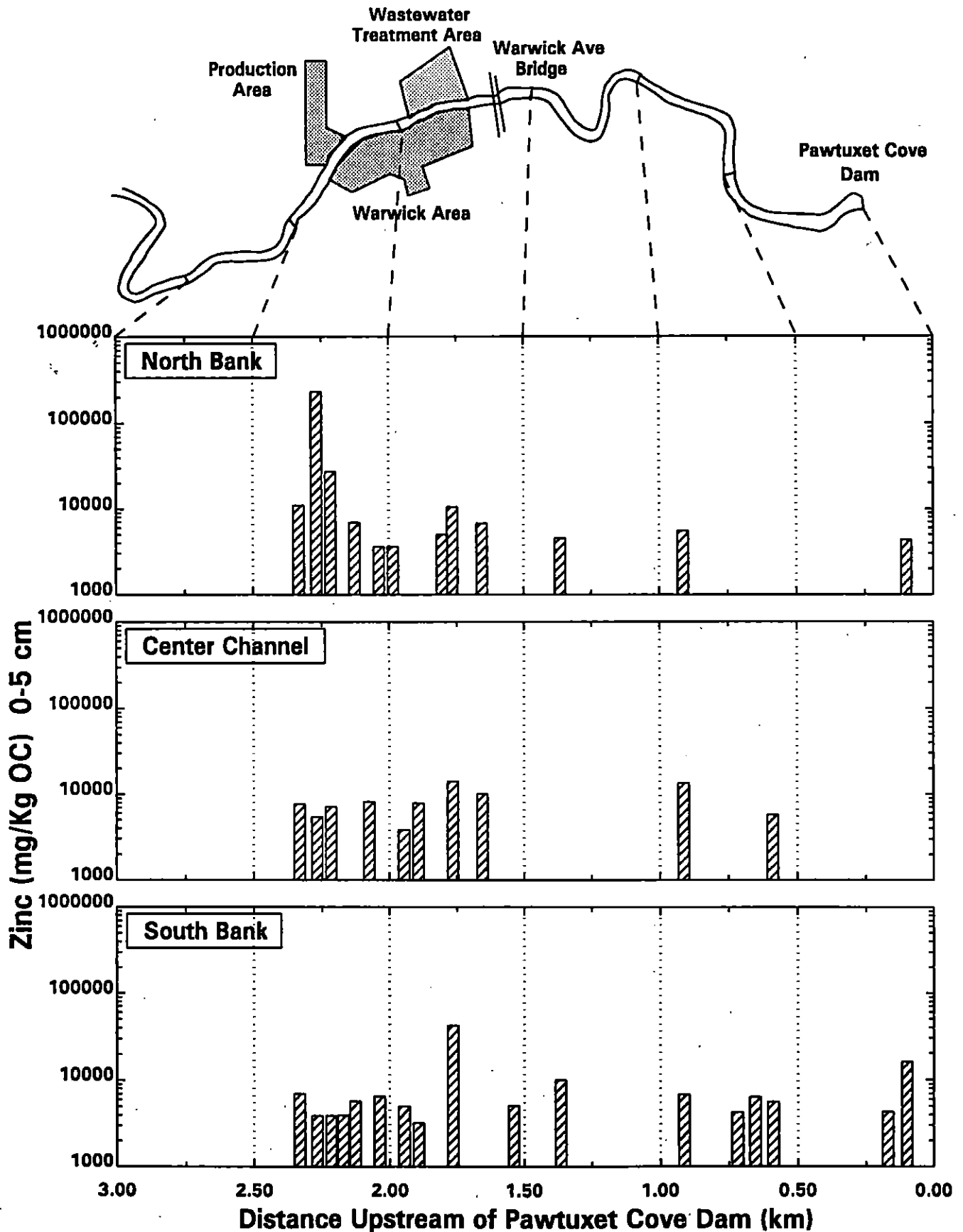
Pawtuxet River

FIGURE 3-20a.   Sediment Sampling for Fate Modeling - Carbon Normalized Zinc
Data - 0-5 cm Layer

Pawtuxet River
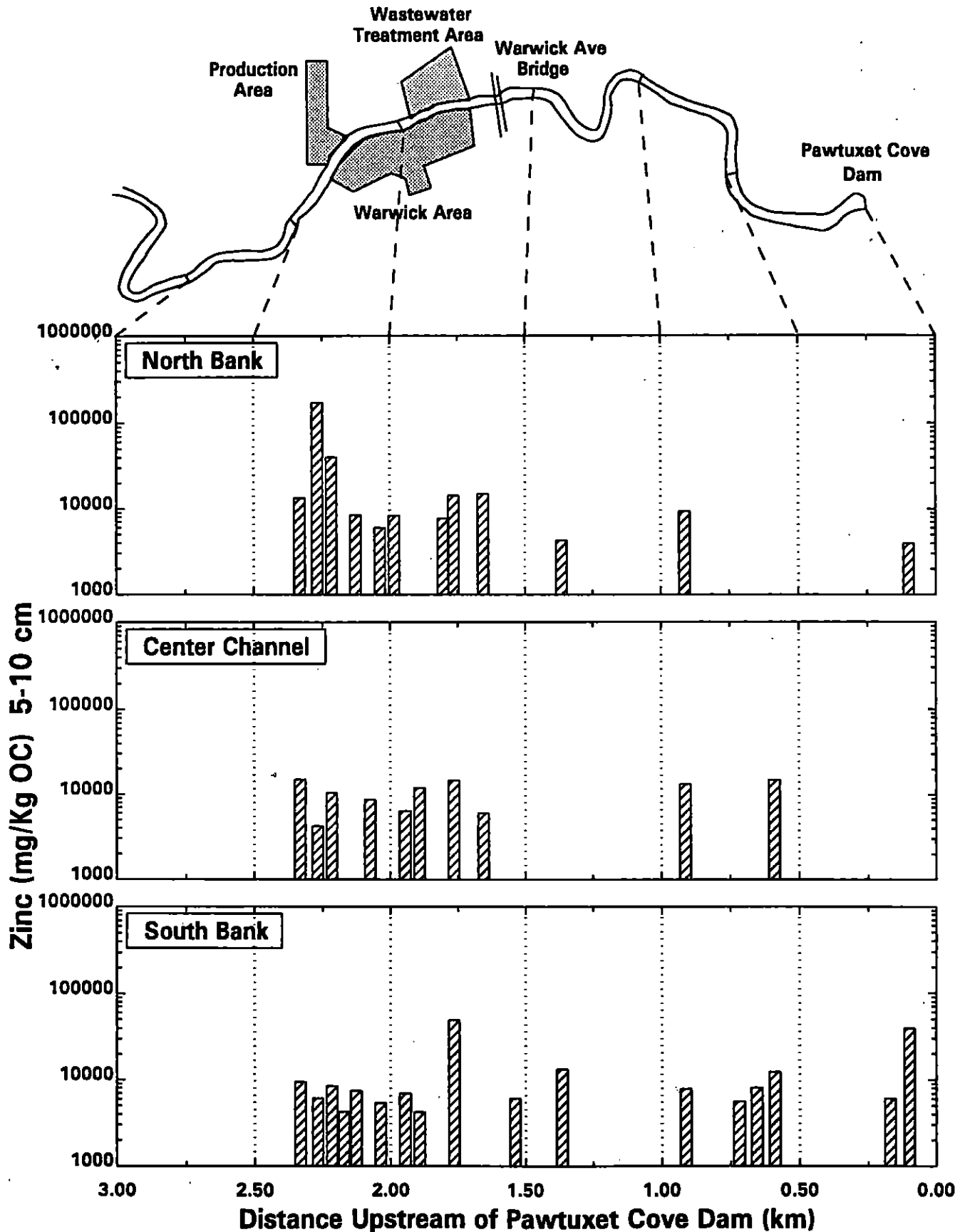
FIGURE 3-20b.   Sediment Sampling for Fate Modeling - Carbon Normalized Zinc
Data - 5-10 cm Layer

Pawtuxet River
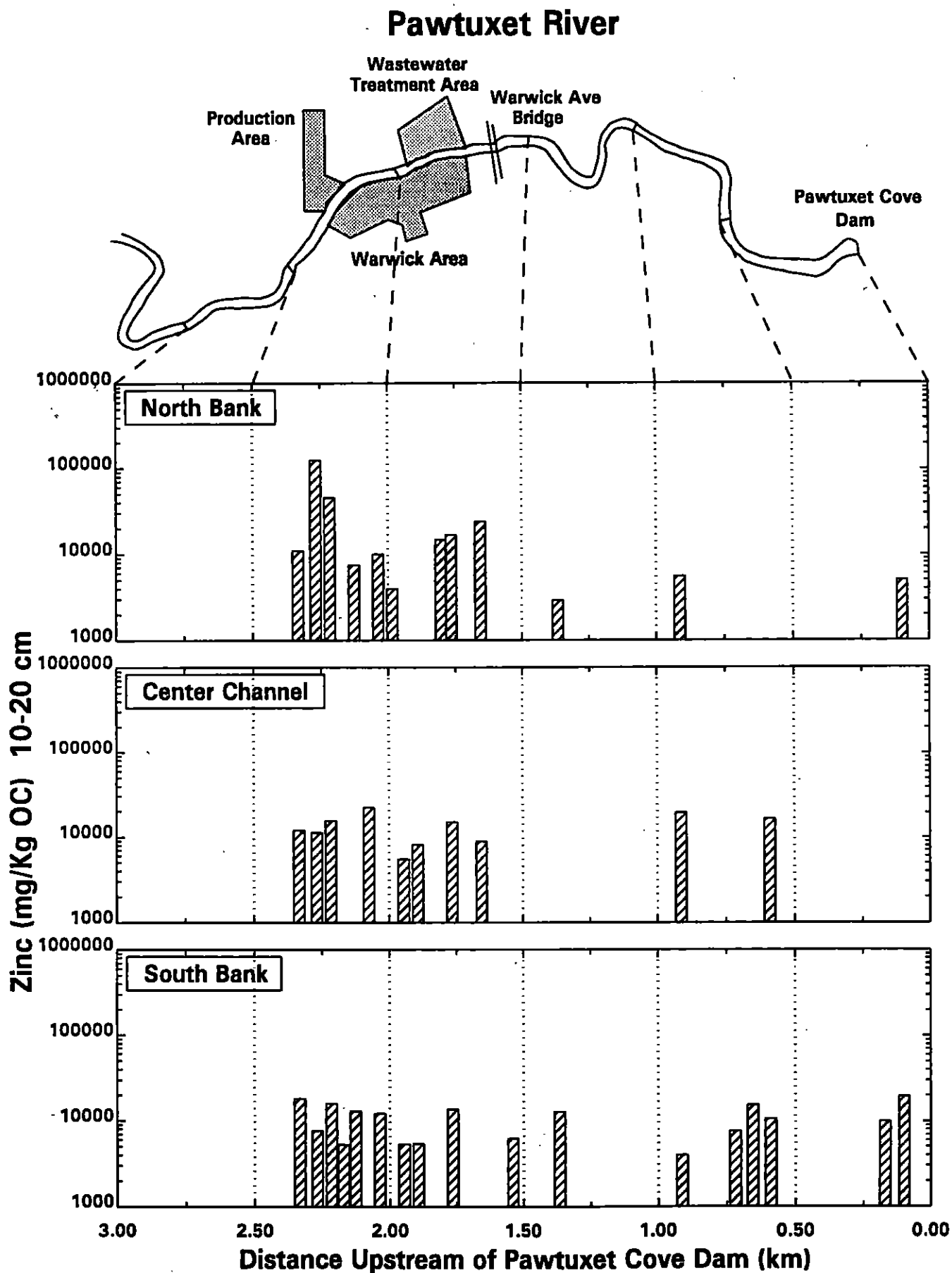
FIGURE 3-20c.   Sediment Sampling Fate Modeling - Carbon Normalized Zinc
Data - 10-20 cm Layer

SECTION 4

HYDRODYNAMIC MODEL DEVELOPMENT AND CALIBRATION

4.1 GOVERNING EQUATIONS

Due to the shallow depth, typically less than 2.5 m, and unstratified flow of the Pawtuxet River, the water column can generally be assumed to be vertically mixed, i.e., the horizontal current velocities and suspended sediment concentrations are approximately uniform in the vertical direction. The laterally heterogeneous sediment bed, with coarse, non-cohesive sediments in the central channel and fine-grained sediments in the near shore areas, makes it necessary to resolve the lateral variation in bottom shear stress. The processes controlling erosion and deposition of cohesive and non-cohesive sediments are significantly different and the local bottom shear stress greatly affects these processes.

Valid approximations to the general three-dimensional equations of motion, after consideration of the above conditions in the Pawtuxet River, are the two-dimensional, vertically-integrated equations. The hydrodynamic equations, conservation of mass and momentum, can be expressed as (Ziegler and Lick, 1986; Gailani et al., 1991)

$$\frac{\partial \eta}{\partial t} + \frac{\partial (uh)}{\partial x} + \frac{\partial (vh)}{\partial y} = 0 \tag{4-1}$$

$$\frac{\partial (uh)}{\partial t} + \frac{\partial (u^2 h)}{\partial x} + \frac{\partial (uvh)}{\partial y} = -gh\frac{\partial \eta}{\partial x} - c_f qu + \frac{\partial}{\partial x}(hA_H \frac{\partial u}{\partial x}) + \frac{\partial}{\partial y}(hA_H \frac{\partial u}{\partial y}) \tag{4-2}$$

$$\frac{\partial (vh)}{\partial t} + \frac{\partial (uvh)}{\partial x} + \frac{\partial (v^2 h)}{\partial y} = -gh\frac{\partial \eta}{\partial y} - c_f qv + \frac{\partial}{\partial x}(hA_H \frac{\partial v}{\partial x}) + \frac{\partial}{\partial y}(hA_H \frac{\partial v}{\partial y}) \tag{4-3}$$

where the total water depth is $h = h_o + \eta$, h_o is the equilibrium water depth, η is the surface displacement from that equilibrium, u and v are velocities in the x- and y-directions respectively, $q = (u^2 + v^2)^{1/2}$, c_f is the spatially-variable bottom friction factor, A_H is the horizontal eddy viscosity, and g is the acceleration due to gravity. The above equations

have been transformed from Cartesian coordinates to orthogonal, curvilinear coordinates in order to more accurately resolve the complex geometry and bathymetry of the Pawtuxet River. The resulting equations were then solved numerically using the semi-implicit version of a well-established hydrodynamic model, ECOM (Blumberg, 1994).

4.2 MODEL DEVELOPMENT

The numerical grid used to discretize the Pawtuxet River was composed of 81 elements; three lateral elements and twenty-seven longitudinal elements were used (Figure 4-1). The grid extends from Cranston to Pawtuxet Cove Dam, a total distance of about 7 km. The model does not allow cross-sectional width variation with increasing stage height. The flow is confined within the bounds of the two-dimensional numerical grid; the shoreline is considered a solid vertical wall.

Bathymetric data for the Pawtuxet River were collected between Cranston and Pawtuxet Cove dam during February 1992. The bathymetric survey was conducted over a four-day period during which the river flow rate was low and approximately steady, ranging from 270 to 290 cfs. About 4600 depth measurements were made using an acoustic depth finder. In shallow areas of the river, where the acoustic depth finder could not be used, river depths were measured along cross-sectional transects using a staff gauge. Location of the river shoreline was also determined during the bathymetric survey. This high resolution data was used to develop an accurate map of the river geometry, which was used as input for the numerical model.

A U.S. Geological Survey (USGS) gaging station has been in operation at Cranston since 1940 (Figure 4-2). The stage height data from this station provides necessary boundary condition information for the upstream inlet of the model. Data for the downstream outlet, at Pawtuxet Cove Dam, were obtained from a pressure transducer installed from March 6, 1992 to June 8, 1992. Rating curves, relating flow rate to stage height, for both locations were generated from the available data.

Cranston flow rate data were analyzed to determine various flow regimes. The average flow rate in the river is 340 cfs and the annual flood is approximately 1200 cfs. In addition, a flood frequency analysis for the lower Pawtuxet River was carried out to estimate the magnitude of various extreme events. An analysis of 51 years of flow data collected at Cranston, from 1940 through 1990, was conducted using a standard USGS method for determining flood flow frequencies (USGS, 1981). This method uses a Log-Pearson Type III distribution to estimate flood flow frequencies. The results of this analysis are tabulated in Table 4-1. The 100-year flood is seen to be over an order of magnitude greater than the mean flow rate and approximately four times larger than the annual flood.

TABLE 4-1. RESULTS OF EXTREME FLOW EVENT ANALYSIS	
Return Period (years)	Flow Rate (cfs)
5	2500
10	2900
20	3400
50	3900
100	4300

4.3 CALIBRATION DESCRIPTION AND RESULTS

The hydrodynamic model was calibrated during a 33-day period that extended from March 3 through April 4, 1992. Two high flow events occurred during this period. Each flood had a peak flow rate that was approximately equal to the annual flood (1200 cfs).

The two variables adjusted during the hydrodynamic calibration were the bottom friction factor, c_f, and the horizontal eddy viscosity, A_H. The friction factor was assumed to be spatially variable according to the local sediment bed type. This variation is necessary to account for the difference in bottom roughness between fine, cohesive sediments and coarse, non-cohesive sediments. The bottom friction factor was set at

0.0025 in areas of fine sediments and increased to 0.0040 for coarse sediment regions. The eddy viscosity had a value of 800 cm^2/s.

Time-variable boundary conditions were prescribed at three locations for the hydrodynamic model, see Figure 4-2. The stage height at Pawtuxet Cove Dam was determined from collected pressure transducer data. USGS gage data collected at Cranston were used to specify the upstream inlet flow rate. The drainage area below Cranston represents 15 percent of the total Pawtuxet River drainage basin with the Pocasset River being the only significant tributary between Cranston and Pawtuxet Cove Dam. So, all watershed runoff below Cranston is assigned to the Pocasset River and the tributary flow rate is determined by using drainage area proration.

Accuracy of the hydrodynamic model was determined by comparing the measured and predicted stage heights at Cranston. The results of the 33-day calibration period are shown on Figure 4-3. Very good agreement between observation and prediction is seen during this period, except the first day of the simulation period, which reflects transients due to model spin-up. The mean value of the absolute relative error, i.e., | predicted - measured | /measured, for the hydrodynamic calibration period was 3.5 percent. The hydrodynamic model tends to slightly over predict stage height, which may be due to the inability of the model to account for cross-sectional width variation with stage height increases.

Figures
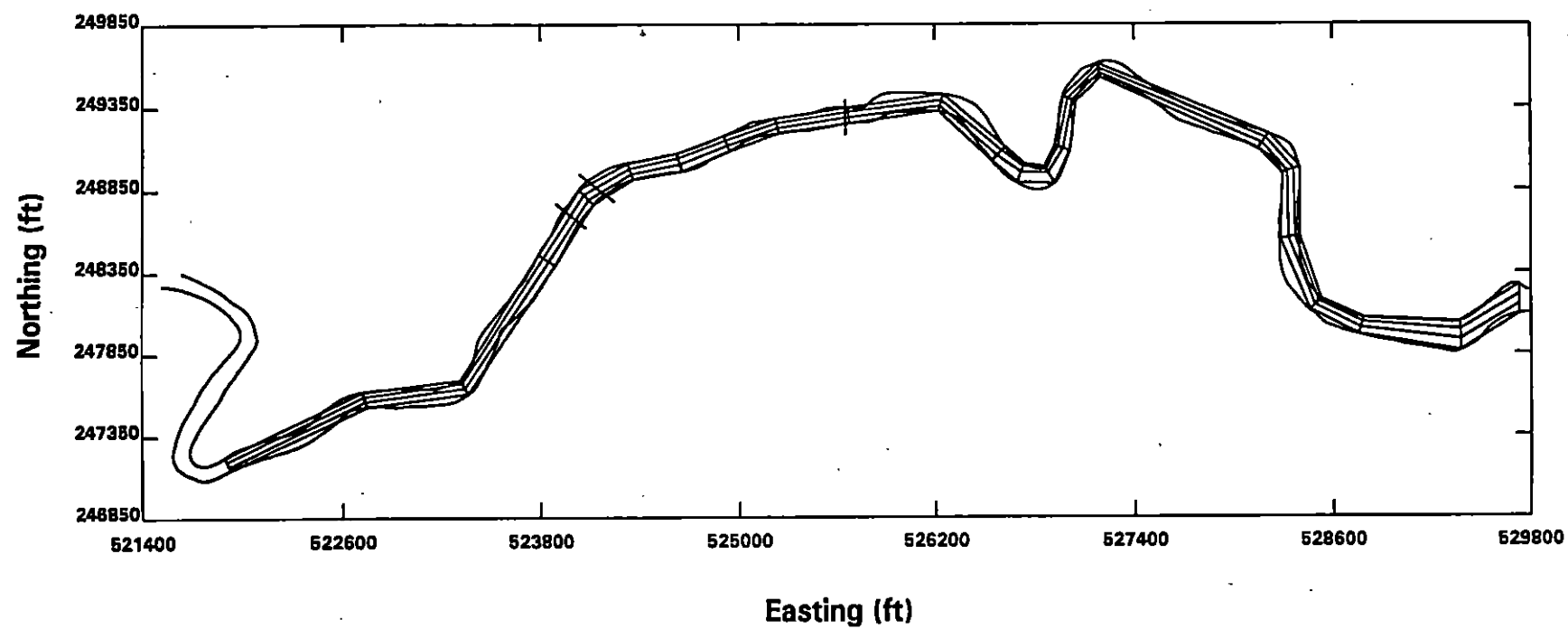
Fig 4-1 Numerical grid for the lower Pawtuxet River
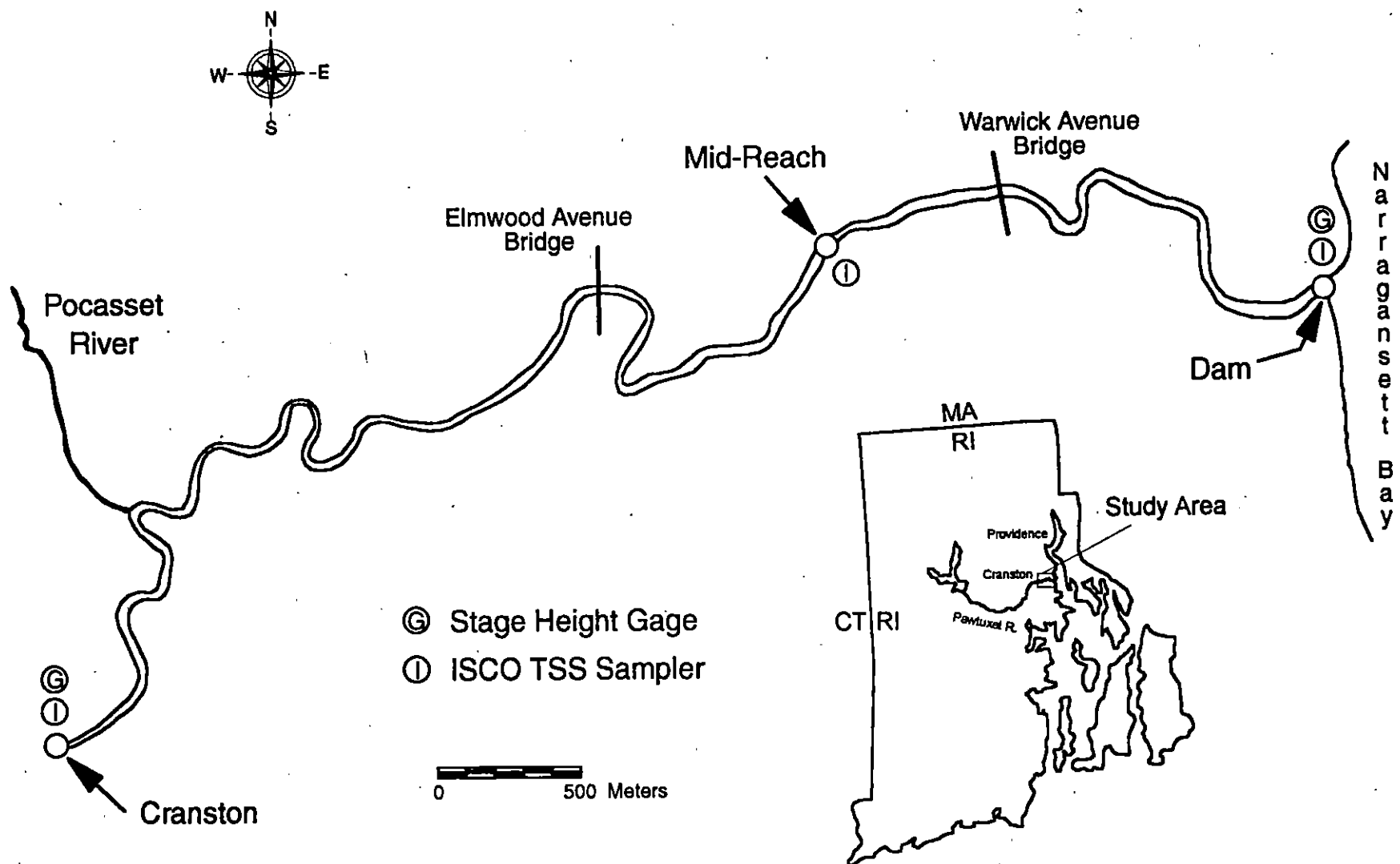
Figure 4-2. Locations of stage height gages and TSS samplers on the Pawtuxet River.
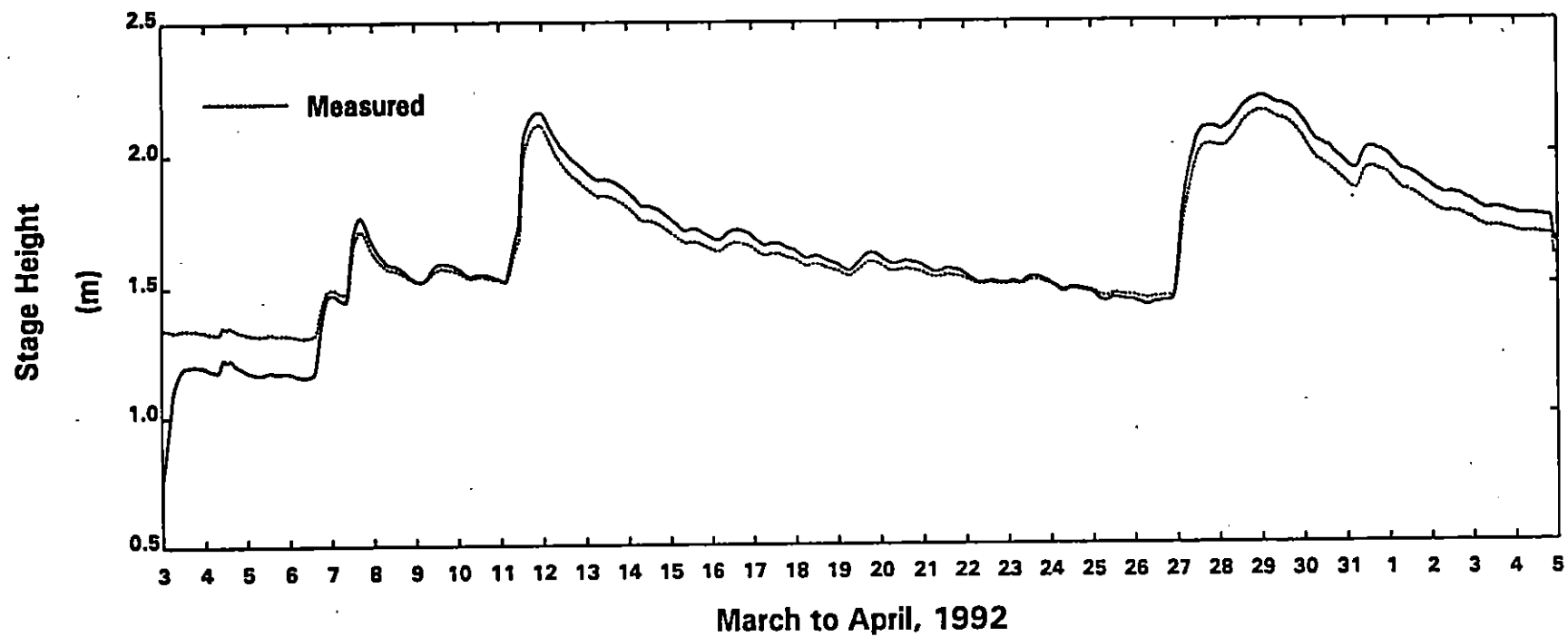
Figure 4-3 Comparison between predicted and observed stage height
at Cranston during 33-day calibration period in 1992

SECTION 5

SEDIMENT TRANSPORT MODEL DEVELOPMENT AND CALIBRATION

5.1 GOVERNING EQUATIONS

5.1.1 Transport

Suspended sediment particles in a river have a large range of sizes, from less than 1 μm clay to fine sand on the order of 250 μm. To simulate the effects of particle size variation realistically, two sediment size classes are modeled in the present study. Class 1 represents cohesive sediments, i.e., clays and silts, with particle diameters of less than 62 μm, while class 2 is composed of coarser, non-cohesive sediments, primarily fine sands with diameters between 62 and 250 μm. Bed load transport was not considered.

A previously developed numerical model for determining the transport and fate of fine-grained sediments, SEDZL, (Ziegler and Lick, 1986; Gailani et al., 1991) was applied to the Pawtuxet River. Modifications to SEDZL were made to provide improved capabilities for predicting the resuspension of non-cohesive sediments. The sediment transport model is coupled to the hydrodynamic model so that lateral variations in sediment bed composition and bottom shear stress can be accounted for properly. The two-dimensional, vertically-integrated sediment transport equation for size-class k (k = 1,2) is (Ziegler and Lick, 1986; Gailani et al., 1991)

$$\frac{\partial(hC_k)}{\partial t} + \frac{\partial(uhC_k)}{\partial x} + \frac{\partial(vhC_k)}{\partial y} = \frac{\partial}{\partial x}(hK_H\frac{\partial C_k}{\partial x}) + \frac{\partial}{\partial y}(hK_H\frac{\partial C_k}{\partial y}) + E_k - D_k \qquad (5\text{-}1)$$

where C_k is the concentration of suspended solids of size-class k, K_H is the horizontal eddy diffusivity, E_k is the resuspension (erosion) flux of class k and D_k is the deposition flux of class k. Results from the hydrodynamic model provide information about the transport

field in Equation (5-1), i.e., u, v and h. Similar to the hydrodynamic equations, Equation (5-1) has been transformed into an orthogonal, curvilinear coordinate system and then solved numerically.

5.1.2 Cohesive Sediment Dynamics

The depositional processes of the two sediment classes are significantly different. Class 1 particles can disaggregate and aggregate into flocs of various sizes and densities. Flocculation processes are dynamic and complex, however, as a first approximation, the median floc diameter can be determined from the following experimentally-based equation (Lick and Lick, 1988; Gailani et al., 1991):

$$d_m = (\frac{\alpha_o}{C_1 G})^{1/2} \qquad (5\text{-}2)$$

where d_m is the median floc diameter (cm), G is the fluid shear stress (dyne/cm^2), C_1 is the concentration of class 1 sediment (g/cm^3) and α_o is an experimentally determined constant. For fine-grained, cohesive sediments in freshwater, $\alpha_o = 10^{-8}$ gm^2/cm^3-s^2.

From laboratory experiments on flocculated, cohesive sediments in freshwater (Burban et al., 1990), a valid first approximation of the settling speed for class 1 sediments, $W_{s,1}$ (cm/s), is

$$W_{s,1} = a \, d_m^b \qquad (5\text{-}3)$$

where:

$$a = B_1(C_1 G)^{-0.85} \qquad (5\text{-}4)$$

$$b = - [0.8 + 0.5\log(C_1 G - B_2)] \qquad (5\text{-}5)$$

and $B_1 = 9.6 \times 10^{-4}$, $B_2 = 7.5 \times 10^{-6}$, and both are experimentally determined constants (Gailani, et al., 1991). The effect of concentration on $W_{s,1}$ is evident on Figure 5-1, where Equation (5-3) is plotted against experimental data. Class 1 settling speeds range from 60 to 160 μm/s and are always less than that for a solid particle of an equal diameter, generally by several orders of magnitude.

The deposition rate, D_1, for class 1 is expressed as

$$D_1 = P_1 \, W_{s,1} \, C_1 \tag{5-6}$$

where P_1 is the probability of deposition or bed incorporation. Due to complex interactions generated by turbulence at the sediment-water interface, only a certain fraction of class 1 sediments that settle onto the sediment bed will become incorporated into the bed. The concept of a probability of deposition has been used in both the STUDH (Ariathuri and Krone, 1976) and the CSTM-H (Hayter and Mehta, 1986) models. The approach proposed by Ariathuri and Krone (1976) has been adapted here. The probability of deposition of class 1 sediments is given by

$$P_1 = \begin{cases} 1 - \dfrac{\tau}{\tau_d} & , \quad \tau \leq \tau_d \\[2mm] 0 & , \quad \tau > \tau_d \end{cases} \tag{5-7}$$

where τ is the bottom shear stress and τ_d is the critical shear stress for deposition of class 1 sediment. Other investigators have estimated the critical shear stress for deposition to range between 0.6 and 11 dynes/cm^2, depending upon sediment type and concentration (Krone, 1962; Mehta and Partheniades, 1975). The critical shear stress for deposition was adjusted during model calibration.

Class 2 sediment is non-cohesive and these particles have a higher settling speed than class 1 particles. The deposition rate for class 2, D_2, is expressed as

$$D_2 = W_{s,2}C_2 \qquad\qquad (5\text{-}8)$$

where $W_{s,2}$ is the settling speed of class 2. The class 2 settling speed, $W_{s,2}$, was used as a calibration parameter in this study and its value is discussed below.

Only a finite amount of material can be resuspended from a fine-grained, cohesive sediment bed exposed to a constant bottom shear stress. This phenomenon, called bed armoring, has been observed and quantified in laboratory (Parchure and Mehta, 1985; Tsai and Lick, 1987; Graham et al., 1992) and field studies (Hawley, 1991; Amos et al., 1992). The amount of fine-grained sediment resuspended from cohesive deposits is given by (Gailani et al., 1991)

$$\epsilon = \frac{a_0}{T_d^m}\left(\frac{\tau - \tau_0}{\tau_0}\right)^n \ , \quad \tau \geq \tau_0 \qquad\qquad (5\text{-}9)$$

where ϵ is the net mass of resuspended sediment per unit surface area (mg/cm^2), a_0 is a system-specific constant, T_d is the time after deposition in days, m and n are dependent upon the deposition environment, and τ_0 is an effective critical stress. Results of previous laboratory and field studies show that appropriate values for the various parameters in Equation (5-9) are: $m = 0.5$, $T_{d,max} = 7$ days, and $\tau_0 = 1$ dyne/cm^2. The values of a_0 and n were determined from field data, see Section 5.3.

Equation (5-9) determines the net resuspension, however, it is the resuspension rate, E, that is needed in the transport equation, Equation (5-1). Experimental results show that the total amount of sediment is not resuspended instantaneously but it is eroded over a one-hour period (Tsai and Lick, 1987; MacIntyre et al., 1990). Thus, the resuspension rate was assumed to be constant and equal to $\epsilon/3600$ sec until all available sediment was eroded. Once the amount ϵ had been resuspended, E was set to zero until further sediment was deposited and available for resuspension or until the shear stress increased (Gailani et al., 1991). The resuspension rate of class k, which is needed in Equation (5-1),

is then given by $E_k = f_k E$, where f_k is the fraction of class k sediment in the surficial layer of the cohesive bed.

A three-dimensional model of the cohesive sediment bed realistically simulates the effects of bed consolidation with depth and horizontal variations in bed composition. Vertical variations of sediment bed consolidation are accounted for by discretizing the bed into seven layers. The time after deposition of the layers increases linearly from one day at the surface, which is composed of freshly deposited sediment, to seven days in the bottom layer. Once deposited sediments have reached the seven-day-old layer, their age no longer increases; all deposited sediments with ages greater than or equal to seven days are treated as seven days old. Previous laboratory flume experiments (Tsai and Lick, 1987; MacIntyre et al., 1990) suggest that consolidation effects are minimal after seven days of consolidation, and are the basis for setting the maximum age of deposited sediments at seven days. The critical shear stress, τ_o, is constant in all layers. The cohesive sediment bed is composed of horizontally varying fractions of class 1 and 2 sediments. Initial values of these fractions were determined from the field study data. The model properly accounts for changes in f_1 and f_2 due to resuspension and deposition during a simulation.

5.1.3 Non-Cohesive Suspended Load

The resuspension of sediment from the non-cohesive portion of the sediment bed in the Pawtuxet River is calculated using a procedure developed by van Rijn (1984). The van Rijn method has been shown to yield good results for predicting suspended load of fine sands (van Rijn, 1984; Garcia and Parker, 1991; van Rijn et al., 1993). Only a brief overview of the van Rijn method will be presented here, for details of the calculation procedure see van Rijn (1984). The first step in the procedure is to compare the bed-shear velocity with the critical bed-shear velocity, based on the local d_{50}, according to Shields. Suspended transport will only occur if the bed-shear velocity exceeds both the Shields criterion for bed load movement and the critical bed-shear velocity for initiation of suspension, u_{crs}^* . If resuspension does occur, the local d_{50} and bed-shear velocity, u^*,

are used to determine the reference concentration at a height of $z = z_0$ above the sediment bed, $C(z_0)$. Finally, the local values of u^*, d_{50} and $C(z_0)$ are used to calculate the suspended load transport rate.

The critical bed-shear velocity for initiation of suspension is set at

$$u_{crs}^* = W_{s,2} \qquad\qquad (5\text{-}10)$$

where $W_{s,2}$ is the settling speed of class 2 sediments. Equation (5-10) is based on the work of Bagnold (1966). As stated during the discussion of deposition processes, $W_{s,2}$ was used as a calibration parameter in this study. Therefore, adjusting $W_{s,2}$ simultaneously varies both the settling speed of non-cohesive sediments and the critical shear velocity for resuspension. The portion of the non-cohesive bed subject to resuspension is assumed to be composed of class 2 sediment only, which is consistent with field data that show low fractions of clays and silts in the non-cohesive areas of the sediment bed. A given value of $W_{s,2}$ also represents a specific particle diameter, d_2, for class 2 sediment. The value of $W_{s,2}$ used to calibrate the model must yield a d_2 that is consistent with particle size data from the Pawtuxet River.

The sediment bed of the Pawtuxet River is heterogeneous with a wide range of particle sizes. Since the non-cohesive bed is graded, armoring effects must be modeled if realistic simulations of suspended transport are to be realized. The non-cohesive bed is assumed to be composed of an active layer, of thickness T_a, overlying the parent bed. Resuspension of class 2 sediment is assumed to occur only from the active layer such that

$$E_2 = f_{2,a} E_N \qquad\qquad (5\text{-}11)$$

where E_2 is the resuspension rate from the graded bed, $f_{2,a}$ is the fraction of class 2 sediment in the active layer, and E_N is the resuspension rate from an ungraded (non-armoring) bed as calculated using the van Rijn method. The fraction of class 2

sediment in the parent bed, $f_{2,p}$, is determined from field data. The active layer thickness is determined using a modified form of the equation proposed by van Niekerk et al. (1992)

$$T_a = \frac{d_{50} \, \tau}{5 \, \tau_{c50}}$$

(5-12)

where τ_{c50} is the critical shear stress necessary to initiate bed load motion for sediment with the local d_{50} and is calculated using the Shields criteria. Changes in the composition of the active layer are made following the method used by Karim and Holly (1986).

5.2 PREVIOUS APPLICATIONS OF SEDIMENT TRANSPORT MODEL

The sediment transport model (SEDZL) described in Section 5.1 has been applied to aquatic systems besides the Pawtuxet River. The model has been used as part of contaminated sediment studies on the following systems: Fox River in Wisconsin (Gailani, et al., 1991); Saginaw River in Michigan (Cardenas, et al., 1994); Buffalo River in New York (Gailani et al., 1994); and Watts Bar Reservoir in Tennessee (Ziegler and Nisbet, 1995). This model was also applied to the Pawtuxet River using a finer numerical grid than the one discussed in Section 5.1; the fine grid model had 360 segments, with 6 lateral and 60 longitudinal segments. This earlier version of the Pawtuxet River sediment transport model was calibrated over the same 33-day period in 1992 used to calibrate the hydrodynamic model (Ziegler and Nisbet, 1994). Computational constraints, due to the need to conduct multi-year simulations, made it necessary to use the 81-segment model considered here.

5.3 MODEL DEVELOPMENT

Two field studies were conducted during the spring of 1992 to collect data for sediment bed property characterization, e.g., grain size distribution, sediment type, porosity and resuspension potential. During the first study, 172 surficial sediment cores were collected between Cranston and Pawtuxet Cove Dam. Each core was analyzed for

grain size distribution and porosity. The primary goal of this study was to create a sediment bed map of the lower Pawtuxet River that delineated areas of cohesive and non-cohesive sediments. The following criteria were used for classifying a core as cohesive: 1) $d_{50} < 250$ μm, where d_{50} is the local median particle diameter; 2) silt/clay content > 15 percent; and 3) moisture content > 75 percent. Using these guidelines, 32 of the 172 sediment cores were classified as cohesive. The cores classified as cohesive were nearly always collected in the near shore regions, within 5 to 7 meters of shore. ·,The mean porosities of the cohesive and non-cohesive cores were 0.77 and 0.55, or bulk densities of 0.61 and 1.19 g/cm^3, respectively.

The sediment core data from the lower Pawtuxet River showed that the sediment bed is laterally heterogeneous and vertically graded. The deeper, central channel is typically composed of a mixture of coarse sand and gravel with varying fractions of fine sand, silt and clay. Fine-grained, cohesive sediment deposits are generally found in narrow strips along the shores, and occupy only 4 to 5 percent of the total sediment bed area. Sediment bed characteristics also vary longitudinally between Cranston and Pawtuxet Cove Dam. For convenience, that portion of the Pawtuxet River considered in this study was divided into two reaches; the upper reach was defined as the section of the river from Cranston to Mid-Reach while the lower reach denotes the length of river between Mid-Reach and Pawtuxet Cove Dam. The upper reach contains coarser sediments, average d_{50} of 11,200 μm, than the lower reach, average d_{50} of 5,400 μm. Localized d_{50} values range from 200 to 24,000 μm. Few areas of cohesive sediment were found in the upper reach; less than 1 percent of the upper reach sediment bed, on an areal basis, is composed of cohesive sediments. In contrast, approximately 11 percent of the lower reach bed is cohesive.

The second field study involved using a portable resuspension device (PRD) to determine the in situ resuspension potential of the cohesive sediment deposits (Tsai and Lick, 1986). Forty-eight surficial cores were collected in areas of cohesive sediment deposits during April 1992. The resuspension potential of each core was determined using

the PRD procedure described in Tsai and Lick (1986). Three effective shear stresses were applied to the cores: 5, 7 and 9 dynes/cm^2.

Examination of the resuspension potential data collected during the PRD study showed that cohesive sediments in the Pawtuxet River can be separated into two categories: muddy and sandy. This stratification of cohesive sediments was based on visual observation of PRD sediment cores and the measured resuspension potential of those cores. Cohesive sediments classified as muddy were found to have a higher resuspension potential than the sandy cohesive sediments. Analysis of the resuspension potential data produced values for a_0 and n of 2.03 and 1.18, respectively, for muddy cohesive sediments. The values of a_0 and n were 0.066 and 2.05 for sandy cohesive sediments, respectively. The values of a_0 were determined by assuming that the in situ age of the sediment bed was seven days. Comparisons between measured and predicted resuspension potentials, using Equation (5-9) and appropriate values of a_0 and n, for muddy and sandy cohesive sediments are shown on Figure 5-2.

Suspended solids data during flood events are necessary for the successful calibration and validation of a riverine sediment transport model. Automated suspended solids samplers were installed at three stations on the Pawtuxet River in 1992: Cranston, Station 4 and Station 6 (Pawtuxet Cove Dam). Additional suspended solids data were collected using automated samplers at two stations in 1994: Station 3 and Station 6. Each automated sampler pumped river water through a pipe, the end of which was positioned approximately at mid-depth in the water column and 5 to 10 m offshore, into one-liter sample bottles. Total suspended solids (TSS) samples were collected every four hours from March 8 to May 28, 1992 and from February 19 to April 17, 1994. If a high flow event did not occur during a particular day, the six collected samples were combined into a composite sample to produce a daily average TSS value.

5.4 CALIBRATION DESCRIPTION AND RESULTS

The TSS data collected during the 1992 and 1994 sampling periods were used to calibrate and validate the sediment transport model over a 789-day period that extended from March 3, 1992 through April 30, 1994. No TSS data were collected at Cranston, which is the upstream limit of the model, after May 28, 1992. Lack of sediment loading data at the upstream boundary of the model during approximately 90 percent of the simulation made it necessary to develop a procedure to estimate accurately the incoming sediment load, both at Cranston and from the Pocasset River.

The methodology developed to estimate sediment load inputs for the model used sediment loading data collected from forty-two rivers in the eastern United States. A detailed description of this data-based procedure is presented in Appendix A. The key idea in this method was the development of a non-dimensional sediment loading function, called the Normalized Sediment Load (NSL) function, which has the form

$$\log L_N = \log a + n \log Q_N + \delta S_L \tag{5-13}$$

$$Q_N = \frac{Q_d}{Q_m} \tag{5-14}$$

and

$$L_N = \frac{L_d}{L_m} \tag{5-15}$$

where L_N = normalized daily sediment load, L_d = daily sediment load, L_m = average daily sediment load under non-flood conditions, Q_N = normalized daily average flow rate, Q_d = daily average flow rate, Q_m = long term mean flow rate, log a and n are functions of drainage basin characteristics, S_L = standard deviation of the log estimate, and δ =

normally distributed random number with mean of zero and standard deviation of one. Thus, given the measured flow rate of the Pawtuxet River, Q_m, an estimate of the sediment load at the upstream boundary of the model can be made for any particular day.

The following values used in Equations (5-14) and (5-15) were calculated from Pawtuxet River data: $Q_m = 340$ cfs and $L_m = 2.4$ tons/day. The parameters in Equation (5-13) were determined using Pawtuxet River characteristics, i.e., $A = 200$ mi^2 and Q_m /$A = 1.70$ cfs/mi^2, and correlations presented in Appendix A. Similar determinations were made for the Pocasset River, where: $Q_m = 60$ cfs, $L_m = 0.43$ tons/day, $A = 36$ mi^2 and Q_m /$A = 1.67$ cfs/mi^2 The resulting parameter values for the Pawtuxet and Pocasset Rivers are listed in Table 5-1.

TABLE 5-1. NSL FUNCTION PARAMETER VALUES					
	Pawtuxet River			Pocasset River		
Q_N	log a	n	S_L	log a	n	S_L
< 2	-0.277	1.35	0.40	-0.262	1.20	0.40
> 2	-0.300	2.47	0.39	-0.280	2.44	0.43

Hence, the incoming sediment load at Cranston was specified by using available TSS data and applying the NSL function during the period that no data was available. Time histories for the flow rate and sediment loading, expressed as daily average TSS values, at Cranston for the 789-day calibration period are shown on Figure 5-3. The sediment loading from the Pocasset River was determined similarly.

Previous studies (Peart and Walling, 1982; Bogen, 1992; Walling et al., 1992) have indicated that changes in suspended load composition occur during flood events. This variation must be included to achieve realistic simulations (Gailani et al., 1991). To account for changes in suspended load composition, the composition of the incoming sediment load was assumed to be 100 percent class 1, i.e., clays and silts, for flow rates less than 400 cfs. The composition was assumed to change to 33 percent class 1 and

67 percent class 2, i.e., fine sands, for flow rates greater than 700 cfs. For flows between 400 and 700 cfs, the composition varied linearly between the two limits. The tributary suspended solids composition was assumed to be equal to that specified at Cranston.

The two model variables adjusted during calibration were the critical shear stress for deposition, τ_d, and the class 2 settling speed, $W_{s,2}$. Modification of bed property values, i.e., d_{50}, in some grid elements was done during initial calibration simulations. Interpolation and extrapolation of available data were used to determine initial bed property values in the modified elements; no bed data were collected in the modified elements. Results of early calibration simulations suggested that the estimated values needed to be reexamined. Adjustments of the interpolated/extrapolated element values were then made based upon the available data. All other parameters used in the sediment transport model were determined from field and laboratory data and were not adjusted during calibration. The eddy diffusivity, K_H, was set equal to the eddy viscosity, A_H.

The best model calibration results were achieved using the following parameter values: $\tau_d = 0.5$ dyne/cm^2 and $W_{s,2} = 7500$ μm/s. This value of $W_{s,2}$ corresponds to a particle diameter of 103 μm, a very fine sand. This effective particle diameter for class 2 sediment is physically consistent with Pawtuxet River sediment bed data, since an average of 22 percent of the sediment bed is composed of fine sands. In addition, fine sands compose a large fraction of the non-cohesive suspended load in most rivers (van Rijn, 1984).

Model accuracy was evaluated using TSS data collected during high flow periods in 1992 and 1994. A 33-day period in 1992, extending from March 3 through April 4, contained two floods, both of which approximately corresponded to the annual flood, with a maximum flow rate at Cranston of 1180 cfs on March 11 and 1240 cfs on March 29. However, the sediment transport response of the river was significantly different during these two high flows. The first flood had maximum TSS concentrations of about 45 mg/l at all three stations while the second flood, which occurred about two weeks later,

generated lower concentrations, with maximum values of about 10 mg/l. An examination of local precipitation records during these two periods showed that 3.6 cm of rain fell during March 11 while 1.8 cm accumulated during March 26. The higher TSS concentrations during the first flood are probably attributable to higher rainfall, which generated more wash load from runoff.

Comparisons between measured and predicted TSS concentrations at Stations 4 and 6 during the 1992 flood period are shown on Figure 5-4. The model predictions are in excellent agreement with observed TSS values during both floods. As another measure of model accuracy, predicted and measured sediment mass discharges at Cranston and Pawtuxet Cove Dam for the three-day periods during the March 11 through 13 and March 27 through 29 floods in 1992 were examined. Sediment mass transported during flood events is important when considering the transport and fate of organic chemicals or heavy metals in the Pawtuxet River. Although the observed sediment load at Cranston was more than two times greater for the first flood (80 metric tons) than the second flood (36 metric tons), measured increases in mass discharge between Cranston and Pawtuxet Cove Dam were very similar. Observed increases in sediment load between the two stations were 39 and 35 metric tons for the first and second floods, respectively. Simulated sediment load increases of 30 metric tons for the March 11 through 13 flood and 20 metric tons for the March 27 through 29 flood compare favorably to the observed values. The model simulations under predict the sediment load increases by 30 and 43 percent during the first and second floods, respectively. These discrepancies can be attributed to underestimated tributary loading, for which no data exists during the two floods, and/or insufficient sediment bed erosion.

Suspended solids data were available for two floods that occurred during a 30-day period in 1994, from March 8 through April 7. The high flow events in 1994 were of greater magnitude than the 1992 floods, with maximum daily average flow rates of 2524 and 1789 cfs being recorded on March 11 and 25, respectively. The March 11 high flow corresponds to a one in five year flood. Similar to the 1992 floods, higher TSS

concentrations were observed during the first flood, maximum of about 80 mg/l, than during the second flood, maximum TSS values ranging from 15 to 20 mg/l.

Model predictions for this 30-day period in 1994 are compared with TSS data collected at Stations 3 and 6 on Figure 5-5. Generally, the model results agree well with measurements. However, the model tends to over predict TSS at Station 6, which is at Pawtuxet Cove Dam, during some days. Efforts to adjust various model parameters, e.g., $W_{s,2}$, so that model over predictions at Station 6 were reduced or eliminated during March 1994 were unsuccessful; reducing over prediction at the dam during March 1994 resulted in poorer agreement between model and data at other locations and times. The possibility exists that installation of the automated TSS sampler at Station 6 in 1994 resulted in unrepresentative measurements under certain flow conditions; the 1994 installation may not have been in the same exact location as the 1992 installation causing inconsistent TSS data sets to be collected. The cause of the model over predictions, due to either model or data limitations, cannot be determined currently. However, this error is not significant when viewed in the context of long-term contaminant fate and transport in the Pawtuxet River. Over predictions at Station 6 primarily occurred during non-flood conditions, when deposition and resuspension rates in the Pawtuxet River were low. The model accurately predicted TSS at Station 6 during the two high flow events in 1994, which was when a majority of the annual deposition and resuspension in the river occurred. Thus, the impact of TSS over prediction during non-flood flows in 1994 on contaminant fate and transport simulations would be minor.

Predicted changes in sediment bed elevation in the three kilometers upstream of Pawtuxet Cove Dam during the calibration period are illustrated on Figure 5-6. Net deposition occurred between Station 3 and the Warwick Avenue bridge, with a maximum bed aggradation of about 1 cm. The central channel generally has lower deposition rates than the near shore regions. Some areas of net erosion occurred downstream of the Warwick Avenue bridge, with typical erosional depths ranging from 0.2 to 0.9 cm. As expected, the highest deposition rates, with a maximum of about 2 cm, were predicted at the dam.

The calibration results show that the model can simulate spatial and temporal TSS trends in the Pawtuxet River over a wide range of flow rates and sediment loadings correctly. In essence, the 1994 flood period results validate the model because all input parameters controlling resuspension and deposition are held constant during the 789-day simulation. Differences in sediment bed characteristics and structure, in both cohesive and non-cohesive model segments, during the calibration period are calculated by the model and simulation results show that the model is functioning realistically and relatively accurately. Initial attempts to simulate the 1994 flood period started the calculation on March 1, 1994 and assumed the same initial bed conditions as in the original 1992 simulation (Ziegler and Nisbet, 1994). These calculations produced poor results and suggested that a long term simulation, starting in 1992, was necessary if the 1994 flood period was to be successfully modeled, as it was after development of the 789-day simulation that has just been presented.

5.5   SENSITIVITY ANALYSIS

The sediment transport model has been calibrated over a two-year period by adjusting two parameters that were not directly measured, i.e., the critical shear stress for deposition, r_d, and class 2 settling speed, $W_{s,2}$. Results of the PRD data analysis also indicated uncertainty in resuspension potential parameter values due to spatial variability of cohesive bed properties (see Figure 5-2). Inherent uncertainty in these resuspension and deposition parameters, though credible results were achieved during model calibration, suggests that the sensitivity of the model to parameter variation should be investigated. So, model sensitivity was tested by varying a_0 in Equation (5-9), r_d, and $W_{s,2}$ because these three parameters can have significant impact on resuspension and deposition fluxes.

Analysis of PRD data yielded 95 percent confidence intervals for a_0 in muddy cohesive and sandy cohesive sediments of 1.01 to 4.10 and 0.036 to 0.120, respectively. The sensitivity of the model to a_0 was evaluated by repeating the 789-day calibration run twice, with the low values (1.01 and 0.036) being used in the first simulation and the high values (4.10 and 0.120) specified in the second simulation. The model was minimally

sensitive to the uncertainty in a_o; predicted TSS concentrations in both sensitivity runs were virtually indistinguishable from the original calibration and differences in predicted bed elevation changes were typically less than 0.1 cm.

The critical shear stress for deposition was decreased and increased by a factor of two, i.e., 0.25 and 1.0 dyne/cm^2. Similar to a_o sensitivity results, the impact of τ_d variation on TSS concentrations was negligible. Bed elevation changes were slightly greater than found for a_o variation but the effects were still minor. Decreasing τ_d reduced net deposition, see Figure 5-7, and increasing τ_d increased the deposition rate, see Figure 5-8.

Class 2 settling speed was doubled, to 15,000 μm/s, which corresponds to a particle diameter of 150 μm and is a fine sand. The model was sensitive to this change in $W_{s,2}$. Minimal differences in TSS concentration during the 1992 flood period were seen, however, noticeable effects on TSS predictions during the 1994 flood period resulted from this increase in $W_{s,2}$, see Figure 5-9. Net deposition increased significantly in some areas, see Figure 5-10, with maximum changes of 3 to 4 cm.

Figures
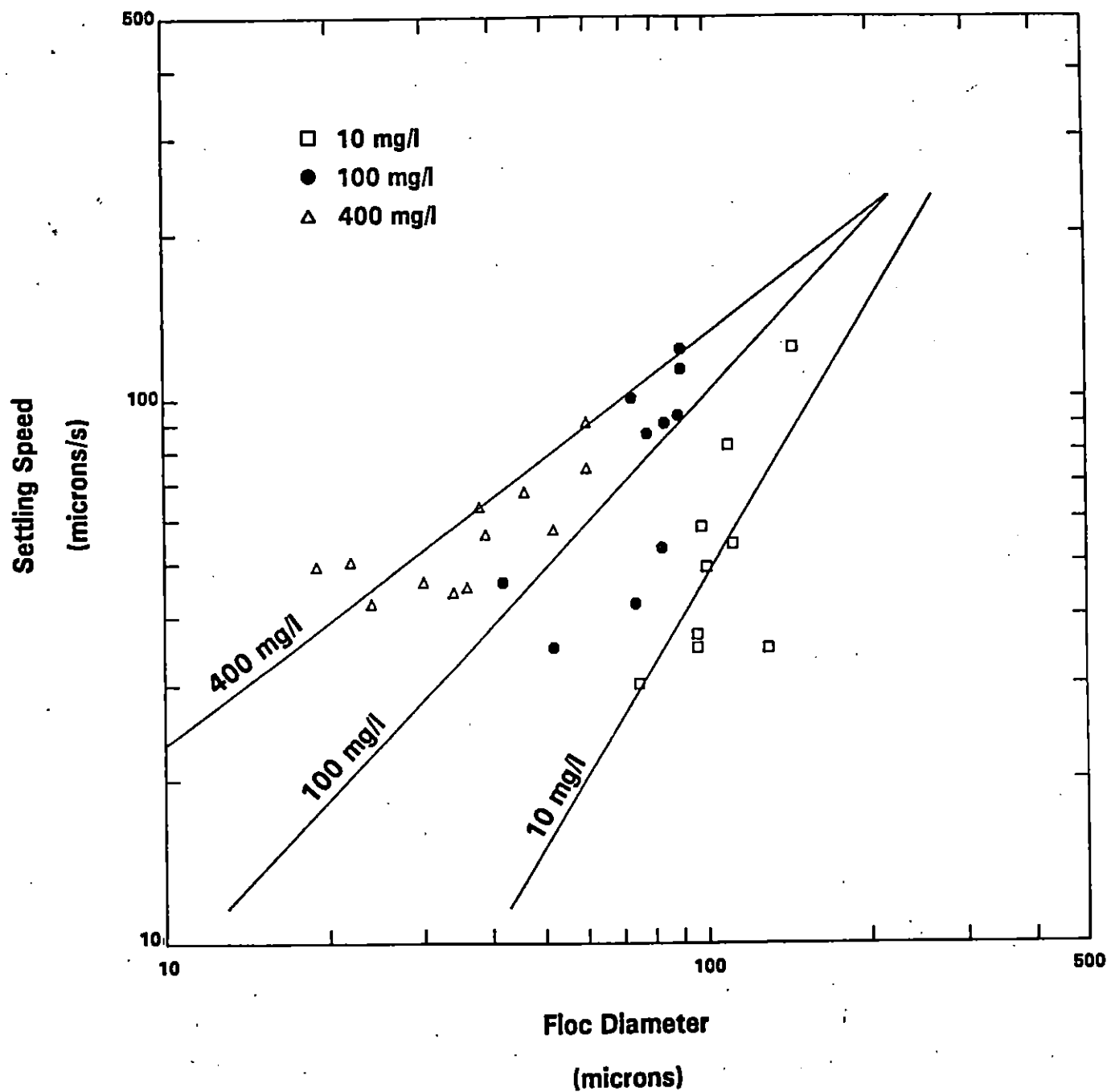
Figure 5-1 Measured and predicted (solid lines) floc setting speeds
for G = 2 dynes/cm^2. Floc settling speed data obtained from Burban et al., 1990
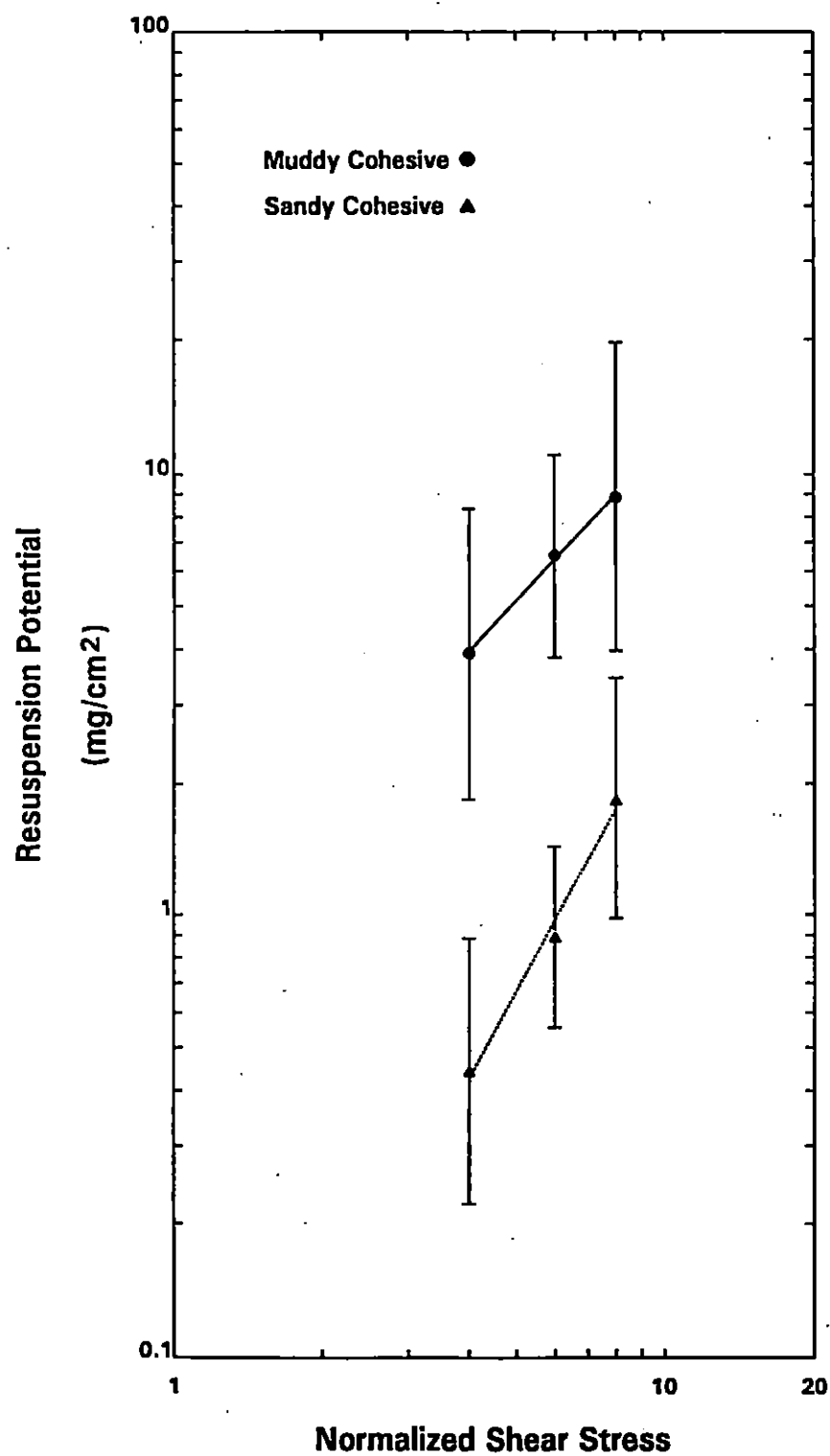
Figure 5-2 Comparison between measured (mean ± 2 standard errors)
and predicted resuspension potential for muddy cohesive (solid line)
and sandy cohesive (dotted line) sediments
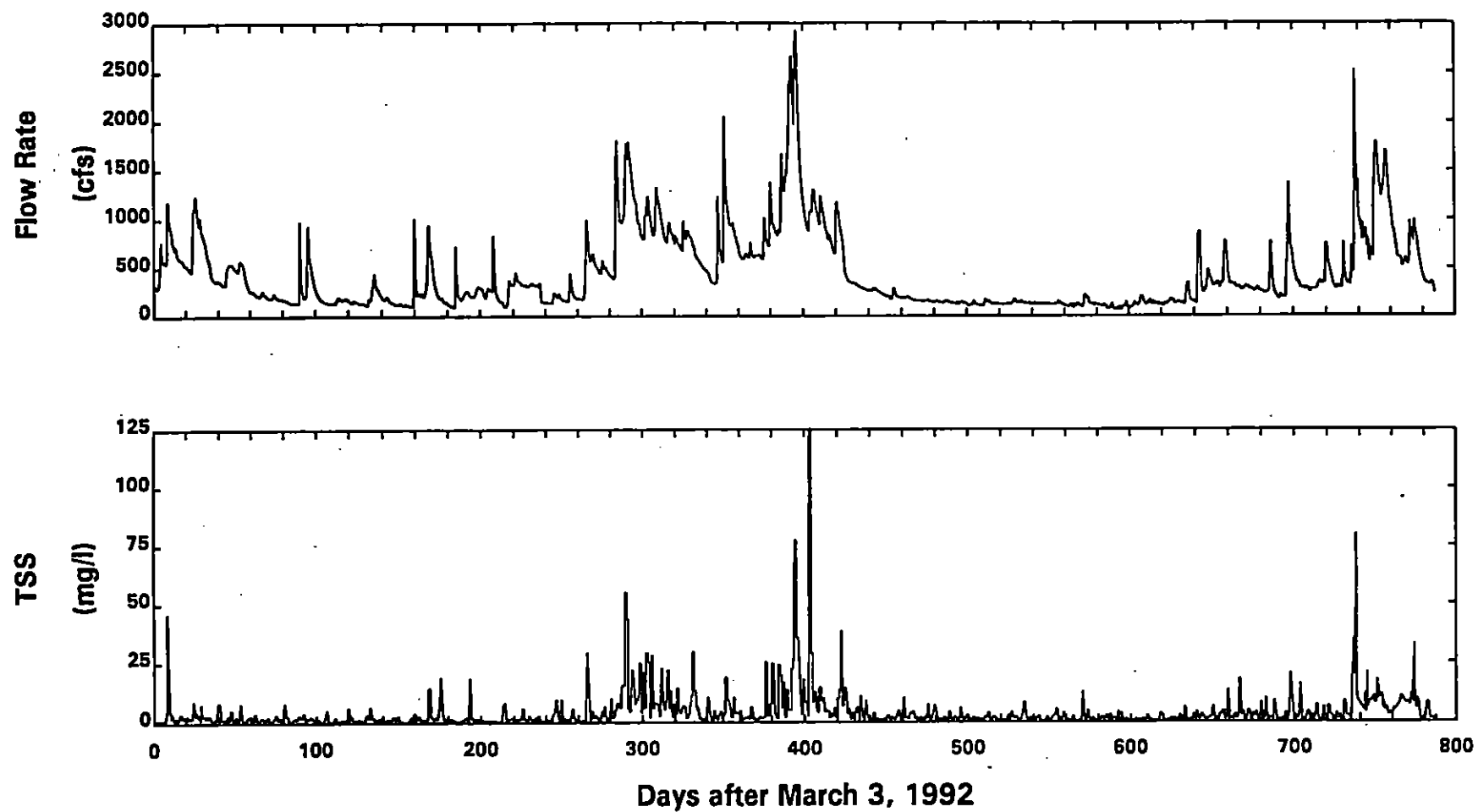
Figure 5-3 Flow rates and TSS concentrations specified at Cranston
during the 789-day calibration period
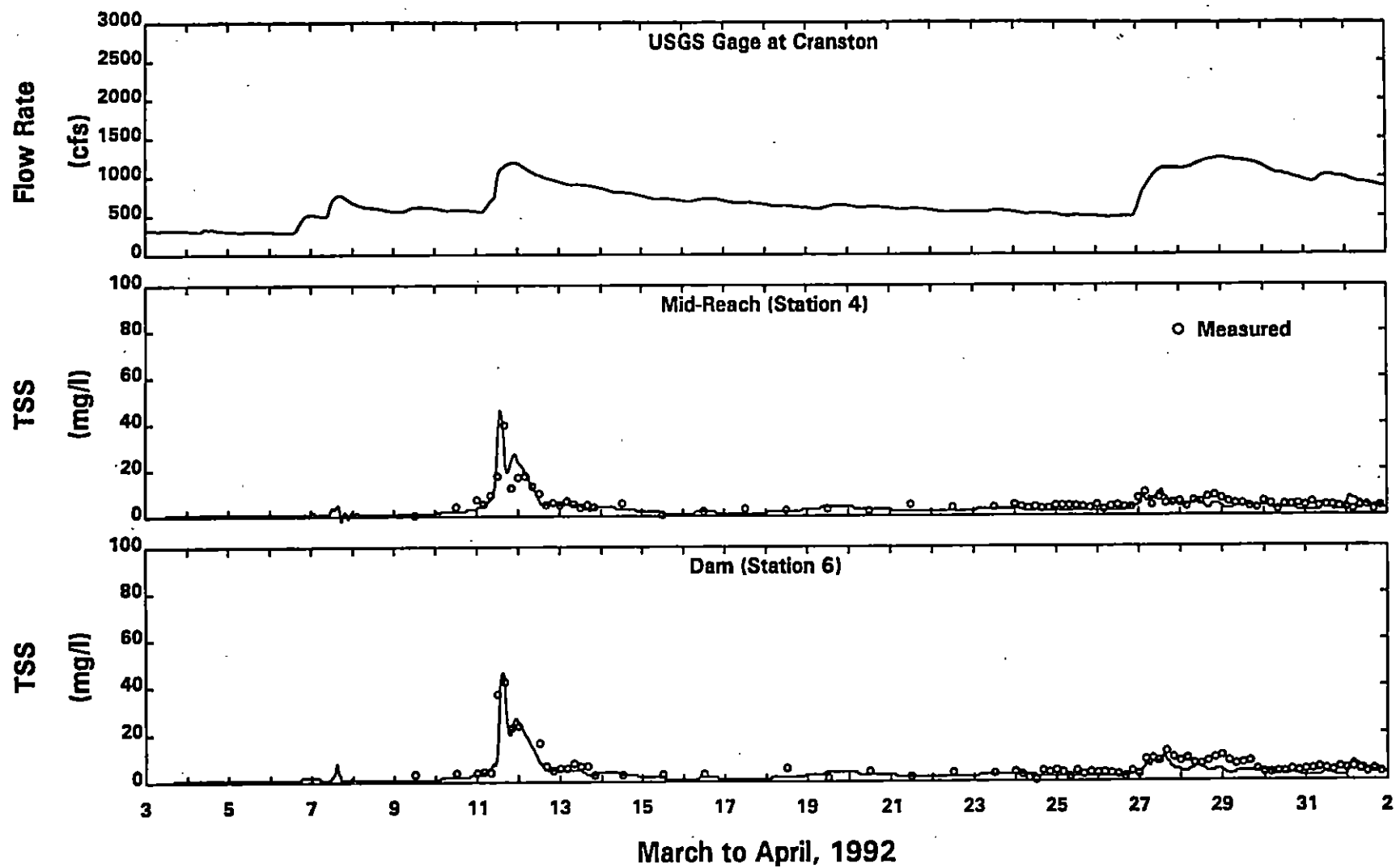
Figure 5-4 Comparison between predicted and measured TSS concentrations
during March and April of 1992
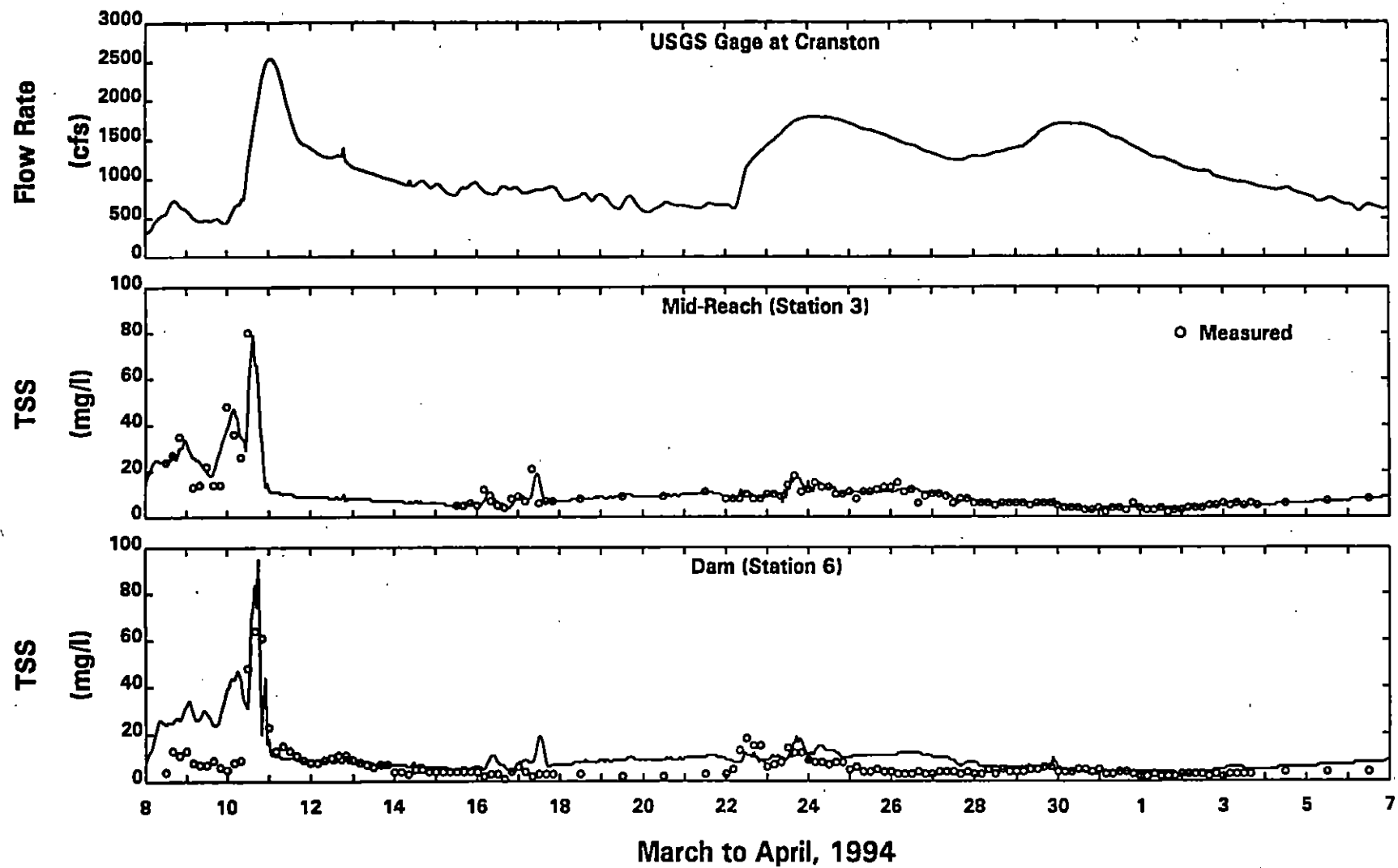
Figure 5-5 Comparison between predicted and measured TSS concentrations during March and April of 1994
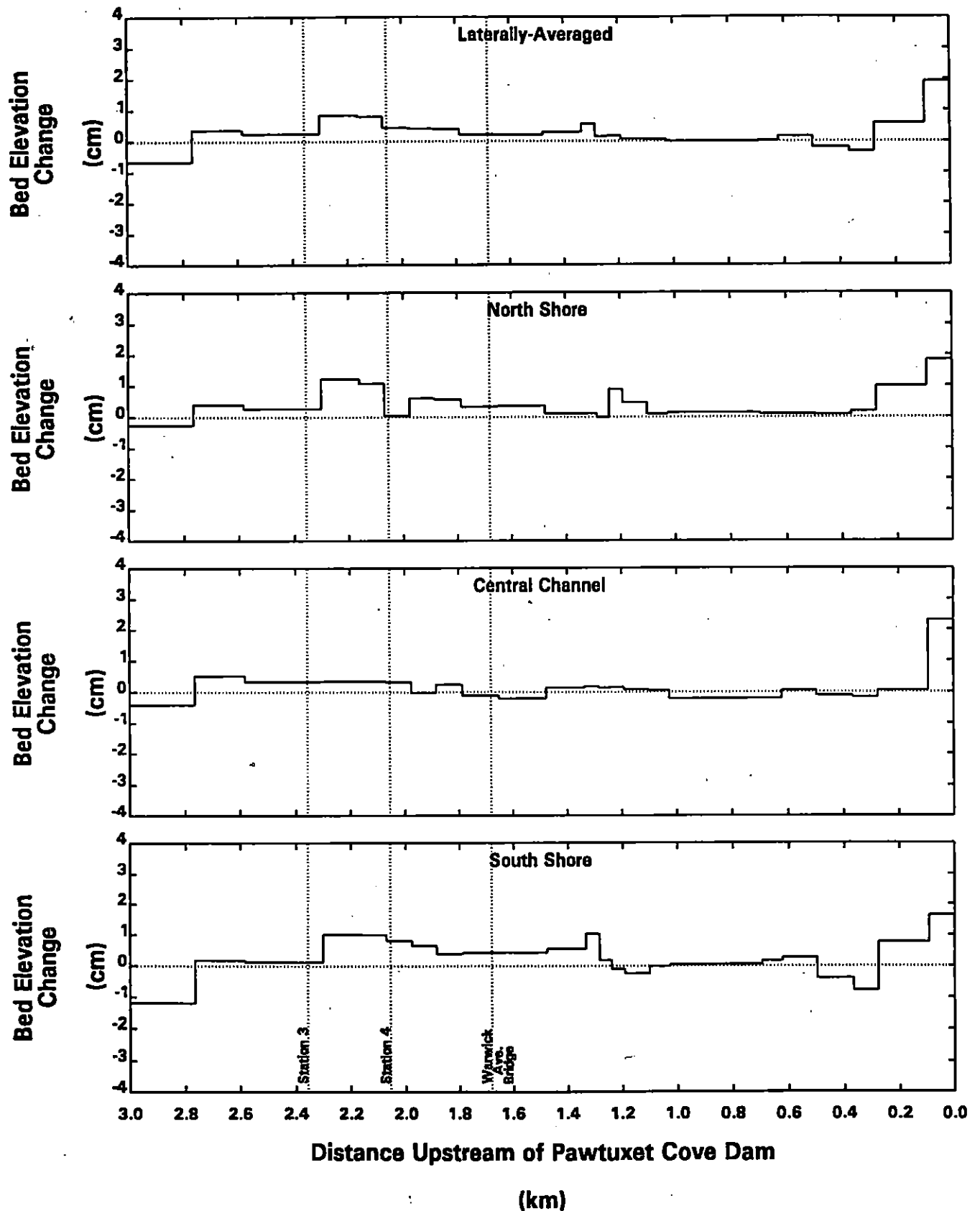
Figure 5-6 Predicted change in sediment bed elevation in the lower
Pawtuxet River during the 789-day calibration period
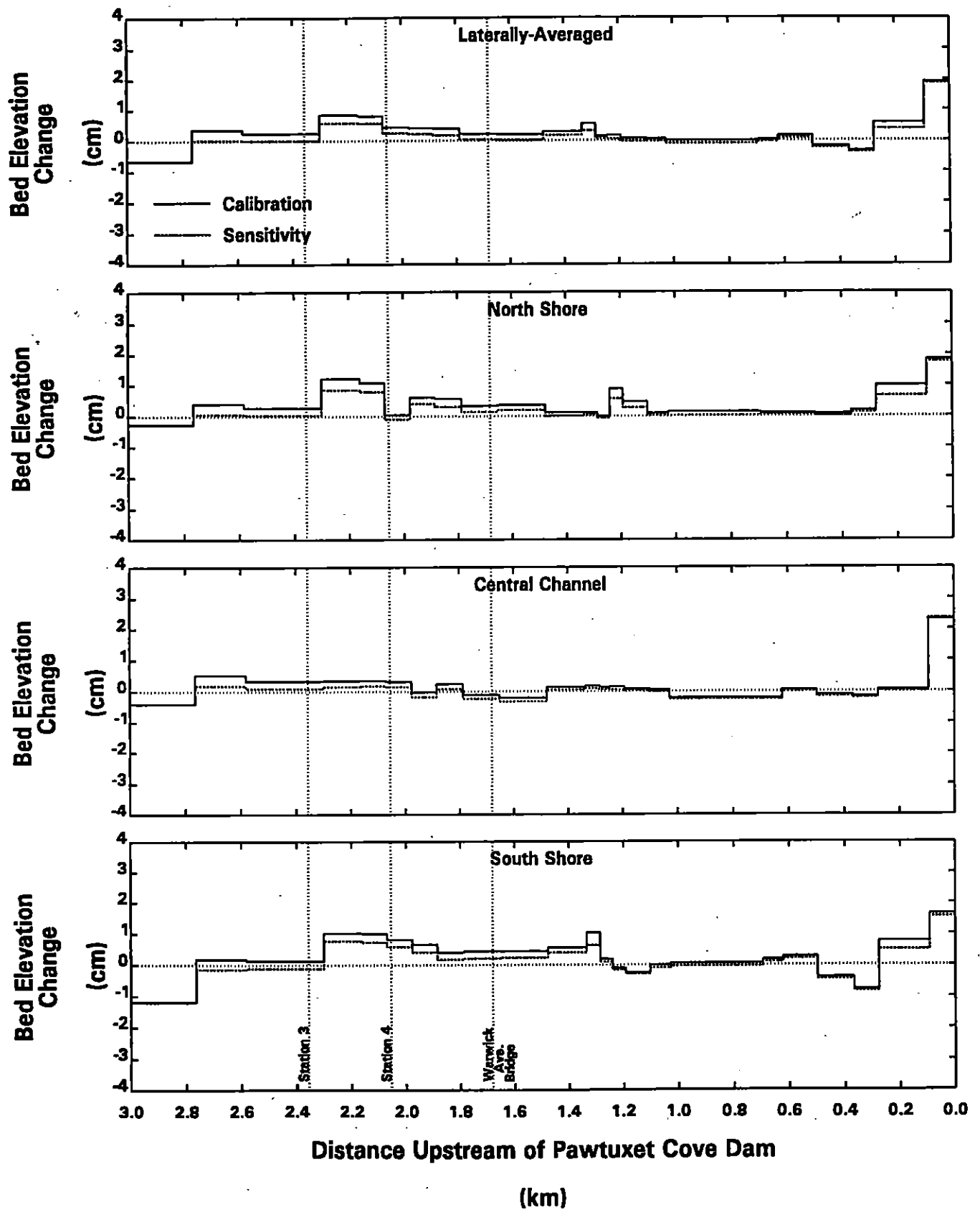
Figure 5-7 Sensitivity of predicted bed elevation changes to a
decrease in the critical shear stress for deposition
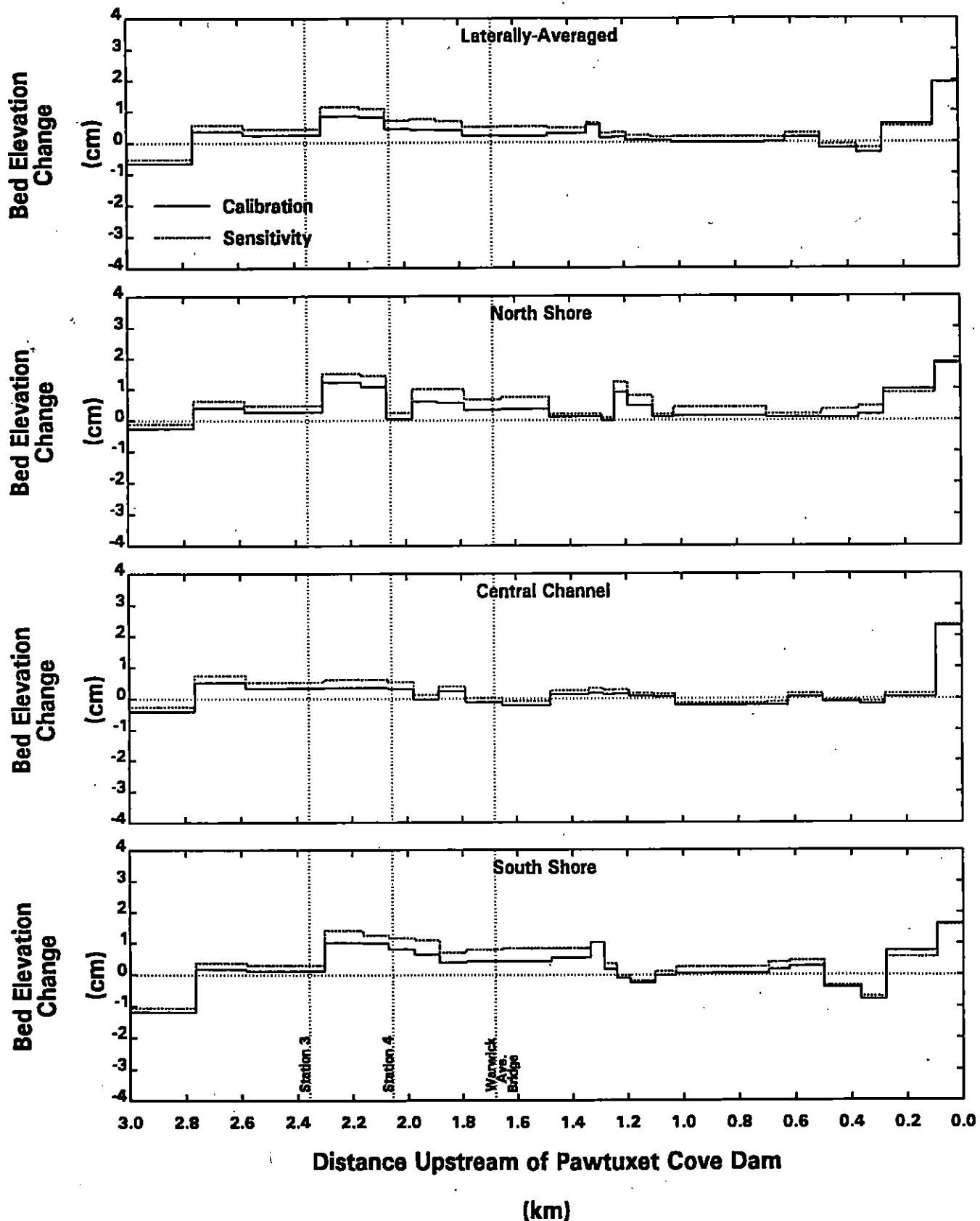
Figure 5-8 Sensitivity of predicted bed elevation changes to an
increase in the critical shear stress for deposition
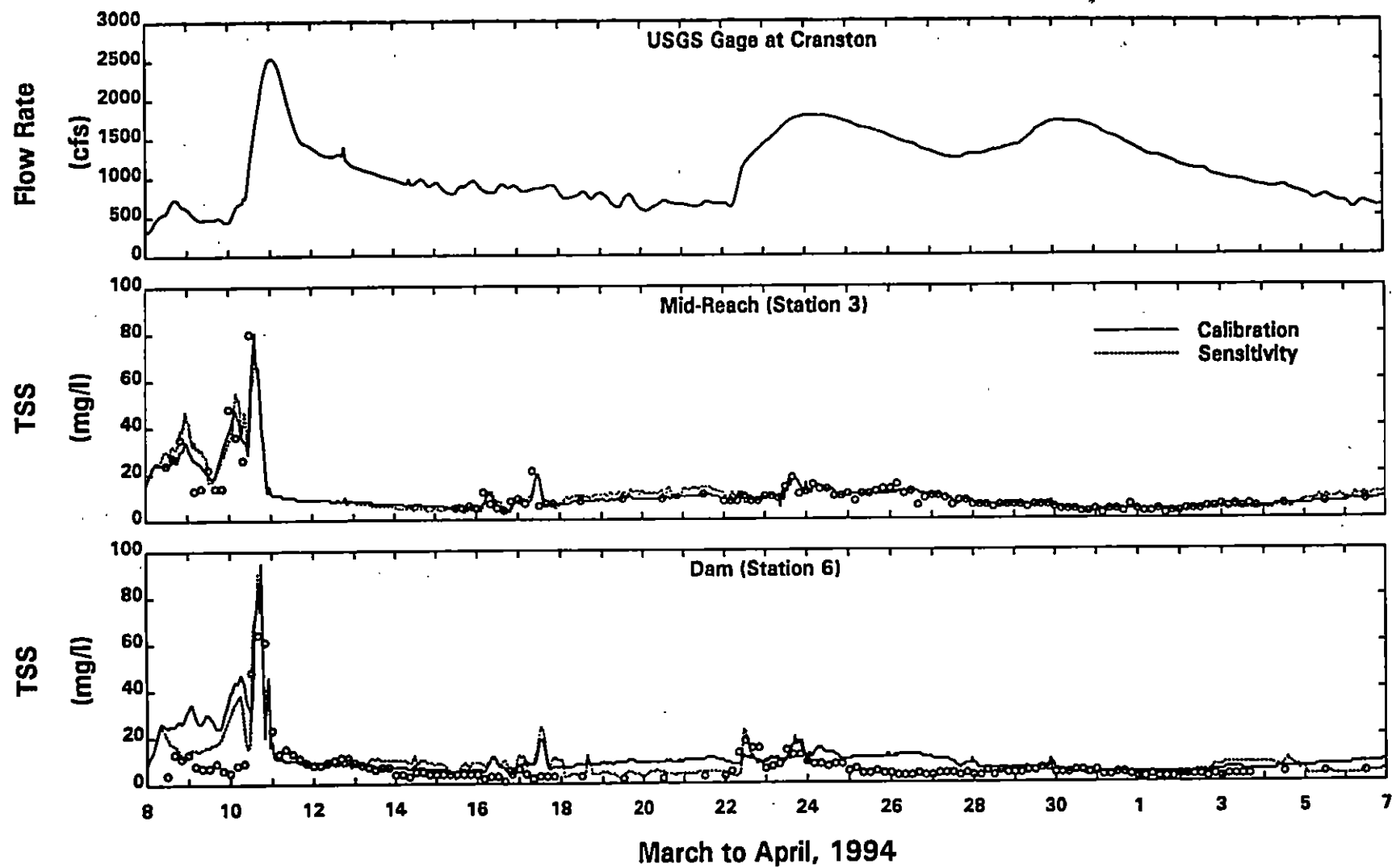
Figure 5-9 Sensitivity of predicted TSS concentrations to an increase in class 2 settling speed
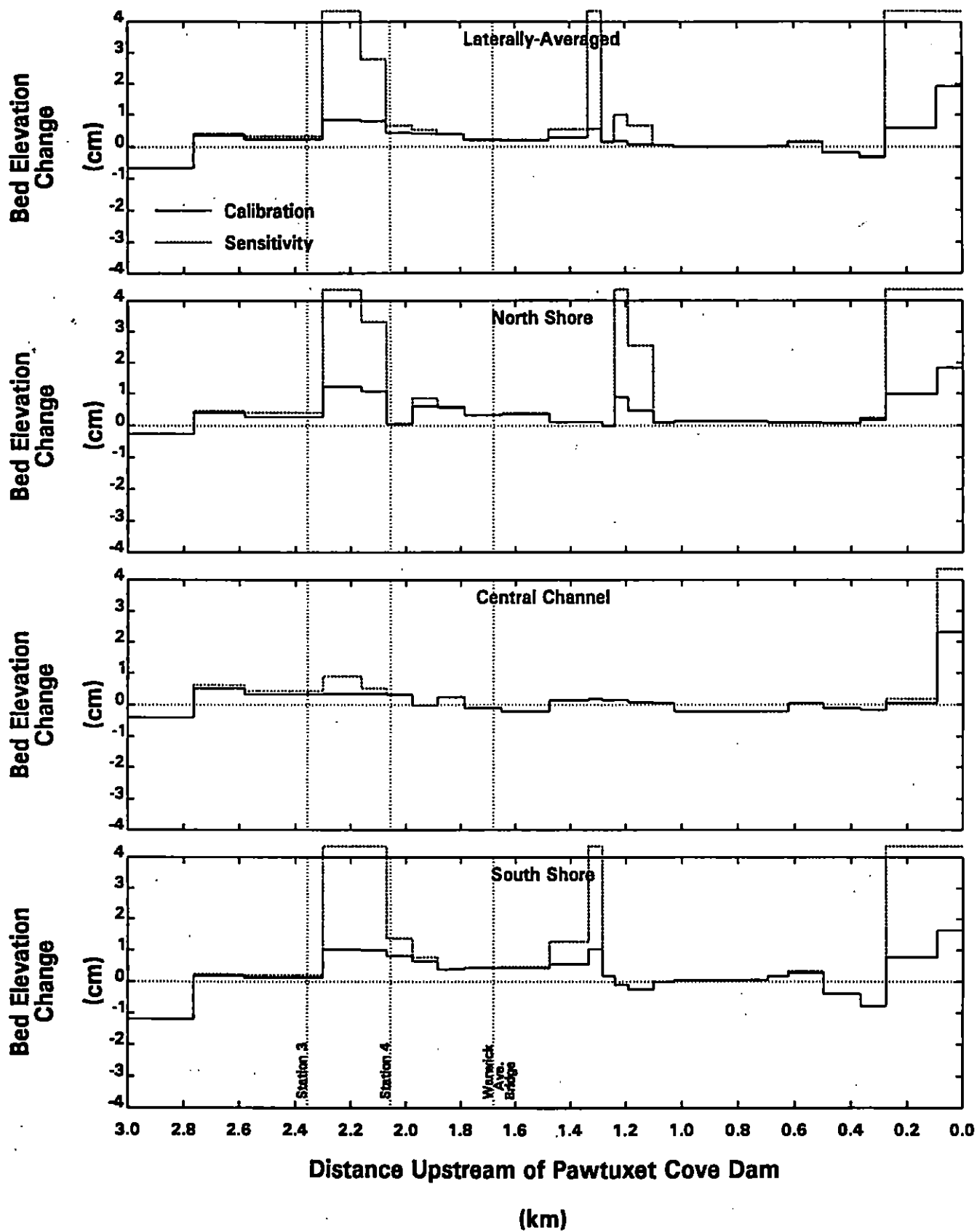
Figure 5-10 Sensitivity of predicted bed elevation changes to an increase in class 2 settling speed

SECTION 6

HYDRODYNAMIC AND SEDIMENT TRANSPORT PROJECTIONS

6.1   DESCRIPTION OF PROJECTIONS

The favorable results of the 789-day calibration simulation suggest that the sediment transport model can be confidently used as a predictive tool.   Therefore, the model was used to forecast the transport and fate of suspended sediments in the Pawtuxet River over an approximately 10.5 year period, which started on May 1, 1994 and ended on December 31, 2004. None of the resuspension or deposition parameters were changed during this projection period, only the flow rates and sediment loads at Cranston and the tributary were varied during this simulation.

6.1.1 Synthetic Hydrograph

Forecasting Pawtuxet River hydrodynamics requires development of a synthetic hydrograph that is realistic. Statistical procedures have been developed to create synthetic hydrographs on annual time scales (Fiering and Jackson, 1971). The method used in the present study employed a lag-one (Markovian) flow model (Fiering and Jackson, 1971) to generate a sequence of annual average flow rates for the Pawtuxet River at Cranston. Thirty-four years of flow rate data, from 1960 through 1993, collected at the Cranston gaging station were used to develop the necessary statistics, e.g., lag-one serial correlation coefficient, for the synthetic hydrograph model. Data obtained at Cranston before 1960 were not used in this analysis because significant differences between pre-1960 and post-1960 flow patterns were observed in the data.

A sequence of annual average flow rates 1000 years long was then created, with the first hundred years being treated as model spin-up. The start of the eleven-year period needed for the model projection was determined by optimizing the matching between the three-year pattern of annual flow rates measured during 1991, 1992 and 1993 with a three-year sequence in the last 900 years of the synthetic hydrograph. This procedure

was used so that the influence of recent flow patterns would be realistically reflected in the projection period hydrograph. An eleven-year sequence of annual flow rates was thus selected in an unbiased manner, see Figure 6-1.

Flow rates are input to the hydrodynamic model on a daily basis, not annually, however. The following procedure was used to develop a daily flow hydrograph based on the annual flow sequence determined from the synthetic hydrograph. Each year in the eleven-year annual flow pattern was optimally matched with one of the thirty-four annual flow rates measured at Cranston between 1960 and 1993. The matching of observed values was done without replacement so that each year of data would only be used once. This method produced the following sequence of annual average flow rates that best matched the synthetic hydrograph: 1968, 1970, 1986, 1978, 1993, 1961, 1967, 1962, 1969, 1971 and 1987.

The daily flow hydrograph needed for model input was then generated by using daily average flow rates measured during each of the eleven years. These annual hydrographs were then connected in the proper sequence to generate input for the hydrodynamic model, see Figure 6-2. The frequency distribution of daily average flows for this eleven-year period was compared with the distribution of flows from the historical record, see Figure 6-3. This comparison shows that this methodology has produced a hydrograph that is representative of flow conditions in the Pawtuxet River.

6.1.2 Solids Loading

The Normalized Sediment Load function described in Section 5.4 was used to generate the sediment loading for the projection period. The daily average flow rates from the synthetic hydrograph were input to the NSL function to calculate daily sediment loads during the eleven-year projection. The resulting TSS concentrations used in the simulation are illustrated on Figure 6-4.

6.2   PROJECTION RESULTS

The main focus of the projection simulation for the sediment transport model was sediment bed elevation changes due to erosion and deposition. Spatial distributions of the average resuspension and deposition rates during the eleven-year projection period are shown on Figure 6-5, along with the calculated rates for the 789-day calibration. Areas of net erosion had nearly the same rates in both calculations. Generally, depositional rates were higher in the projection than during the calibration, with a maximum difference of about 0.2 to 0.3 cm/year near the dam.

6.3   INSIGHTS GAINED FROM DATA ANALYSIS AND MODELING RESULTS

The reach extending from near Station 3 to Warwick Avenue bridge is generally a depositional environment, with the highest deposition rates (~0.5 cm/year) occurring in the shallower areas along the north and south shores. The cause of sediment deposition in this area is a change in the gradient of the Pawtuxet River. The upper 4 km of the river, extending from Cranston to a point about 0.5 km upstream of Station 3, has a relatively high gradient, which results in high current velocities. The sediment bed in this reach is primarily composed of coarse sands and gravels because of the higher velocities; very little fine-grained sediment deposits in the upper portion of the study area. The river gradient decreases significantly about 0.5 km upstream of Station 3 causing the current velocities to decline. The lower velocities make it possible for some of the suspended sediment load to deposit between Station 3 and Warwick Avenue bridge; the Pawtuxet River in the vicinity of the Ciba facility is a natural depositional environment due to a change in the river gradient.

Deposition decreases downstream of Warwick Avenue bridge, particularly in the central channel, until the dam is reached. The reduction of deposition in this area is caused by higher current velocities due to a decrease in the cross-sectional area of the flow. Deposition rates start to increase about 0.2 km upstream of the dam due to backwater effects; the highest deposition rates occur at the dam, as expected.

6.4 COUPLING TO CHEMICAL FATE AND TRANSPORT MODEL

The primary purpose of developing hydrodynamic and sediment transport models for the Pawtuxet River was to provide information for the chemical fate and transport model. This objective was accomplished by coupling the models together. Output from the hydrodynamic model, i.e., current velocities and water volumes, was transferred to the chemical fate model for both the calibration and projection simulations. Similarly, deposition and resuspension fluxes at the sediment-water interface were calculated by the sediment transport model and then output for use in the solids transport component of the chemical fate model.

The chemical fate model used the same numerical grid as the hydrodynamic and sediment transport models, so time-variable transport information for the chemical fate model had to be provided for each grid element during the calibration and projection simulations. Due to computational constraints, output from the hydrodynamic and sediment transport models was averaged on a daily basis for use as input to the chemical fate model. The accuracy of the chemical fate model was not compromised by this temporal averaging because the effects of hourly time-scale events were realistically simulated by the hydrodynamic and sediment transport models; the daily average values include the impacts of short-term events.

Figures
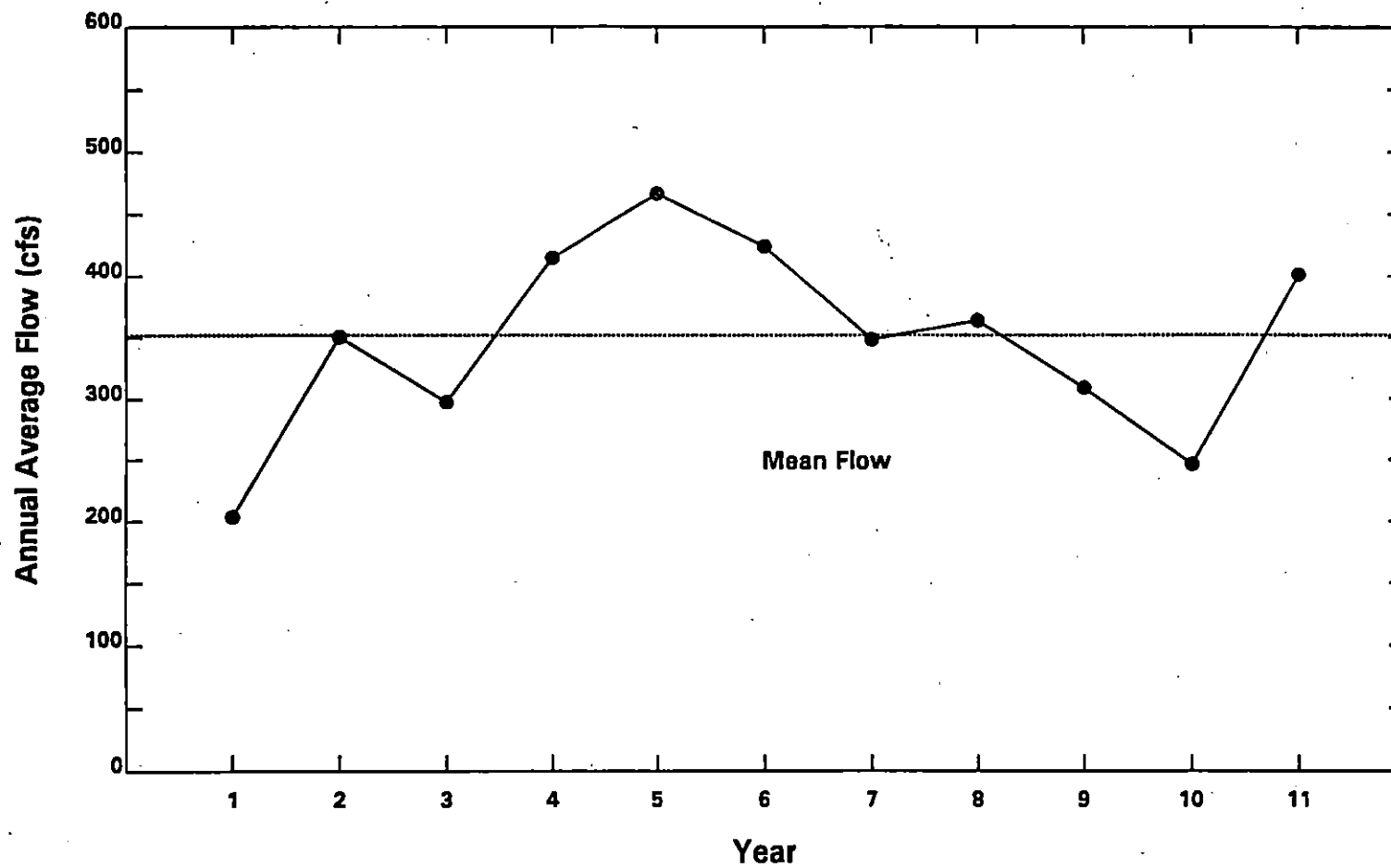
Figure 6-1 Synthetically-generated annual average flow rates
at Cranston for the eleven-year projection simulation
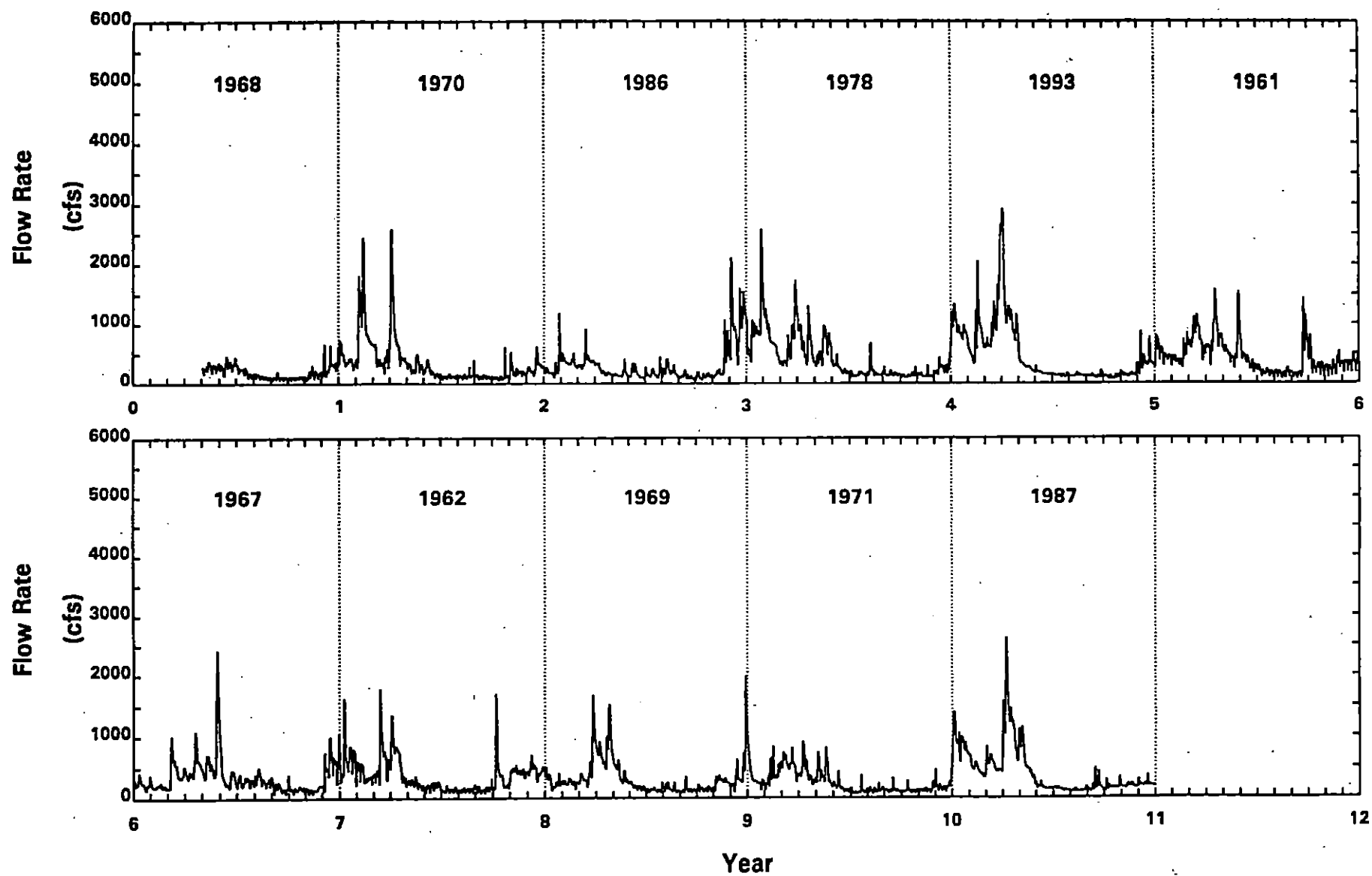
Figure 6-2 Daily average flow rates specified at Crantson
for the eleven-year projection simulation
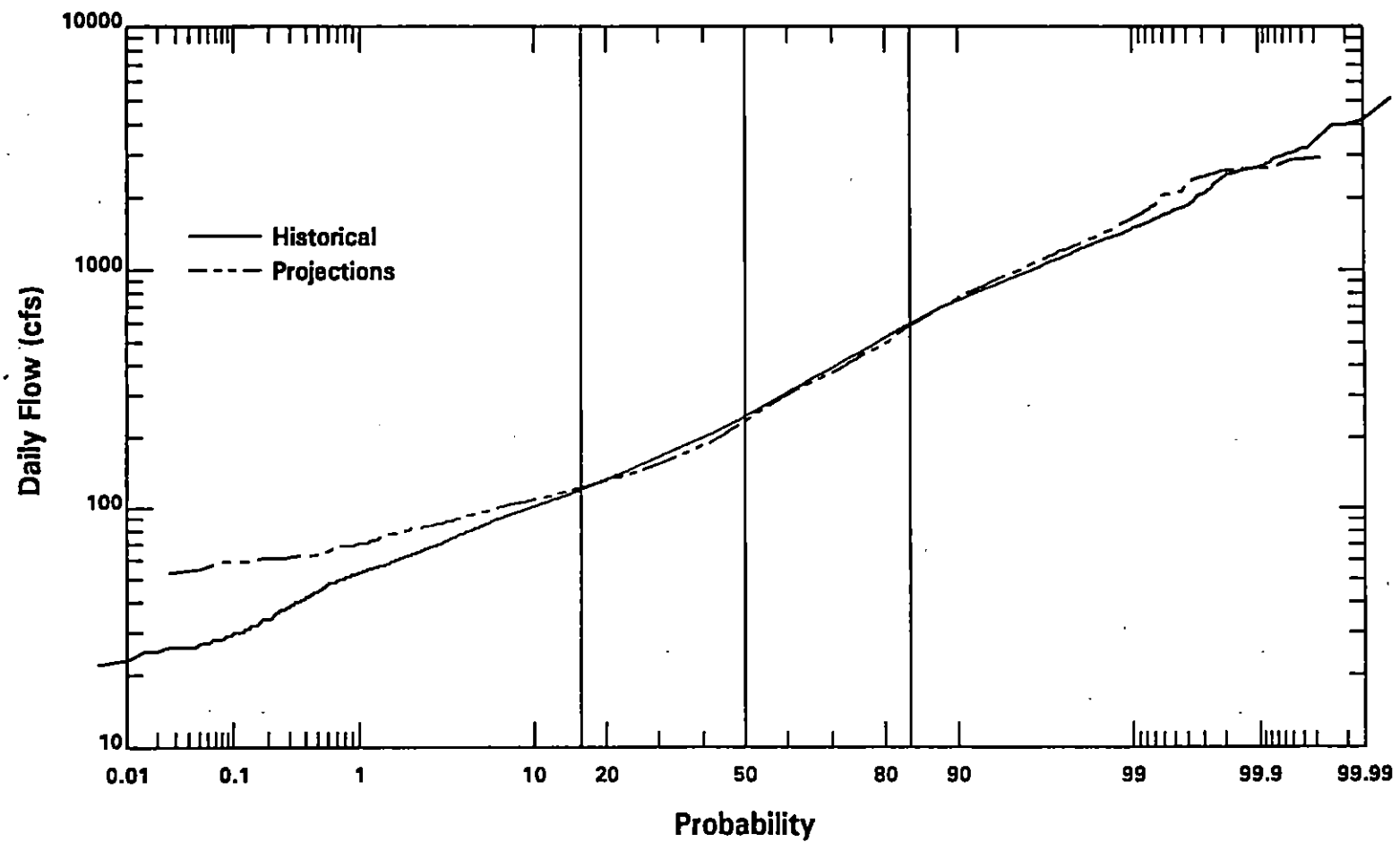
Figure 6-3 Comparison between frequency distributions of historical
and synthetic hydrograph flow rates at Cranston
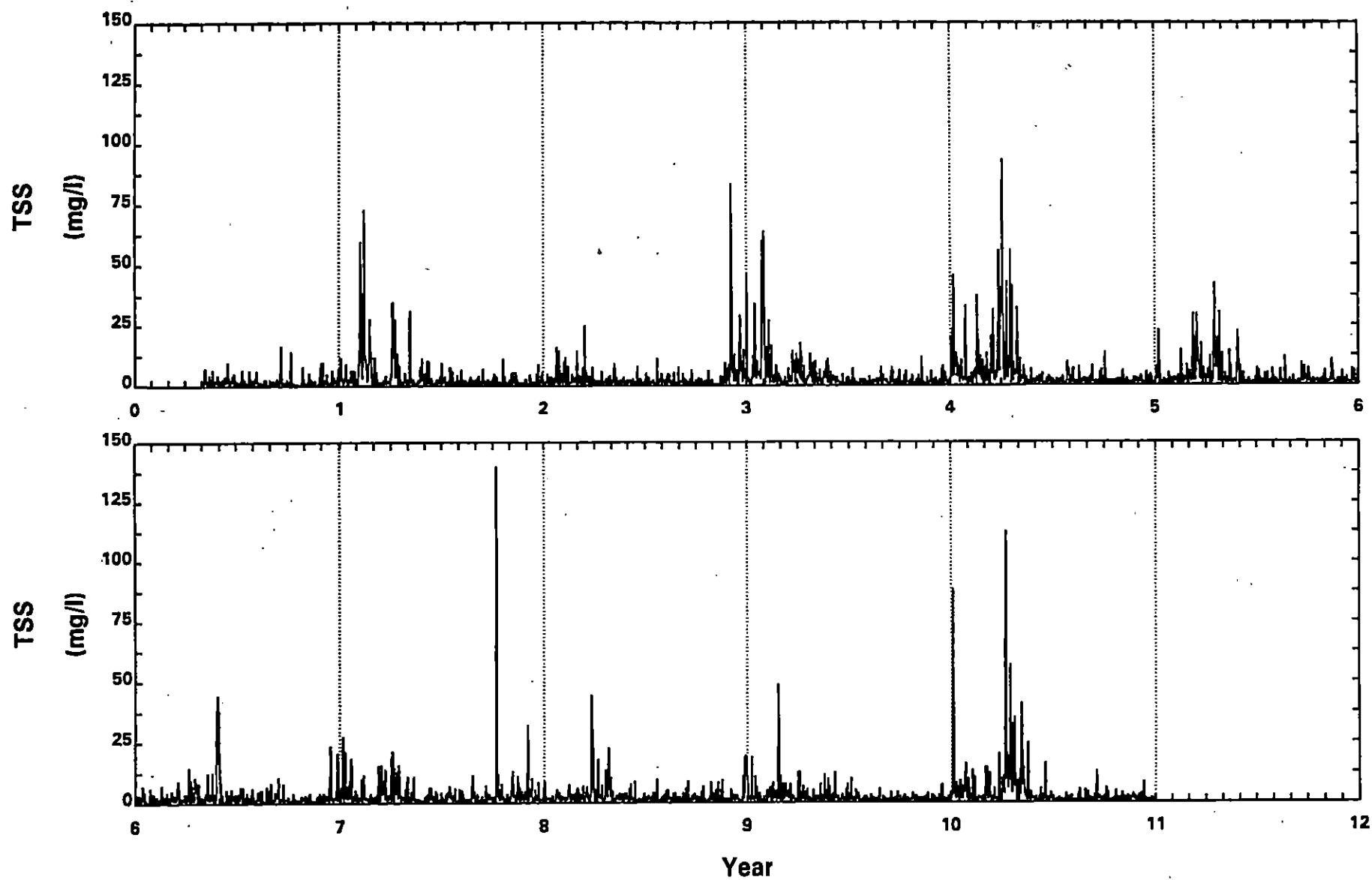
Figure 6-4 Daily average TSS concentrations specified at Cranston
during the eleven-year projection simulation
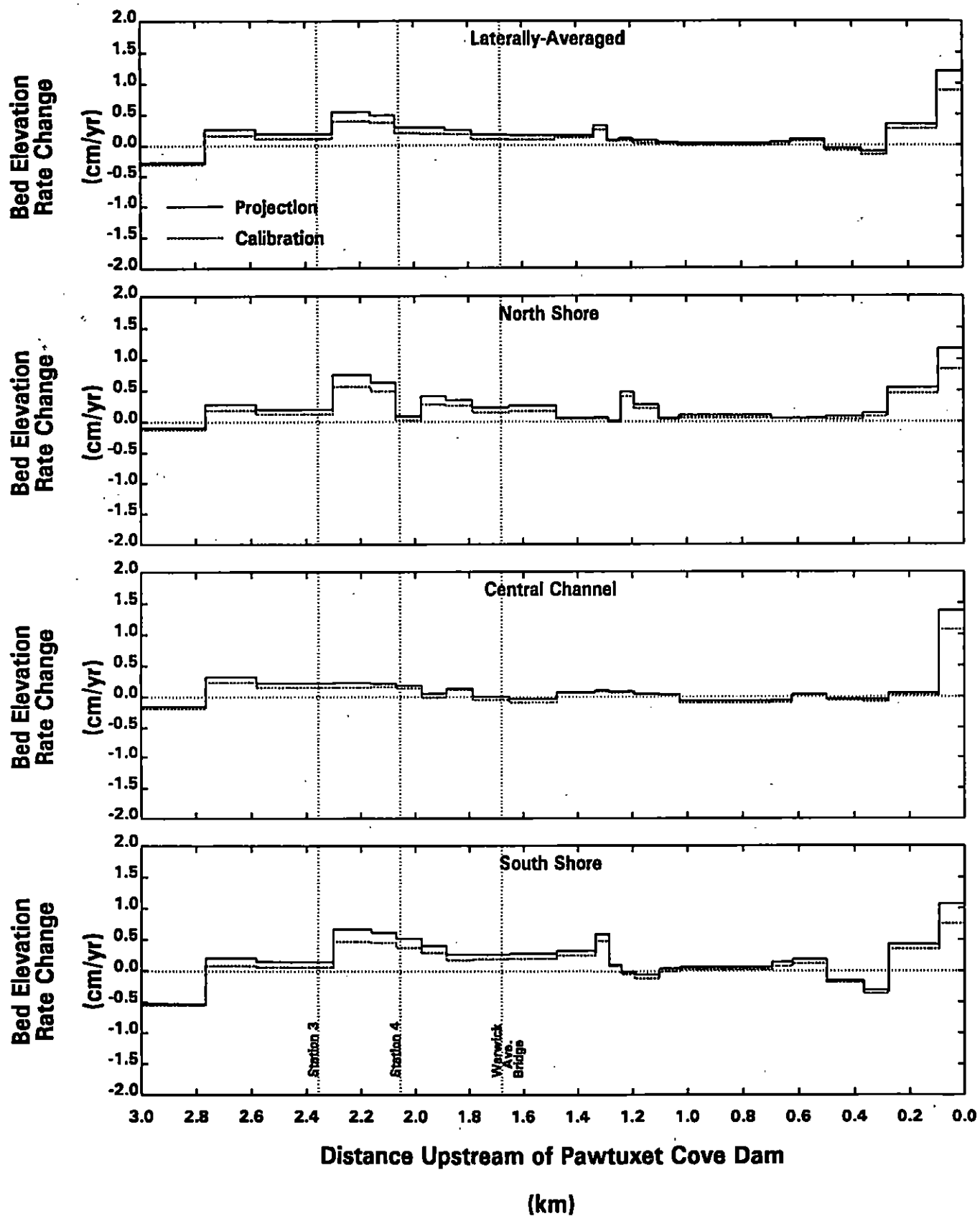
Figure 6-5 Comparison between bed elevation rate changes in the lower Pawtuxet River for the calibration and projection simulations

SECTION 7

WATER COLUMN AND SEDIMENT CONTAMINANT FATE MODEL

7.1   BASIC EQUATIONS

The processes that determine the fate of toxic chemicals in surface water systems may be divided into two classes; (a) transport and (b) transfer and reaction. Transport is the physical movement of the chemical caused by the net advective movement of water, mixing, and the scouring and deposition of solids to which the chemical may be adsorbed. It is specified by the flow and dispersion characteristics in the water column and the settling velocity and resuspension rate of the solids. Transfer and reaction include movement of the chemical between the air, water, and solid phases of the system and transformation or degradation of the chemical. The processes involved in transfer and reaction are volatilization, adsorption, biodegradation, ionization, hydrolysis and photolysis. The latter three processes are not significant with regard to the chemicals modeled in the Pawtuxet River.

Consider the concentration, C_d, to be the dissolved component of the chemical in water. It interacts with the particulate component of the chemical at concentration C_p, through an adsorption-desorption reaction with the suspended solids. The particulate concentration can be expressed as:

$$C_p = rm \tag{7-1}$$

where

C_p = particulate concentration $[M/L^3]$

r   = mass of chemical/unit mass of solids $[M/M]$

m   = concentration of the solids $[M/L^3]$

The equations governing the distribution of the dissolved and particulate components in any surface water system may be written as follows (Connolly, 1984):

$$\frac{\partial C_d}{\partial t} = \frac{\partial}{\partial x}\left(E_x \frac{\partial C_d}{\partial x}\right) + \frac{\partial}{\partial y}\left(E_y \frac{\partial C_d}{\partial y}\right) + \frac{\partial}{\partial z}\left(E_z \frac{\partial C_d}{\partial z}\right) - \frac{\partial}{\partial x} u_x C_d \qquad (7\text{-}2)$$

$$- \frac{\partial}{\partial y} u_y C_d - \frac{\partial}{\partial z} u_z C_d - K_0 m C_d + K_2 C_p \pm S_1 \; (s,y,z,t)$$

$$\frac{\partial C_p}{\partial t} = \frac{\partial}{\partial x}\left(E_x \frac{\partial C_p}{\partial x}\right) + \frac{\partial}{\partial y}\left(E_y \frac{\partial C_p}{\partial y}\right) + \frac{\partial}{\partial z}\left(E_z \frac{\partial C_p}{\partial z}\right) - \frac{\partial}{\partial x} u_x C_p \qquad (7\text{-}3)$$

$$- \frac{\partial}{\partial y} u_y C_p - \frac{\partial}{\partial z} u_z C_p + \frac{\partial}{\partial z} w_s C_p + K_0 m C_d - K_2 C_p \pm S_2 \; (s,y,z,t)$$

in which

C_d	=	concentration of the dissolved component $[M/L^3]$
E	=	dispersion coefficient $[L^2/T]$
u	=	velocity $[L/T]$
w_s	=	settling velocity of the particulates $[L/T]$
K_0	=	adsorption coefficient $[L^3/(M\bullet T)]$
K_2	=	desorption coefficient $[T^{-1}]$
x,y,z	=	coordinate directions $[L]$
t	=	time $[T]$
S_i	=	sources and sinks of the component due to reactions, phase transfers and resuspension of contaminated bed sediment

The first three terms in each equation represent dispersion or mixing due to temporal and spatial velocity gradients and density differences within the natural water system. The next three terms represent the longitudinal, lateral and vertical advection,

respectively. The seventh term in Equation (7-3) accounts for the vertical advection of the particulate component due to settling. The following two terms define the rates of adsorption and desorption, respectively. The last term accounts for the resuspension of contaminated bed sediment and the chemical and biological reactions and volatilization that may produce or degrade the component.

Note that since the distributions of the dissolved and particulate components depend on the concentration of the solids, m, an expression equivalent to Equations 7-2 and 7-3 is written for the distribution of solids:

$$\frac{\partial m}{\partial t} = \frac{\partial}{\partial x} (E_x \frac{\partial m}{\partial x}) + \frac{\partial}{\partial y} (E_y \frac{\partial m}{\partial y}) \frac{\partial}{\partial z} (E_z \frac{\partial m}{\partial z}) - \frac{\partial}{\partial x} u_x m \qquad (7-4)$$

$$- \frac{\partial}{\partial y} u_y m - \frac{\partial}{\partial z} u_z m + \frac{\partial}{\partial z} w_s m$$

In addition to sorption to suspended solids, hydrophobic chemicals can complex with dissolved, or colloidal, organic matter, DOC. Equations similar to 7-3 and 7-4 can be written for DOC complexed chemical, C_{doc}, and dissolved organic carbon. The total chemical, C_t, can be calculated from the sum of the dissolved and sorbed phases:

$$C_T = \phi C_d + C_p + \phi C_{doc} \qquad (7-5)$$

where ϕ = porosity (liquid volume/total volume)

which can also be expressed as:

$$= \phi C_d + rm + \phi r_{doc} \, m_{doc} \qquad (7-6)$$

where:

r_{doc} = chemical complexed with dissolved organic carbon [m/m]

m_{doc} = dissolved organic carbon concentration [m/l^3]

Adsorption is generally viewed as a rapid process relative to other processes affecting the chemicals being modeled. Following the conventional assumption, local instantaneous equilibrium is assumed (DiToro, et al., 1981; Connolly, 1984; Thomann and Mueller, 1987; O'Connor, 1988), and therefore the sorbed forms in equation 7-6 can be expressed in terms of the dissolved concentration:

$$C_T = \left[\phi + \pi m + \phi K_{doc}\, m_{doc} \right] C_d \qquad (7\text{-}7)$$

where:

$$\pi \quad = \quad f_{oc}\, K_{oc}$$

f_{oc} = organic fraction of solid particles [M/M]

K_{oc} = partition coefficient to particulate organic carbon, POC $[L^3/M]$

K_{doc} = $\beta\, K_{oc}$ $[L^3/M]$

β = ratio of DOC partition coefficient to POC partition coefficient

A dissolved fraction, f_d, can be calculated from equation 7-7:

$$f_d = \frac{C_d}{C_T} = \frac{1}{\phi + \pi m + \phi K_{doc}\, m_{doc}} \qquad (7\text{-}8)$$

as can the fraction sorbed to solids, f_p,

$$f_p = \frac{C_p}{C_T} = \frac{\pi m}{\phi + \pi m + \phi\, K_{doc}\, m_{doc}} \qquad (7\text{-}9)$$

and the fraction complexed to DOC, f_{doc}

$$f_{doc} = \frac{C_{doc}}{C_T} = \frac{K_{doc}\,m_{doc}}{\phi + \pi m + \phi K_{doc}\,m_{doc}} \qquad (7\text{-}10)$$

For modeling the fate of metals in sediments, an additional partitioning must be included: the precipitation of the metal as a metal sulfide. This is presented in detail in Section 7.3.3, below. Equations 7-8, 7-9 and 7-10 provide a computational benefit by allowing the total chemical to be represented in the modeling framework by a single equation instead of equations for each form. An equation describing the distribution of total chemical is obtained by summing the equations for the dissolved and sorbed phases:

$$\frac{\partial c_T}{\partial t} = \frac{\partial}{\partial x}\left(E_x \frac{\partial c_T}{\partial x}\right) + \frac{\partial}{\partial y}\left(E_y \frac{\partial c_T}{\partial y}\right) + \frac{\partial}{\partial z}\left(E_z \frac{\partial c_T}{\partial z}\right) \qquad (7\text{-}11)$$

$$-\frac{\partial u_x c_T}{\partial x} - \frac{\partial u_y c_T}{\partial y} - \frac{\partial u_z c_T}{\partial z} + \frac{\partial}{\partial z}\,w_s\,(f_p\,c_T)\ \pm S$$

Equations analogous to Equations 7-4 and 7-11 are written for the bed. Interactions between the water column and bed are specified by boundary conditions at the water-bed interface. Together the water column and bed equations form the system of general mass balance equations needed to model chemical fate in surface waters. Analytical solution of these equations is not possible and an upgraded version of the WASTOX modeling framework (Connolly and Winfield, 1984) is used to numerically solve a finite difference approximation of the mass balance equations.

7.2 PREVIOUS APPLICATION OF MODELS

There is a well established precedent for quantitative models in water quality analyses of both fresh and marine environments. Over the past 30 or more years, extensive work has been done to establish the modeling approach, which has been employed by the EPA and many state and regional agencies to address specific problems. Early modeling was directed primarily to dissolved oxygen and eutrophication problems

and, as documented in many instances with intensive data, played a significant role in ongoing water quality improvement.

More recent efforts have included modeling the transport and fate of potentially toxic substances. While many of these studies are still in various stages of development, a sufficient number of projects employing mathematical models have been completed, and acceptance in the general approach has been established. As EPA's Science Advisory Board has recognized, "Mathematical models of the phenomena provide an essential element of the analysis and understanding" (U.S. EPA, 1989).

Notable examples of toxics modeling with direct relevance to the problem in the Pawtuxet River are:

1.   The analyses of Kepone in the fresh and marine stretches of the James River over a period of approximately two decades preceding and following the banning of this chemical.   Hydrodynamic,   suspended   bed   solids,   physical. and   chemical mechanisms, and food chain analyses were individually modeled and incorporated in a overall framework to address environmental questions. The analysis indicated that a no-action plan was the most feasible remedial alternative.

2.   PCB analysis is the Saginaw River, sponsored by General Motors Corporation. The work determined the time required to reduce PCB concentrations in both the water and bed of the River. In addition, EPA sponsored a modeling study of the physical chemical fate of PCBs in Saginaw Bay.

3.   An EPA study, presently underway, is addressing PCB problems in Green Bay, Wisconsin including the elements of sources, transport, fate and food chain. This study is similar to the Kepone analysis in the James River.

7.3   SPECIFICATION OF MODEL INPUT PARAMETERS

7.3.1 Transport

The equations describing the transport of dissolved and particulate material in the Pawtuxet River include terms for velocity and dispersion in the lateral and longitudinal direction, as well as settling and resuspension rates that transport solids and sorbed chemical between the water column and sediment. Each of these terms were calculated in the hydrodynamic and sediment transport model components. The chemical fate and transport model uses the same computational grid as the hydrodynamic and sediment transport models, and therefore time variable transport information is available for each contaminant fate model segment. Transport information provided by the hydrodynamic and sediment transport components was averaged over a one day period in order to realistically incorporate the effects of shorter term events, and yet keep the data files containing the transport information within disk storage limitations.

7.3.2 Sorption Parameters - Organic Chemicals

The partition coefficient describes the distribution of a chemical between dissolved and particulate phases, in particular organic carbon. Values for the partition coefficient may be obtained from laboratory experiments, field data and/or other more easily measured physical-chemical parameters. The carbon referenced partition coefficient, Koc, correlates with the octanol-water partition coefficient, K_{ow}, of the chemical. For this project a direct linear relationship between K_{oc} and K_{ow} was assumed, consistent with a data summary conducted to support sediment quality criteria (USEPA, 1993).

$$K_{oc} = K_{ow} \tag{7-12}$$

The assigned K_{ow} values for each chemical are presented in Table 7-1. Also presented in Table 7-1 are the range of K_{ow} values found in the literature reviews, K_{ow} values calculated based on a single pore water measurement taken during the Phase II sediment

sampling and values provided by a computer program, SPARC (Karickhoff, et.al., 1991) that estimates chemical constants based on molecular structure. The final K_{ow} value used in the model for each chemical was determined by weighing literature and calculated values against the chemical model calibration and using the K_{ow} value that most closely represented the dynamics of the Pawtuxet River system. Model sensitivity runs were used to assess the importance of the range of K_{ow} values.

TABLE 7-1. CHEMICAL OCTANOL - WATER PARTITION COEFFICIENTS			
Chemical	Value Used in Model	Range of Literature Values	Calculated Value
Chlorobenzene	2.84[a]	2.13 - 3.00[b]	3.35[c]
Naphthalene	3.35[a]	3.01 - 4.70[b]	3.53[c]
Total PCB	6.00[b]	5.6 - 6.5[b]	5.02[c]
Tinuvin 328	6.71[c]	-	6.71[c], 8.33[d]

[a] Handbook of Environmental Fate and Exposure Data for Organic Chemicals, P.H. Howard
[b] Illustrated Handbook of Physical - Chemical Properties and Environmental Fate for Organic Chemicals, Vol. 1 - Mackay, Shiu & Ma
[c] Calculated based on Field Measurements of one pore water sample
[d] Calculated using SPARC

The partition coefficient is then obtained from:

$$K_p = f_{oc} * K_{oc} \qquad \text{(7-13)}$$

The fraction organic carbon, f_{oc}, values assigned to the bed solids are based on five field surveys conducted on the Pawtuxet River between January 1990 and July 1994. The f_{oc} value for each model segment is the average of all measurements in the segment. From these segment averages, f_{oc} values were interpolated for model segments for which f_{oc} data were unavailable. Figure 7-1 presents the f_{oc} data and assigned values for each model segment. The f_{oc} assigned to the water column solids was based on water column total and volatile suspended solids.

Partitioning to the dissolved organic carbon, DOC, phase in the water and sediment was modeled in a manner analogous to the partitioning to solids described above. The partion coefficient for DOC is expressed as:

$$K_{doc} = \beta * K_{ow} \tag{7-14}$$

Based on measurements in other systems β values of 0.20 and 0.06 were assigned for the sediment and water column, respectively. Water column DOC levels were assigned at 4.0 mg/l, a typical value for this type system (Thurman, 1985).

7.3.3 Partitioning of Zinc in Sediment

Metals in sediment are generally viewed as being partitioned among three phases: dissolved, sorbed and precipitated. Dissolved metal includes free metal ion and inorganic and organic metal complexes. Sorbed metal is associated with various components of the particulate matter, including iron and manganese oxides and organic matter. Precipitated metal is mostly complexed with the acid-volatile sulfide (AVS) in the sediment. The total metal concentration is thus the sum of the three components:

$$c_T = \phi c_d + c_p + c_{avs} \tag{7-15}$$

where:

c_T	=	total metal concentration (mass per unit total volume)
ϕ	=	the porosity of the sediment
c_d	=	dissolved metal concentration (mass per unit pore water volume)
c_p	=	sorbed metal concentration (mass per unit total volume)
c_{avs}	=	precipitated metal concentration (mass per unit total volume)

The precipitated component was calculated from measured concentrations of total metal and AVS. The AVS available to zinc was determined by subtraction of the molar concentration of copper; the only competing metal of significance in the sediment. Where

the molar concentration of total zinc exceeded the available AVS, c_{avs} was assumed to equal the AVS. Otherwise, c_{avs} was assumed to equal c_T.

Dissolved and sorbed zinc were assumed to be in an equilibrium described by a langmuir isotherm:

$$c_p = \frac{mr_m \, \pi c_d}{r_m + \pi c_d} \qquad (7\text{-}16)$$

where:

m = concentration of particulate matter (mass per unit total volume)

r_m = sorptive capacity of the particulate matter (mass per mass of particulate matter)

π = partition coefficient

At low metals concentrations ($\pi \, c_d << r_m$) the relationship reduces to the linear partitioning used for the organic chemicals, i.e.:

$$c_p = m\pi c_d \qquad (7\text{-}17)$$

At high metals concentrations ($\pi \, c_d >> r_m$) the particulate concentration reaches a maximum:

$$c_p = mr_m \qquad (7\text{-}18)$$

The values of the sorptive capacity and the partition coefficient are functions the composition of the particulate matter. Additionally, the partition coefficient varies with pH and the presence of competing sorptive phases in the water. In natural sediments, organic matter appears to be the significant particulate component. Sorptive capacities and partition coefficients between the organic matter (expressed as organic carbon) and the free metal ion (K_{oc}) measured as part of the EPA effort to develop sediment quality criteria

for metals are shown in Table 7-2. These data indicate significant differences among metals that preclude direct extrapolation to zinc. Observations that the bonding strength and complex stability of zinc onto humic or fulvic acids is less than either copper or lead and similar to or slightly greater than cadmium (Förstner and Wittman, 1979; Pettersson et al., 1993), provide some basis for inference.

Table 7-2. Organic carbon partition coefficients and binding capacity of organic carbon for copper,cadmium and lead (USEPA, 1994).				
	K_{oc} (l/kg OC)			Capacity mg/kgOC
	pH 6	pH 7	pH 8	
Copper	390,000	2,700,000	2,000,000	118,000
Cadmium	21,000	250,000	910,000	54,000
Lead	250,000	350,000	-	340,000

Measurements conducted on the pore water and bulk sediment of a core collected in the Pawtuxet River as part of the RIFS (Table 7-3) were used with the EPA data to establish values of r_m and K_{oc}.

Table 7-3. Zinc, TOC and AVS concentrations measured in a sediment core from the Production Area	
pore water Zn	6.9 mg/l
sediment Zn	1800 mg/kg
sediment TOC	7.9 %
sediment AVS	340 mg/kg (10 mmol/kg)

To determine a value of K_{oc} from the Pawtuxet data, sorbed zinc was calculated by subtraction of precipitated zinc from sediment zinc. The molar concentration of precipitated zinc was assumed to be equal to the molar concentration of AVS; a reasonable assumption because zinc is the dominant metal species in the sediment. Thus,

the precipitated zinc equals 650 mg/kg (10 mmol/kg x 65 mg/mmol) and the sorbed zinc equals 1150 mg/kg. The concentration sorbed per unit carbon is 14,600 mg/kgOC and K_{oc} is 2100 l/kgOC. This partition coefficient value is ten to one thousand times lower than the values shown in Table 7-2, suggesting that the sorbed concentration may be at or near the sorption capacity. The sorbed concentration is of the same order as the sorptive capacities in Table 7-2: about a factor of four lower than the cadmium value and a factor of eight lower than the copper value. Therefore, the Pawtuxet data are presumed to provide an estimate of the sorptive capacity of the Pawtuxet sediments. Lacking site specific data for the linear partition coefficient K_{oc}, a value of 10^5 was assumed. This value is consistent with the EPA data at neutral pH.

7.3.4 Volatilization

The flux, j, of toxic chemical across the air-water interface due to volatilization from surface waters is described by the following equation:

$$j = K_{OL}(\frac{P}{H} - c)$$

(7-19)

where

K_{OL} = overall mass transfer coefficient

P = partial pressure of the chemical in the atmosphere

H = Henry's constant

For the organic chemicals being modeled the partial pressure in the atmosphere is small and Equation (7-14) reduces to:

$$j = -K_{OL}c$$

(7-20)

The rate of transfer of chemical given by K_{OL} is controlled by properties of the chemical and conditions at the air-water interface. The value of K_{OL} is computed using the two film

theory first proposed by Lewis and Whitman (1924). This theory assumes that the rate of transfer is controlled by diffusion through laminar layers at the air-water interface in which the concentration gradients driving transfer are localized. The transfer rate coefficients are defined as follows:

$$\frac{1}{K_{OL}} = \frac{1}{K_L} + \frac{RT}{HK_G} \qquad (7\text{-}21)$$

where:

K_L = liquid mass transfer coefficient

K_G = gas mass transfer coefficient

R = the gas constant

T = absolute temperature

Mackay and Yeun (1983) demonstrated the validity of this equation for organic chemicals under environmentally relevant conditions. The liquid and gas transfer coefficients in Equation (7-16) are dependent on turbulence at the interface, temperature, and properties of the chemical such as diffusivity. Empirical correlations have been developed relating these coefficients either directly to physical parameters including wind velocity, molecular weight and diffusivity of the chemical, and the density and viscosity of the water (Southworth, 1979a,b: Mackay and Yeun, 1983) or to transfer coefficients of oxygen and water vapor (Liss and Slater, 1974). These correlations are useful but their general applicability have not been tested. The former were developed considering only a region of the full spectrum of environmental conditions, particularly with regard to the effect of winds. The latter are based on theoretical reasoning but have not been extensively compared to prototype data. O'Connor (1983) presented a theoretical development of the liquid transfer coefficient applicable to the full range of hydrodynamic conditions. This approach is incorporated in the model.

Henry's Law constants used in the model for each chemical, and the range in literature values, are presented in Table 7-4. Model sensitivity runs are used to assess the significance of these differences.

TABLE 7-4. HENRY'S CONSTANT		
Chemical	Model Value	Literature Range
Chlorobenzene	350^a	$237 - 545^b$
Naphthalene	48^a	$29.2 - 123.95^b$
Total PCB	20^b	$1.72 - 47.59^b$
Tinuvin 328	$<<1^d$	-
Zinc	-	-
[a] Handbook of Environmental Fate and Exposure Data form Organic Chemicals, P.H. Howard [b] Illustrated Handbook of Physical - Chemical Properties and Environmental Fate for Organic Chemicals, Vol. 1 - Mackay, Shiu & Ma [d] Calculated using SPARC		

The liquid film mass transfer coefficient was calculated using the O'Connor-Dobbins reaeration equation, modified by differences in diffusivity between oxygen and these chemicals. The gas film mass transfer coefficient was assumed to be constant at 100 m/d, a value appropriate for riverine systems (O'Connor, 1983).

7.3.5 Mass Transfer Rate Coefficients for Diffusion in Sediments

The mass transfer coefficient for diffusion between the sediment pore water and the overlying water column was set to 0.2 cm/d for all five chemicals. The transfer is controlled by the dynamics occurring in the water layer and is difficult to assign prior. The value of 0.2, which is slightly greater than molecular diffusion, was determined in the model calibration process. Diffusion within the pore water of the sediment layer and between the pore water of the sediment layer and sediment boundary was assigned at the molecular diffusion rate, except for zinc. The sediment-sediment diffusion mass transfer

coefficient for zinc was assigned at a rate slightly lower than the molecular diffusion rate, 0.20 cm/d vs 0.24 cm/d.

DIFFUSIVE EXCHANGE		
Chemical	Water-Sediment Diffusion (cm/d)	Sediment-Sediment Diffusion (cm/d)
Chlorobenzene	0.20	0.16
Naphthalene	0.20	0.15
Total PCB	0.20	0.09
Tinuvin 328	0.20	0.08
Zinc	0.20	0.20

7.3.6 Biodegradation

The rate of biodegradation is a function of the size and activity of the bacterial populations, the amount and activity of the bacterial enzyme(s) attacking the substrate, and the availability of substrate (contaminants). There are many difficulties inherent in estimating the processes that determine biodegradation activity. The growth kinetics of the complex bacterial populations degrading a toxic chemical under environmental conditions are not well understood. The presence of competing substrates, other bacteria, the toxicity of the chemical to the degrading bacteria, and the possibilities of adaptation to the chemical or co-metabolism make quantification of changes in the population difficult. In order to calculate conservative estimates of future contaminant concentrations, it is assumed that the chemicals studied are not subject to biodegradation processes.

7.3.7 External Inputs

Groundwater enters the river near the location of the Ciba facility production area and transports measurable amounts of chlorobenzene and naphthalene into the river. PCB,

Tinuvin 328, and Zinc sorb more strongly to the solid substrate through which the groundwater flows, and therefore groundwater advection does not represent a significant pathway for these chemicals. The degree to which a chemical can be transported via groundwater flow is reflected in the chemical Kow value; chemicals with lower Kow values are transported more easily than those chemicals with higher Kow values.

Based on hydrogeological analyses, the groundwater flow entering the river is only a small fraction of the total flow of the river and does not impact the river hydrodynamically. However, this flow and the associated concentrations of Chlorobenzene and Naphthalene combined to produce measurable mass fluxes to the river; 0.5 lb/day for Chlorobenzene and 0.01 lb/day for Naphthalene. The mass flux of chlorobenzene was estimated from a mass balance calculation based on daily river flow and increases in water column chlorobenzene concentrations observed between stations 3 and 4. Naphthalene data at stations 3 and 4 were too variable to use in the same manner. However, in a pore water sample obtained from the sediments along the production area bulkhead, chlorobenzene was measured at 15,000 ug/l and naphthalene at less than 500 ug/l. Assuming the ratio of the loads to be equal to the ratio of the pore water concentrations (less than 0.033) a naphthalene load of less than 0.017 lb/d was calculated, and a value of 0.01 was used in the analysis.

7.3.8 Boundary and Initial Conditions

Upstream boundary conditions for the water column are based on monitoring data collected in 1992 and 1994, supplemented with USGS data for PCBs and zinc which was retrieved from USEPA's STORET database (Figure 7-2). While data for chlorobenzene, naphthalene, and zinc include some non-detected results, there were a sufficient number of valid data points that a maximum likelihood estimator (MLE) algorithm (Aithchinson, 1957) could be used to evaluate the mean and standard deviation of concentrations of each chemical (Table 7-1). Based on these statistics, time variable boundary conditions were randomly generated with the aid of a monte carlo program. The daily values specified in the model input have means and standard deviations that match those derived

from the data analysis. PCB and Tinuvin 328 data did not provide enough information to apply the MLE technique and therefore, temporally constant boundary conditions were assigned for these chemicals. PCB concentrations were set at 5 ng/l, approximately half of the detection limit used in the water column monitoring conducted as part of this effort. Tinuvin 328, was not measured in any of the water column monitoring and was assigned as zero.

Chemical	Statistics	
	Mean, $\bar{x}$	Standard Deviation, s
Chlorobenzene	1.32	0.66
Naphthalene	0.32	0.51
Zinc	26.60	0.43

The sediment boundary and initial conditions were both calculated in the same manner using data collected during the Phase II sediment sampling for the contaminant fate and transport model (except chlorobenzene which is supplemented with Release characterization data). Data from 0-5 cm sediment cores were used in the initial condition calculation while 5-10 cm sediment cores were used to determine boundary conditions. As with the foc values, chemical values for each model segment were averaged and from these segment averages, chemical values were interpolated for model segments for which chemical data were unavailable.

7.4 CALIBRATION

Calibration of a contaminant fate model involves comparison of model and data on several time scales, including: time of travel, storm event, seasonal and decadal. The time of travel scale provides an assessment of volatilization and fluxes between the water column and sediment (i.e., diffusion, settling and resuspension) by comparing observed and computed spatial changes in water column concentration. The storm event and seasonal scales provide further assessment of these processes by comparing observed and

computed water column concentrations under different flow regimes. The decadal time scale provide an assessment of the rate of sedimentation by comparison of observed and computed changes in sediment concentrations. In this study, as in most other cases, data does not exist at all of the relevant time scales. In particular, sediment contaminant measurements are not available on the decadal time scale nor during storm events. This lack of data is compensated for by the independent calibration/validation of the sediment transport model from which the resuspension, settling and sedimentation rates are derived.

Given the data limitations, the focus of the calibration is the processes that control the spatial distributions in the water column under low to moderate flow conditions: volatilization, partitioning, diffusion and settling. In most cases the descriptions of these processes were derived from independent studies and were not adjusted during calibration. In essence the calibration was a validation of these process descriptions. Diffusion and zinc partitioning were exceptions to this, in that independent information was limited. The diffusion rates were established in calibration, in concert with the groundwater loadings, such that the model best reproduced the spatial changes observed in the water column and maintained pore water contaminant concentrations consistent with observed data. The zinc partitioning was similarly defined by comparison to the pore water zinc measurements.

An approximate two year period (3/3/92 to 4/30/94) was used for calibration. The measured sediment concentrations were used to establish initial conditions and the model was compared to water column contaminant concentrations measured during the early portion of this period. Changes in bed concentrations over this period were also examined to determine that the calibrated diffusion rates were consistent with the expectation, based on limited historical data, that the bed concentrations would not change dramatically over a two year period.

Figures 7-3a&b present comparisons of computed water column chlorobenzene concentrations to data collected in 12 surveys between May and July 1992. In general, chlorobenzene concentrations decreases slightly from kilometer point 6.9 to 2.2 due to volatilization. At the facility reach, the water column concentration increases due to the

groundwater source at this location. The computed increase generally reproduces the observed change in this region.

Figure 7-4 shows the initial (dashed line) and final (solid line) sediment chlorobenzene concentrations for the north bank, center channel, and south bank of the river. Concentrations on the north bank of the river increased slightly over the two year period, generally by less than 0.1 mg/kg. The peak concentration at the facility location remained constant at approximately 3000 mg/kg. The center channel and the south bank sediment concentrations change very little. In general the computed changes tend to reduce initial spatial gradients.

A sensitivity analysis of the chlorobenzene model is summarized on Figure 7-5, through presentation of sediment concentrations along the north bank of the river. The model shows virtually no response to changes in resuspension or deposition of cohesive sediments. Changes in resuspension are accomplished by using the 95 percent confidence limits for the mean of the resuspension parameter a_o (Eq. 5-9), which represents an approximate halving and doubling of this parameter. Increased and decreased deposition of cohesive sediments correspond to a halving and doubling of the critical shear stress for deposition. Sediment concentrations are not sensitive to these changes, however, because of the relatively low partitioning of chlorobenzene and the limited amounts of resuspension and cohesive sediment deposition within the study area. An increase in the deposition of non-cohesive particles (doubling of the settling velocity) produces an increase of approximately 0.05 mg/kg in two locations where deposition is more significant. A halving and doubling of the water column-sediment diffusive exchange coefficient produces changes in sediment chlorobenzene concentrations of approximately 25 percent or less. A factor of 10 variation in the partition coefficient (log Kow of 2.25 to 3.25) produces a range in computed sediment concentrations of approximately a factor of 5. This range in Kow encompasses most of the range of values reported in the literature (see Table 7-1). Computed sediment concentrations are not sensitive to variation of Henry's constant within limits reported in the literature (see table 7-4). In areas of low chlorobenzene concentration, a fairly linear response to changes in water column boundary

conditions is computed, indicating these areas are in equilibrium with water column chlorobenzene concentration. In locations where concentrations are above 0.1 mg/kg, the sediment is not sensitive to changes in water column concentrations.

Naphthalene water column concentrations are plotted with data collected in 1992 on Figures 7-6a&b. Spatial patterns observed from these data are much less consistent than the chlorobenzene data. Increases in concentration near the facility are not observed in most data sets and no significant increase is calculated by the model. Computed spatial patterns generally decrease slightly from upstream to downstream. The water column data generally vary more than the computed concentrations. Computed sediment naphthalene concentrations (Figure 7-7) show patterns similar to chlorobenzene. The peak concentration near the facility remains fairly constant, at about 140 mg/kg. Concentrations in the remainder of the north side of the river increase, in most cases by less than a few hundredths of a mg/kg. Spatial gradients in the center channel and south bank tend to reduce.

A sensitivity analysis of the naphthalene model is summarized on Figure 7-8, again using sediment concentrations from segments along the north bank. Similar to chlorobenzene, changes in resuspension parameters do not noticeably affect sediment naphthalene concentrations. Doubling and halving of the critical shear stress for cohesive sediment deposition produces changes of less than 0.01 mg/kg. Doubling the settling velocity of non-cohesive solids produces an increase of roughly 0.05 mg/kg in two locations. Halving and doubling the diffusion coefficient between the water and sediment produces changes of near 20 percent, or less, in computed sediment concentrations. An order of magnitude range in Kow results in a factor of three to almost an order of magnitude range in sediment naphthalene concentrations in most locations. Peak concentrations, above 0.1 mg/kg are less sensitive to this change. Computed sediment concentrations are not sensitive to changes in Henry's constant within limits reported in the literature. Changes in upstream water column boundary conditions produce fairly linear responses in computed sediment concentration in locations where concentration are less

than a few hundredths of a mg/kg. Peak concentrations are fairly insensitive to changes in upstream boundary conditions.

Computed water column PCB concentrations are plotted with available data on Figure 7-9a&b. The majority of water column PCB data are below the detection limit of approximately 11 ng/l. For May 28, 1992, when data are above the detection limit, boundary conditions at Cranston and for the Pocasset River were assigned to reproduce the upstream data. The computed decrease downstream of km 5.5 is due to deposition and diffusion into the sediment. Boundary condition for the remainder of the simulation were assigned at 5 ng/l, approximately half of the detection limit. Sediment PCB concentrations (Figure 7-10) change very little during the two year calibration, suggesting that the processes affecting PCB concentrations are fairly slow.

Sensitivity analyses for PCB (Figure 7-11) indicate very minor changes in sediment concentrations in response to approximately halving and doubling the resuspension parameter, a_o. This is due to the limited erosion within the study area. Halving and doubling the critical shear stress for cohesive solids deposition results in changes of less than a few hundredths of a mg/kg, suggesting that the sediments are close to being in equilibrium with the assigned water column concentration (boundary condition = 5 ng/l). Increased non-cohesive deposition provides dilution to the elevated concentrations near the facility, but little change downstream of this location. PCB concentrations are not sensitive to the water column-sediment diffusion coefficient because the sorption characteristics of PCB keep the majority in the particulate form. A factor of 10 range in Kow (log Kow = 5.5 to 6.5) results in less than a factor of 2 range in computed sediment concentration, with several areas showing considerably less than a factor of 2 variation. Sediment concentrations are not sensitive to a range of Henry's constant from 2 top 100. Sensitivity to upstream boundary conditions was evaluated by replacing the temporally constant calibration concentration of 5 ng/l with values of 11 ng/l (the detection limit) and 1 ng/l. Areas of lower concentration were affected by several tenths of a mg/kg, however peak concentrations were not affected.

Water column data for Tinuvin 328 were consistently below the detection limits, which varied between roughly 1 and 10 ug/l. Because of the lack of data for comparison, water column results for Tinuvin are not presented graphically. Sediment Tinuvin 328 concentrations (Figure 7-12) do not vary significantly during the calibration period. The most noticeable changes occur at the Pawtuxet Cove Dam where deposition of relatively clean solids dilutes in-place concentrations.

Sensitivity analyses for Tinuvin are presented on Figure 7-13. Tinuvin is not sensitive to resuspension, and because water column concentrations are so low, changes in deposition of cohesive solids do not affect sediment concentrations. Increased deposition of non-cohesive solids (factor of 2 increase in settling speed) provides increased dilution, which is most significant at the upstream end of the facility reach and upstream of the Pawtuxet Cove Dam. Near the facility this additional dilution decreases concentrations by almost a factor of 10 and by almost two orders of magnitude near the dam.

Water column zinc data and computed concentrations are presented on Figures 7-14a&b. Both model and data indicate fairly uniform concentrations from upstream to downstream, although the data are more variable than the computed concentrations. An increase in concentration is calculated near the location of the peak sediment zinc concentrations, however the magnitude of the increase is small relative to the variability in the water column data. Sediment zinc results (Figure 7-15) indicate a reduction in concentration in locations where levels are greater than approximately 600 mg/kg and increasing levels in locations where concentrations are below 600 mg/kg. This is in response to contaminant concentrations on solids depositing from the water column. The peak just upstream of the facility reach decreases from approximately 4000 mg/kg to 2000 mg/kg.

Figure 7-16 presents the zinc sensitivity analyses. Sediment zinc concentrations are unaffected by approximately halving and doubling the resuspension parameter, a_0. Because of the elevated water column concentrations of zinc, changes in cohesive

sediment deposition affect the amount of sorbed zinc deposited to the sediment. A halving and doubling of the critical shear stress for deposition results in changes in sediment zinc concentrations of 20 to 50 percent in some locations. A doubling of the settling velocity of non-cohesive solids produces a dramatic decrease at the peak, from approximately 2000 to 700 mg/kg. Upstream of the Pawtuxet Cove Dam the increased settling velocity raises zinc concentrations by 40 to 90 percent, reaching levels of between 400 and 500 mg/kg. These changes are driven by the concentration of zinc on the non-cohesive particles.

In the vicinity of the Facility, zinc concentrations exceed the sorption capacity of the solids and as result, halving and doubling the diffusive exchange between the water column and bed produces almost a 50 percent change in the computed zinc concentration. Sediments in other portions of the study area are not sensitive to the diffusive exchange rate because of the relatively small fraction of zinc in the dissolved phase. An order of magnitude increase and decrease in the partition coefficient produces changes of a factor of 2 or more in computed sediment zinc concentrations, due to changes in contaminant concentrations on depositing solids. In a similar fashion a 50 percent increase or decrease in water column boundary conditions affects the concentration of zinc on depositing solids which results in sediment concentration changes of as much as 20 to 40 percent at some locations.

Figures
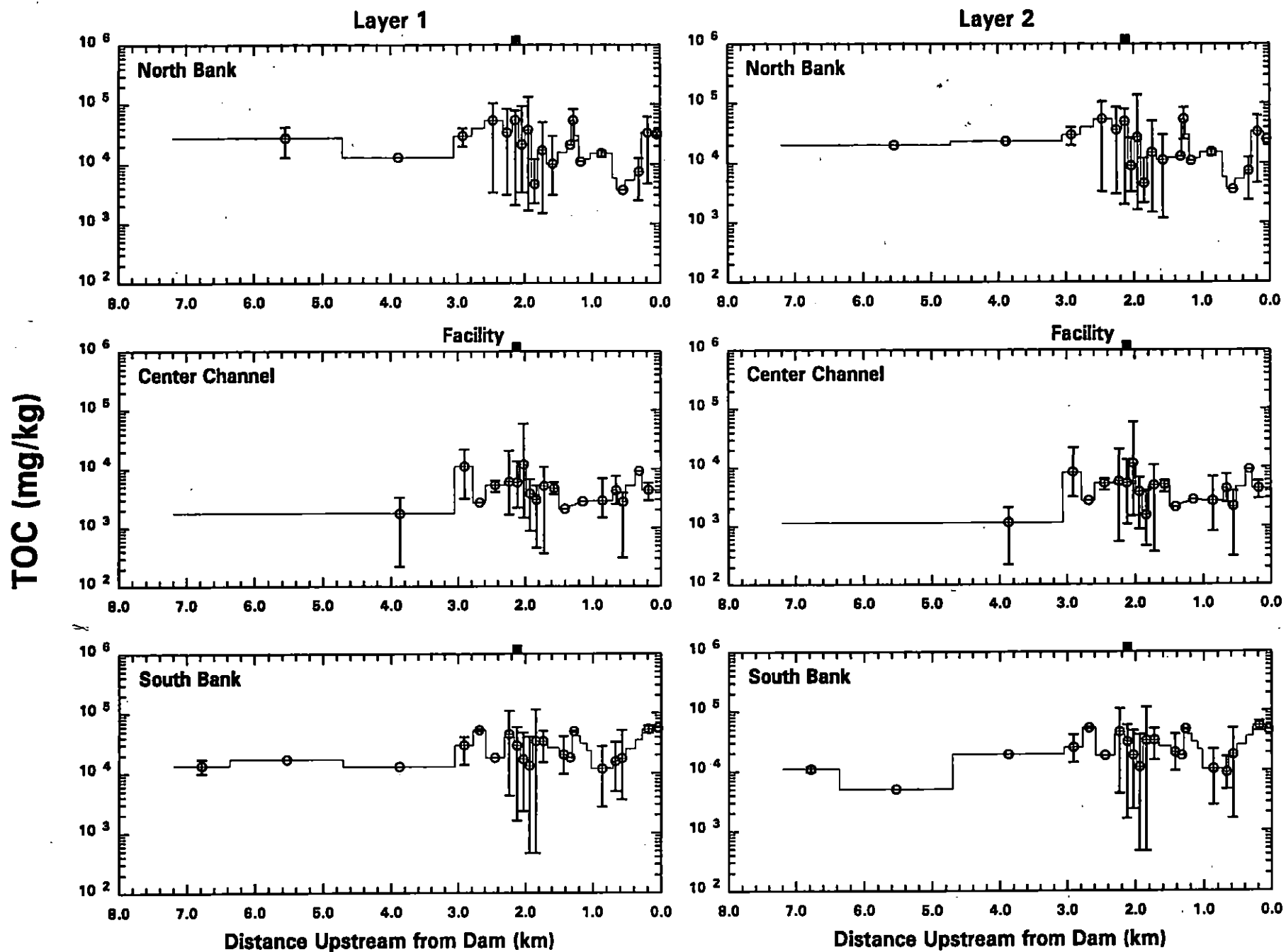
FIGURE 7-1. Total organic carbon sediment concentrations (○ - data, mean and range — - model
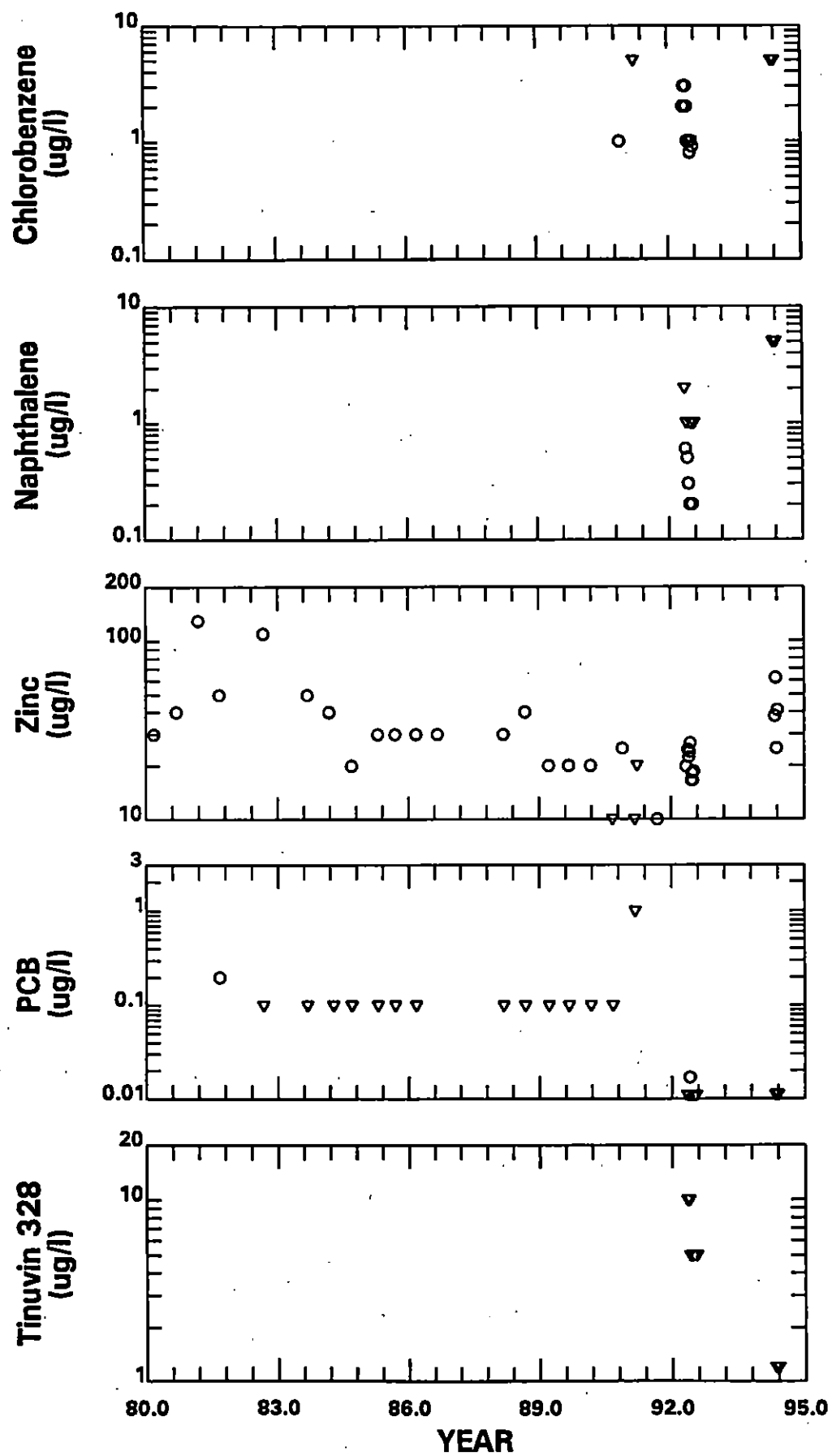
FIGURE 7-2.   Upstream boundary water column data
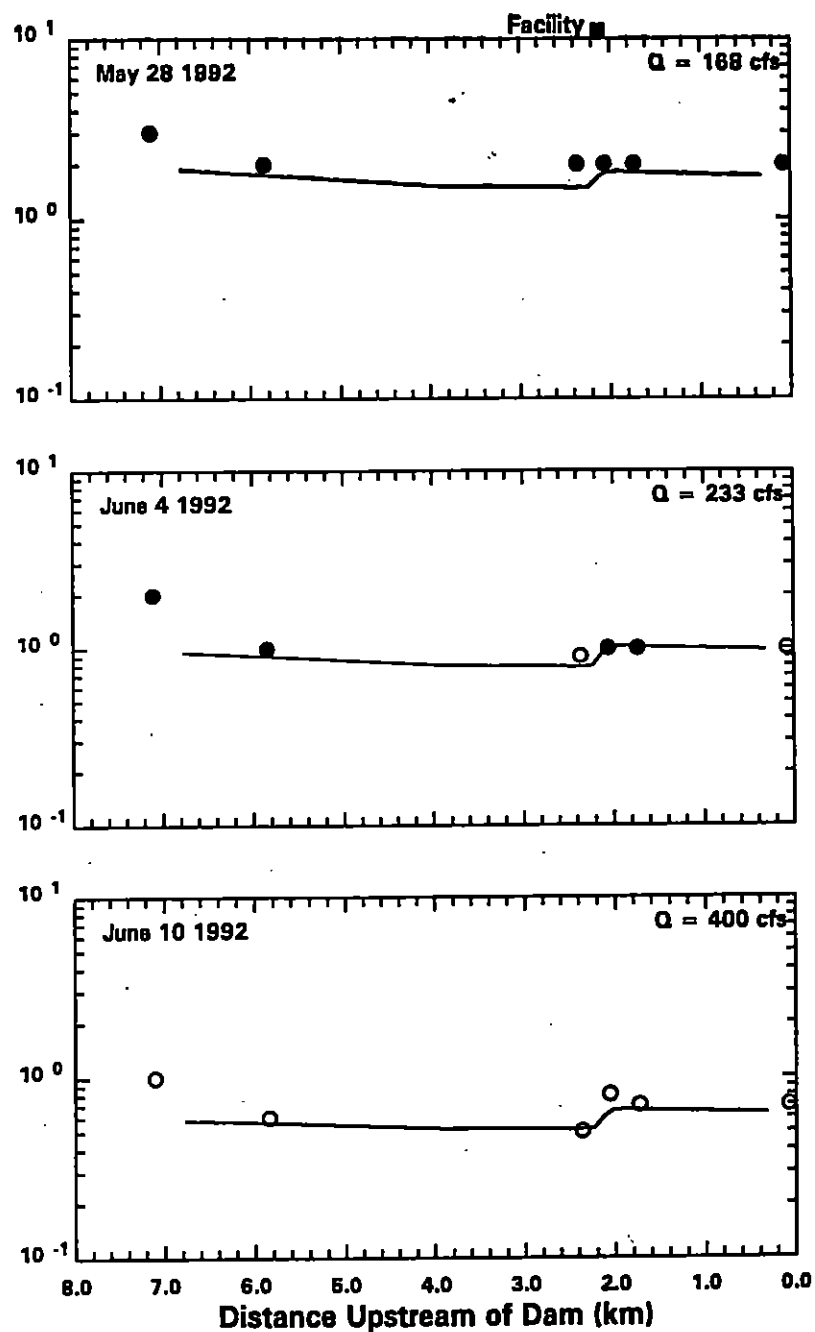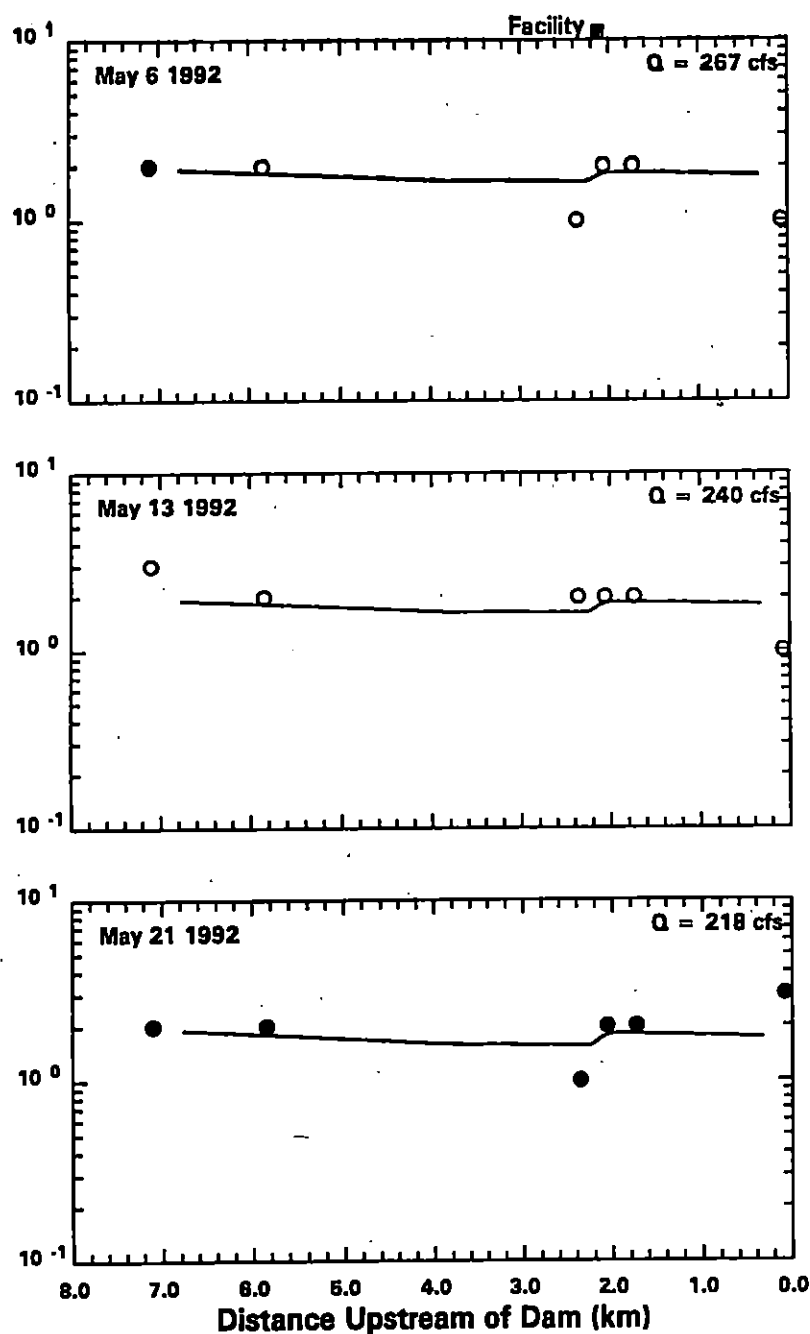
FIGURE 7-3a. Chlorobenzene Calibration - Water Column Concentrations
(— model ● measured, ○ estimate, ∇ non-detect)
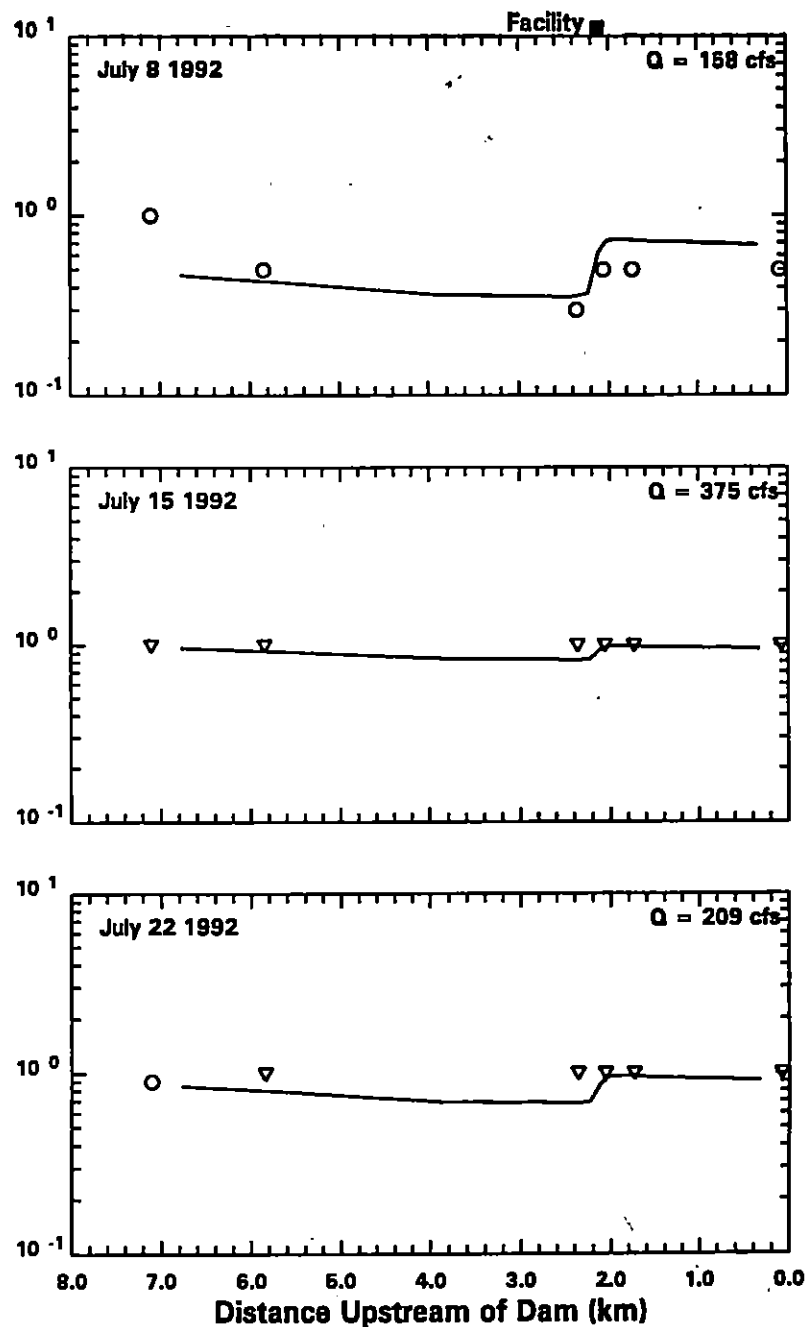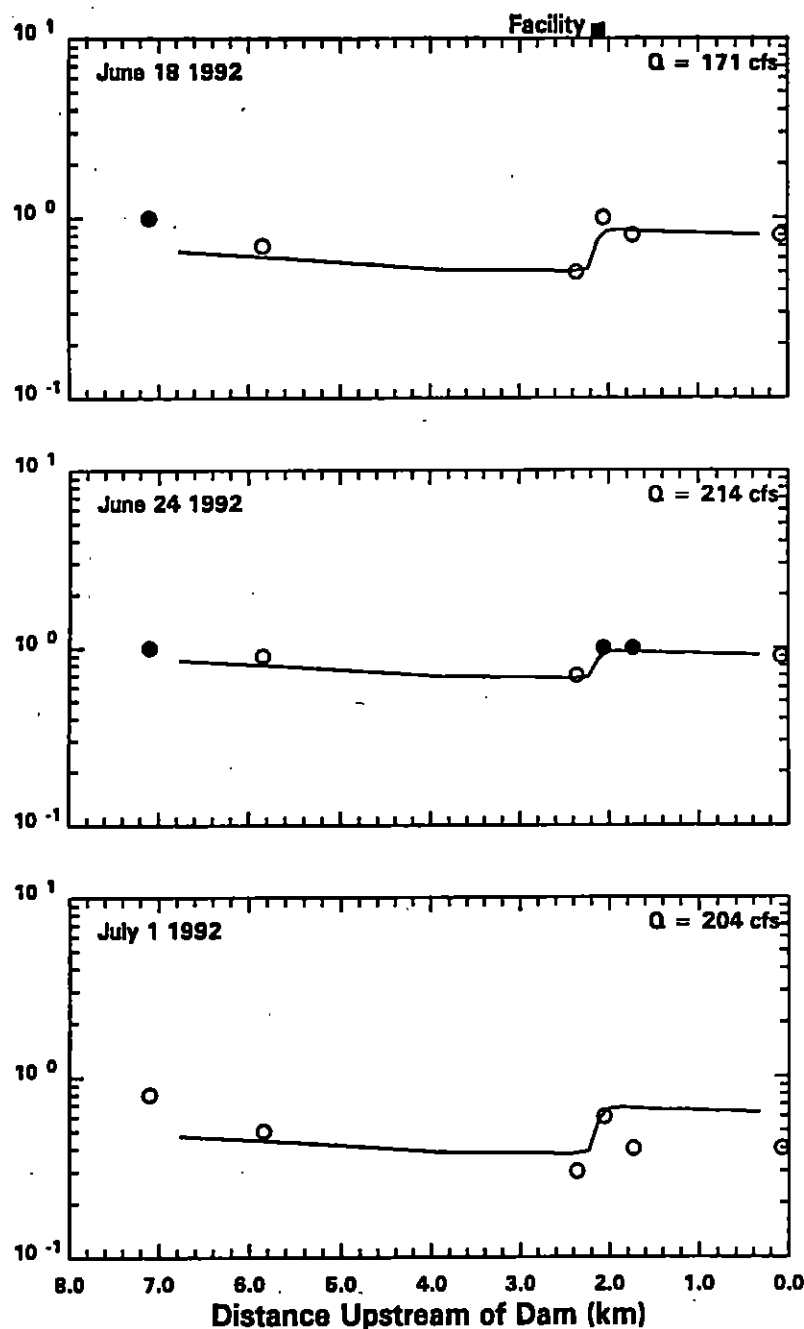
FIGURE 7-3b. Chlorobenzene Calibration - Water Column Concentrations
(— model ● measured, ○ estimate, ∇ non-detect)

Pawtuxet River
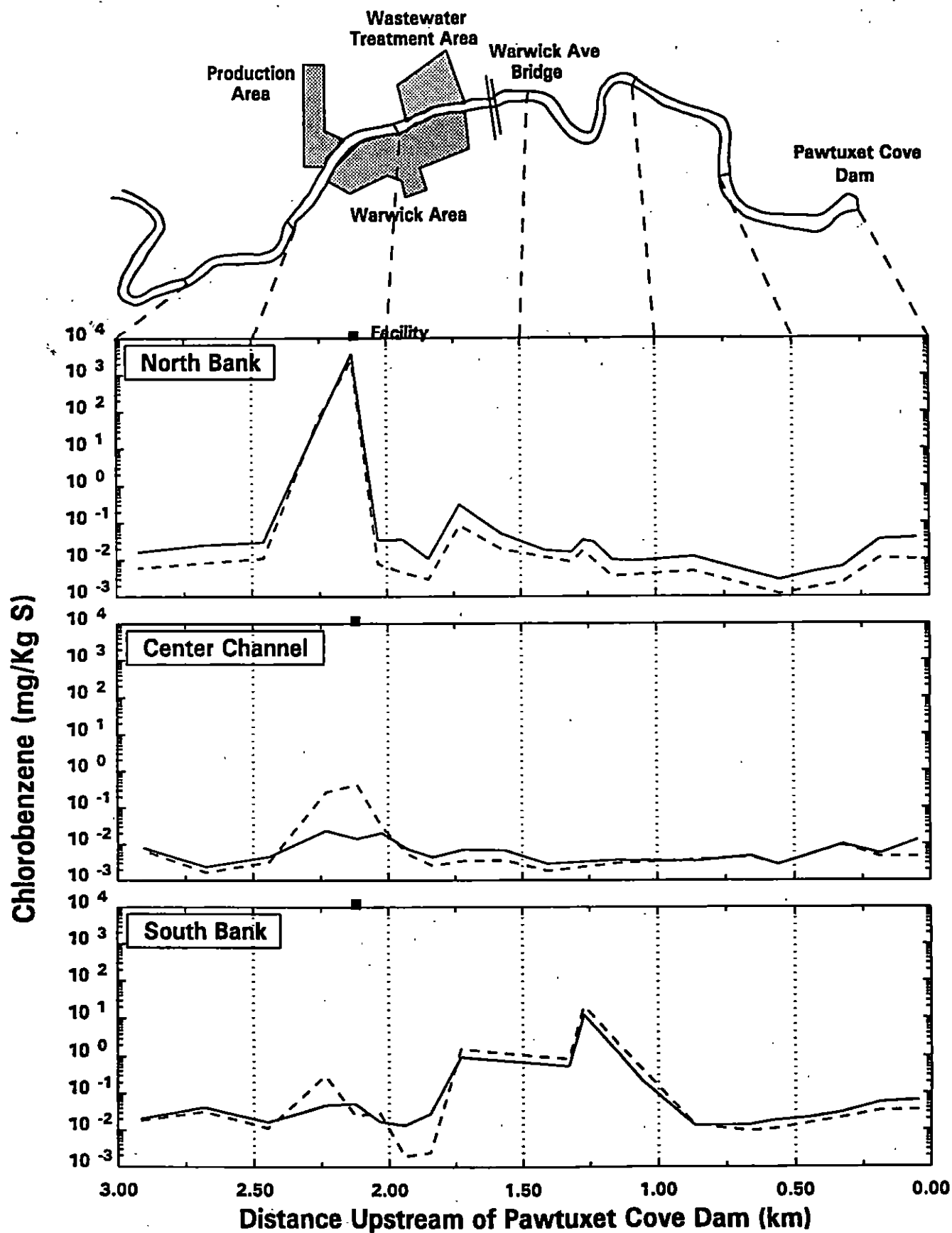
FIGURE 7-4.   Chlorobenzene Calibration - Sediment Concentrations
(--- 3/3/92 — 4/30/94)
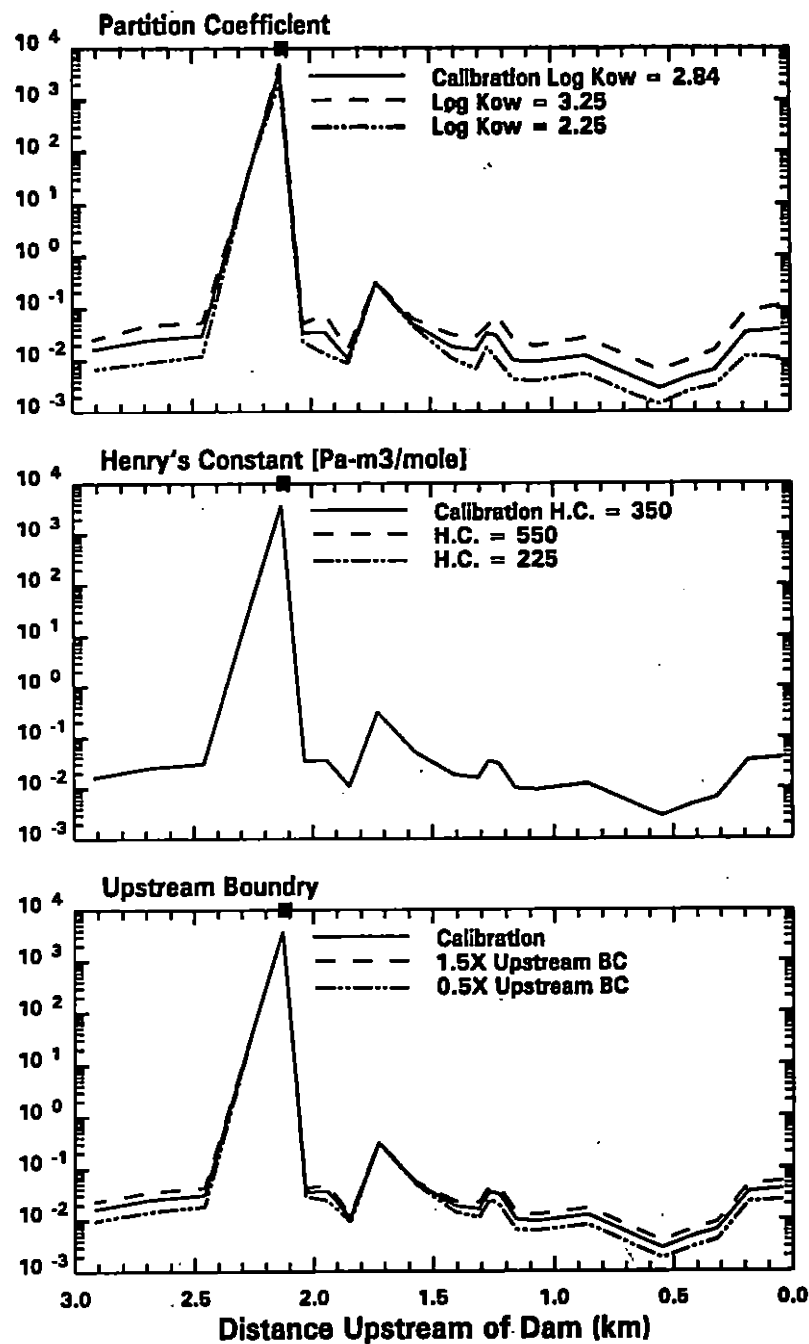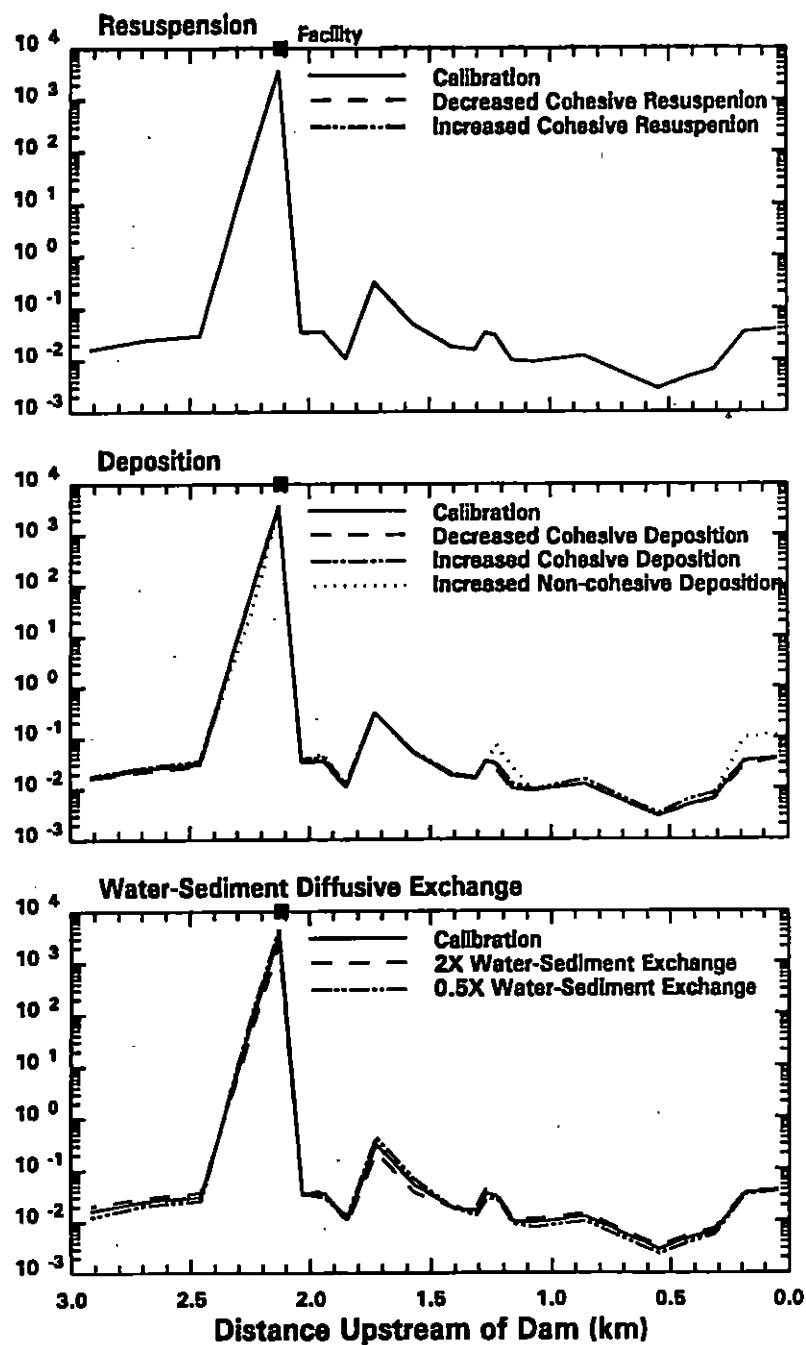
FIGURE 7-5.   Chlorobenzene Calibration Sensitivity Runs - Sediment Concentrations
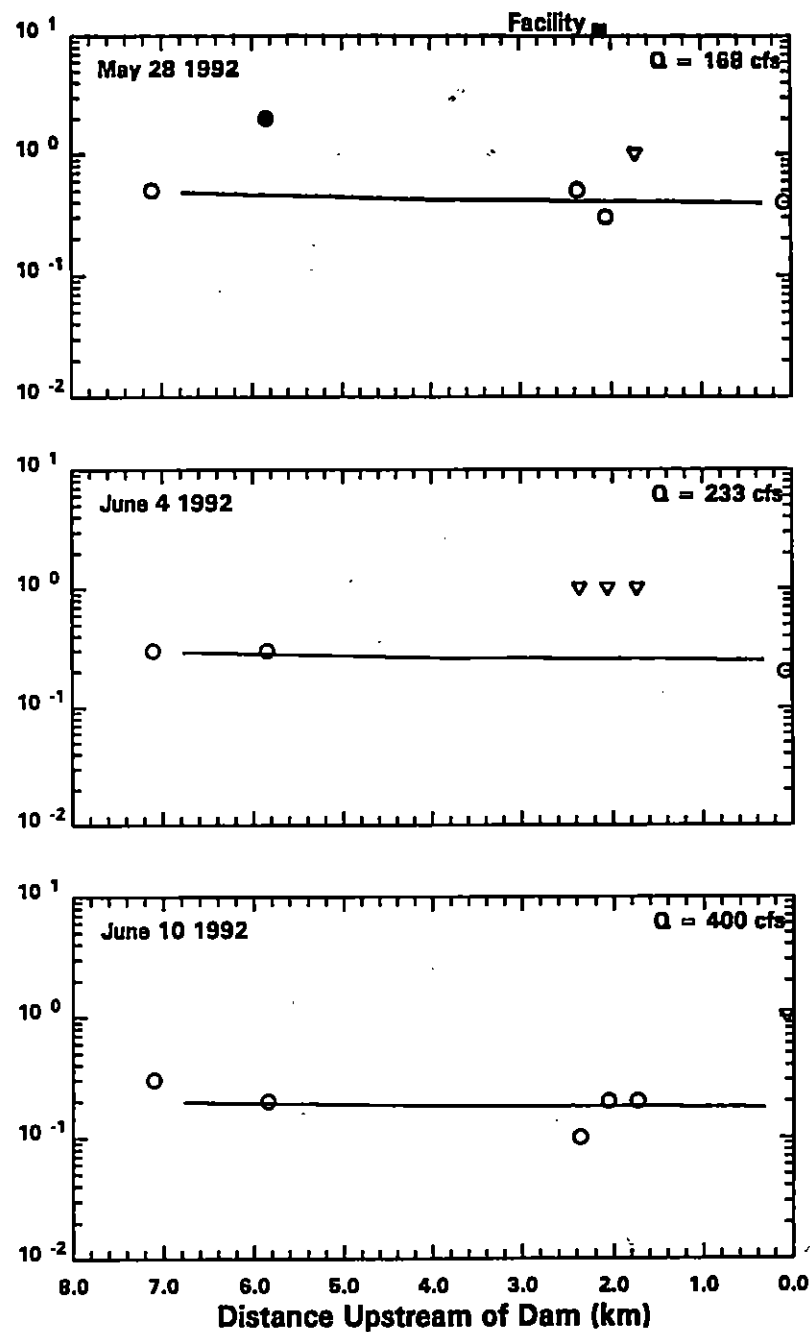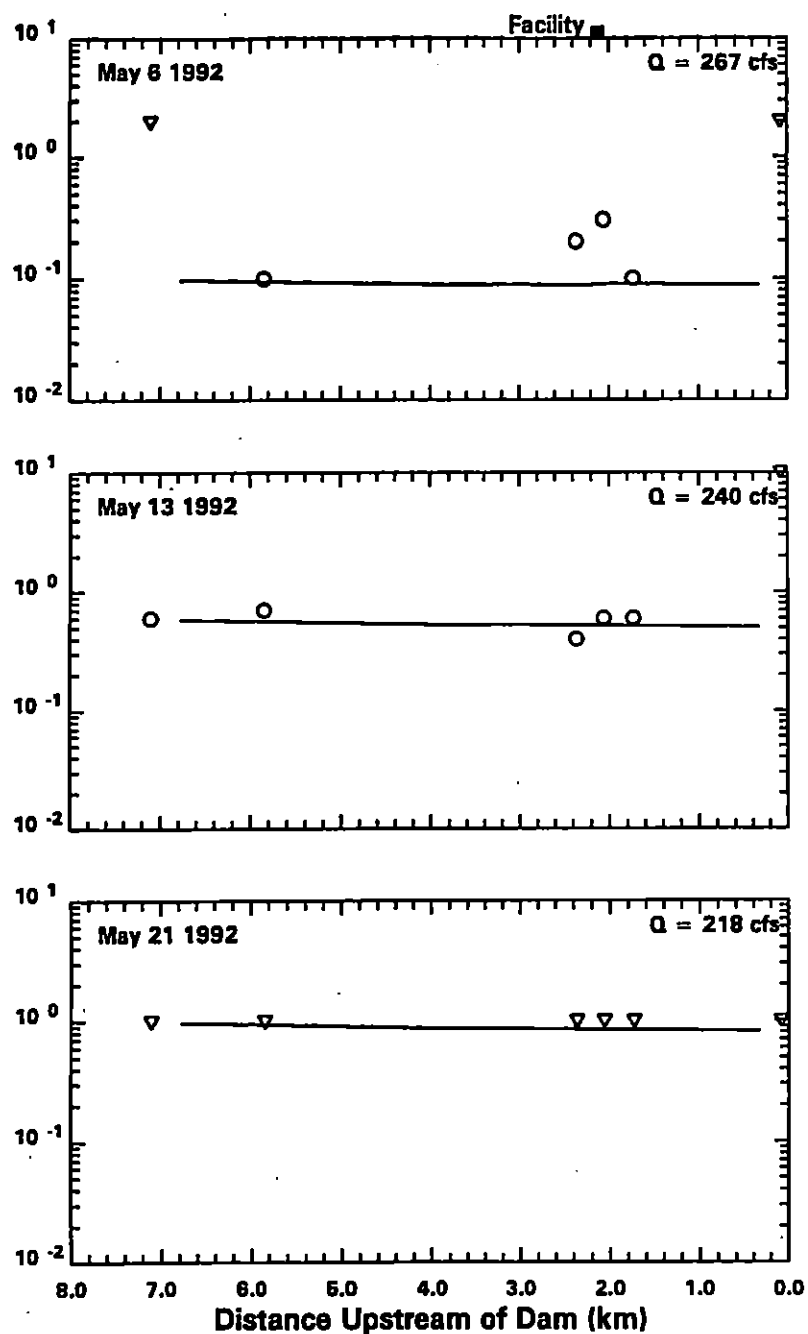
FIGURE 7-6a. Naphthalene Calibration - Water Column Concentrations
(— model ● measured, ○ estimate, ∇ non-detect)
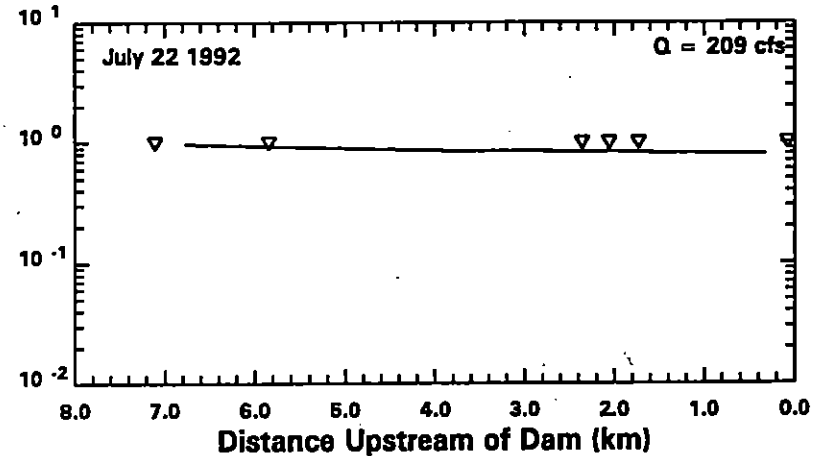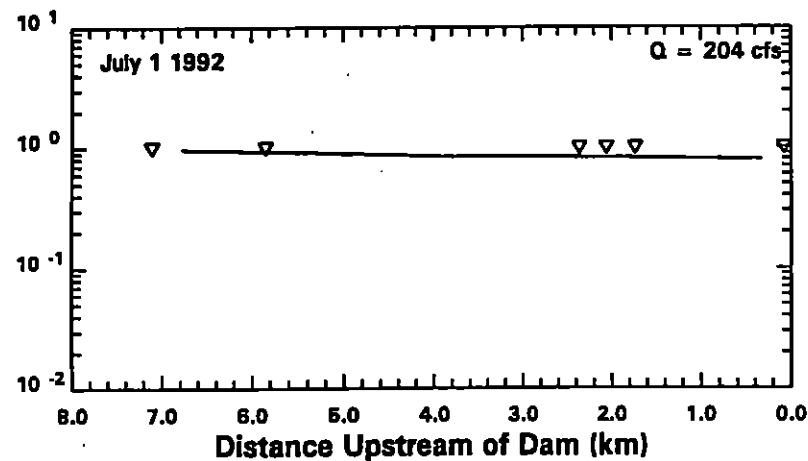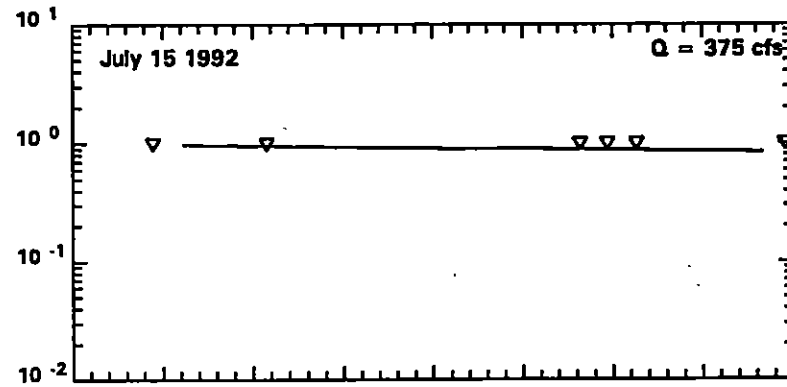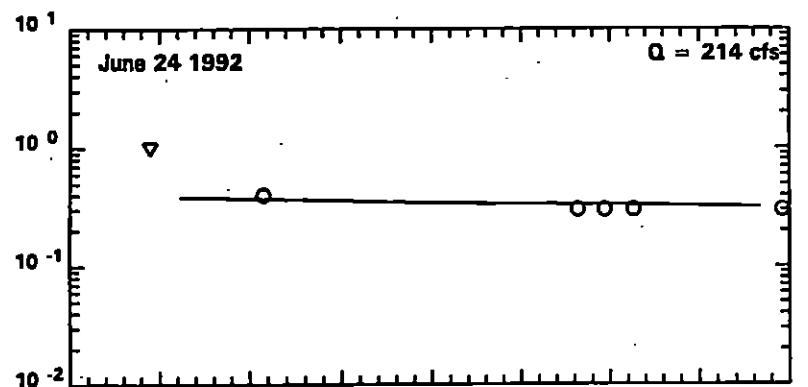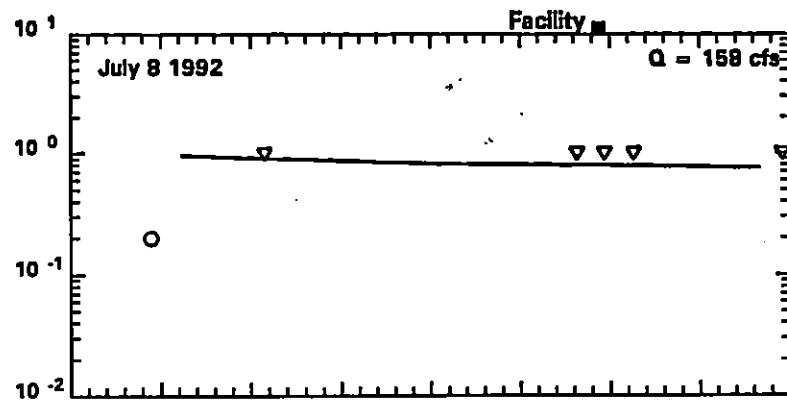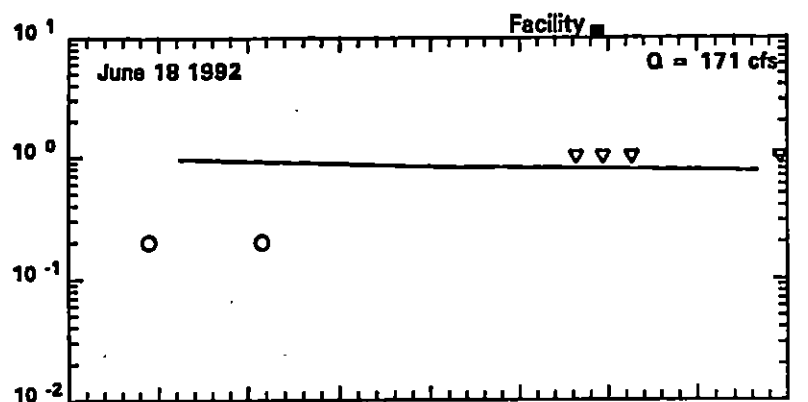
FIGURE 7-6b. Naphthalene Calibration - Water Column Concentrations
(— model ● measured, ○ estimate, ▽ non-detect)

Pawtuxet River
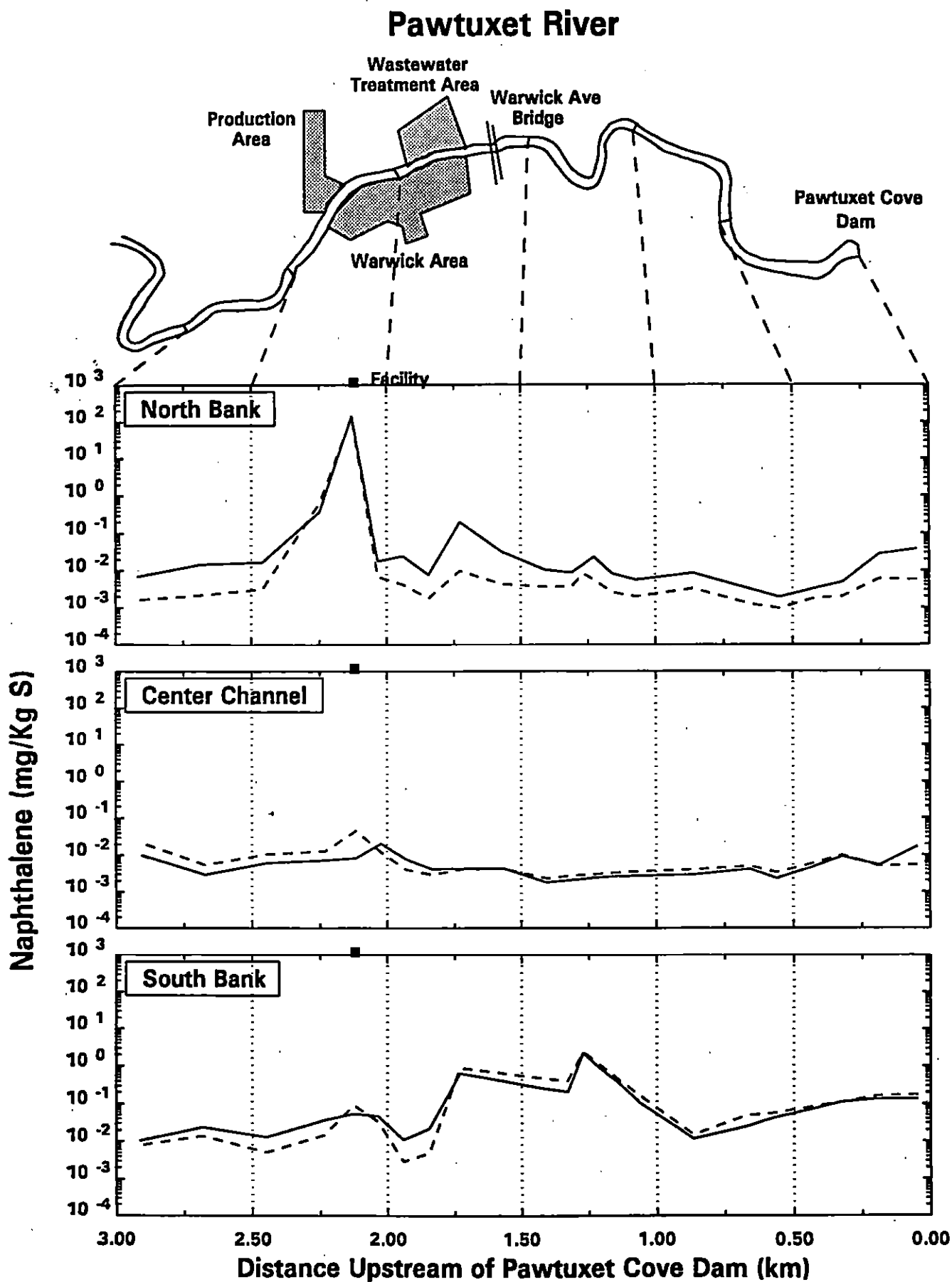
FIGURE 7-7.   Naphthalene Calibration - Sediment Concentrations
(--- 3/3/92 — 4/30/94)
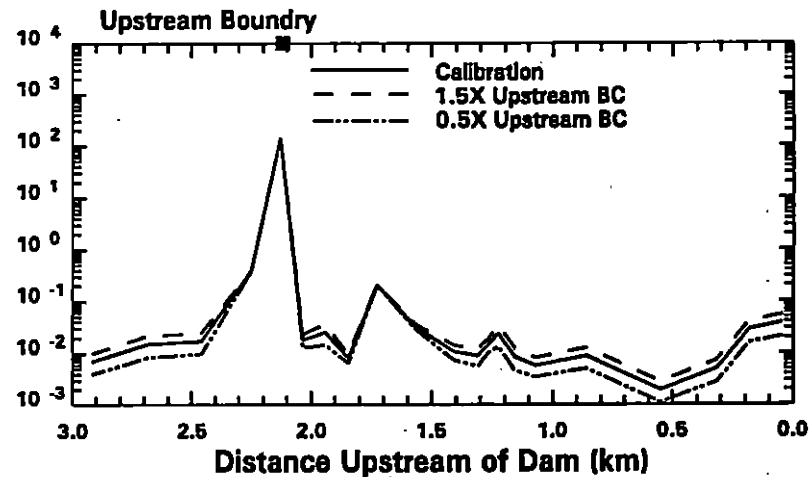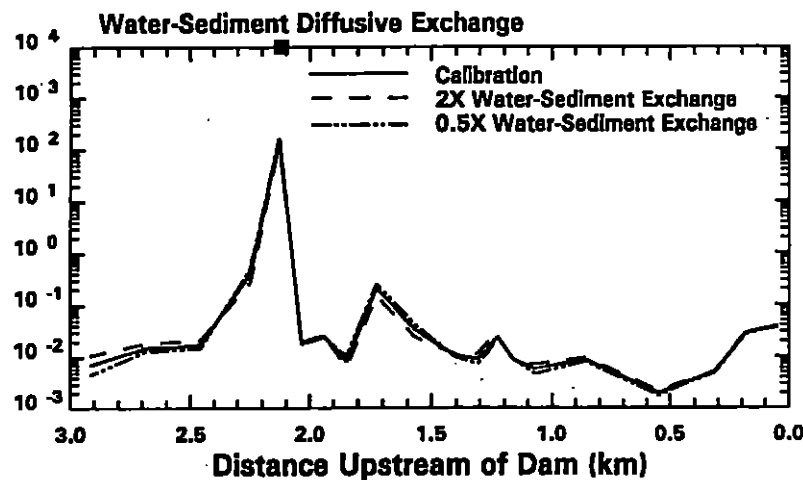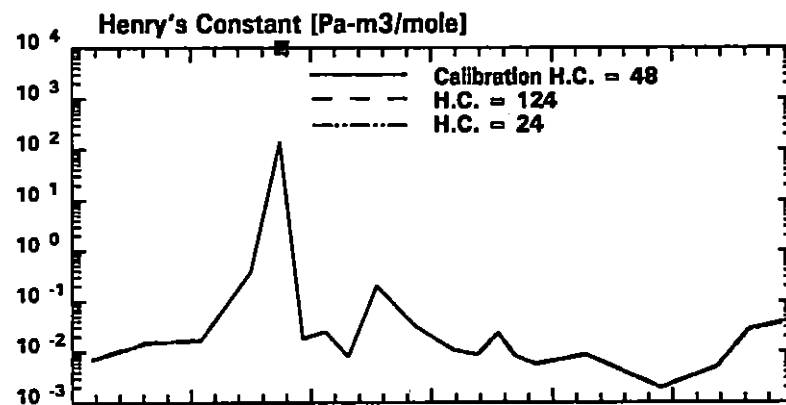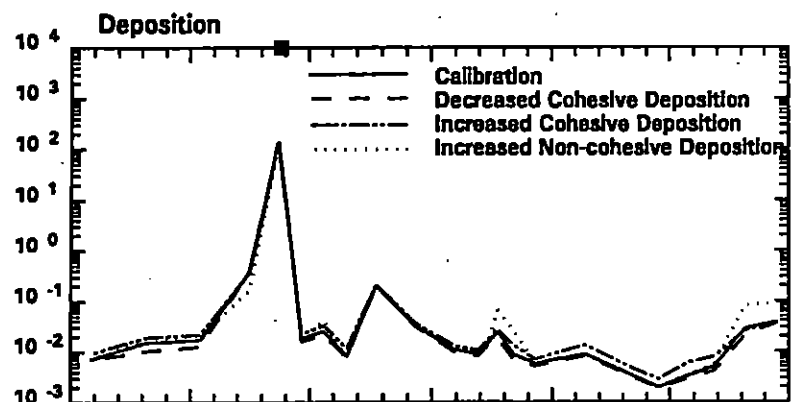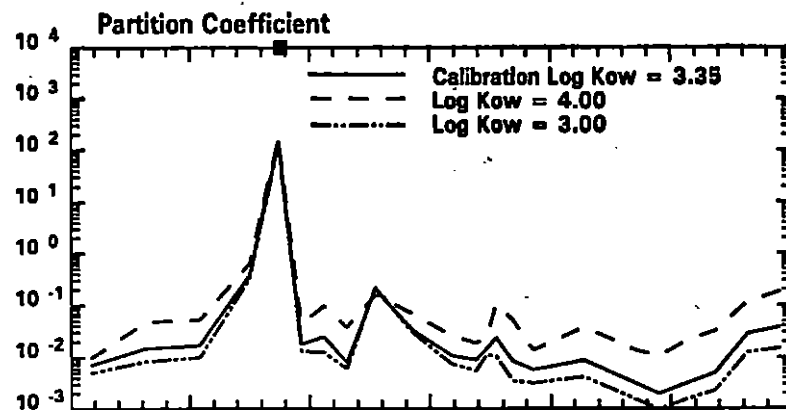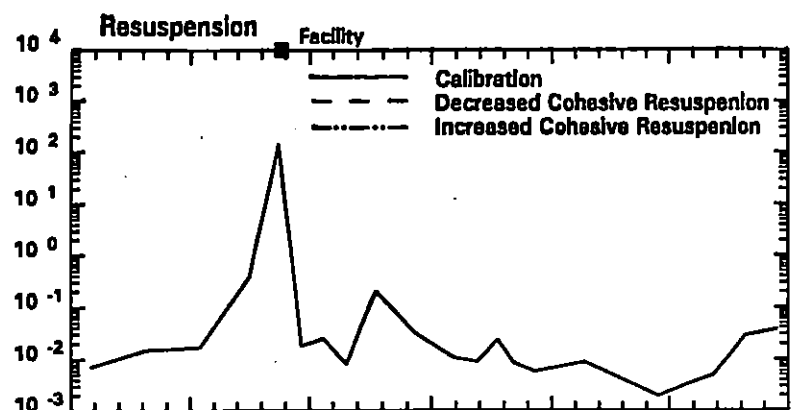
FIGURE 7-8. Naphthalene Calibration Sensitivity Runs - Sediment Concentrations
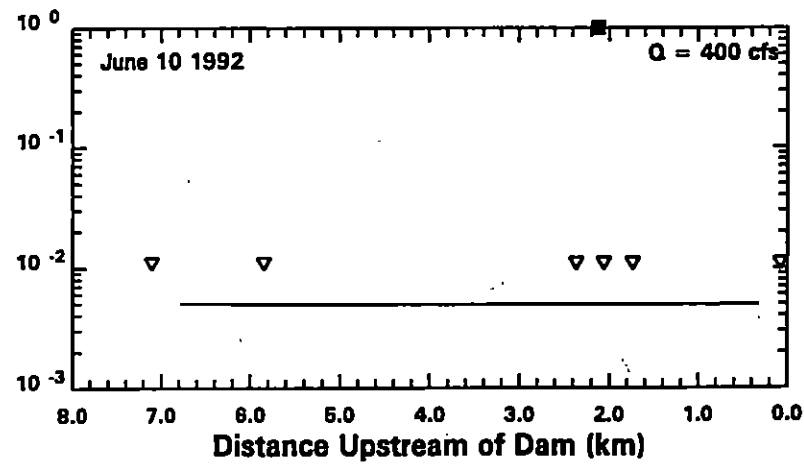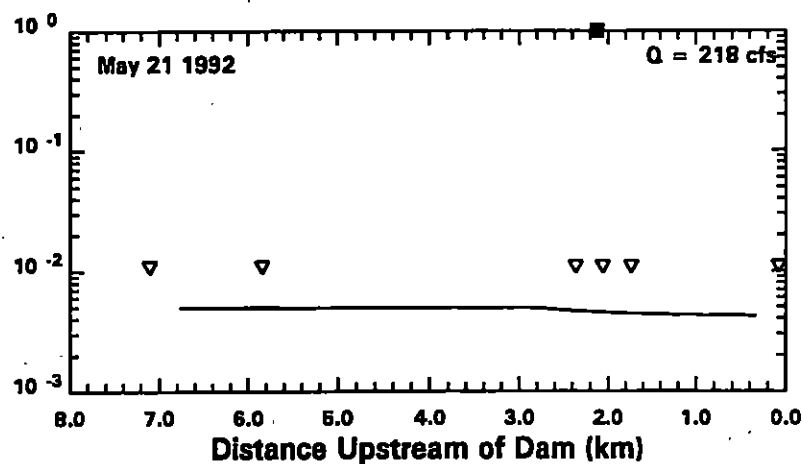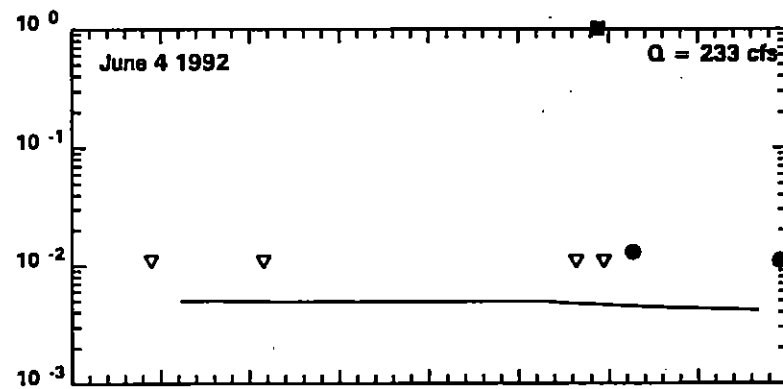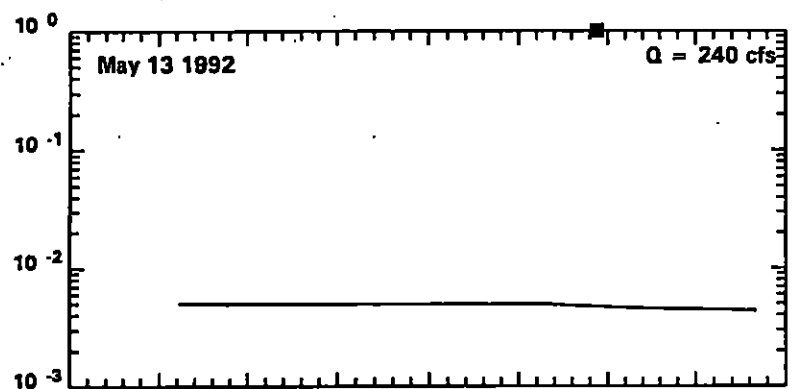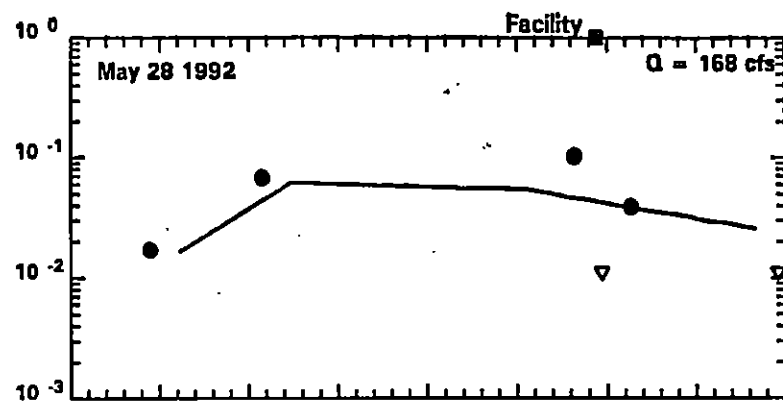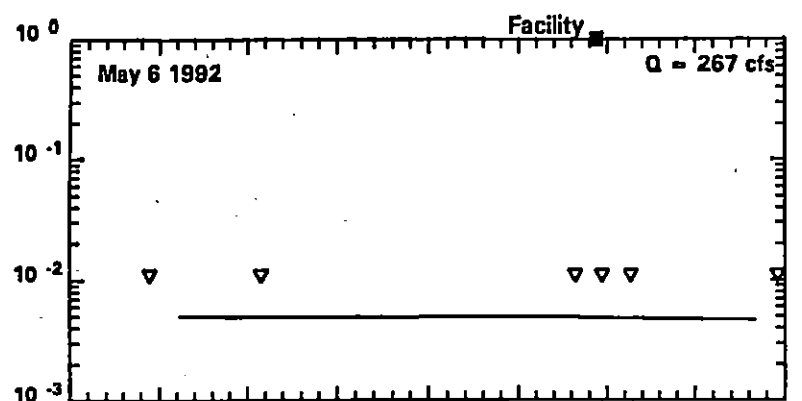
FIGURE 7-9a. Total PCB Calibration - Water Column Concentrations
(— model ● measured, ○ estimate, ∇ non-detect)
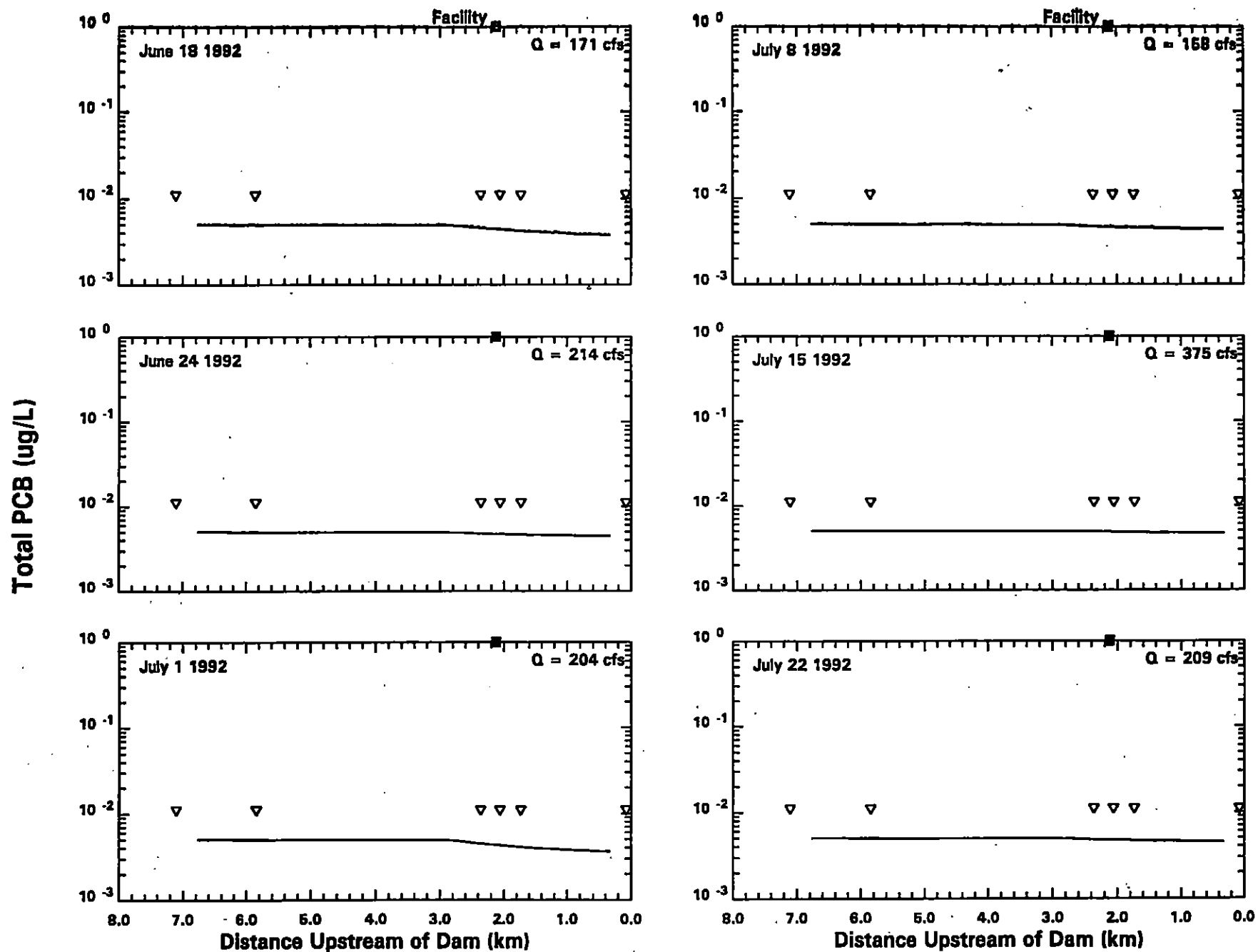
FIGURE 7-9b. Total PCB Calibration - Water Column Concentrations
(— model ● measured, ○ estimate, ▽ non-detect)
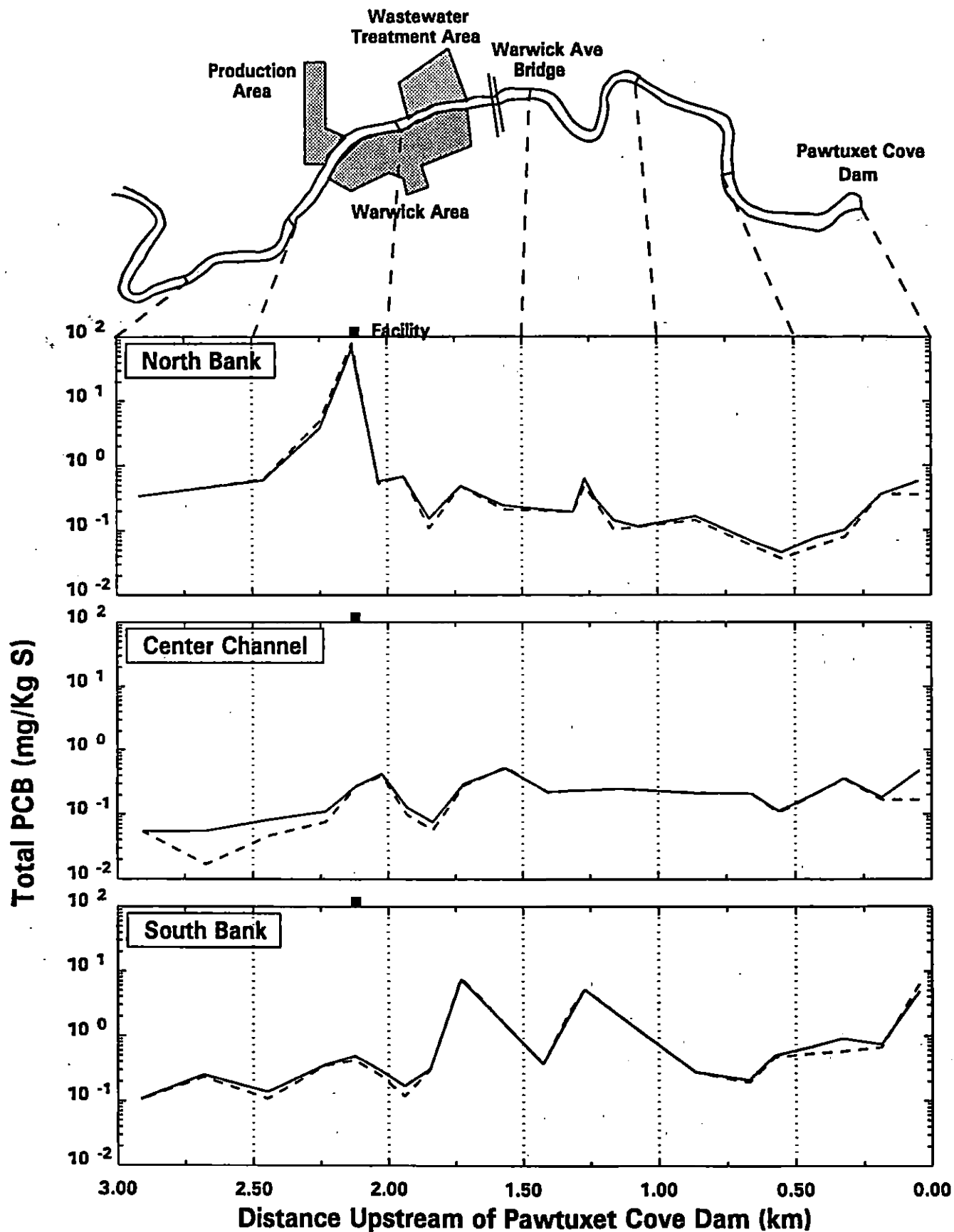
Pawtuxet River

FIGURE 7-10.   Total PCB Calibration - Sediment Concentrations
(--- 3/3/92 — 4/30/94)
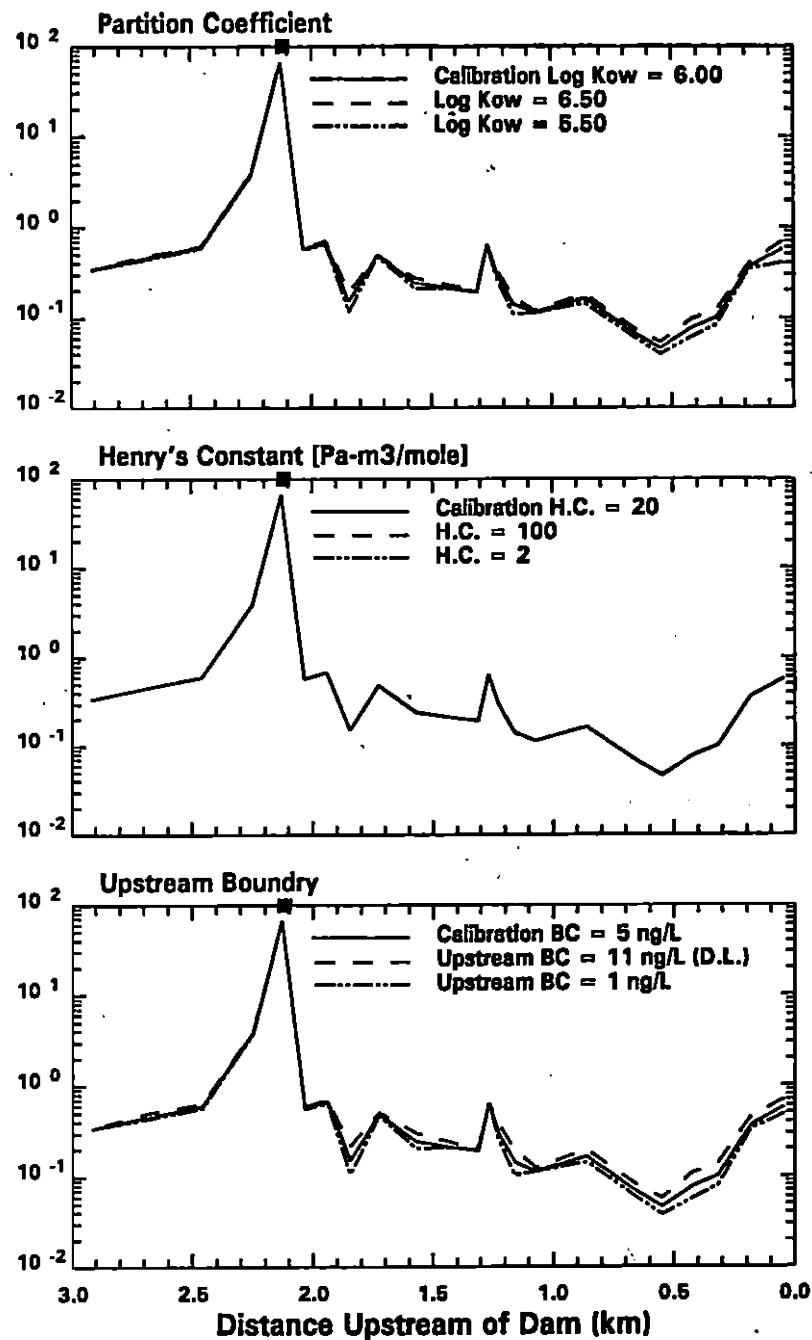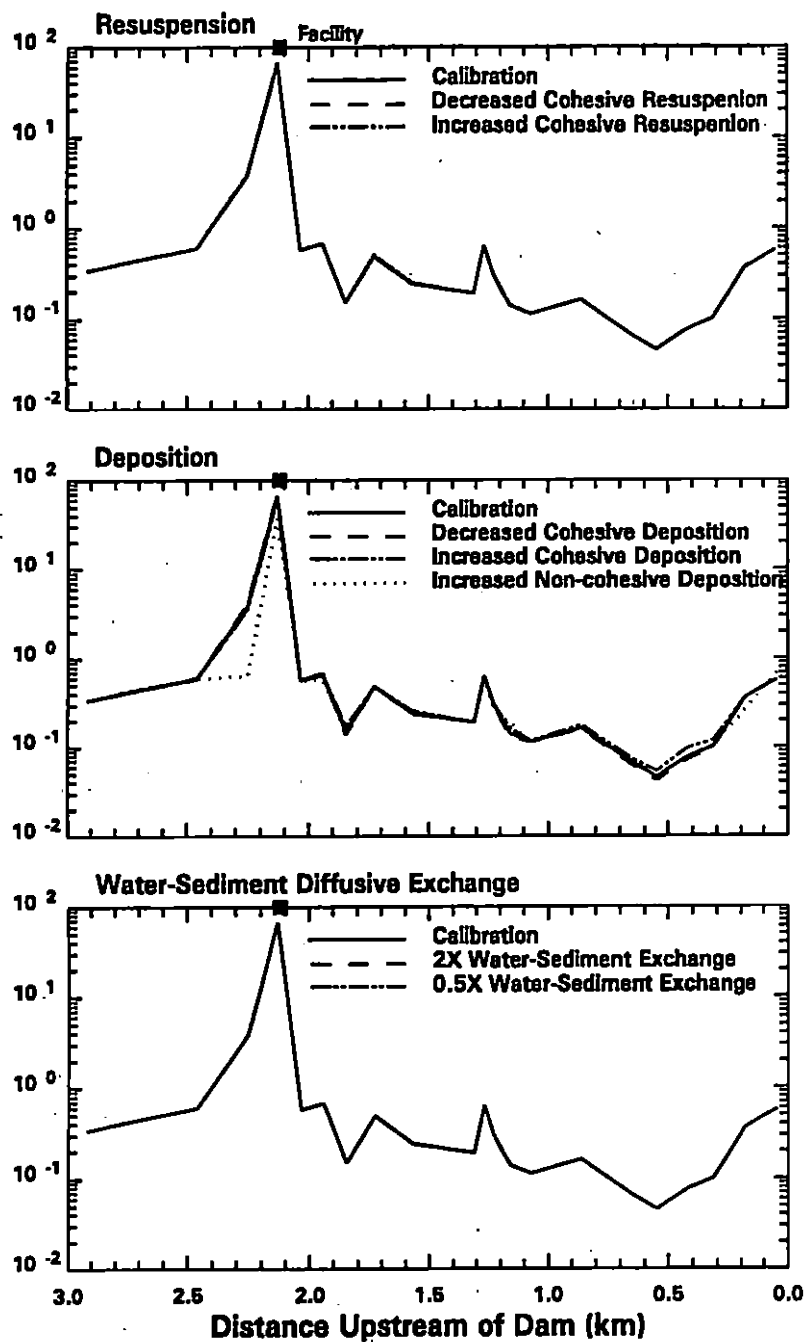
FIGURE 7-11. Total PCB Calibration Sensitivity Runs - Sediment Concentrations

Pawtuxet River
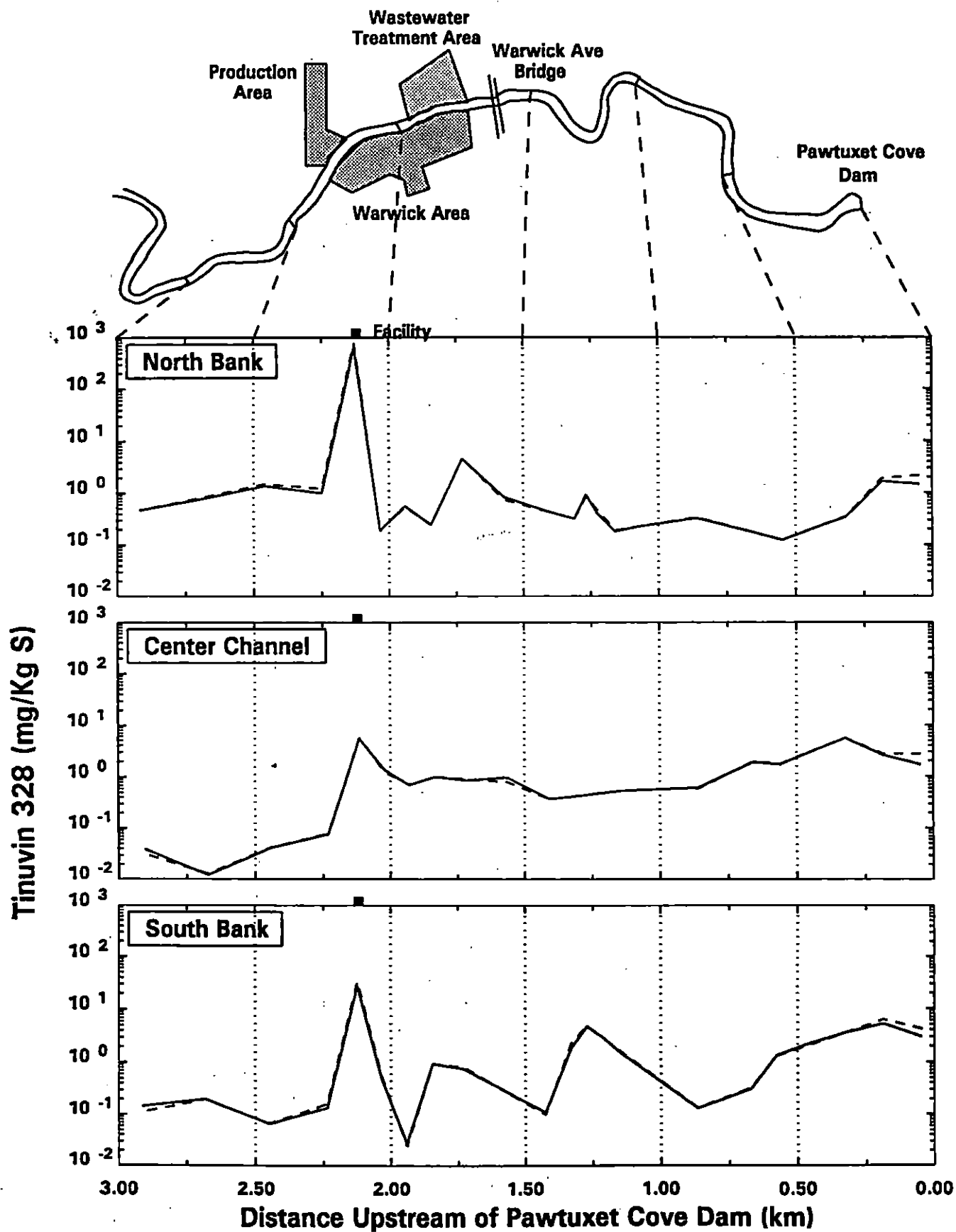
FIGURE 7-12.   Tinuvin 328 Calibration - Sediment Concentrations
(--- 3/3/92 — 4/30/94)
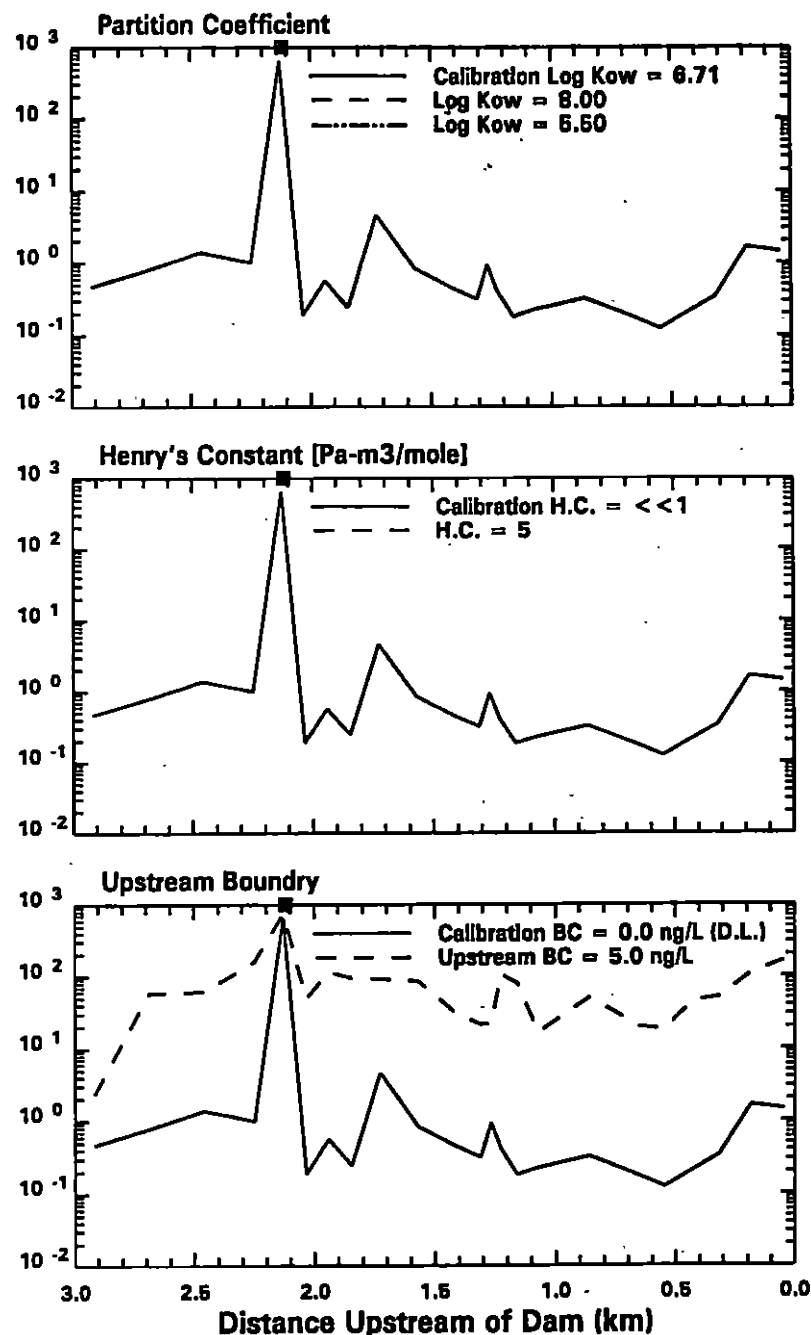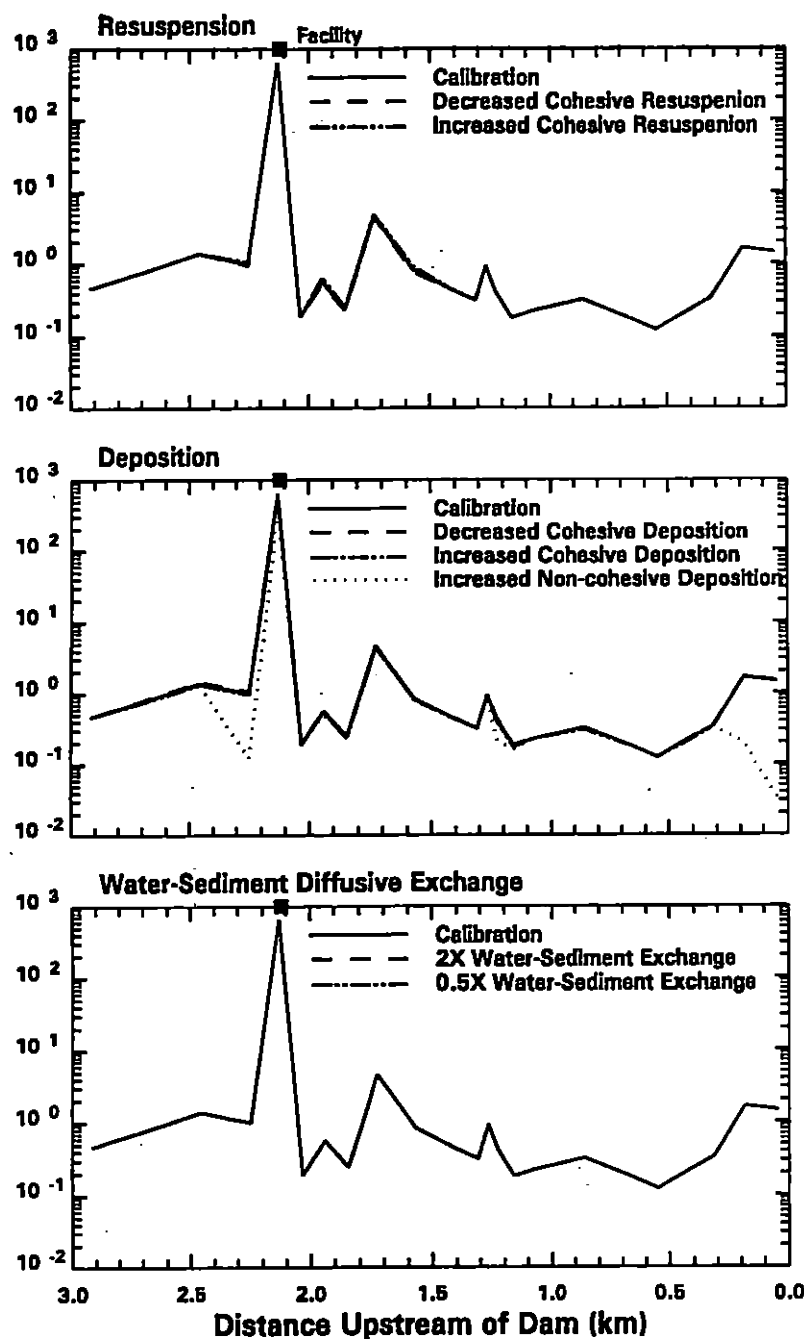
FIGURE 7-13.   Tinuvin 328 Calibration Sensitivity Runs - Sediment Concentrations
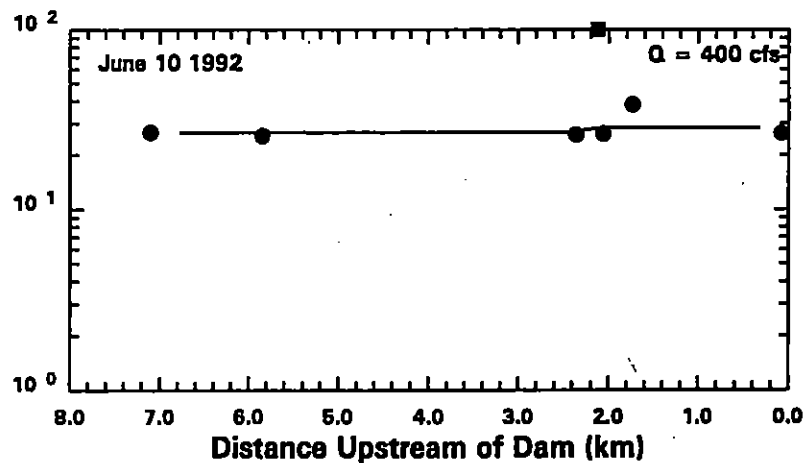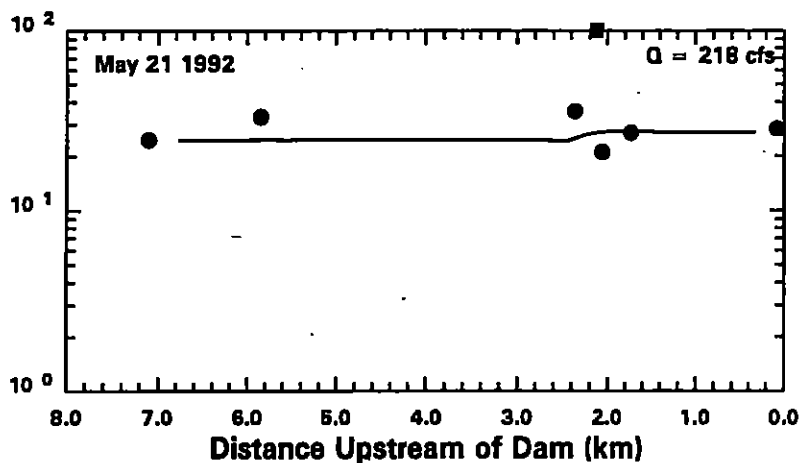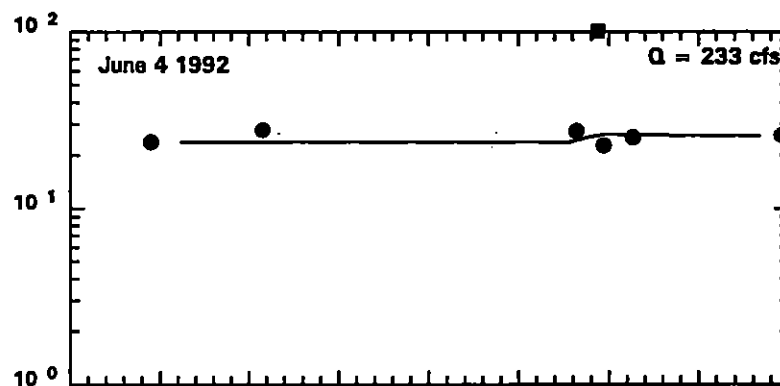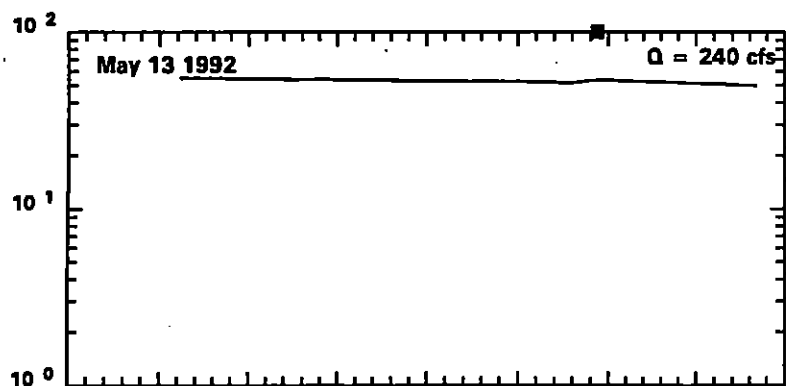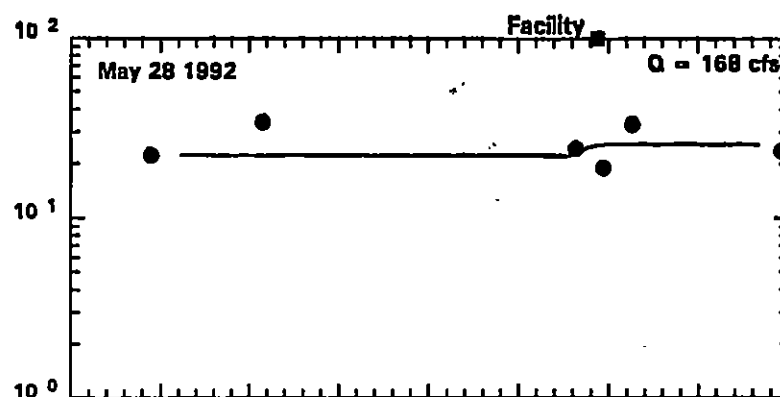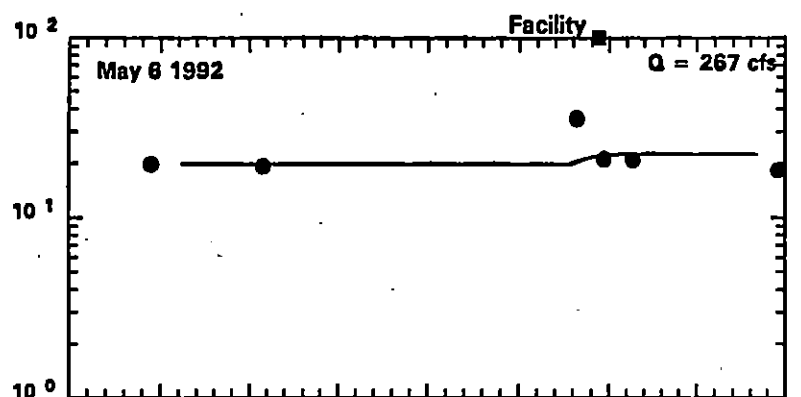
FIGURE 7-14a. Zinc Calibration - Water Column Concentrations (— model ● measured, ○ estimate, ▽ non-detect)
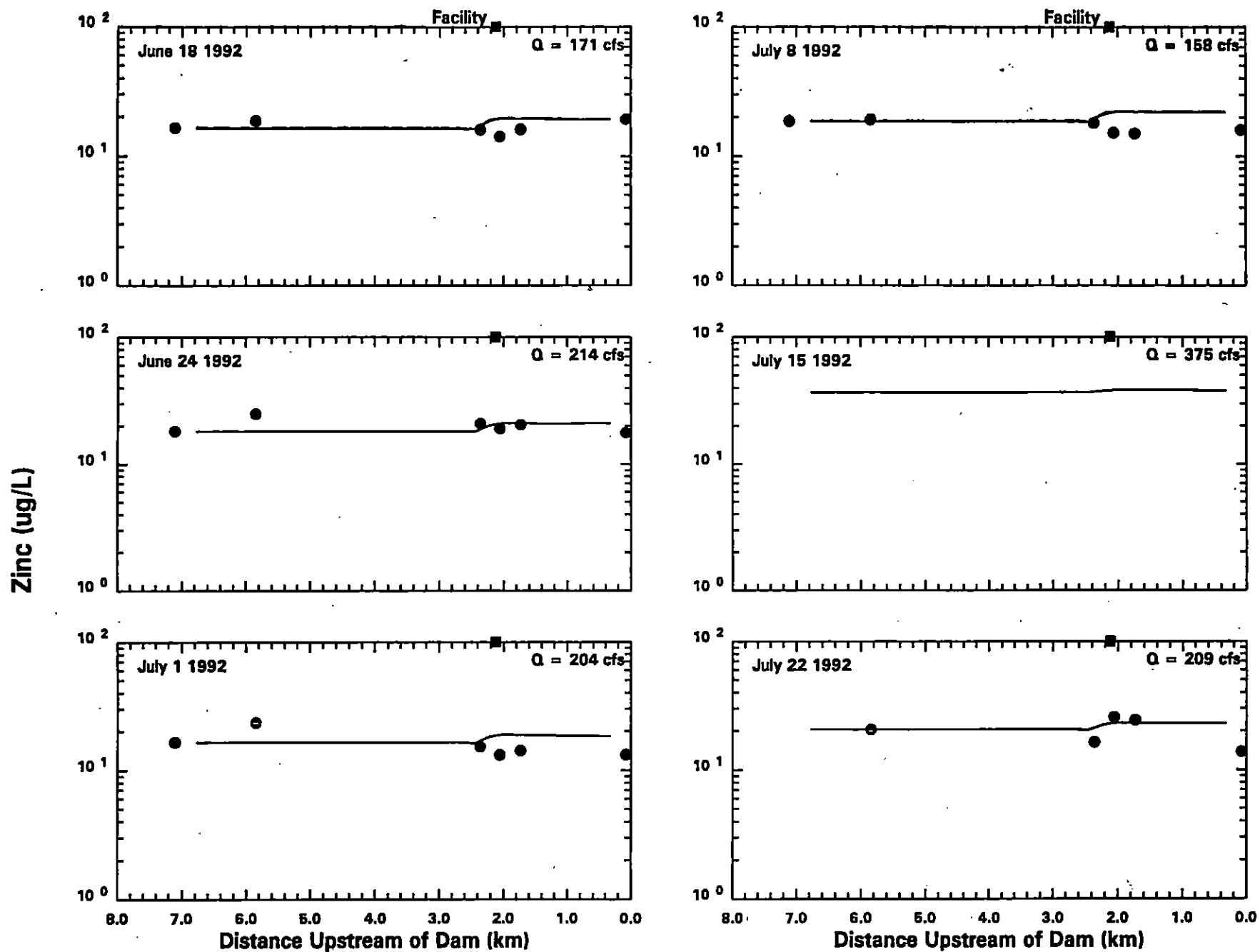
FIGURE 7-14b. Zinc Calibration - Water Column Concentrations (— model
● measured, ○ estimate, ∇ non-detect)

Pawtuxet River
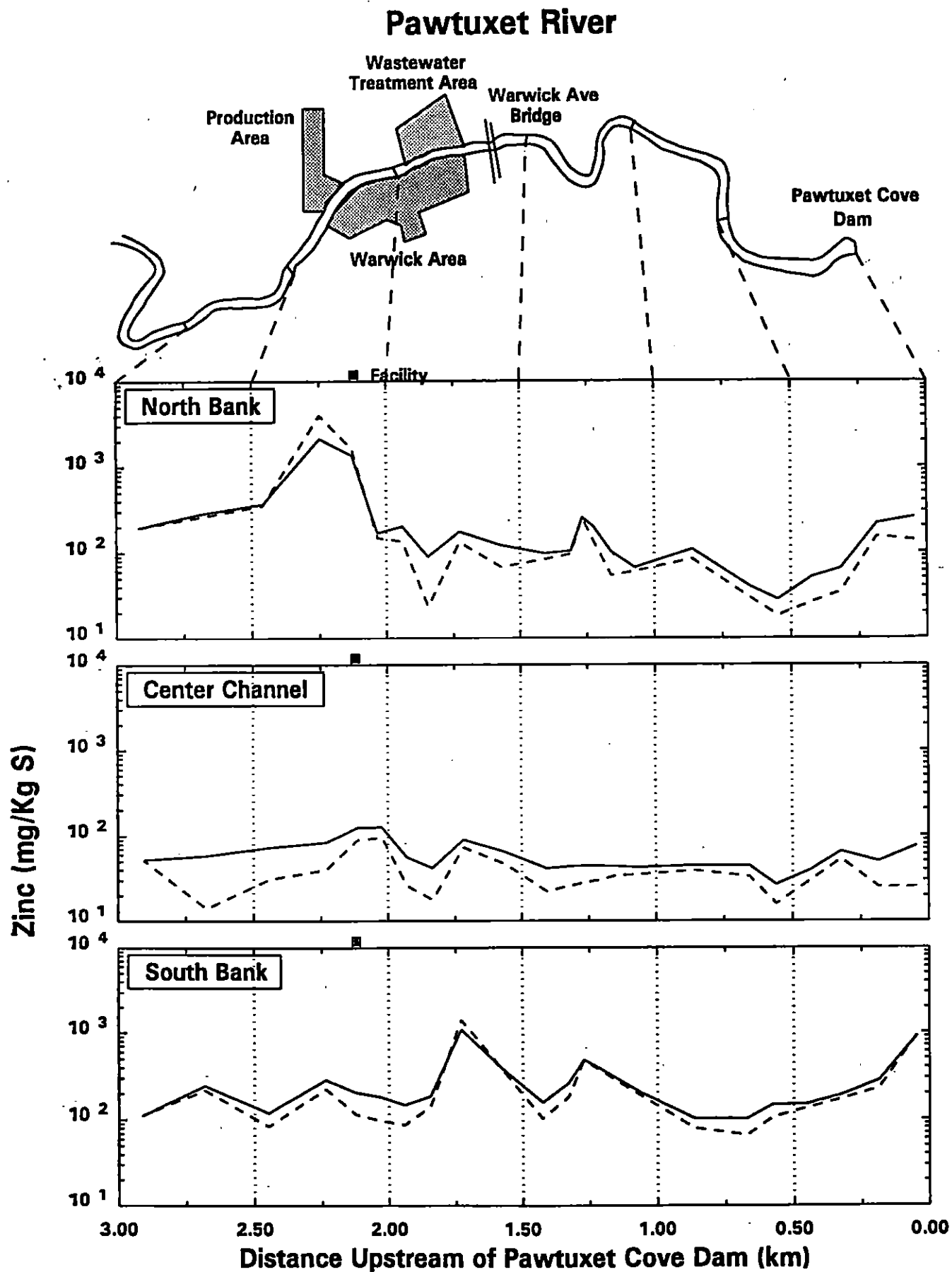
FIGURE 7-15.   Zinc Calibration - Sediment Concentrations
(--- 3/3/92 — 4/30/94)
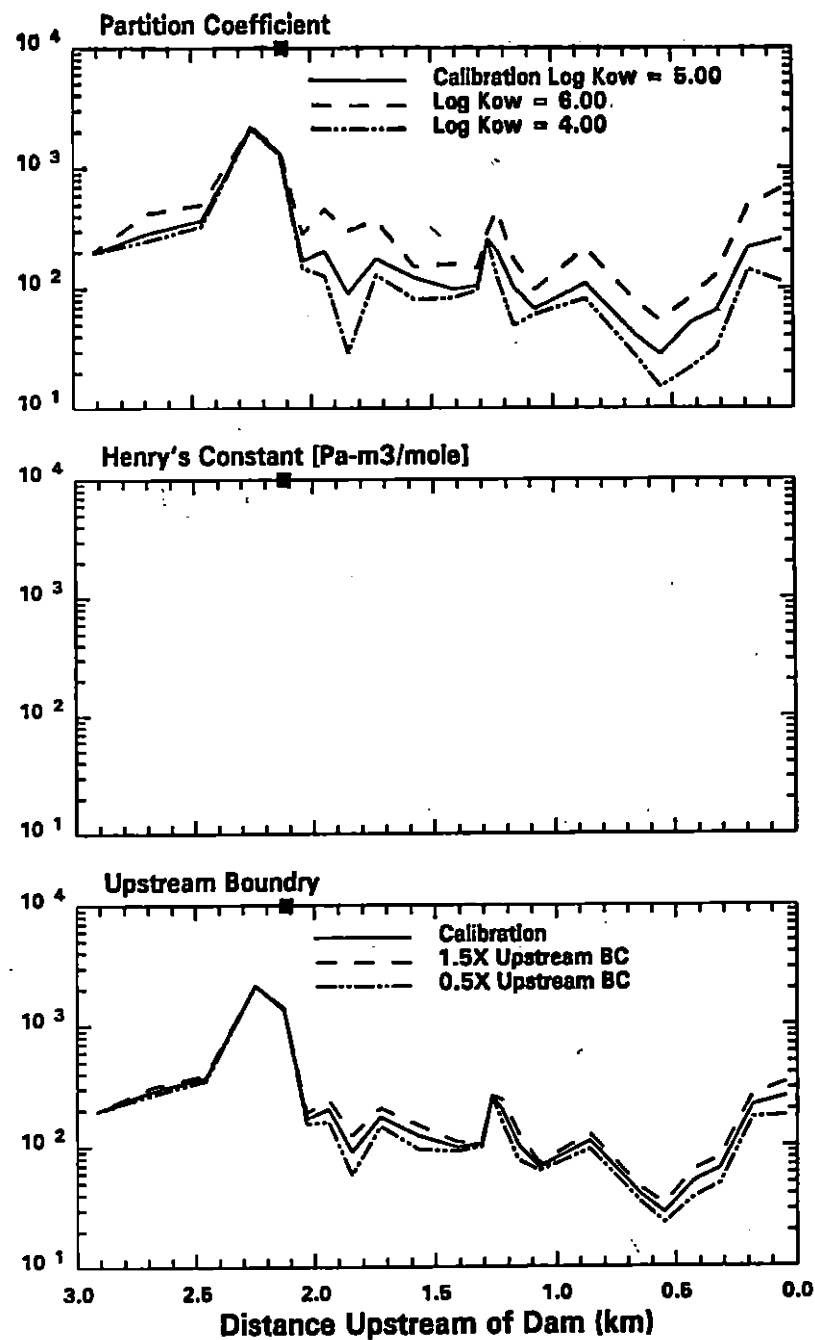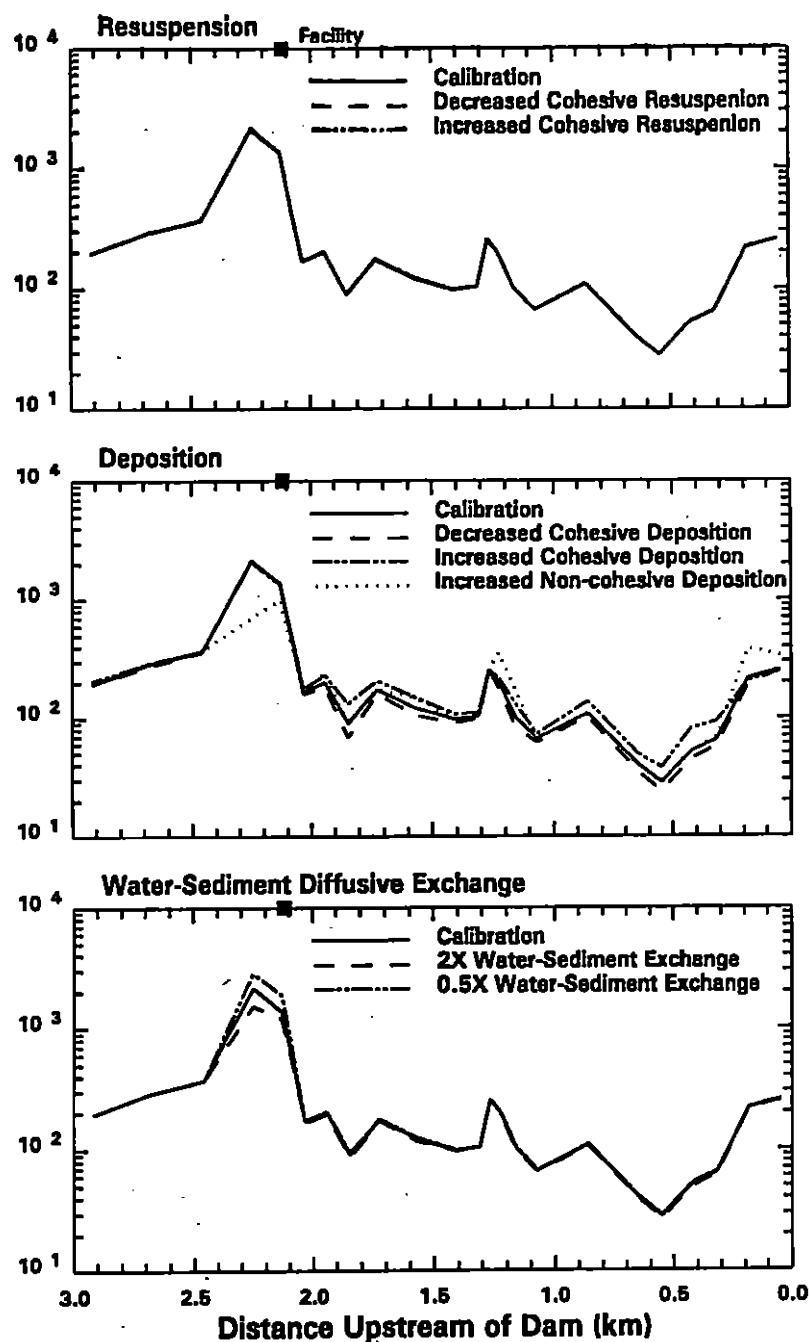
FIGURE 7-16. Zinc Calibration Sensitivity Runs - Sediment Concentrations

SECTION 8

PROJECTIONS OF FUTURE CONTAMINANT CONCENTRATIONS

The purpose of projection analyses presented in this section is to estimate contaminant concentrations in the future and assess the effectiveness of potential alternate remedial actions. Projection analyses are performed for a period of approximately 10.6 years. Hydrodynamic and sediment transport simulations, described in section 6, provide daily values of flow and dispersion between each model grid element and settling and resuspension fluxes of solids between each water column grid element and its adjacent surface sediment grid element. The synthetic hydrograph developed for the projection analyses (see Section 6) approximates the historical river flows measured at Cranston, and therefore, the projection results are based on expected long term flow conditions. Concentrations calculated at the end of the calibration are assigned as initial conditions in the projections. Upstream boundary water column concentrations are assigned based on recent data, in the same manner used in the calibration analysis (Section 7). Changes in chemical concentrations in the sediment are calculated throughout the simulation in response to diffusive exchange with the overlying water and deeper sediment, and particle exchange due to settling and resuspension.

8.1 PROJECTION SCENARIOS

The first projection run provides a baseline for comparison to subsequent runs that simulate alternate remedial actions. This no action projection predicts future concentrations if no remediation occurs.

The second projection run simulates the effect of a groundwater capture system installed along the bulkhead of the production area. This system is designed to capture groundwater moving under the production area towards the river. In addition to preventing groundwater migration from the production area, the system will reverse the hydraulic gradient and draw approximately 0.1 cfs of river water through the sediments along the

bulkhead toward the groundwater capture wells. The effect of this remediation alternative is represented in the model by 1) discontinuing the groundwater source of chlorobenzene and naphthalene and 2) including an advective flow from the river through the sediment segments adjacent to the bulkhead.

The number of sediment layers included in the projection runs was initially set to 2 (0-5, and 5-10 cm) based on the erosional characteristics calculated in the sediment transport modeling. Chemical concentrations in the zone from 10-20 cm were assigned as a boundary condition to the overlying sediment layer. Because the advective flow through the sediments along the bulkhead would affect the chemical concentrations in the 10-20 cm layer, the boundary condition in this area had to be represented differently than in the remainder of the river. The solution to this complication was to add 10 additional sediment layers (at 10 cm each) below the two existing layers in the four grid elements affected by the groundwater reversal. By adding these layers, the chemical concentrations in the upper 70 cm change over time in response to the downward pore water advection. Concentrations below 70 cm can be influenced by diffusion from the assigned boundary condition, with the degree of influence determined by the partition coefficient. Projection results from the upper 10 cm are the focus of the comparison between remediation alternatives, while results below 70 cm are ignored.

The third projection case evaluates the combined effect of the groundwater capture system and excavation of a limited portion of the sediments along the production area bulkhead. The excavation of sediments from the area of the former coffer dam took place in the fall of 1995. The excavation is represented in the model by reducing the initial conditions of chemical concentrations in the sediment in the grid element affected by the excavation. It is assumed that the concentration of the chemicals being modeled is zero in the certified clean backfill material. Based on this assumption, initial conditions in the grid element affected by the excavation are recomputed, weighted by the fraction of the area removed by the excavation.

8.2   PROJECTION RESULTS

Projection results of sediment concentrations are presented on subsequent figures as temporal plots at three locations and as spatial plots of initial and final concentrations. Figures 8-1 to 8-10 present time series results of computed sediment concentrations in the 0-5 and 5-10 cm layers, for each of the 5 chemicals modeled. The letters A, B, and C, shown on the sketch of the river indicate the locations on the north side of the river for which temporal results are presented. Location A is the former coffer dam, where the highest concentrations of organic chemicals were observed. Location B is near the end of the facility reach, adjacent to the waste water treatment area, and location C is upstream of the Pawtuxet Cove Dam. Three lines (legend in lower panel) are plotted in each panel to indicate the concentrations calculated in the three projection cases. In several instances concentrations from one or more scenarios are essentially the same and the lines overplot. Spatial plots for each of the five chemicals modeled are presented on Figures 8-11 to 8-20. The three panels on these figures present results for the three lateral divisions of the model segmentation indicated as the north and south banks, and center channel. Initial conditions from the base case run and final concentrations from each projection case are presented, as indicated by the legend in the top panel.

8.2.1 No Action

If no remedial actions are taken, the model indicates that natural attenuation will cause a reduction of contaminant levels in the area of the former coffer dam. This reduction occurs largely through burial of sediments by less contaminated solids. The rate and extent of the reductions are dependent on the sedimentation rate and the contaminant concentrations on the water column solids. The concentrations of chlorobenzene, naphthalene, PCBs and Tinuvin 328 on water column solids are several orders of magnitude lower than in the surface sediment. Thus, the contaminated sediments are being buried by essentially clean solids. As a result, the sedimentation rate is the main determinant of the rate at which the surficial sediment concentrations decline and all of these chemicals are projected to have similar reductions in coffer dam area surficial

sediment contamination. Reductions of about 70 percent are predicted by the year 2004: chlorobenzene declines from about 4000 mg/kg to about 1000 mg/kg; naphthalene from about 140 mg/kg to 40 mg/kg; PCBs from about 70 mg/kg to 20 mg/kg; and Tinuvin 328 from about 650 mg/kg to about 200 mg/kg (Figures 8-1 to 8-4). In contrast, the surficial sediment zinc concentration declines by less than 25 percent; about 1200 mg/kg to about 900 mg/kg (Figure 8-5). This smaller reduction is the result of relatively high zinc concentrations on water column solids.

Concentrations in the coffer dam area subsurface sediments (5-10 cm) decline to a lesser extent than the surficial sediments (0-5 cm), reflecting the transport of contaminated sediments from the surface layer to the subsurface layer. The reductions vary depending on the initial concentration gradient in the sediments. The net decline of PCBs is near zero (Figure 8-8). For all the other contaminants a decline of about 20 percent occurs (Figures 8-6, 8-7, 8-9 & 8-10).

Outside the coffer dam area, concentration changes are less dramatic. In general, the surficial sediments appear to be at or near steady-state with the water column and little change occurs. The greatest change occurs with zinc: concentrations increase by about a factor of two in most of the study area (Figure 8-15). Tinuvin 328 concentrations tend to decline slightly and the other contaminants remain approximately constant (Figures 8-11 to 8-14). Along the north bank of the river downstream of km. 2, concentrations of chlorobenzene and naphthalene increase during the projection due to diffusive exchange with the deep sediment boundary. The relatively little deposition at this location does not provide sufficient clean solids to dilute the contaminants diffusing from below. However, at most other locations outside the vicinity of the production area, changes in calculated sediment concentrations are primarily due to deposition of solids from the water column, which are generally cleaner than bed sediments.

8.2.2 Groundwater Capture

The groundwater capture system has a significant impact on the concentrations of chlorobenzene and naphthalene in the coffer dam area (Figures 8-1, 8-2, 8-6 & 8-7). Sediment chlorobenzene declines from about 4000 mg/kg to less than 0.1 mg/kg within about 500 days in the top 5 cm and within about 600 days in the 5-10 cm layer. Naphthalene declines more slowly due to its higher partition coefficient, going from about 140 mg/kg to about 0.05 mg/kg in about 1000 days in the surface layer and about 1400 days in the subsurface layer. After achieving the cited levels, concentrations remain relatively constant. A continuing decline does not occur because the overlying water being advected into the sediment by the groundwater pumping system is contaminated. In essence , the sediment becomes contaminated at the same level as the water column.

The groundwater capture system has no significant effect on chlorobenzene and naphthalene concentrations outside of the coffer dam area (Figures 8-11, 8- 12, 8-16 & 8-17). Current chlorobenzene and naphthalene fluxes from the coffer dam sediments to the water column contribute little to the contamination of the sediments in other areas. Thus, the elimination of those fluxes by the capture system has almost no impact on the sediments in other areas.

Peak sediment zinc concentrations are reduced by a factor of two, from approximately 1800 (end of base case) to 900 mg/kg as a result of the 10.6 year operation of the groundwater capture system. It is noted that the peak zinc concentration (Figures 8-15 & 8-20) is located slightly upstream of the location of the peak concentrations of the organic chemicals. Sediment organic carbon concentrations at this location are lower than at the location of the former coffer dam. Because of the lower organic carbon content, a greater fraction of zinc is in the dissolved form at this location, and therefore the groundwater capture system has more of an effect at the location of the peak zinc concentration than at the former coffer dam. Outside of the vicinity of the production area, sediment zinc concentrations are not affected by the operation of the groundwater capture system.

The groundwater capture system has virtually no effect on PCB or Tinuvin 328 concentrations in any portion of the study area (Figures 8-14, 8-15, 8-18 & 8-19). Higher partition coefficients for these chemicals (compared to chlorobenzene and naphthalene) keep most of the chemical in the sorbed phase, and as a result advection of river water through the sediments does not significantly affect the total concentration.

8.2.3 Groundwater Capture and Sediment Excavation

Excavation of sediments from the former coffer dam area is represented by the reduction of initial concentrations in the sediments of one model grid element. After this reduction in concentration due to excavation, chlorobenzene and naphthalene concentrations at the former coffer dam area continue to decrease due to the groundwater capture system. The incremental effect of the excavation on chlorobenzene and naphthalene is a reduction in the time required to bring the sediment into equilibrium with the concentrations in the overlying water (Figures 8-1, 8-2, 8-6 & .8-7). Chlorobenzene concentrations reach equilibrium with the overlying water 150 to 300 days earlier (0-5 and 5-10 cm layers, respectively) and naphthalene concentration reach equilibrium approximately 400 to 500 days earlier. The combination of excavation and groundwater capture does not affect sediment concentrations of chlorobenzene and naphthalene away from the production area.

The more significant effect of excavation is the reduction in PCB, Tinuvin 328 and zinc concentrations in the vicinity of the former coffer dam area. PCB concentrations in this area, computed at the end of the excavation projection, are approximately a factor of 30 less than concentrations computed in either the base case or groundwater capture simulations (Figures 8-3 & 8-8). Tinuvin 328 concentrations are reduced by more than 3 orders of magnitude in this area (Figures 8-4 & 8-9). Excavation reduces zinc concentrations in the former coffer dam area from between 1000 to 3000 mg/kg (0-5 and 5-10 cm layers) down to approximately 200 mg/kg (Figures 8-5 & 8-10). However, during the course of the approximately 10.6 year projection, deposition of zinc contaminated solids from the water column increases concentrations to over 500 mg/kg in the top 5 cm

and to over 300 mg/kg in the 5-10 cm layer. For each of the five chemicals, neither the groundwater capture system nor excavation of sediments from the former coffer dam have an effect on sediment concentrations outside of the vicinity of the production area. Downstream concentrations are essentially the same in each projection run.

8.3 SUMMARY OF PROJECTION ANALYSES

Figures 8-21a-c summarize projection results for three locations: 1) the former coffer dam area, where peak concentration of the 4 organic chemicals are presently observed, 2) on the south bank just upstream of the sharp bend in the river near km 1.25, and 3) on the south bank of the river immediately upstream of the Pawtuxet Cove dam. The latter two locations represent areas where peak concentrations of some of the 5 chemicals are calculated at the end of the projections. Zinc concentrations are presented for a forth location, along the bulkhead of the production area upstream of the former coffer dam area. Peak concentrations of zinc are currently observed at this location.

The groundwater capture is effective in reducing peak concentrations of chlorobenzene and naphthalene near the former coffer dam area, and would be expected to be equally effective in reducing concentrations of other chemicals with similar partition coefficients. At this location both chemicals are reduced to concentrations less than 0.1 mg/kg, which can be compared to base case final concentrations of chlorobenzene of about 1000 mg/kg and 40 mg/kg of naphthalene. The groundwater capture system also produces approximately a factor of 2 reduction in the peak zinc concentration. The groundwater capture system does not significantly affect sediment PCB or Tinuvin 328 concentrations. The concentrations of PCBs and Tinuvin in the former coffer dam area are significantly reduced by the excavation of sediments in that area. Ten years after excavation PCB concentrations in the former coffer dam area are calculated at 0.6 an 1.6 mg/kg in the top 5cm and 5-10 cm layers, respectively. These concentrations represent approximately a factor of 30 reduction compared to the concentrations calculated at the end of the base case run (22 and 45 mg/kg in the same two layers).

Sediment contaminant concentrations in areas away from Ciba's production area are not significantly affected by either remedial action, because current mass fluxes out of the production area reach do not significantly affect downstream sediment concentrations. The combination of the two remedial actions, does however, reduce the peak concentrations of each of the chemicals modeled.

Figures

Pawtuxet River
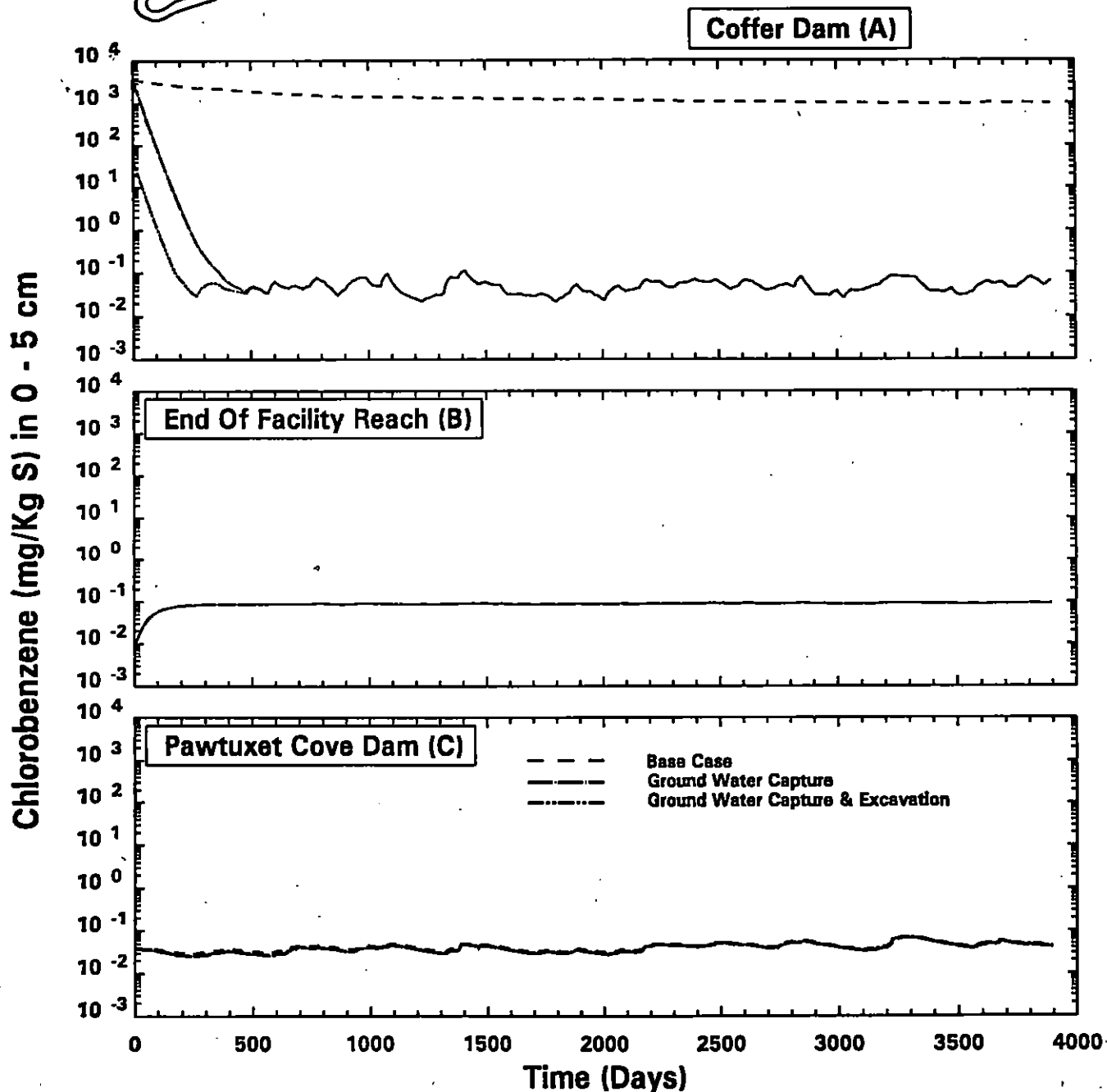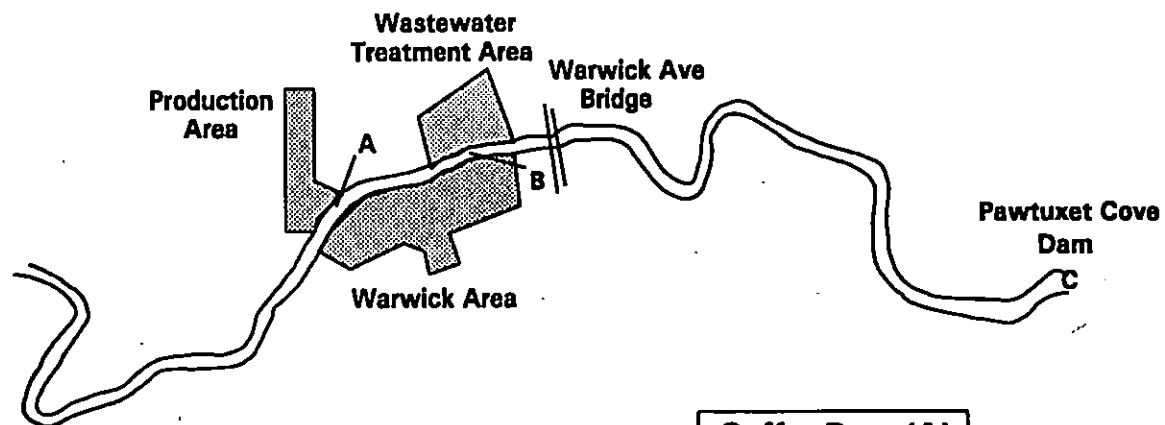
FIGURE 8-1. Comparison of Temporal Distributions of Chlorobenzene Projections - 0-5 cm Layer
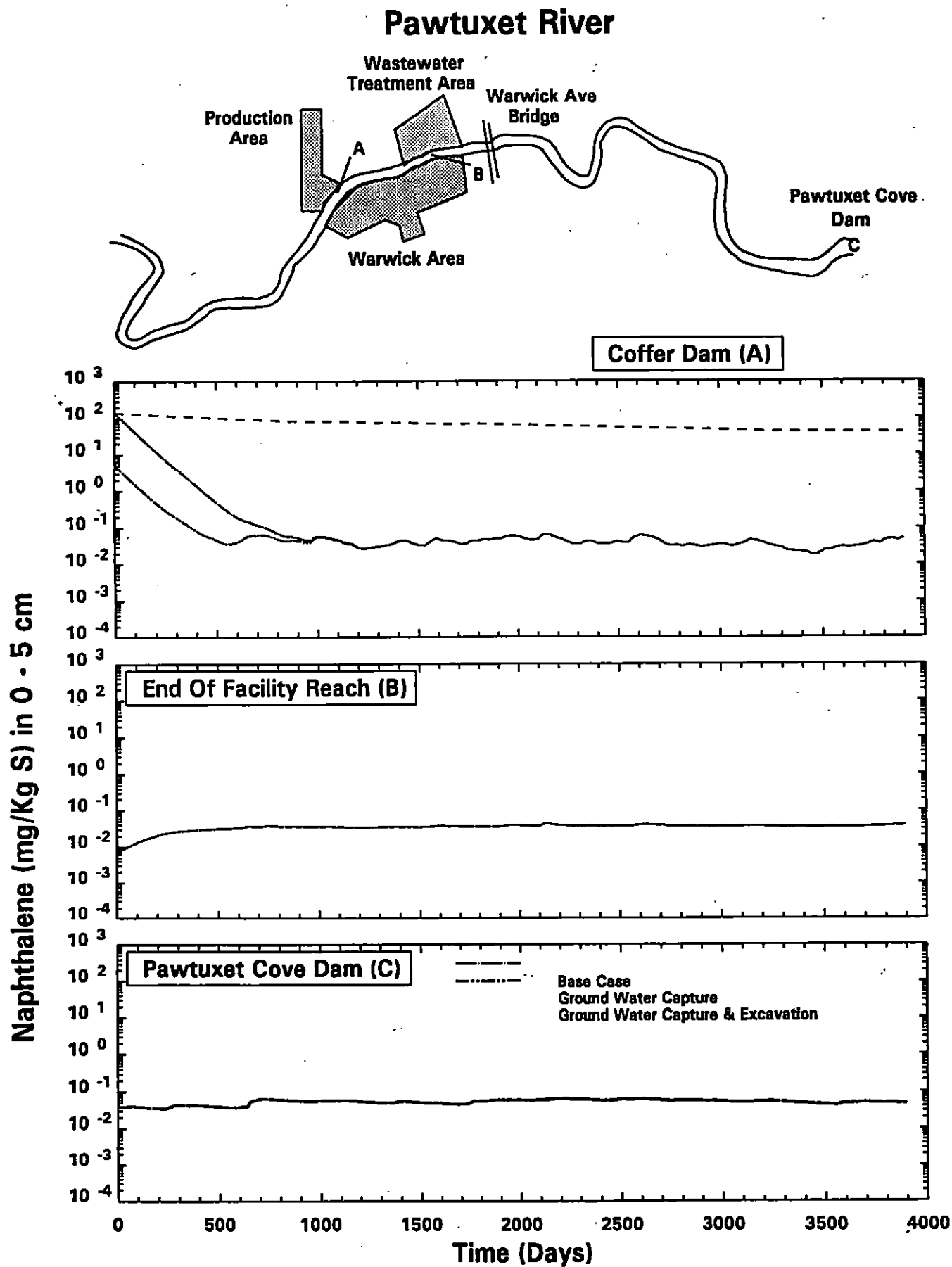
Pawtuxet River

FIGURE 8-2.   Comparison of Temporal Distributions of Naphthalene Projections - 0-5 cm Layer
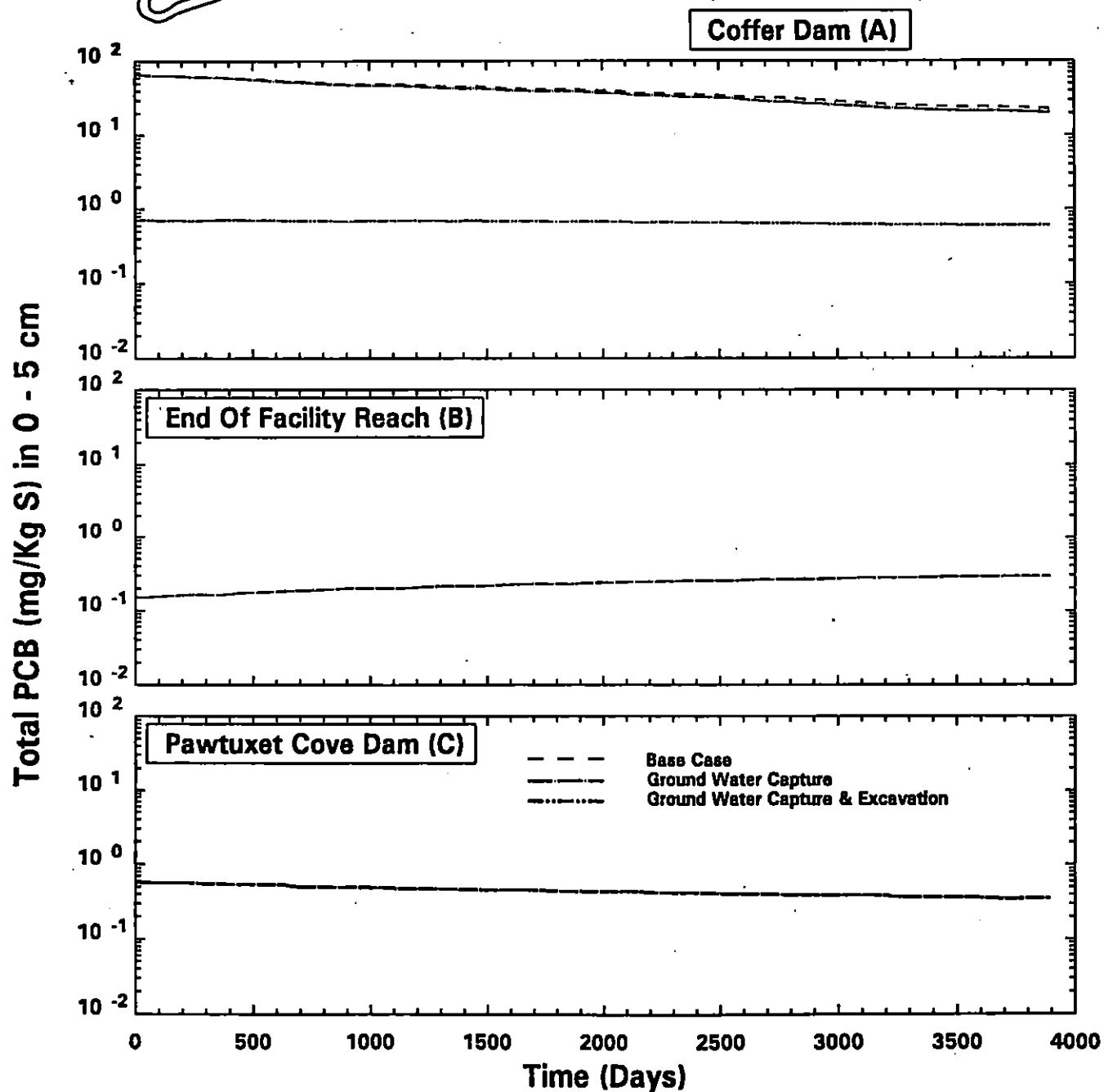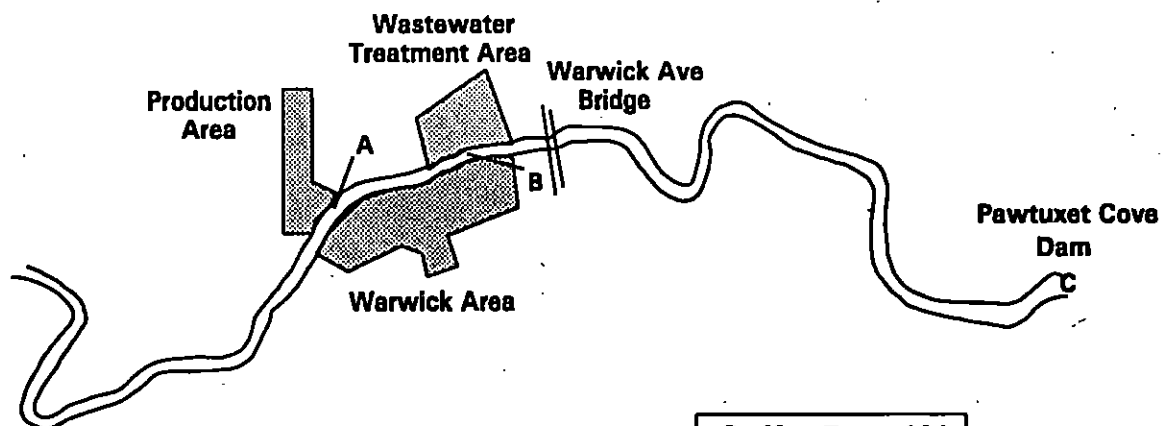
Pawtuxet River

FIGURE 8-3. Comparison of Temporal Distributions of PCB Projections - 0-5 cm Layer
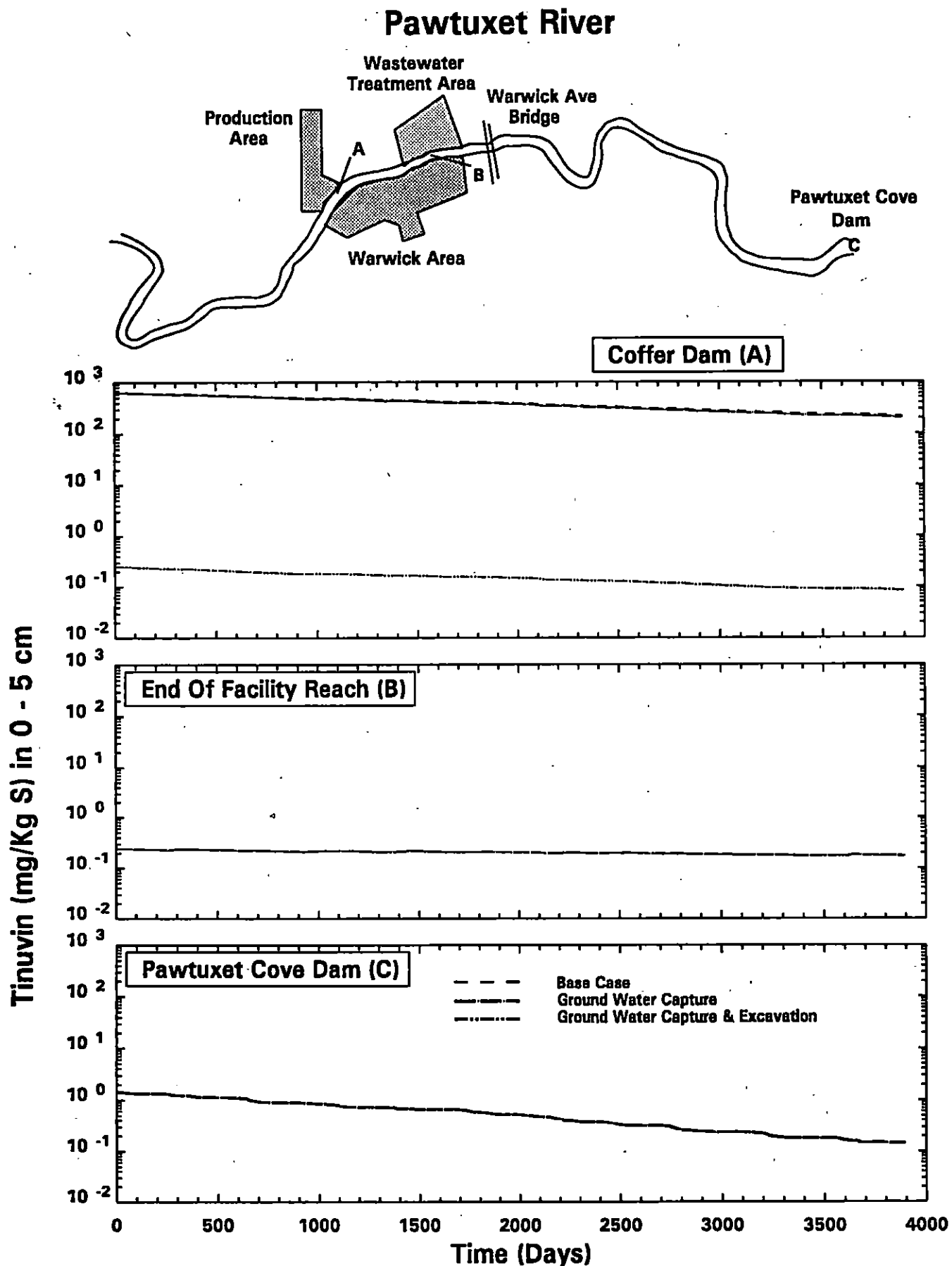
Pawtuxet River

FIGURE 8-4.   Comparison of Temporal Distributions of Tinuvin 328 Projections
- 0-5 cm Layer

Pawtuxet River
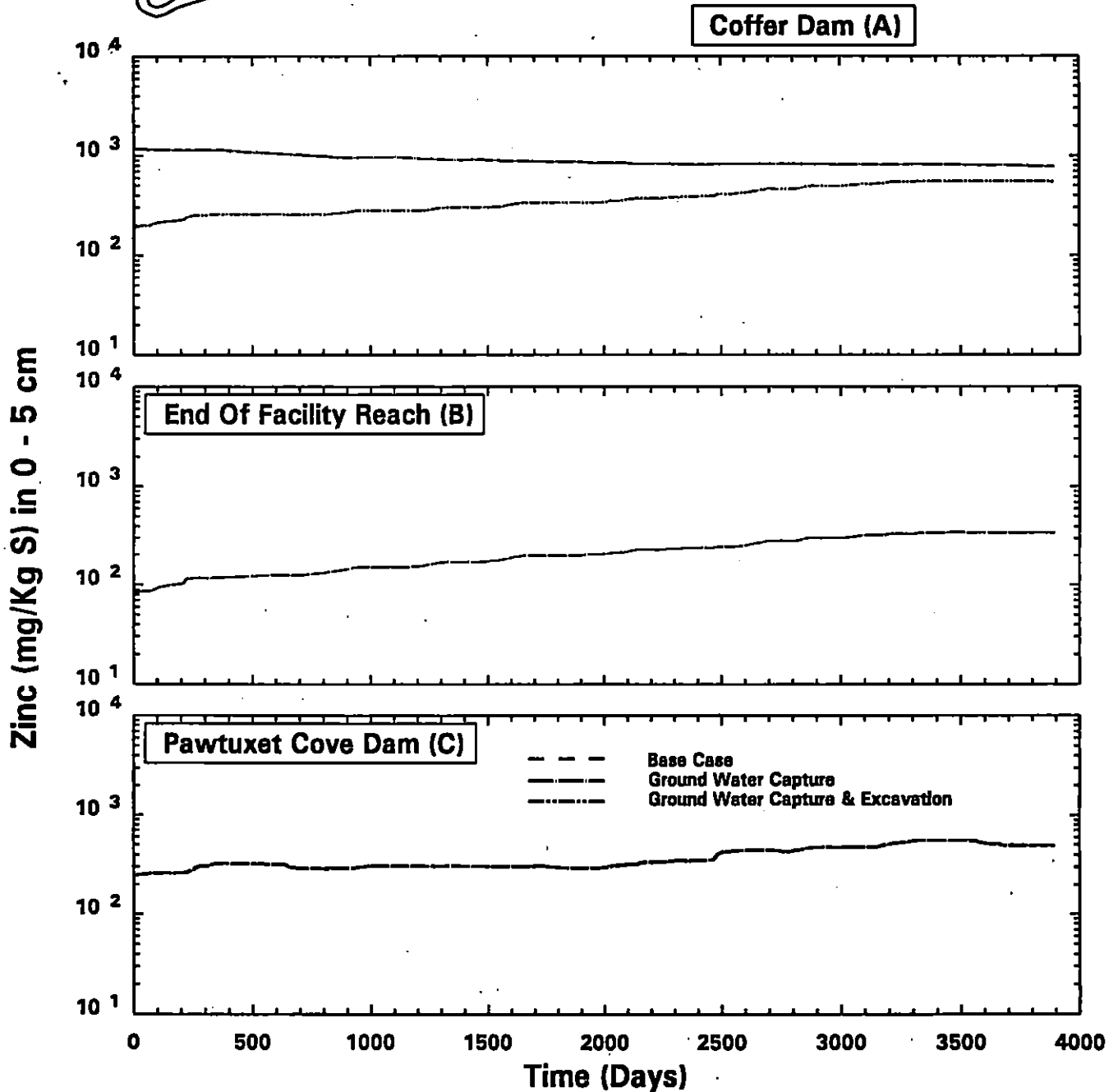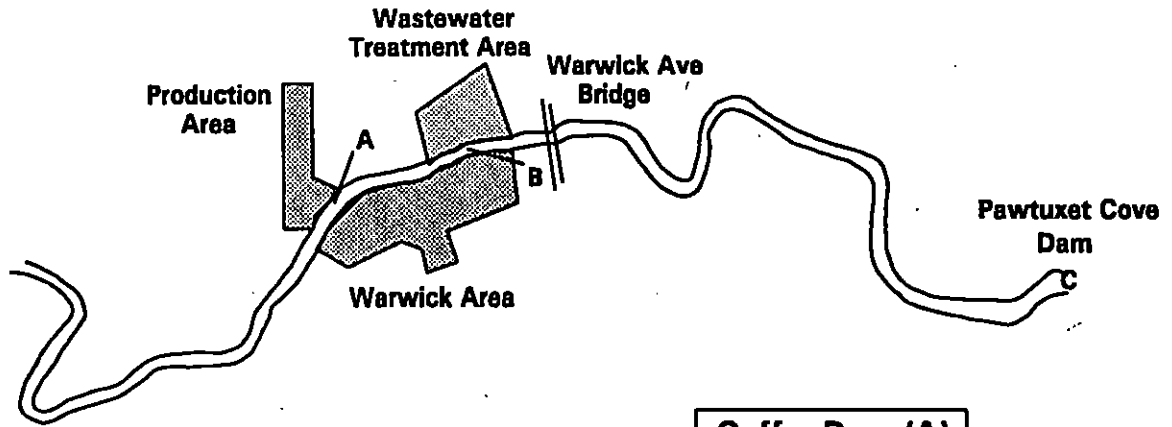
FIGURE 8-5.   Comparison of Temporal Distributions of Zinc Projections - 0-5 cm Layer
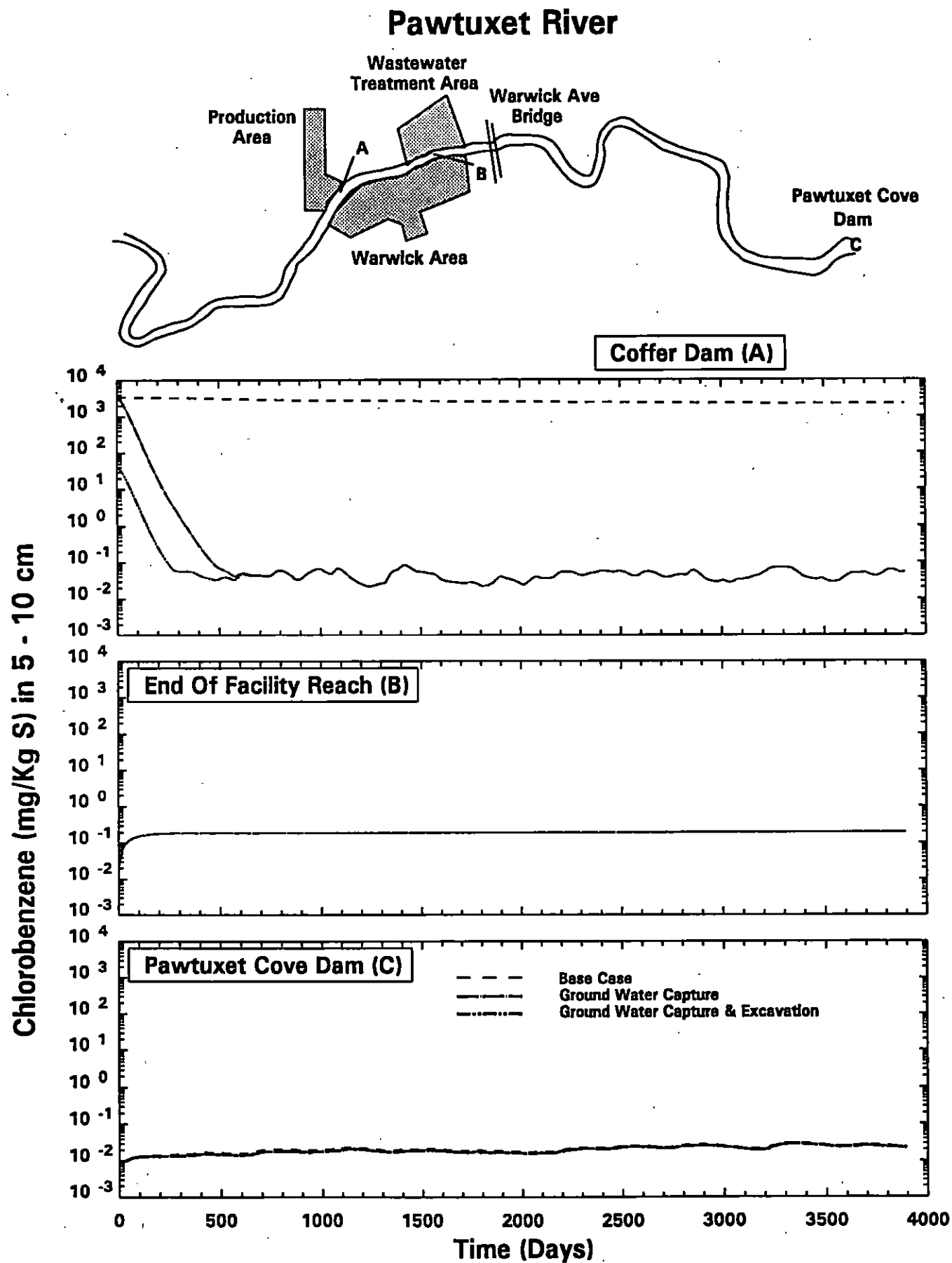
FIGURE 8-6.   Comparison of Temporal Distributions of Chlorobenzene
Projections - 5-10 cm Layer
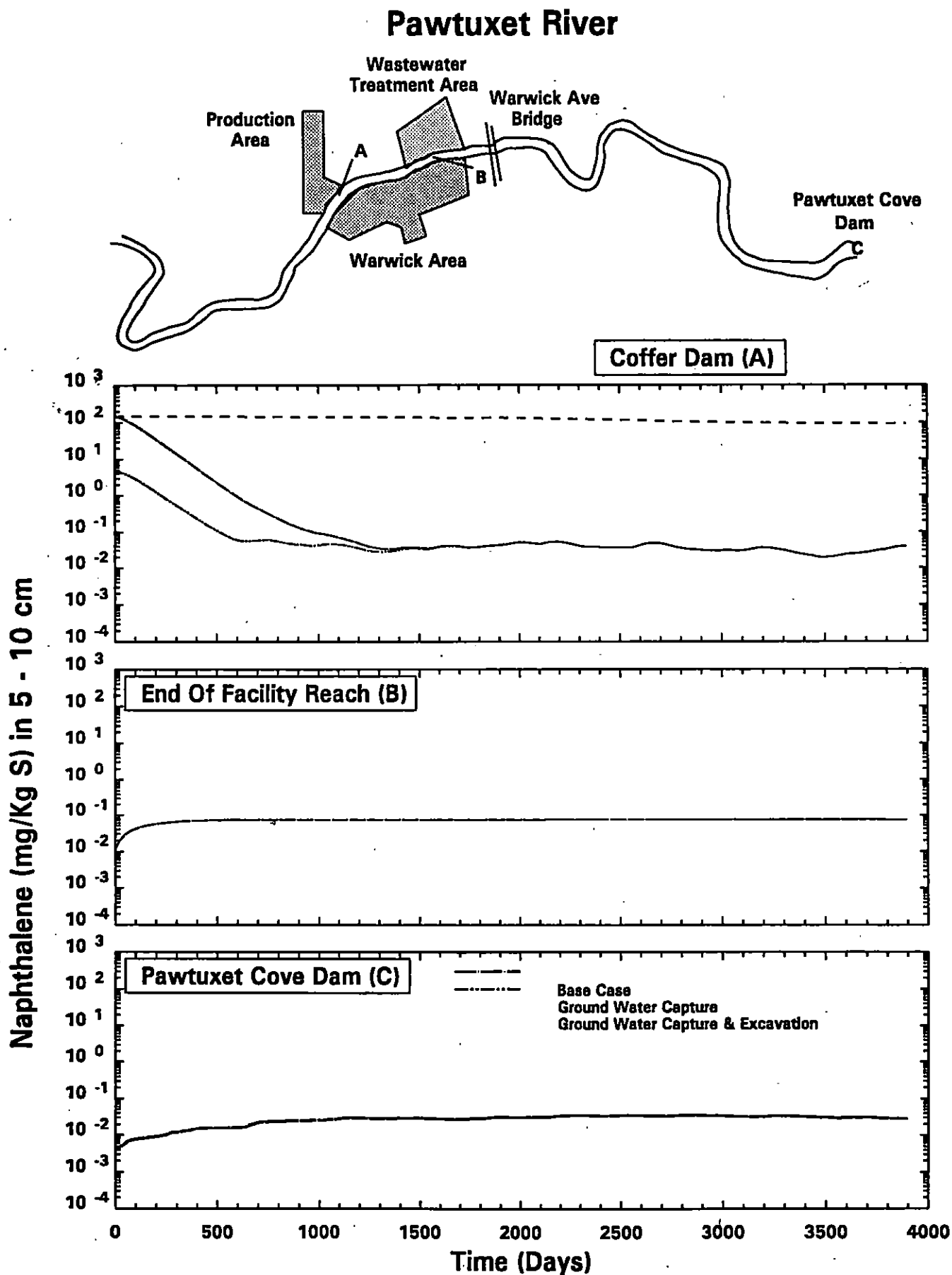
Pawtuxet River

FIGURE 8-7.   Comparison of Temporal Distributions of Naphthalene
Projections - 5-10 cm Layer
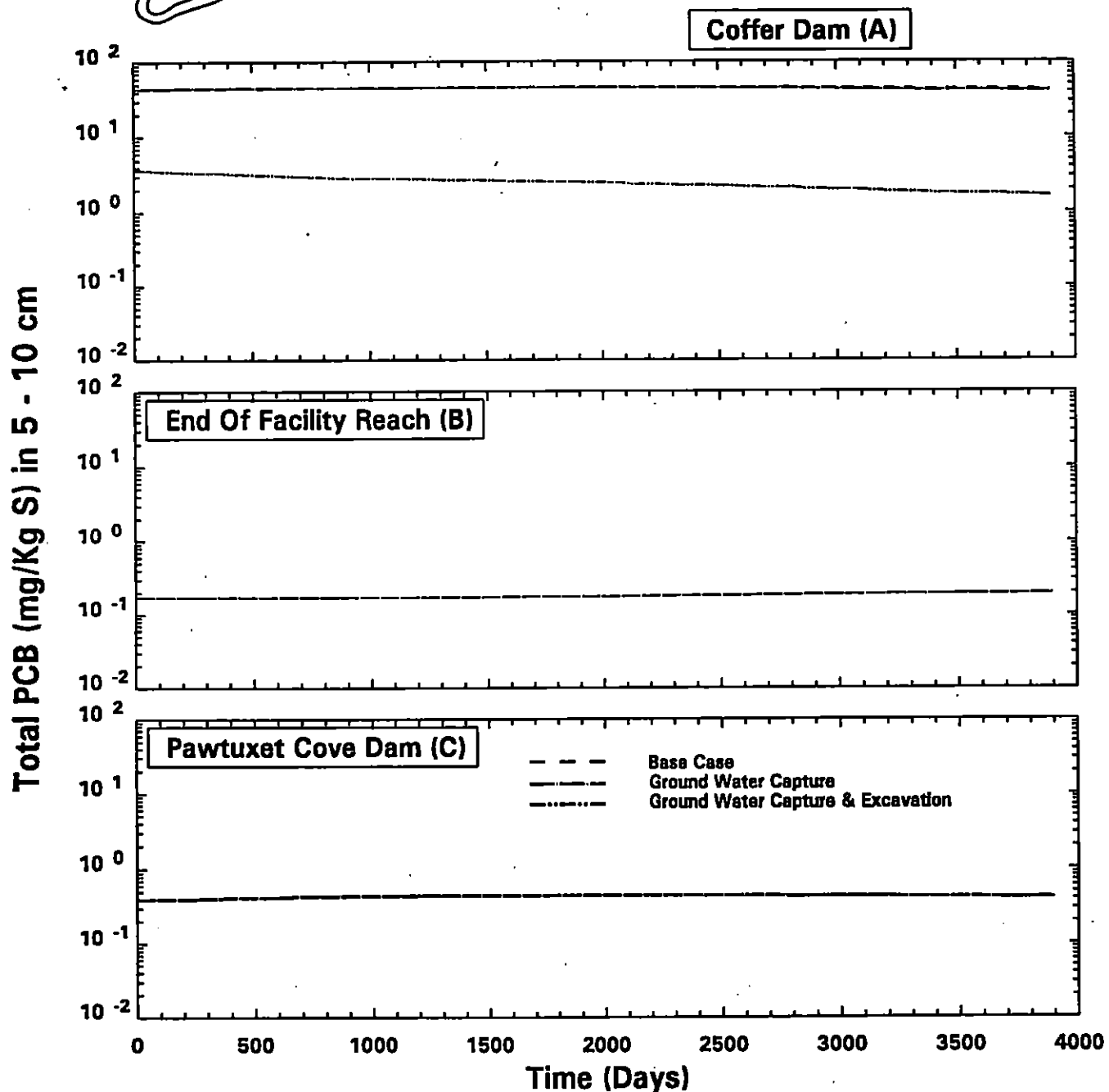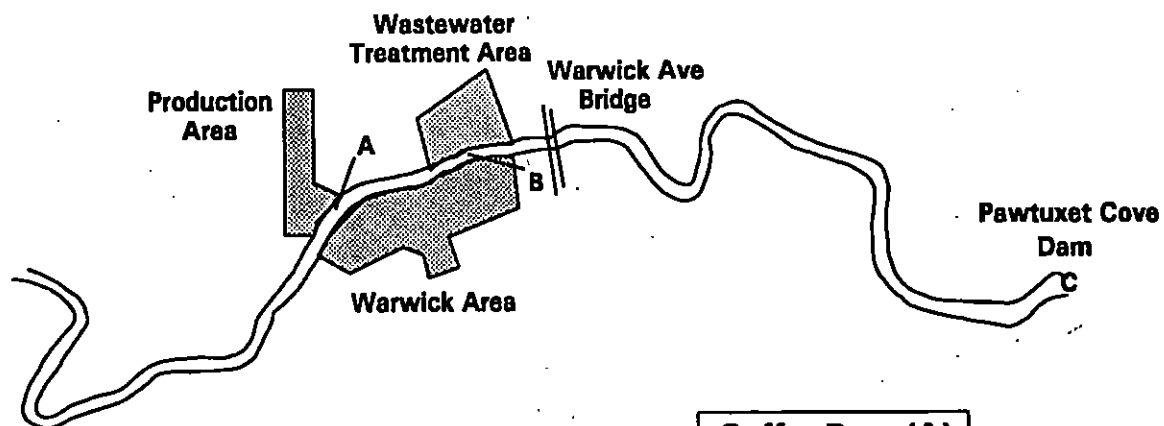
Pawtuxet River

FIGURE 8-8.   Comparison of Temporal Distributions of PCB Projections - 5-10 cm Layer
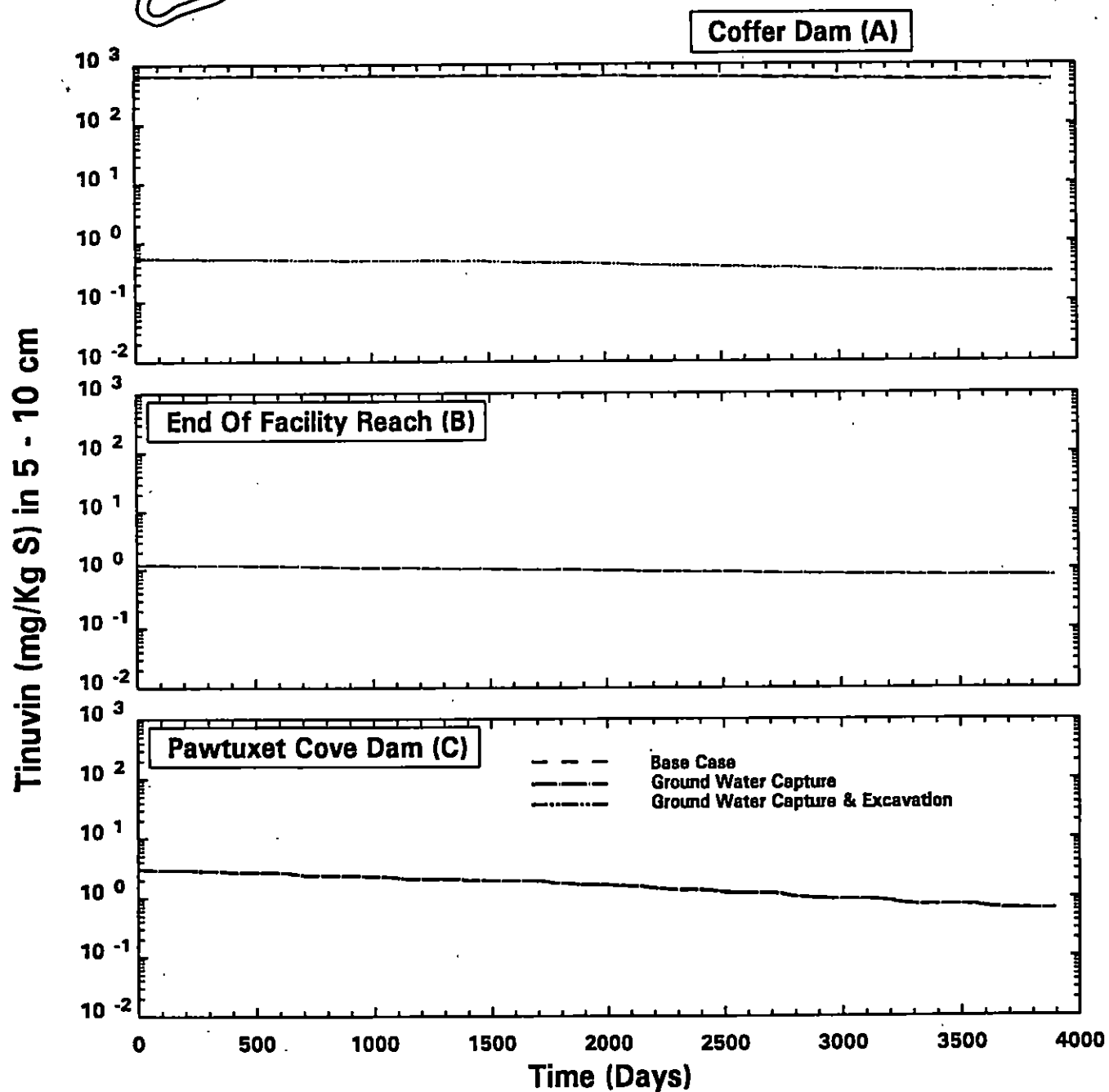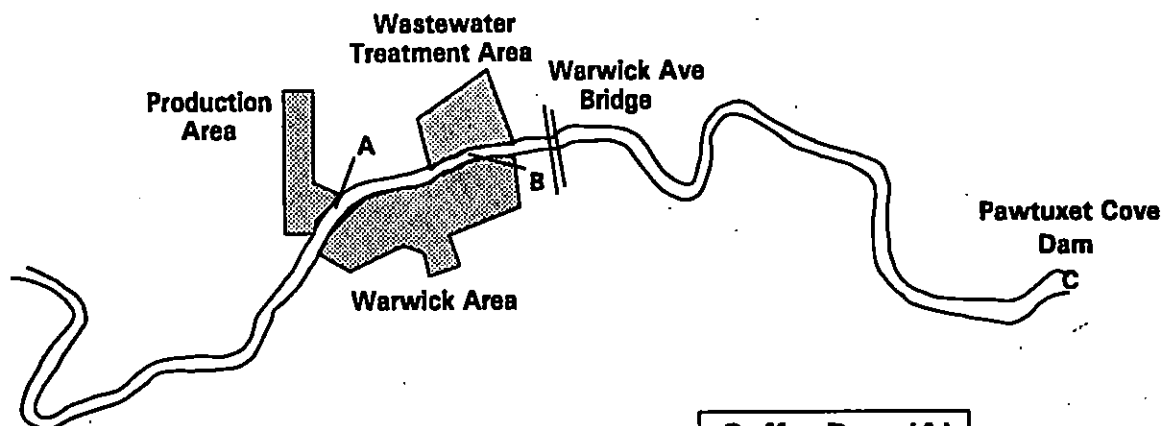
Pawtuxet River

FIGURE 8-9. Comparison of Temporal Distributions of Tinuvin 328 Projections
- 5-10 cm Layer
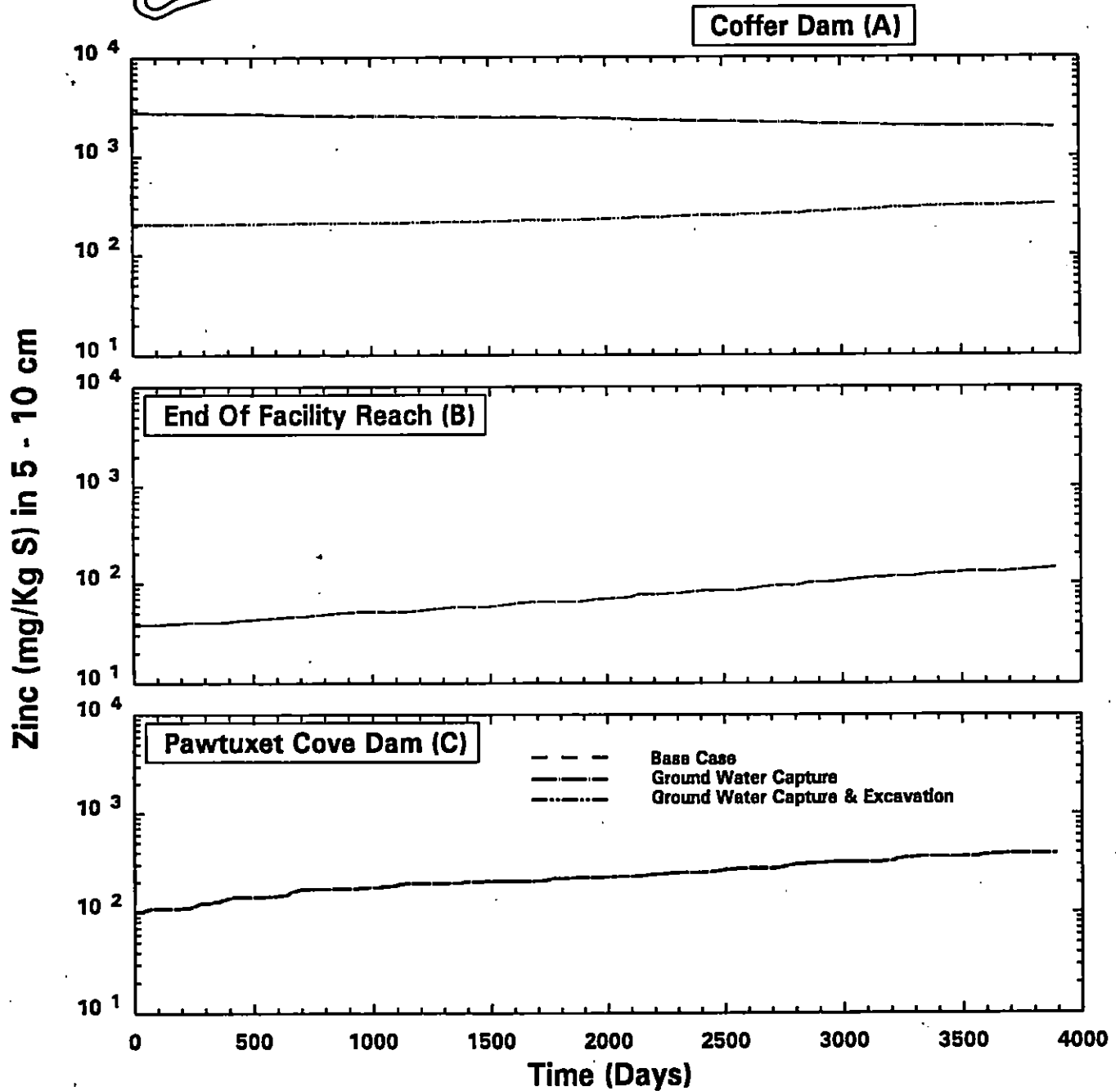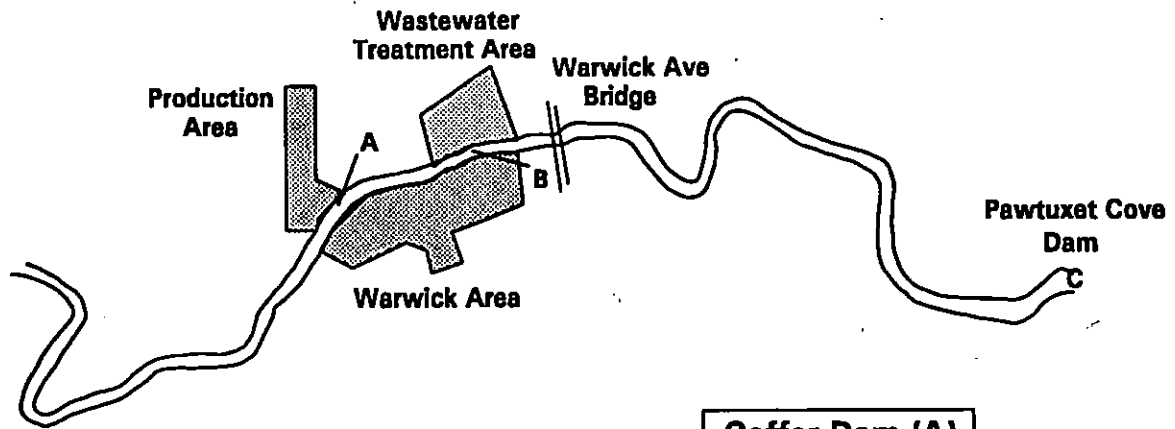
Pawtuxet River

FIGURE 8-10.   Comparison of Temporal Distributions of Zinc Projections - 5-10 cm Layer
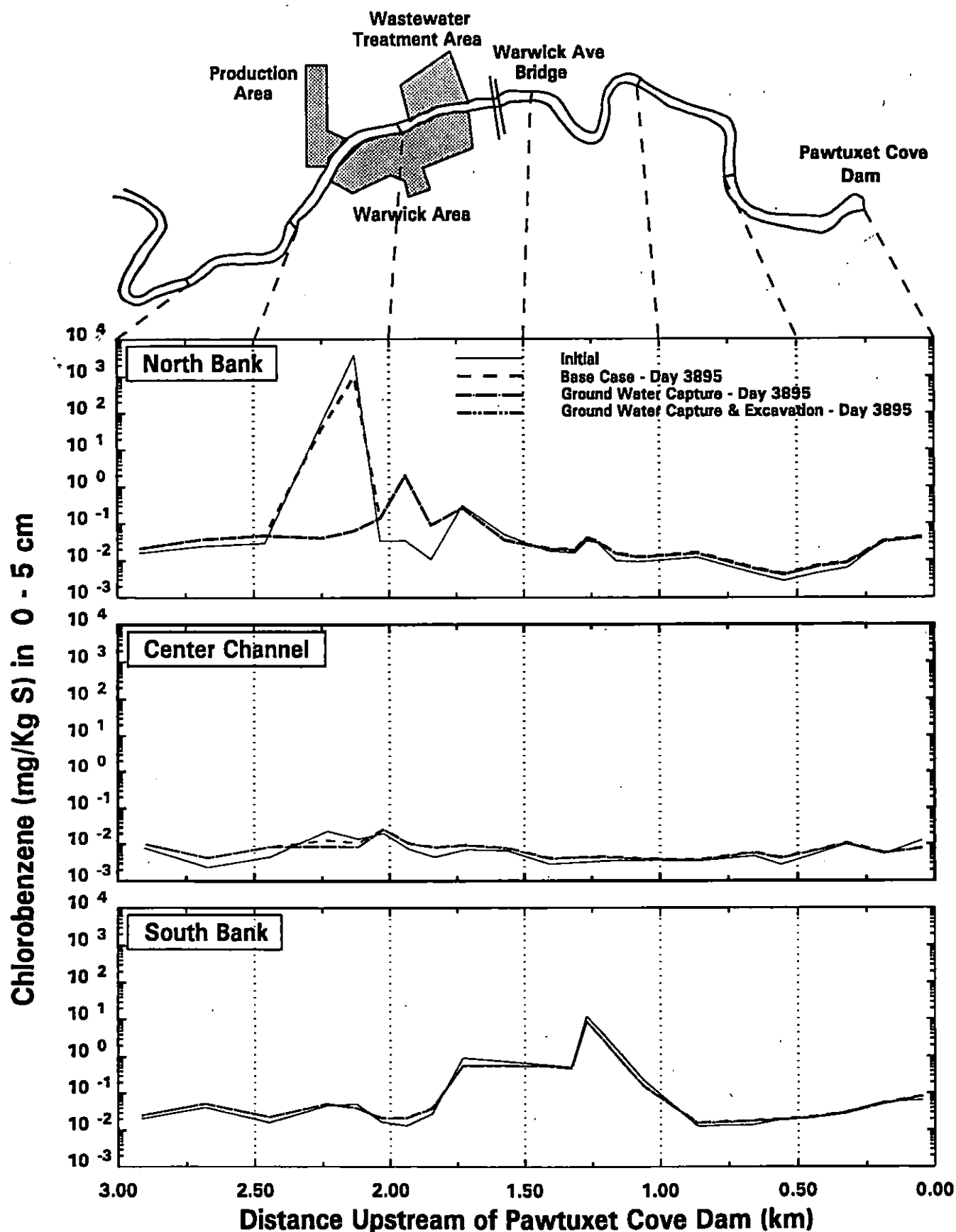
Pawtuxet River

FIGURE 8-11.   Comparison of Spatial Distributions of Chlorobenzene Projections - 0-5 cm Layer
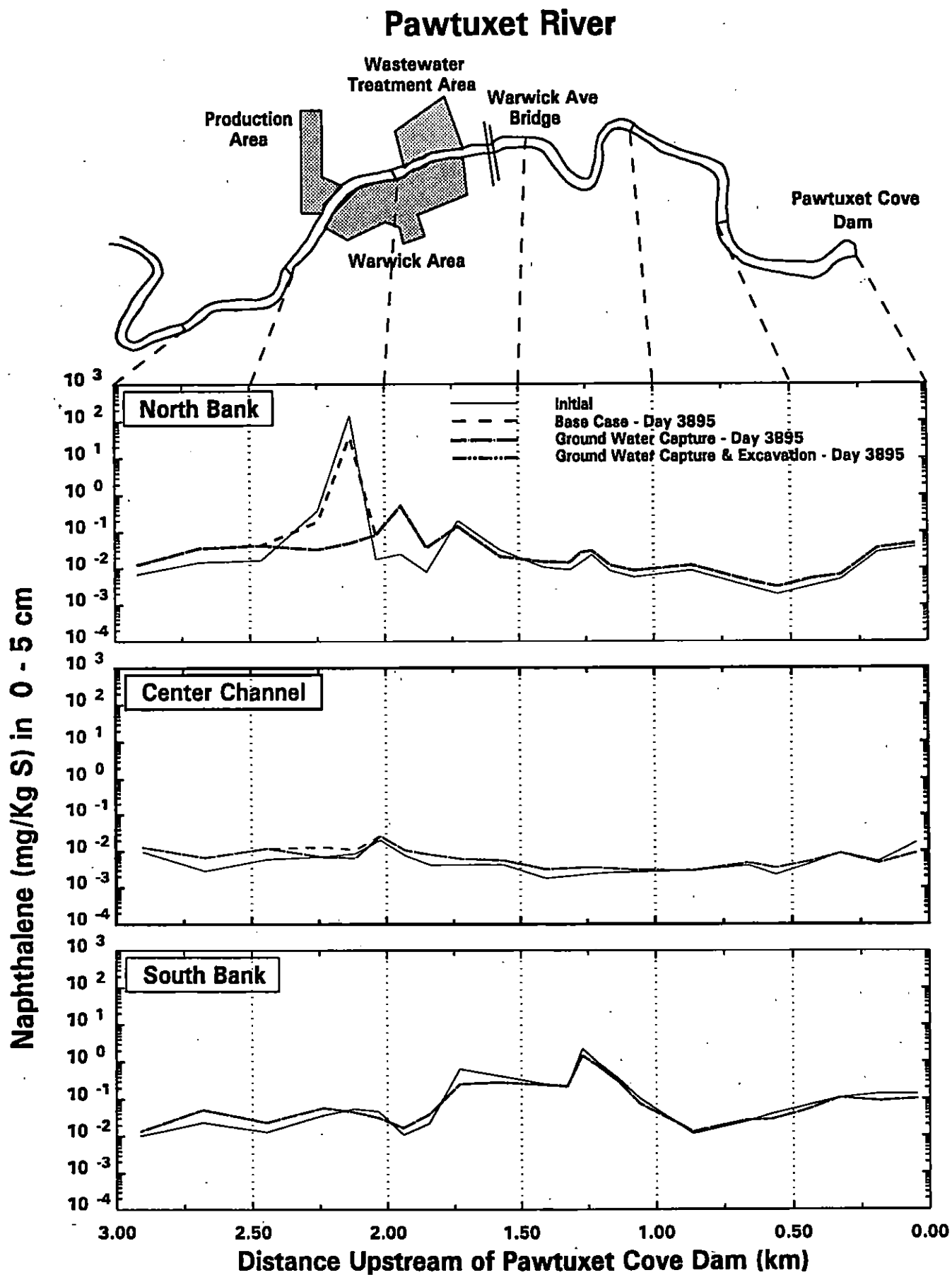
Pawtuxet River

FIGURE 8-12.   Comparison of Spatial Distributions of Naphthalene Projections -
0-5 cm Layer
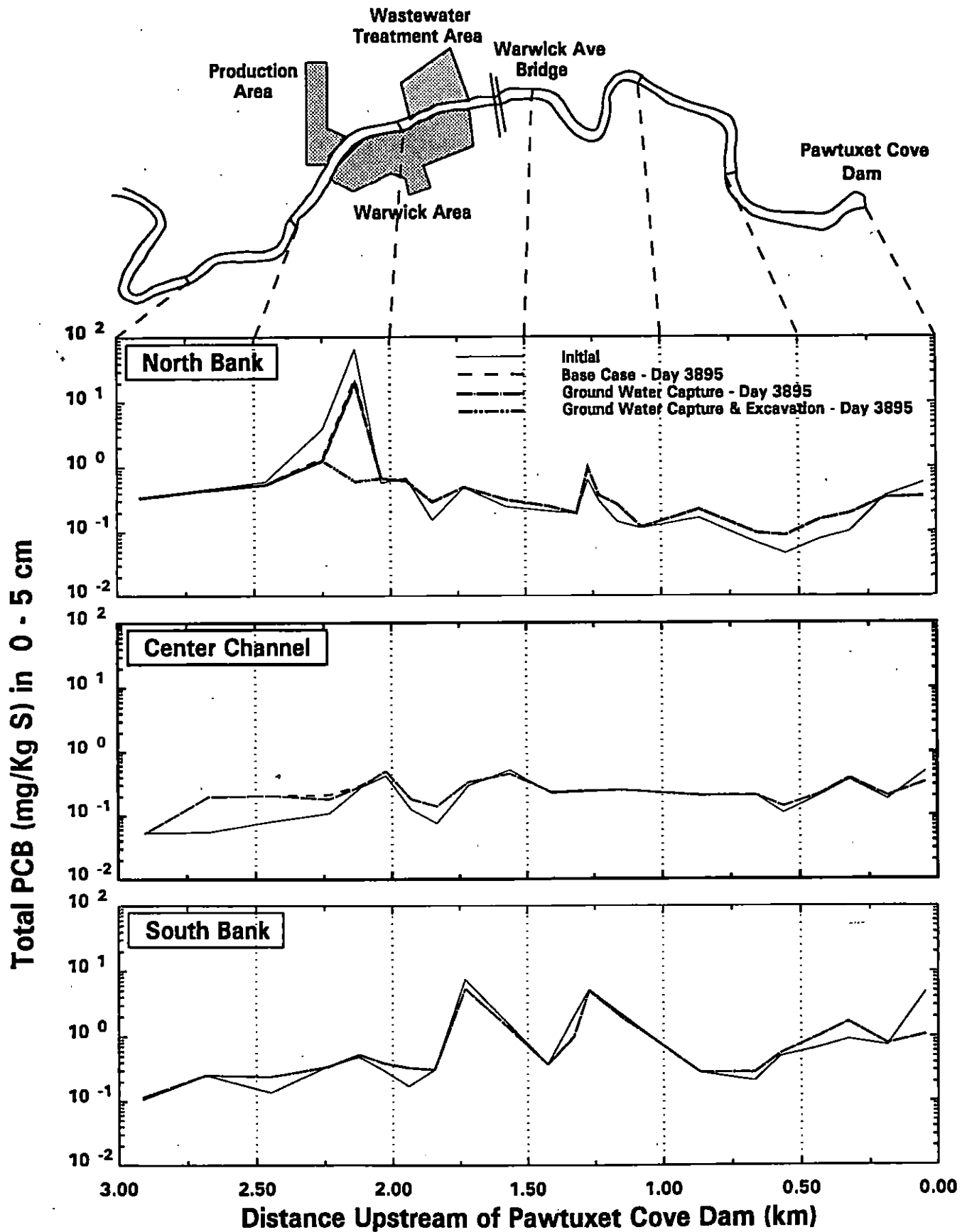
FIGURE 8-13. Comparison of Spatial Distributions of PCB Projections - 0-5 cm Layer

Pawtuxet River
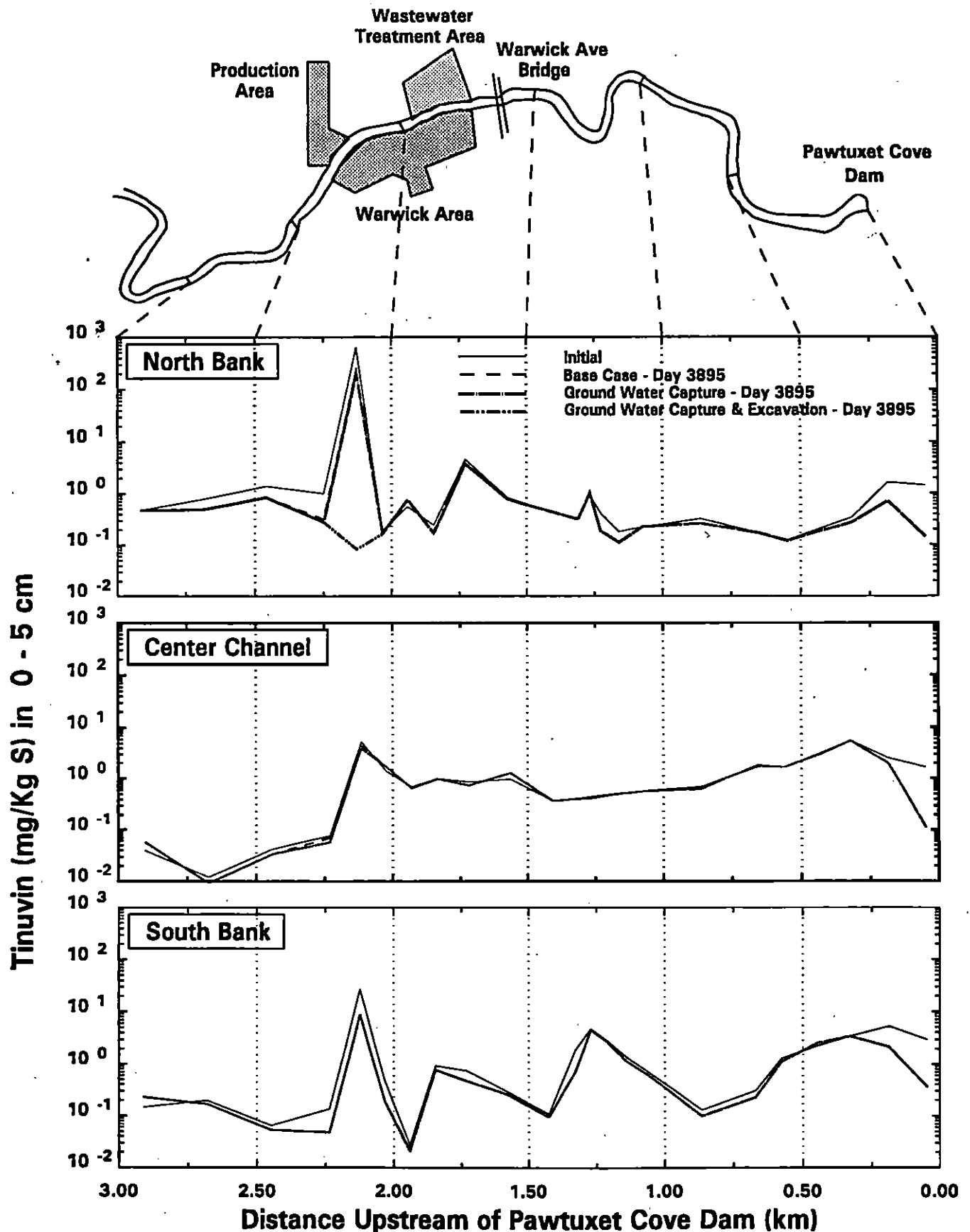
FIGURE 8-14. Comparison of Spatial Distributions of Tinuvin 328 Projections - 0-5 cm Layer
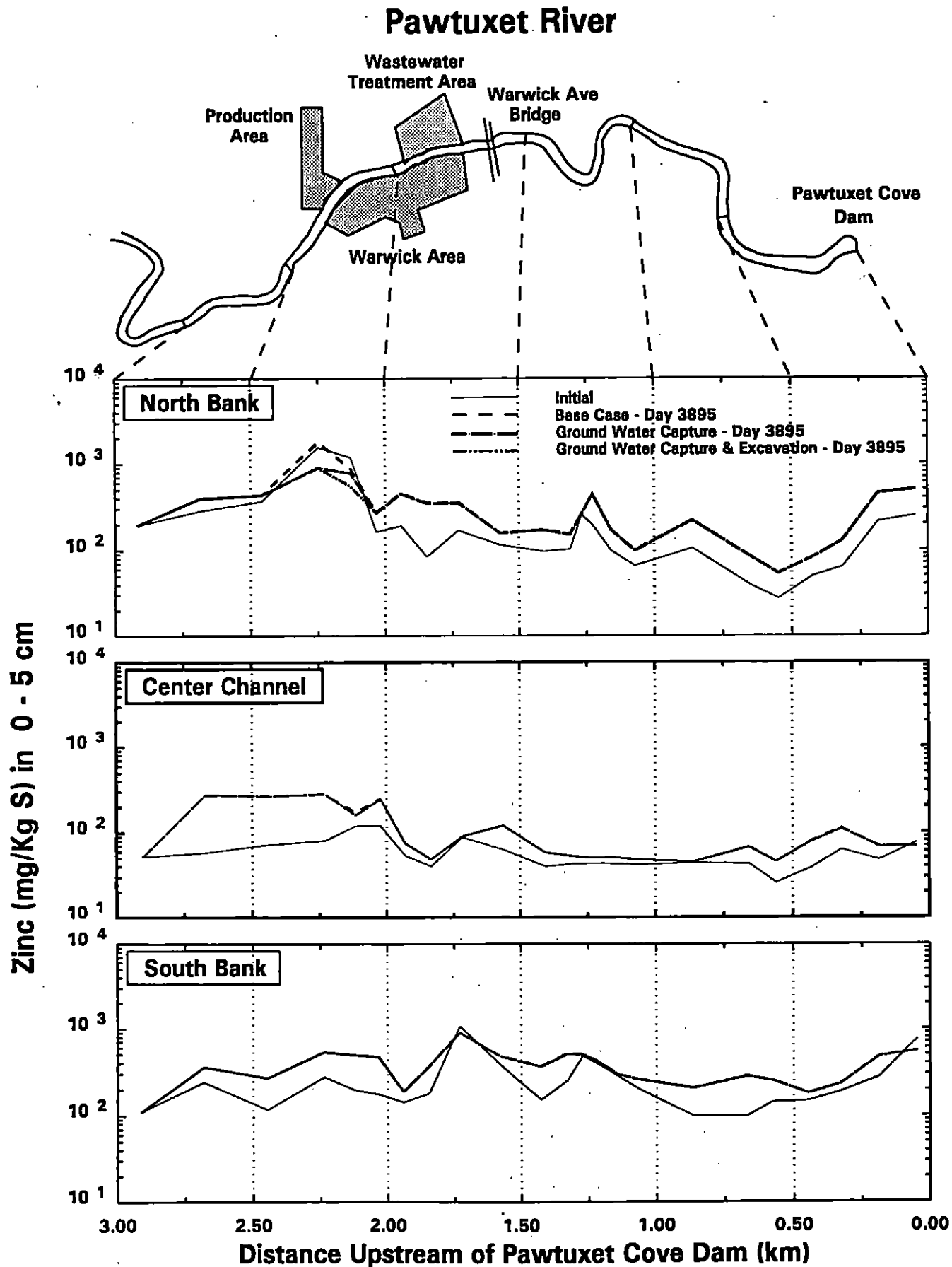
FIGURE 8-15. Comparison of Spatial Distributions of Zinc Projections - 0-5 cm Layer
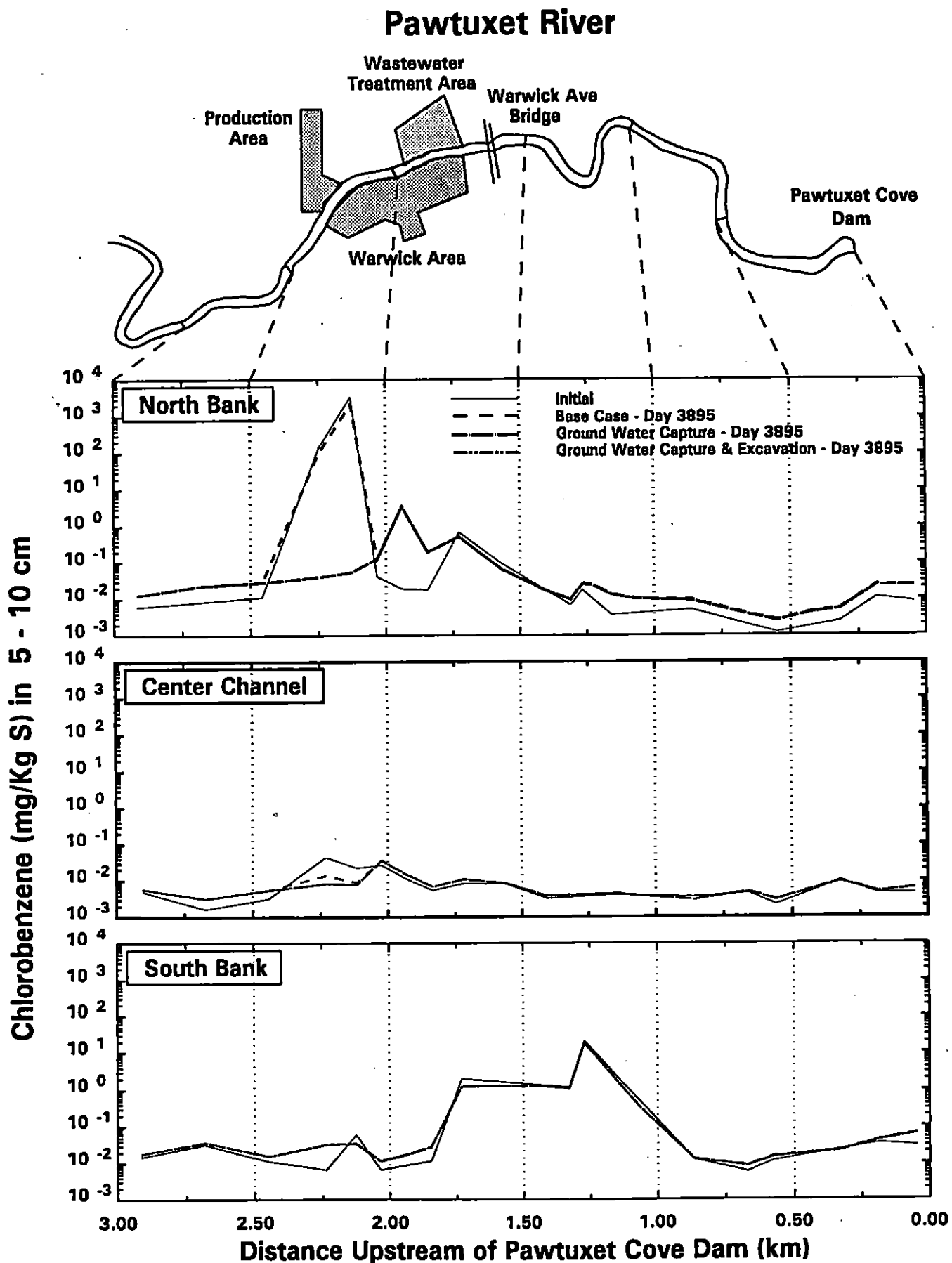
Pawtuxet River

FIGURE 8-16. Comparison of Spatial Distributions of Chlorobenzene Projections
- 5-10 cm Layer
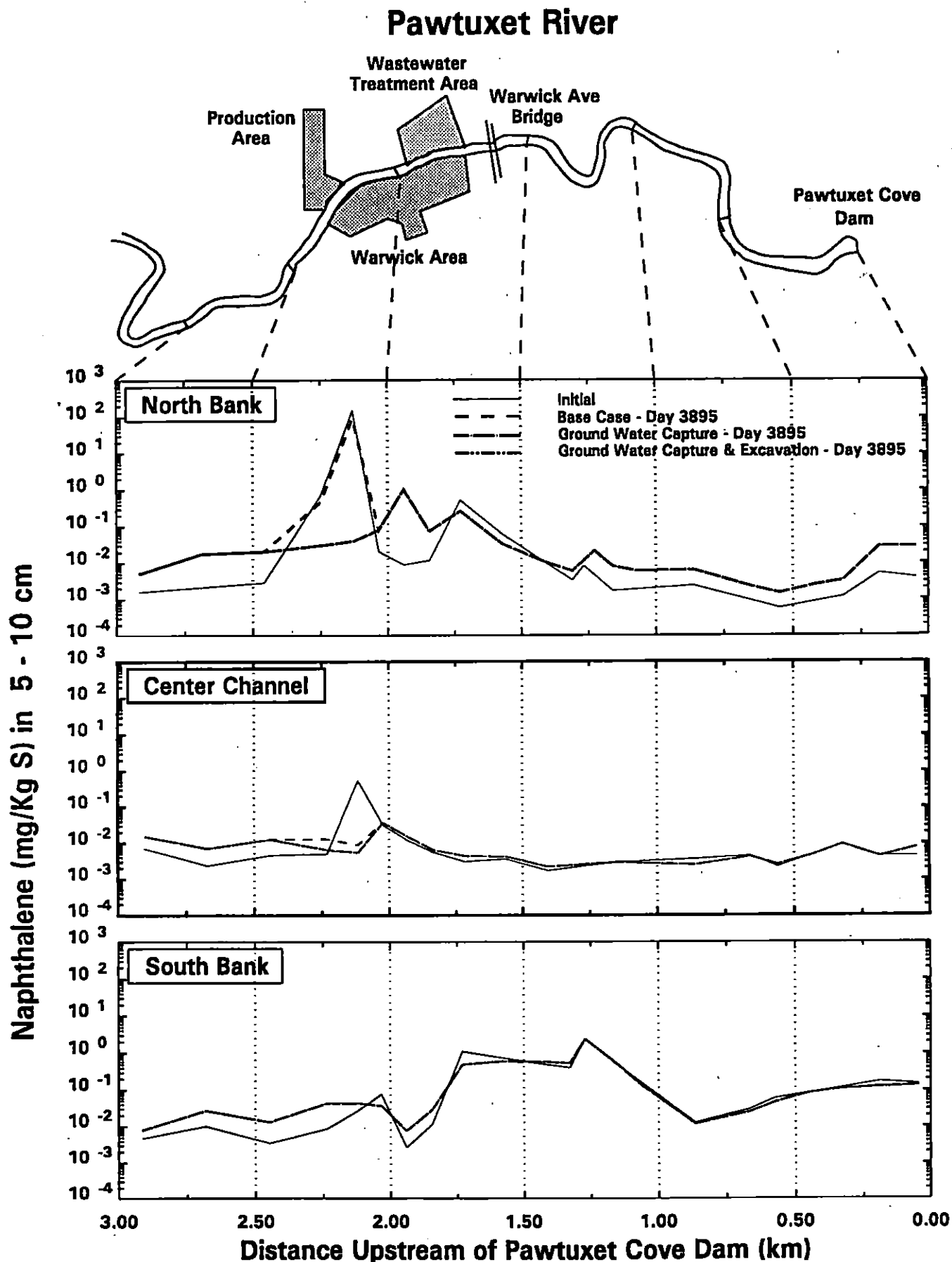
FIGURE 8-17. Comparison of Spatial Distributions of Naphthalene Projections -
5-10 cm Layer
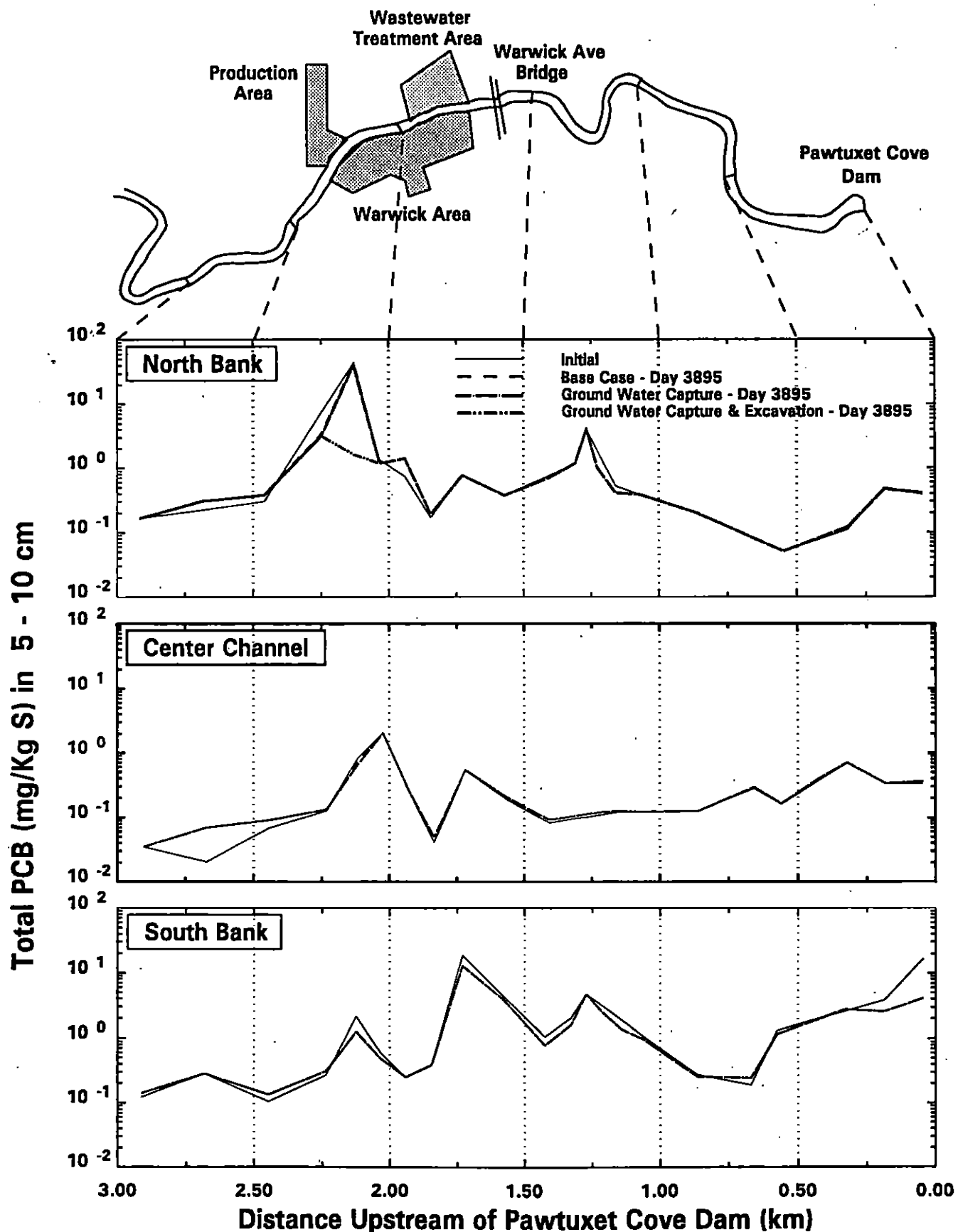
Pawtuxet River

FIGURE 8-18.   Comparison of Spatial Distributions of PCB Projections - 5-10 cm Layer
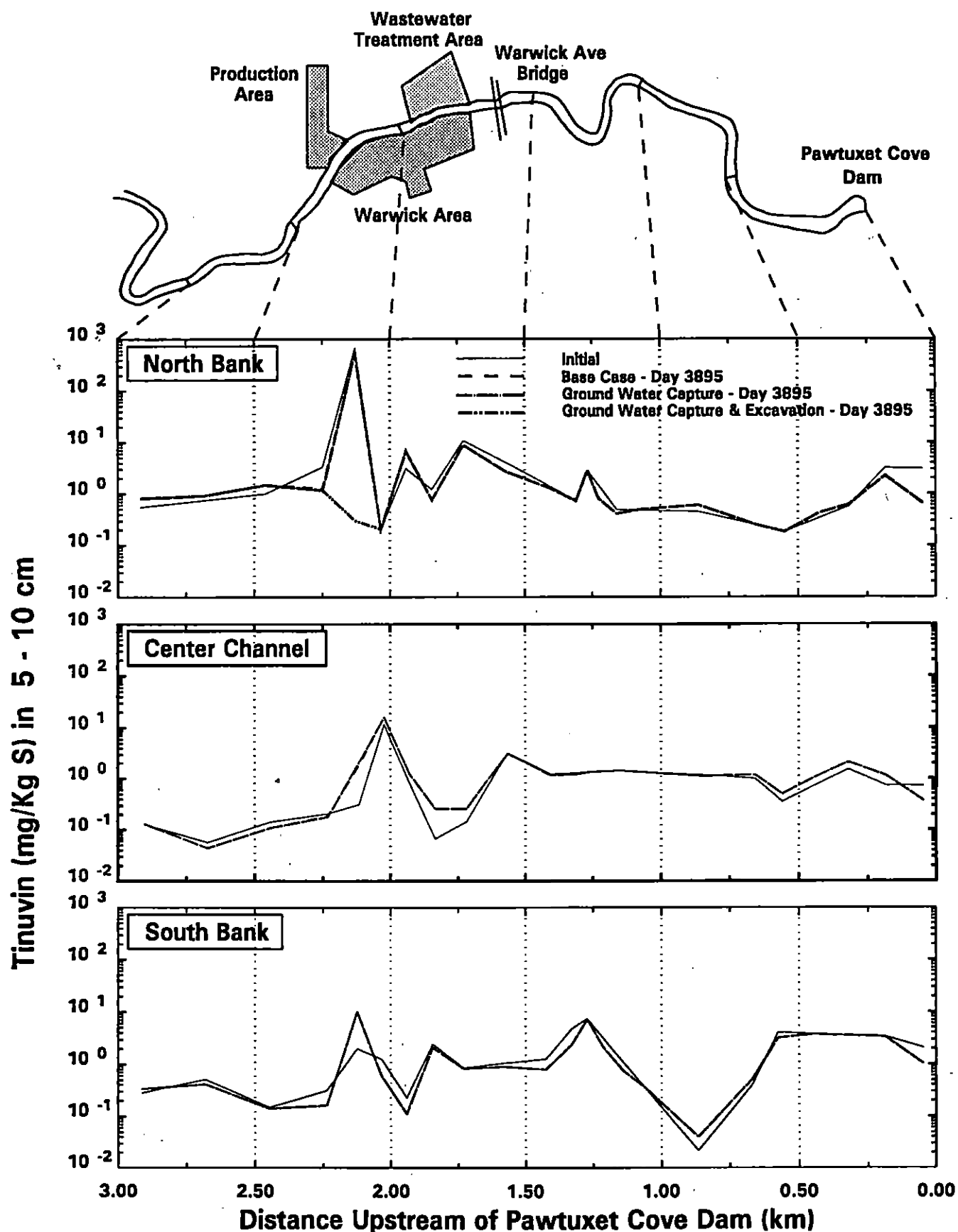
FIGURE 8-19.   Comparison of Spatial Distributions of Tinuvin 328 Projections -
5-10 cm Layer

Pawtuxet River
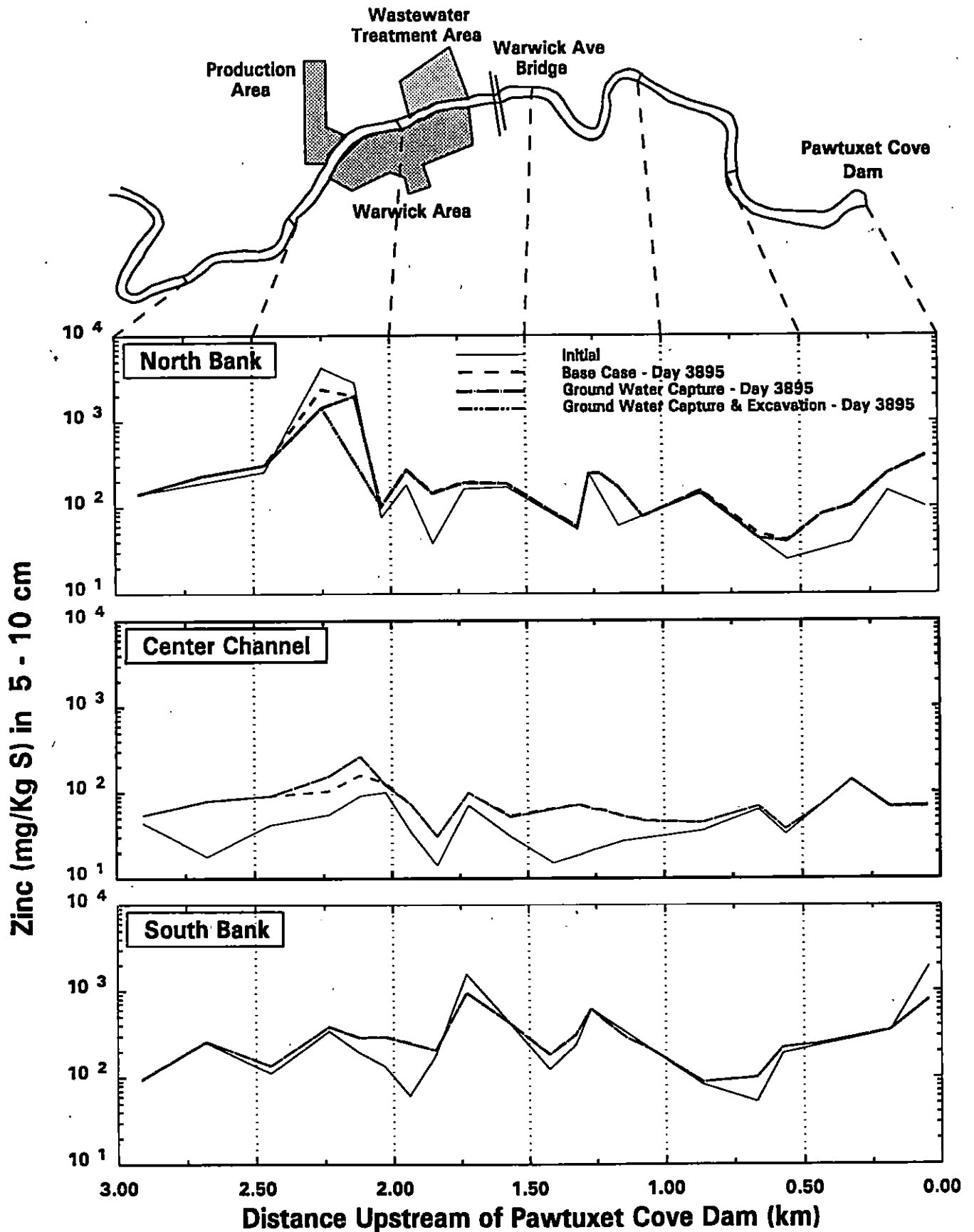
FIGURE 8-20.   Comparison of Spatial Distributions of Zinc Projections - 5-10 cm Layer
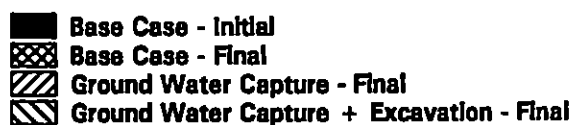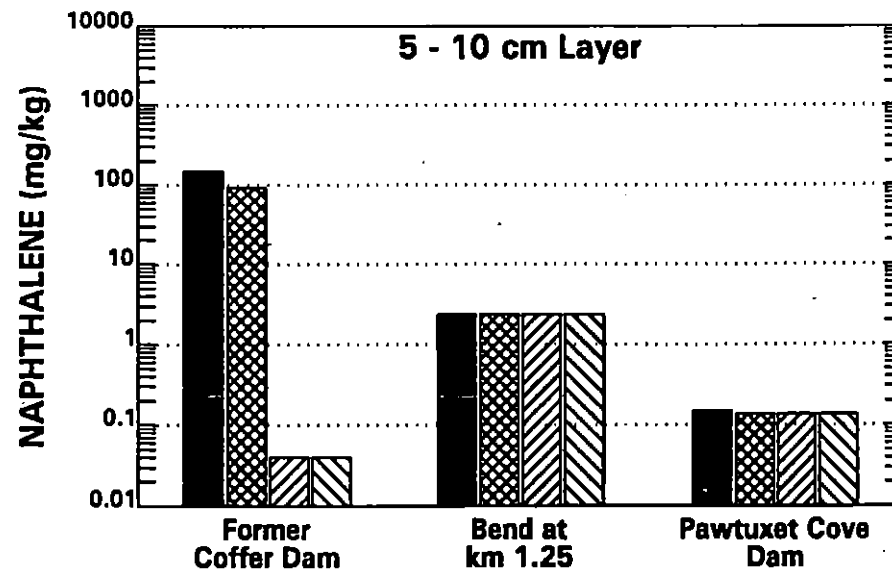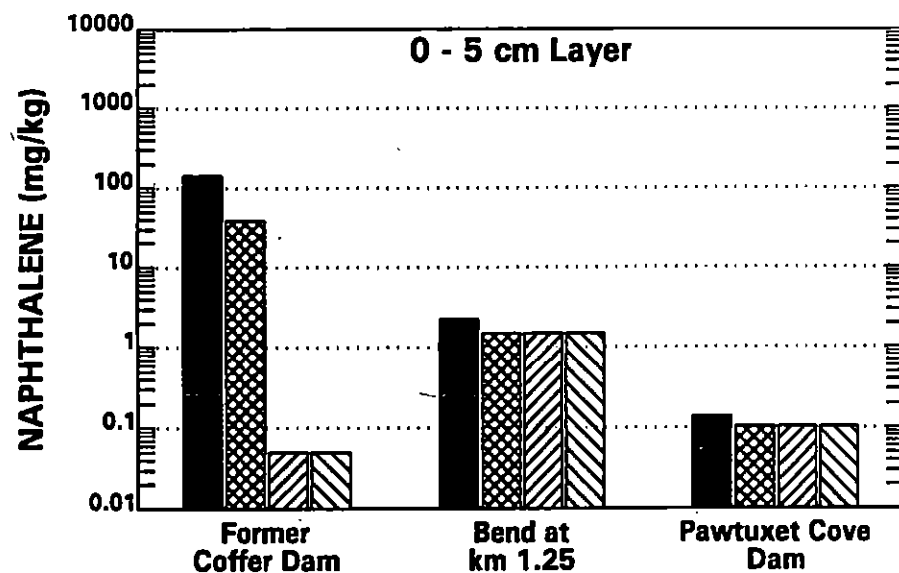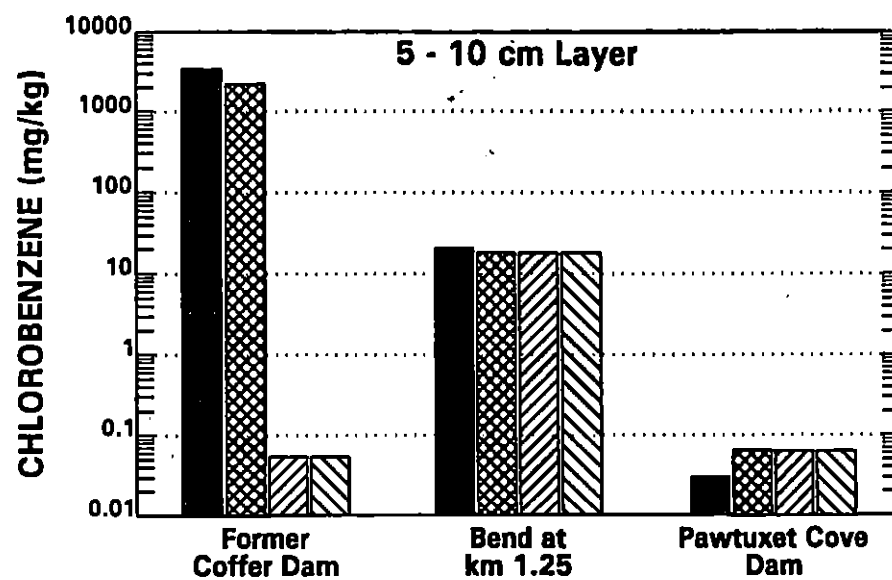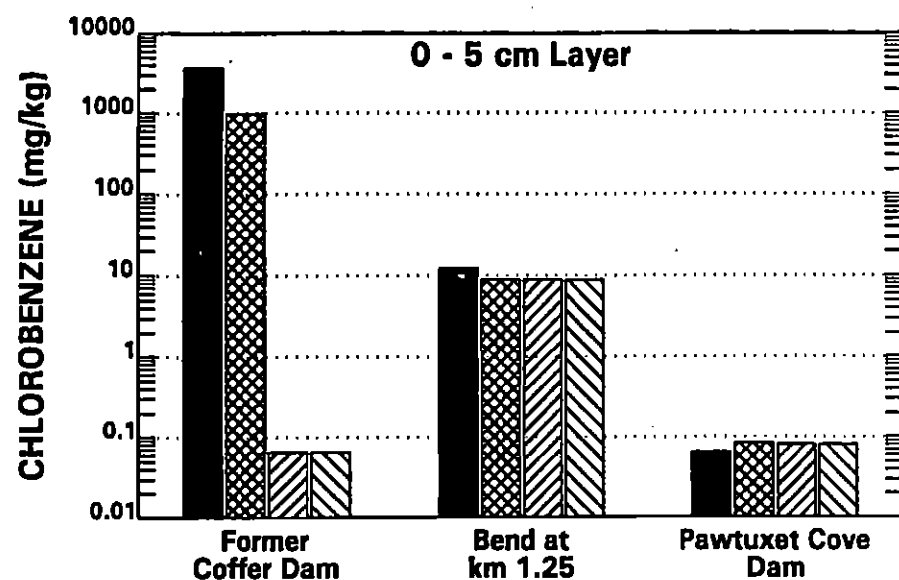
FIGURE 8-21a. Comparison of Present and Future Contaminant Concentrations for Base Case and Alternate Projections - Chlorobenzene & Naphthalene
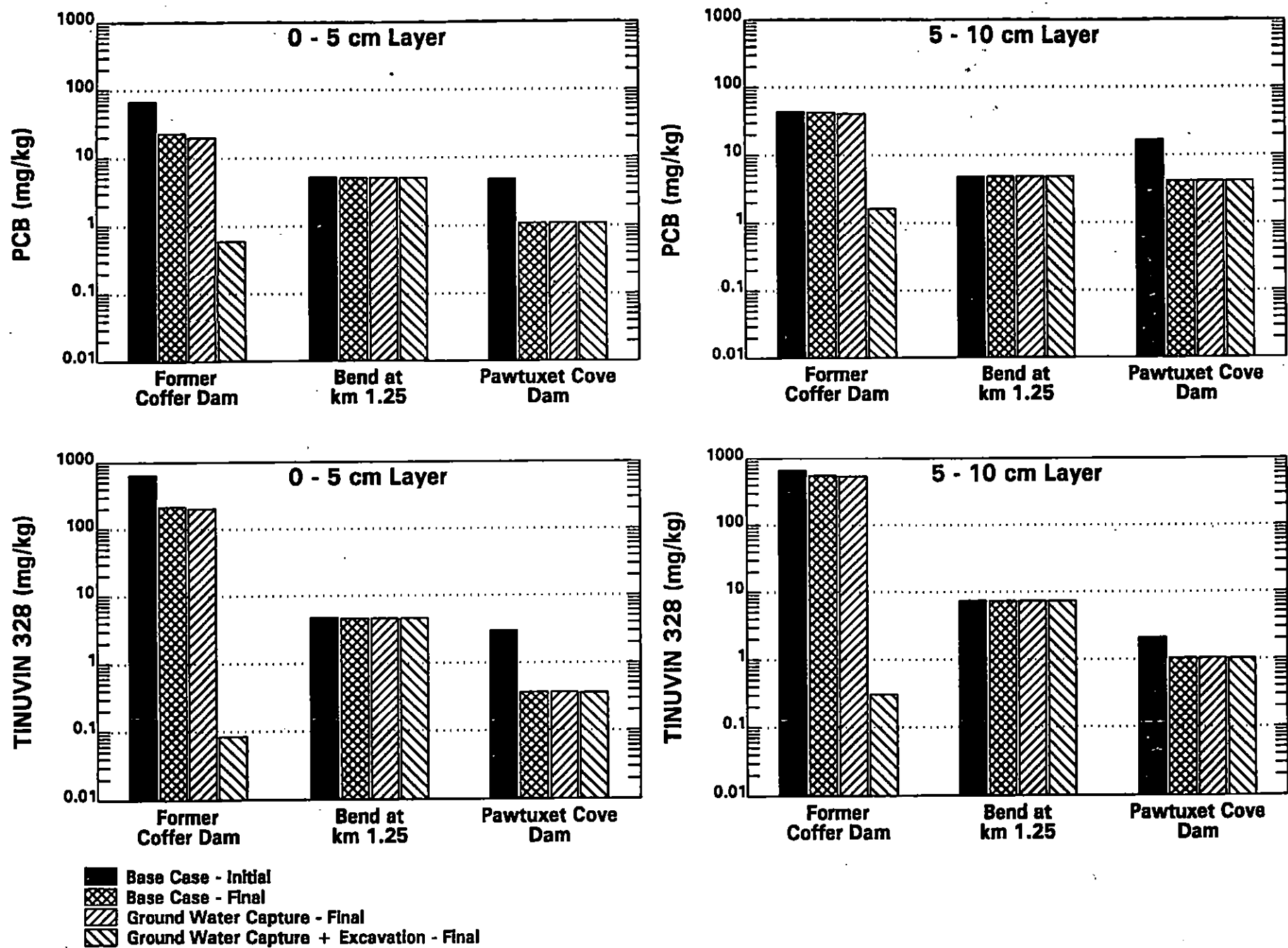
FIGURE 8-21b.   Comparison of Present and Future Contaminant Concentrations
for Base Case and Alternate Projections - PCBs & Tinuvin 328
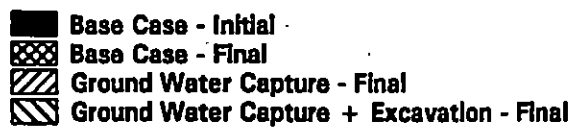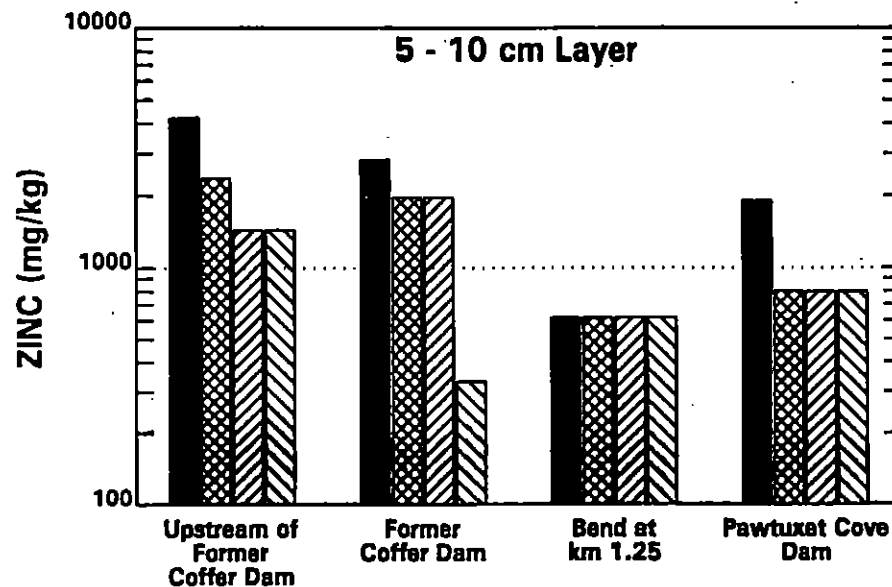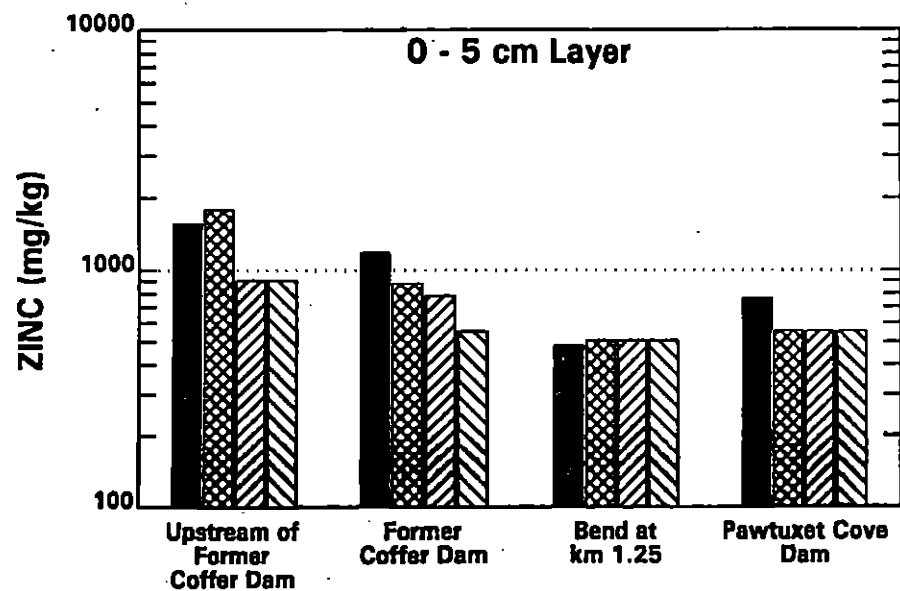
FIGURE 8-21c.   Comparison of Present and Future Contaminant Concentrations
for Base Case and Alternate Projections - Zinc

SECTION 9

SUMMARY AND CONCLUSIONS

The primary objective of the modeling analyses described in this report is to provide a quantitative evaluation of the effect of alternate remedial measures on contaminant concentrations in the Pawtuxet River. In order to accomplish this objective, a coupled hydrodynamic - sediment transport - contaminant transport and fate modeling framework has been applied to the lower Pawtuxet River. The framework represents the state-of-the-art in scientific understanding of the relevant environmental mechanisms influencing the transport and fate of contaminants in surface waters. Modeling analyses have been performed for 5 chemicals:

- Chlorobenzene
- Naphthalene
- PCBs
- Tinuvin 328
- Zinc

These five chemicals were selected because they cover a range of physical/chemical properties, they were used or produced at the facility, and/or because of the toxicological significance of concentrations measured in the Phase I Release Characterization.

To varying degrees, each of the five chemicals selected for modeling sorb to particulate material in the water column and sediment. The transport of these chemicals, therefore, is influenced by the movement of the surface water and the settling and resuspension of particulate material. The first two submodels (hydrodynamic and sediment transport) calculate spatial and temporal distributions of the movement of water and solids. The contaminant fate submodel uses this transport information, as well as chemical properties that affect transfer processes, to calculate the fate and transport of each chemical. The contaminant fate and transport model includes such processes as

dissolved-particulate partitioning, volatilization, settling, resuspension, and diffusion. The results of the transport and fate model are estimates of future contaminant concentrations, which vary in response to alternate remediation activities.

The significant findings from these analyses are:

- The lower 2.8 km of the study area (from approximately 0.5 km upstream of the Facility to the Pawtuxet Cove Dam) is, in general, a depositional area. Net resuspension is calculated in only very limited areas. Net deposition begins roughly 0.5 km upstream of the facility in response to a reduction in the slope of the river bed. Net deposition rates in the shallower near shore areas are higher than in the more stable center channel. Only a limited number of areas have net deposition rates greater than 0.5 cm/yr, with the highest rates (1 to 1.5 cm/yr) calculated in the area upstream of the Pawtuxet Cove Dam.

- Re-deposition of sediments resuspended from within the study area is not a significant component in the depositional processes in the study area. Therefore, sediment contaminant concentrations in downstream areas are not significantly affected by resuspension of contaminated sediment from areas within the study area.

- Deposition in the lower 2.8 km of the study area results in gradual burial of surfical sediments with upstream water column solids. The change in contaminant concentrations due to this burial is a function of the local deposition rate and the relative concentration of contaminants in the sediment and on the depositing solids.

- In the area of the former coffer dam, approximately a 70 percent reduction in surfical sediment concentrations of chlorobenzene, naphthalene, PCBs and Tinuvin 328 is calculated after 10.6 years in the base case projection, where no remedial actions are implemented. This is due to the high deposition rate in this location and the fact that measured sediment concentrations at this location are several orders

of magnitude higher than concentrations sorbed to the water column solids. For these chemicals the sediments are being buried by essentially clean solids. By contrast, zinc concentrations on the water column solids are closer to the sediment concentrations and a reduction in sediment concentrations of zinc of only 20 percent is calculated after 10.6 years.

- Sediment concentrations of chlorobenzene, naphthalene and PCBs are fairly constant in locations away from the former cofferdam area, indicating that sediment - water column exchanges of these chemicals are near equilibrium. Most locations in the lower 2.8 kilometers of the study area experienced an increase in zinc concentrations in the sediment due to deposition of zinc contaminated solids. The contaminated water column solids are associated with zinc entering the study area at the upstream boundary. Tinuvin 328 concentrations in most of the lower 2.8 km of the study area decreased in response to deposition of uncontaminated solids.

- Contaminant concentrations in sediments of areas away from Ciba's production area are not significantly affected by either remedial action, because current mass fluxes out of the sediments adjacent to the production area do not significantly affect the sediments in the downstream Pawtuxet River.

- Operation of the groundwater capture system along the production area bulkhead is effective in reducing peak concentrations of chlorobenzene and naphthalene near the former coffer dam area. This remedial action should be equally effective in reducing the concentrations of other chemicals with similar partition coefficients. During the first two years of operation, chlorobenzene concentrations in the top 10 cm of the sediment of the former coffer dam area decrease from over 3000 mg/kg to less than 0.1 mg/kg. In the first three years of operation of the groundwater capture system, naphthalene concentrations in the same area decrease from over 100 mg/kg to less than 0.1 mg/kg. These significant reductions are due to river water advecting through the sediment, desorbing chlorobenzene and naphthalene as it flows toward the groundwater capture well. The groundwater capture system

results in approximately a 40 percent reduction in the peak zinc concentration. Operation of the groundwater capture system does not significantly affect the concentrations of PCBs or Tinuvin 328. Areas away from the former cofferdam area are not affected by the operation of the groundwater capture system.

- Excavation of sediment from the former coffer dam area is effective in reducing concentrations of PCB, Tinuvin 328, and zinc at that location. Ten years after excavation, PCB concentrations in the top 5 cm and 5-10 cm layers are calculated at 0.6 and 1.6 mg/kg, respectively. These represent substantial reductions compared to concentrations calculated in the base case (no remedial action), which were 22 and 45 mg/kg in the top 5 cm and 5-10 cm layers. Tinuvin concentrations of 0.08 and 0.3 mg/kg in the top 5 and 5-10 cm layers, calculated ten years after excavation are significantly lower than concentrations calculated at the end of the no action simulation (213 and 550 mg/kg in the top 5 and 5-10 cm layers). Zinc concentrations in the 0-5 and 5-10 cm layers are initially reduced from between 1000 and 3000 mg/kg to approximately 200 mg/kg as a result of the excavation. Deposition of contaminated solids from upstream gradually increases the sediment concentrations of zinc to approximately 550 and 330 mg/kg in the two layers, during the 10.6 year simulation.

- The combination of the two remedial actions produces substantial reductions in the peak concentrations of each of the five chemicals modeled. Table 9-1 summarizes the reduction in contaminant concentration in sediments near the production area, calculated over the course of the 10.6 year projection analyses. The indicated reductions of chlorobenzene and naphthalene concentrations are achieved in the first 2 and 3 years, respectively.

Table

Table 9-1. Effect of Remedial Actions on Contaminant Concentrations in Sediments Adjacent to the Ciba Production Area over 10.6 Year Projection			
Chemical	Effective Action	Concentration at Production Area (mg/kg)	
		Initial	Final
Chlorobenzene	Groundwater Capture	3700	0.06[1]
Naphthalene	Groundwater Capture	150	0.05[2]
PCBs	Excavation	66	1.6
Tinuvin 328	Excavation	640	0.3
Zinc	Excavation	2800	330

Note:
[1] Achieved after 2 years
[2] Achieved after 3 years

SECTION 10

REFERENCES

Acitchinson, J. and J.A.C. Brown, 1957. The Lognormal Distribution. Cambridge University Press, London.

Amos, C.L., J. Grant, G.R. Daborn and K. Black, 1992. Sea Carousel-A Benthic, Annular Flume, Estuarine, Coastal and Shelf Science, 34:557-577.

Ankley, G.T., N.A. Thomas, D.M. Di Toro, D.J. Hansen, J.D. Mahony, W.J. Berry, R.C. Swartz, R.A. Hoke; A.W. Garrison, H.E. Allen and C.S. Zarba, 1994. Assessing Potential Bioavailability of Metals in Sediments: A Proposed Approach, Envir. Manage., 18(3):331-337.

Ariathurai, R. and R.B. Krone, 1976. Finite Element Model for Cohesive Sediment Transport, J. Hydr. Div. ASCE, 102(3):323-338.

Bagnold, R.A., 1966. An Approach to the Sediment Transport Problem for General Physics, Geological Survey Professional Paper 422-I, Washington, D.C.

Blumberg, A.F., 1994. A Primer for ECOMsi, Technical Report, HydroQual, Inc., Mahwah, New Jersey.

Bogen, J., 1992. Monitoring Grain Size of Suspended Sediment in Rivers, In: Erosion and Sediment Transport Monitoring Programmes in River Basins, IAHS Pub. No. 210, pp. 183-190.

Burban, P.Y., Y.J. Xu, J. McNeil and W. Lick, 1990. Settling Speeds of Flocs in Fresh Water and Seawater, J. Geophys. Res., 95(C10): 18,213-18,220.

Cardenas, M., J. Gailani, C.K. Ziegler and W. Lick, 1994. Sediment Transport in the Lower Saginaw River, <u>Austral. J. Mar. Fresh. Res.</u>, in press.

CDM Federal Programs Corporation, 1993a. <u>Toms River Monitoring, Revised Draft Phase I Report, Baseline Characterization of the Toms River and Wetlands in the Vicinity of the Ciba-Geigy Toms River, New Jersey, Plant</u>, CMD Document No. 7720-022-DR-BTCD.

CDM Federal Programs Corporation, 1993b. <u>Revised Draft, Wetland Characterization and Ecological Assessment Winding River Park and Ciba-Geigy Toms River Chemical Plant, Toms River, New Jersey</u>, CDM Document No. 7720-027-DR-BTCN.

Connolly, J.P. and R.P. Winfield, 10984. WASTOX, A framework for Modeling Toxic Chemicals in Aquatic Systems, Part 1: Exposure Concentration, USEPA Gulf Breeze Florida, EPA 600/3-84-077.

Di Toro, D.M., J.D. Mahony, D.J. Hansen, K.J. Scott, M.B. Hicks, S.M. Mayr and M.S. Redmond, 1990. Toxicity of Cadmium in Sediments: The Role of Acid Volatile Sulfide, <u>Envir. Tox. Chem.</u>, 9:1489-1504.

Di Toro, D.M., J.D. Mahony, D.J. Hansen, K.J. Scott, A.R. Carlson and G.T. Ankley, 1992. Acid Volatile Sulfide Predicts the Acute Toxicity of Cadmium and Nickel in Sediments, <u>Envir. Sci. Tech.</u>, 26(1):96-101.

Fiering, M.B. and B.B. Jackson, 1971. <u>Synthetic Streamflows</u>, American Geophysical Union, Washington, D.C.

Förstner, U. and G.T.W. Wittman. 1979. *Metal Pollution in the Aquatic Environment.* Springer-Verlag, New York, 486 p.

Gailani, J., C.K. Ziegler and W. Lick, 1991. Transport of Suspended Solids in the Lower Fox River, J. Great Lakes Res., 17(4):479-494.

Gailani, J., W. Lick, M.K. Pickens, C.K. Ziegler and D.D. Endicott, 1994. Sediment and Contaminant Transport in the Buffalo River, USEPA report, Grosse Ile, Michigan.

Garcia, M. and G. Parker, 1991. Entrainment of Bed Sediment into Suspension, ASCE J. Hydr. Engr., 117:414-435.

Graham, D.I., P.W. James, T.E.R. Jones, J.M. Davies and E.A. Delo, 1992. Measurement and Prediction of Surface Shear Stress in Annular Flume, ASCE J. Hyd. Engr., 118:1270-1286.

Hawley, N., 1991. Preliminary Observations of Sediment Erosion from a Bottom Resting Flume, J. Great Lakes Res., 17(3):361-367.

Hayter, E.J. and A.J. Mehta, 1986. Modelling Cohesive Sediment Transport in Estuarial Waters, Appl. Math. Modelling, 10:294-303.

Howard, P.H., 1990. Handbook of Environmental Fate and Exposure Data for Organic Chemicals. Lewis Publishers, Chelsea, Michigan.

Karickhoff, S.W., V.K. McDaniel, C. Melton,A. N. Vellino, D.N. Nute, and L.A. Carreira, 1991. Predicting Chemical Reactivity by Computer. Environmental Toxicology and Chemistry, Vol 10 pp 1405-1461.

Karim, M.F. and F.M. Holly, 1986. Armoring and Sorting Simulation in Alluvial Rivers, ASCE J. Hydr. Engr., 112:705-715.

Krone, R.B., 1962. Flume Studies of the Transport of Sediment in Estuarial Processes, Final Report, Hydraulic Engineering Laboratory and Sanitary Engineering Research Laboratory, University of California, Berkeley, California.

Lick, W. and J. Lick, 1988. Aggregation and Disaggregation of Fine-Grained Lake Sediments, J. Great Lakes Res., 14(4):514-523.

MacIntyre, S., W. Lick, and C.H. Tsai, 1990. Variability of Entrainment of Cohesive Sediments in Freshwater, Biogeochemistry, 9:187-209.

Mackay, D., W.Y. Shiu, and K.C. Ma, 1992. Illustrated Handbook of Physical - Chemical Properties and Environmental Fate for Organic Chemicals, Vol. 1, Lewis Publishers, Chelsea, Michigan.

Mehta, A.J. and E. Partheniades, 1975. An Investigation of the Depositional Properties of Flocculated Fine Sediments, J. Hydr.Res., 12(4):361-609.

Parchure, T.M. and A.J. Mehta, 1985. Erosion of Soft Cohesive Sediment Deposits, ASCE J. Hyd. Engr., 111:1308-1326.

Peart, M.R. and D.E. Walling, 1982. Particle Size Characteristics of Fluvial Suspended Sediment, In: Recent Developments in the Explanation and Prediction of Erosion and Sediment Yield, IAHS Pub. No. 137, pp. 397-407.

Pettersson, C. K. Håkansson, S. Karlsson and B. Allard. 1993. Metal Speciation in a Humic Surface Water System Polluted by Acidic Leachates from a Mine Deposit in Sweden. Wat. Res. 27(5):863-871.

Quinn,J.G., E.J. Hoffman, .S. Latimer, and C.G. Carey. A Study of the Water Quality of the Pawtuxet River: Chemical Monitoring and Computer Modeling of Pollutants. Univ. Rhode Island Grad. School of Oceanography, 1985.

STORET. Water Quality Inventory and Retrieval from USEPA's STORET database, 1992.

Tsai, C.H. and W. Lick, 1986. A Portable Device for Measuring Sediment Resuspension, J. Great Lakes Res., 12(4):314-321.

Tsai, C.H. and W. Lick, 1987. Resuspension of Sediments from Long Island Sound, Wat. Sci. Tech., 21(6/7):155-184.

Thurman, E.M., 1985. Organic Geochemistry of Natural Waters. Martinus Nijhoff/Dr. W. Junk Publishers, Dordrecht, Netherlands.

U.S. Geological Survey, 1981. Guidelines for Determining Flood Flow Frequency, Bulletin No. 17B.

USEPA. 1994. Briefing Report to the EPA Science Advisory Board on the Equilibrium Partitioning Approach to Predicting Metal Bioavailability in Sediments and the Derivation of Sediment Quality Criteria for Metals. Office of Water and Office of Research and Development, Washington, D.C.

USEPA, 1993. Technical Basis for Deriving Sediment Quality Criteria for Nonionic Organic Contaminants for the Protection of Benthic Organisms by Using Equilibrium Partitioning. USEPA, Washington DC, EPA-822-R-93-011, September 1993.

Van Niekerk, A., K.R. Vogel, R.L. Slingerland and J.S. Bridge, 1992. Routing of Heterogeneous Sediments Over Movable Bed: Model Development, ASCE J. Hydr. Engr., 118:246-279.

Van Rijn, L.C., 1984. Sediment Transport, Part II: Suspended Load Transport, ASCE J. Hydr. Engr., 110:1613-1638.

Van Rijn, L.C., M.W.C. Nieuwjaar, T.V.D. Kaay, E. Nap and A.V. Kampen, 1993. Transport of Fine Sands by Currents and Waves, ASCE J. Water., Port, Coast. and Ocean Engr., 119:123-143.

Walling, D.E., B.W. Webb and J.C. Woodward, 1992. Some Sampling Considerations in the Design of Effective Strategies for Monitoring Sediment-Associated Transport, in: Erosion and Sediment Transport Monitoring Programs in River Basins, IAHS Pub. No. 210, pp. 183-190.

Ziegler, C.K. and W. Lick, 1986. A Numerical Model of the Resuspension, Deposition and Transport of Fine-Grained Sediments in Shallow Water, USCB Report ME-86-3.

Ziegler, C.K. and B. Nisbet, 1994. Fine-Grained Sediment Transport in Pawtuxet River, Rhode Island, ASCE J. Hydr. Engr., 120(5):561-576.

Ziegler, C.K. and B.S. Nisbet, 1995. Long-Term Simulation of Fine-Grained Sediment Transport in a Large Reservoir, ASCE J. Hydr. Engr., in press.

APPENDIX A

AN EMPIRICAL METHOD FOR ESTIMATING
SUSPENDED SEDIMENT LOADS IN RIVERS

APPENDIX A
AN EMPIRICAL METHOD FOR ESTIMATING SUSPENDED
SEDIMENT LOADS IN RIVERS

A.1   INTRODUCTION

Engineers and scientists studying riverine systems must frequently estimate suspended sediment loads.   Two examples illustrate the importance of accurately .determined sediment loads in rivers.   First, net annual deposition is a primary factor controlling the long-term fate of hydrophobic organic chemicals, e.g., PCBs and dioxin, in rivers and the burial rate is greatly affected by the annual sediment load.   Secondly, reservoir sedimentation is a problem for which accurately determining the total sediment load delivered to a reservoir over long time periods by the tributary river, or rivers, is critical for predicting changes in the storage capacity of a reservoir.

Other types of problems, in addition to the previous examples, are routinely encountered that require accurate hindcasts or forecasts of sediment discharge rates on seasonal or annual time scales.   In many cases, the loading time history needs to be specified in addition to the total mass of suspended sediment discharged by a river over a particular period.   This requirement means that the estimated sediment loading should reflect the observed behavior of rivers wherein a large fraction of the annual sediment load is transported during a relatively small number of high flow events, or floods, each year [Walling et al., 1992].

The difficulty of accurately measuring sediment loads in rivers, particularly during floods, is well known [Walling and Webb, 1981; Thomas, 1985; Ferguson, 1987; Walling et al., 1992].   Data collection problems are related to the importance of flood-period sediment discharge to the annual load.   Suspended sediment sampling programs must be carefully designed if accurate loading data are to be obtained and particular emphasis must be placed on sediment loading during high flow events.

Even if accurate sediment discharge data are available for a river that is of interest for a specific study, these data are usually collected during a limited period of time. Investigators are frequently faced with the task of using a restricted sediment loading data set to predict the response of a river during periods when no data are available. A variety of procedures have been used to predict suspended sediment discharge based upon existing data [Ferguson, 1987; Parker and Troutman, 1989]. The most widely used approach is the sediment rating curve, which is a relation of the form

$$C = aQ^n \qquad\qquad\qquad (A-1)$$

where C = suspended sediment concentration and Q = flow rate. The parameters in Equation (A-1), a and n, are determined from a log linear regression analysis of the available data. While Equation (A-1) does provide predictive capability of C in a river, and hence sediment load, the rating curve approach has been shown to usually under-predict sediment loads [Walling, 1977; Ferguson, 1987]. A method to correct for rating curve bias has been proposed [Ferguson, 1986] but subsequent evaluation of this correction procedure questioned its effectiveness [Walling and Webb, 1988].

While methods exist for predicting sediment loads in rivers that have available suspended sediment load data, situations are commonly encountered where little or no loading data has been collected for a river of interest. One possible method for estimating sediment loads in cases where little or no data exist is to use gross soil erosion estimates, e.g., tons/km²-year, for the drainage basin under consideration. The amount of eroded sediment transported into the river is the product of the gross soil erosion and a constant, termed the delivery ratio. Delivery ratios depend upon a number of drainage basin characteristics, including size, topography and land use [Robinson, 1977; Dickinson et al., 1986]. However, this method can produce a high degree of uncertainty in predicted annual loads, especially if the gross soil erosion and delivery ratio are not well known for a particular riverine system.

The above discussion indicates a need for an improved methodology to predict sediment loads in rivers, on seasonal or annual time scales, during periods when very

limited or no sediment discharge data are available. An attempt has been made in the current study to develop such a procedure. The next section presents an analysis of existing sediment discharge data from a variety of rivers in the eastern United States that results in the development of a non-dimensional sediment loading function. The predictive capabilities of this non-dimensional formulation are evaluated in the third and fourth sections. A summary of the proposed methodology, highlighting its advantages and limitations, concludes the paper.

A.2 DATA ANALYSIS AND MODEL DEVELOPMENT

The U.S. Geological Survey (USGS) collects sediment discharge data at numerous locations on rivers throughout the United States. The currently available sediment load data base consists of 1552 stations, with daily sediment discharge records ranging in length from 2 days to 45 years at these stations. Generally, daily sediment discharge at a particular station is determined from suspended sediment concentration and flow rate data. However, daily sediment load may be estimated on days when no suspended sediment concentration data are collected. This estimate is based upon flow rate, observed suspended sediment concentrations before and after the period of no data collection, and measured sediment discharges on days with similar flow rates. The analysis presented in this paper does not consider the possible errors or biases in the determination of sediment discharge values.

A typical sediment discharge analysis involves developing a sediment rating curve, e.g., Equation (A-1), for a particular river. If issues concerning the accuracy and precision of sediment rating curves are neglected, this approach could be applied to a large number of rivers using the USGS sediment loading and flow rate data. A major problem with this approach is that identifying general trends in the rating curves of rivers with different characteristics, e.g., drainage area, mean flow rate and mean sediment load, would be very difficult.

An attempt has been made in the present study to overcome this obstacle by normalizing both sediment discharge and flow rate and then examining the relationships between normalized sediment discharge and normalized flow rate for a wide range of rivers. For a given river, the daily average flow rate, Q_d, is normalized with respect to the long term mean flow rate, Q_m, yielding

$$Q_N = \frac{Q_d}{Q_m} \qquad (A-2)$$

where Q_N = normalized daily average flow rate. This normalization was chosen because, generally, Q_m can be determined from available data.

A useful normalization of the daily sediment discharge, L_d, is less clear and various methods could be proposed. The quantity used here to normalize L_d is the mean daily sediment discharge under non-flood conditions, L_m, so that

$$L_N = \frac{L_d}{L_m} \qquad (A-3)$$

where L_N = normalized sediment discharge.

Non-flood conditions are defined as all flows where the daily average flow rate is less than or equal to twice the mean flow rate, i.e., $Q_N \leq 2$. This criterion was chosen for two reasons. First, examination of rating curves for a number of rivers suggested that a transition in the rating curve generally occurs when $Q_N \cong 2$, i.e., the slope of the log-linear regression line changes. Second, an important goal of this analysis was to develop predictive capabilities of sediment loads in rivers using data that are available or relatively easy to measure. The importance and difficulty of accurately measuring sediment discharge during floods was mentioned earlier in this paper and obtaining this type of data is a significant challenge on any river. However, reliable estimates of L_d, and therefore L_m, under non-flood conditions for a particular river are usually easy to obtain from available data or from a non-flood sediment discharge study.

The normalization procedure was first applied to rivers with the longest record lengths because the USGS sediment discharge data base is quite large and applying the procedure to all rivers prohibitive. Twenty-five rivers were selected with periods of record that ranged from 33 to 45 years. The initial focus of the data analysis was flood flows, i.e., $Q_N > 2$, because of the significant contribution of flood discharge to the annual sediment load of a river. The normalized sediment discharge plots for $Q_N > 2$ were informative. First, graphs of the proposed normalizations were similar over a large range of river sizes, indicating that this type of analysis held promise for producing a predictive model. Second, the impact of load hysteresis during floods was discovered to vary significantly between different geographic regions. Generally, rivers in the western and midwestern United States have dramatically different sediment load trends during the rising and falling limbs of a flood hydrograph. In contrast, the daily sediment load of rivers in the eastern United States tends to exhibit minor hysteresis effects during floods.

The normalization analysis was then extended to non-flood flows and, similar to the flood event regime, discernible geographic differences were observed. An example of regional variability, in both flow regimes, is illustrated by three rivers from different areas (Figure A-1): Animas River, New Mexico; Iowa River, Iowa; and Roanoke River, Virginia. The sediment load data were binned into groups of equal size, e.g., same fraction of the total population, and the log mean $\pm$ two standard deviations of each data group then plotted on Figure A-1. Normalized sediment loads in the Roanoke River have lower variability than the rivers in New Mexico and Iowa, which was found to be typical of rivers in the eastern United States when compared to rivers in the midwestern or western regions. The log means of L_N during flood flows, i.e., $Q_N \geq 2$, are also higher for the Roanoke River, by about a factor of five, than the Animas and Iowa Rivers.

One of the motivating factors behind the development of the methodology presented in this paper was the authors' involvement in a contaminant fate and transport study on the Pawtuxet River in Rhode Island. The sediment transport model developed for the Pawtuxet River [Ziegler and Nisbet, 1994] was calibrated over a 789 day period, beginning in March 1992 and extending to May 1994. Sediment loading data were only
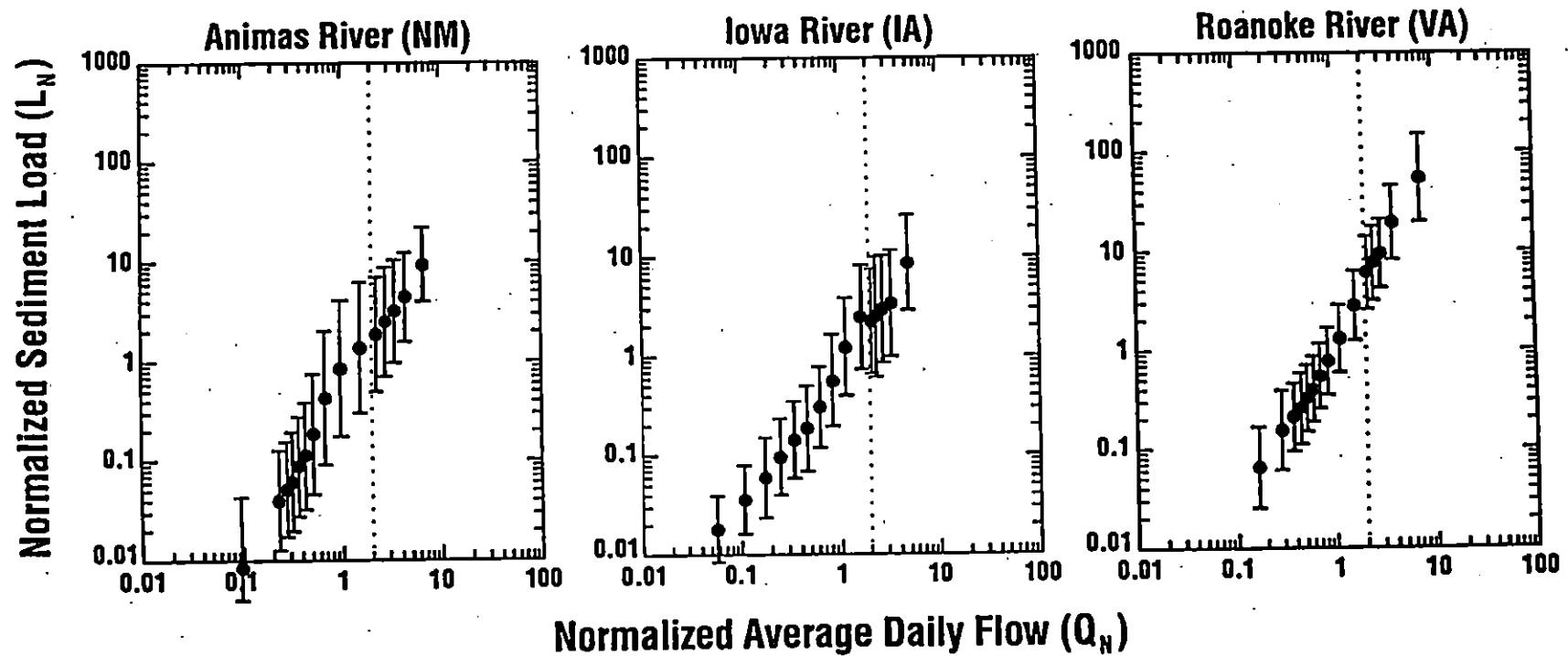
Figure A-1. Normalized sediment load plots for rivers in New Mexico, Iowa and Virginia. Log mean values, ± two standard deviations, of binned data are shown.

available for approximately 90 days during this period and an adequate sediment rating curve could not be developed from the data. A great need existed for estimating daily sediment loads for the 700 day period for which no data existed. The procedures described in this paper evolved from this lack of necessary sediment loading information for the Pawtuxet River sediment transport model. However, differences in the normalized sediment discharge plots of rivers from various geographic regions, particularly during floods, precluded development of a generic model for the entire United States. The focus of this study is thus limited to a region of the eastern United States, including the Pawtuxet River, that extends along the Atlantic seaboard from North Carolina to New England and westward to Ohio, see Figure A-2.

Twenty-nine rivers were selected from the region under consideration. The characteristics of these rivers are listed in Table A-1 and their locations are shown on Figure A-2. As can be seen in Table A-1, these rivers encompass a wide range of characteristics: drainage area, A, ranging from 2.4 to 62,400 km^2; mean flow rates from 0.048 to 980 m^3/s; and L_m ranging from 0.082 to 2440 tons/day. The mean non-flood sediment load, L_m, of each river was determined by averaging L_d on all days in the record for which $Q_N \leq 2$.

Normalized sediment discharge plots are presented on Figure A-3 for four rivers that span the range of river sizes included in the present analysis, from a small stream with A < 3 km^2 to a large river with A ~ 13,000 km^2. Normalized sediment load data are presented as log means with ± two standard deviations; L_N data were binned using 5% increments of the population along the Q_N axis. The solid lines on this figure are the result of separate log linear regressions of the low flow and high flow data; the log linear regressions were performed on all of the data, not on the log means of the binned data.

Several observations can be made about the plots on Figure A-3. First, a break or transition in the data is evident near $Q_N = 2$, which lends support to the choice of this normalized flow rate as a criterion for defining the non-flood regime. Second, the normalized sediment load plots are similar from one river to the next. Finally, the log
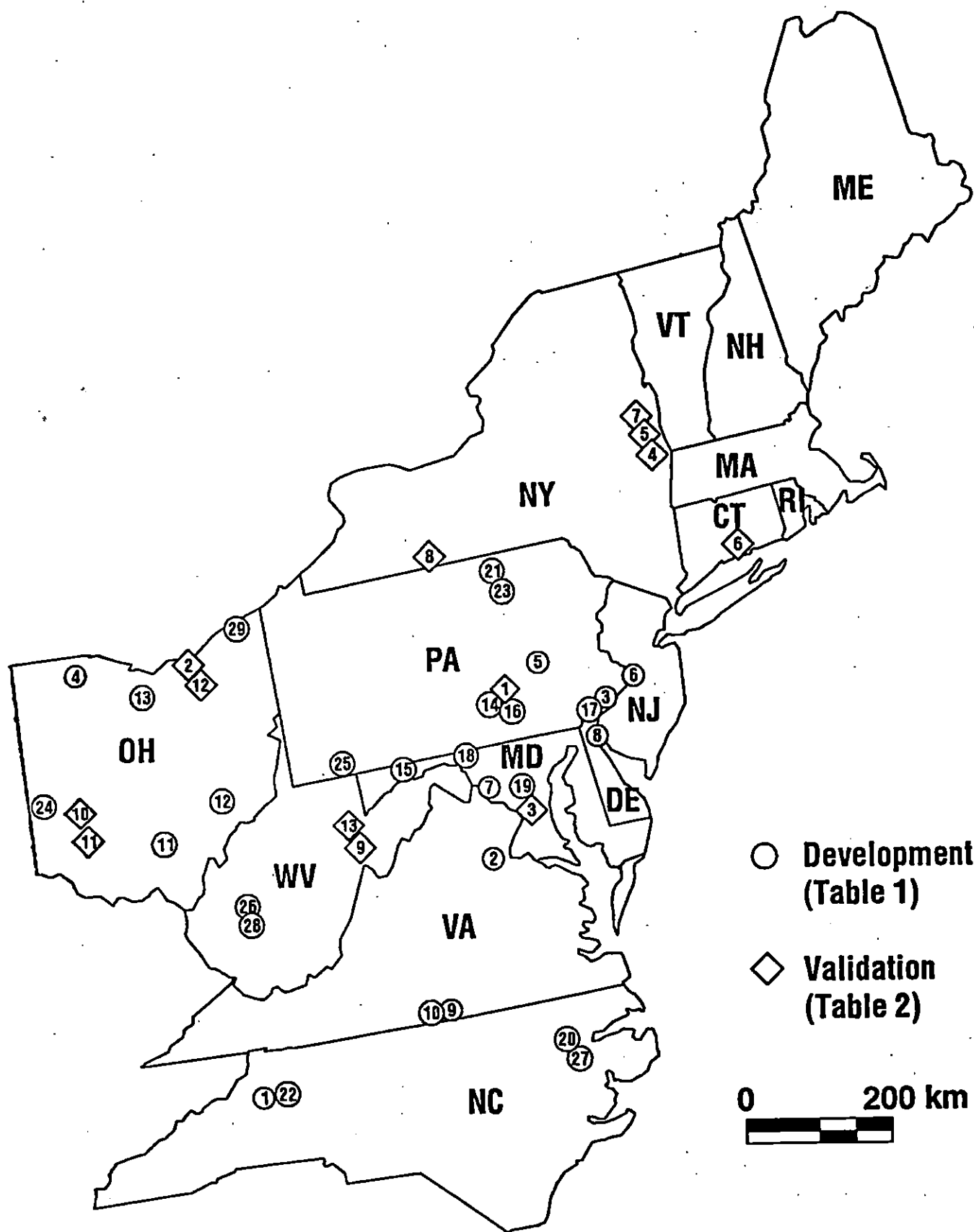
Figure A-2. Region in eastern United States considered in present analysis. Reference numbers for rivers are listed in Tables A-1 and A-2.

Station Location (Figure A-2 reference number)	Record Length (years)	A (km^2)	Q_m (m^3/s)	Data-Based L_m (tons/day)
Yadkin R. at Yadkin College, NC (1)	42.8	5910	87	892
Rappahannock R. at Remingon, VA (2)	42.5	1610	19	35
Schuylkill R. at Manayunk, PA (3)	38.9	4740	78	124
Maumee R. at Waterville, OH (4)	43.5	16,400	146	419
Schuylkill R. at Berne, PA (5)	34.0	920	20	63
Delaware R. at Trenton, NJ (6)	32.6	6150	327	397
Potomac R. at Point of Rocks, MD (7)	33.0	25,000	276	2440
Brandywine C. at Wilmington, DE (8)	33.9	810	13	21
Roanoke R. at Randolph, VA (9)	27.8	7710	83	335
Dan R. at Paces, VA (10)	27.3	6610	79	563
Scioto r. at Higby, OH (11)	29.0	13,300	133	684
Muskingum R. at Dresden, OH (12)	22.0	15,530	165	592
Sandusky R. near Fremont, OH (13)	43.0	3240	29	89
Bixier Run near Loysville, PA (14)	17.4	39	0.42	0.34
NB Potomac R. near Cumberland, MD (15)	18.0	2270	38	69
Susquehanna R. at Harrisburg, PA (16)	19.1	62,400	980	1513
Brandywine Cr. at Chadds Ford, PA (17)	15.0	740	12	19
Conococheague Cr. at Fairview, MD (18)	14.0	1280	21	40
NWB Anacostia R. near Colesville, MD (19)	13.0	55	0.65	3.6
Tar R. at Tarboro, NC (20)	10.0	5660	62	137
Elk Run near Mainesburg, PA (21)	13.0	26	0.29	0.082
Third C. near Stony Point, NC (22)	12.3	13	0.18	0.36
Corey C. near Mainesburg, PA (23)	13.4	32	0.31	0.12
Stillwater R. at Pleasant Hill, OH (24)	12.0	1300	12	21
Stony Fork Trib. near Gibbon Glade, PA (25)	12.0	2.4	0.048	0.18
Coal R. at Tornado, WV (26)	11.8	2230	35	123
Chicod C. near Simpson, NC (27)	11.5	117	1.4	1.7
Little Coal R. at Danville, WV (28)	11.1	700	12	64
Grand R. near Painesville, OH (29)	11.0	1780	30	328

TABLE A-1. DRAINAGE BASIN CHARACTERISTICS OF RIVERS USED IN MODEL DEVELOPMENT
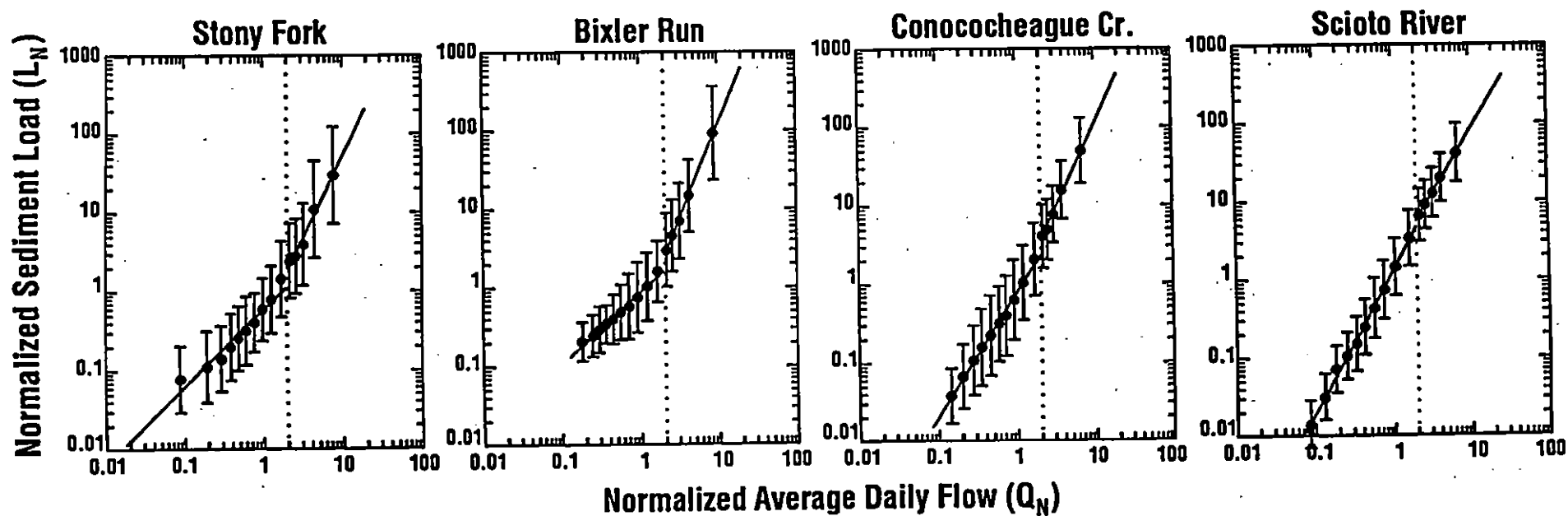
Figure A-3. Normalized sediment load plots for several rivers used in model development. Log mean values, ± two standard deviations, of binned data are shown. Solid lines indicate results of log linear regression analysis using the normalized data.

standard deviation of L_N is approximately constant with respect to Q_N, as can be seen on Figure A-3 from the relatively constant width of the standard deviation bars.

Sediment discharge hysteresis during floods was also examined for these twenty-nine rivers. Somewhat surprisingly, the difference between normalized sediment load curves developed for flows on the rising and falling limbs of flood hydrographs was minor (results not shown). Thus, stratifying flood flow regimes will not significantly improve daily sediment load predictions for rivers in the eastern United States.

These trends in the normalized sediment discharge plots indicate the possibility of developing a generalized function relating L_N to Q_N which would be applicable to rivers over a wide range of drainage basin sizes and mean flow rates. Such a generalized function has been developed and it is similar to a conventional sediment rating curve, i.e., Equation (A-1), except for three important differences. First, non-dimensionalizing the loading function produces a generalized expression that is applicable to many rivers. Second, variations in the sediment discharge characteristics among riverine systems are accounted for by making the parameters a and n in Equation (A-1) functions of river characteristics. Third, a stochastic component has been added to the non-dimensional version of Equation (A-1) to account for observed variability in sediment loads. Equation (A-1) is completely deterministic, meaning that a single suspended sediment concentration, or sediment discharge, corresponding to the median or geometric mean of the distribution, will be predicted at a specific flow rate. The deterministic method is not completely realistic because the sediment load at a particular flow rate can be highly variable. An important benefit of including the stochastic component, in addition to generating more realistic daily sediment loads, is that it improves the predictive capabilities of the method, as will be demonstrated later in this paper.

The modified form of Equation (A-1), expressed in log linear form, is

$$\log L_N = \log a + n \log Q_N + \delta S_L \qquad \text{(A-4)}$$

where $\log a$ and n are functions of drainage basin characteristics, S_L = standard deviation of the log estimate, and δ = normally distributed random number with mean of zero and standard deviation of one. Hereafter, Equation (A-4) will be referred to as the Normalized Sediment Load (NSL) function.

The motivation for including a stochastic component in the NSL function, i.e., δS_L, is to account for natural variability in L_N at a particular Q_N and to more accurately predict L_N. The tendency of sediment rating curves developed from log linear regression analysis to underestimate sediment loads in rivers has been recognized [Walling, 1977; Ferguson, 1986; Walling and Webb, 1988]. The typical development of a sediment rating curve ignores the variability not captured by log-linear regression. The resulting equation, e.g., Equation (A-1), predicts the median solids loading at any flow. The sediment rating curve under-predicts the mean load because the data are log-normally distributed. This bias is eliminated by including the estimate of residual variance in the log-linear form of the equation. The random nature of the NSL function will not make it possible to accurately predict sediment loads on short time scales, e.g., hourly or daily, however, it will increase the accuracy of predicted sediment loads over seasonal or annual time scales.

Parameter values in the NSL function, i.e., $\log a$, n and S_L, were determined in the following manner. First, log linear regression was used to determine the best fit line for L_N as a function of Q_N for each of the twenty-nine rivers. To account for observed differences in the variation of L_N under non-flood and flood conditions, the flow regime was stratified prior to regression analysis, with $Q_N = 2$ being chosen as the break point between non-flood and flood flows. Thus, two best fit lines, one for $Q_N \leq 2$ and another for $Q_N > 2$, were determined for each river. The results of the regression analyses yielded values of $\log a$, n and S_L, for $Q_N \leq 2$ and $Q_N > 2$, for each river.

Attempts were then made to develop generalized expressions for $\log a$, n and S_L that were applicable over a wide range of river sizes. Correlations between the three

A-12

parameters, log a, n and S_L, and five drainage basin characteristics, A, Q_m, L_m, Q_m/A and L_m/A, were examined using results from the regression analyses of the twenty-nine rivers. The analyses indicated that log a, n and S_L were not significantly correlated with many of the five drainage basin characteristics. This result suggested that mean values of log a, n and S_L, for the two flow regimes of $Q_N \leq 2$ and $Q_N > 2$, could be used when applying the NSL function. However, statistically significant correlation, even though it was relatively low, did exist between the NSL function parameters and either Q_m/A or A. Preliminary tests of the NSL function indicated that accounting for parameter variability with respect to Q_m/A or A, as opposed to using mean values, did improve the accuracy of Equation (A-4). The following relationships, stratified for $Q_N \leq 2$ and $Q_N > 2$, were determined from the correlation analyses

$$\log a = \begin{cases} 0.478 - 40.6 \dfrac{Q_m}{A} & , \quad Q_N \leq 2 \\[2mm] 0.714 - 54.5 \dfrac{Q_m}{A} & , \quad Q_N > 2 \end{cases} \tag{A-5}$$

$$n = \begin{cases} 0.794 + 0.205 \log A & , \quad Q_N \leq 2 \\[2mm] 1.18 + 69.3 \dfrac{Q_m}{A} & , \quad Q_N > 2 \end{cases} \tag{A-6}$$

$$S_L = \begin{cases} 0.40 & , \quad Q_N \leq 2 \\ 0.546 - 0.0572 \log A & , \quad Q_N > 2 \end{cases} \tag{A-7}$$

where A and Q_m have units of km^2 and m^3/s, respectively. The correlation plots corresponding to Equations (A-5) through (A-7) are presented on Figure A-4.

The predictive capability of the NSL function, utilizing Equations (A-5) through (A-7) to determine log a, n and S_L, was initially tested by applying these equations to the twenty-nine rivers used in the model development process. This check, while not a

A-13
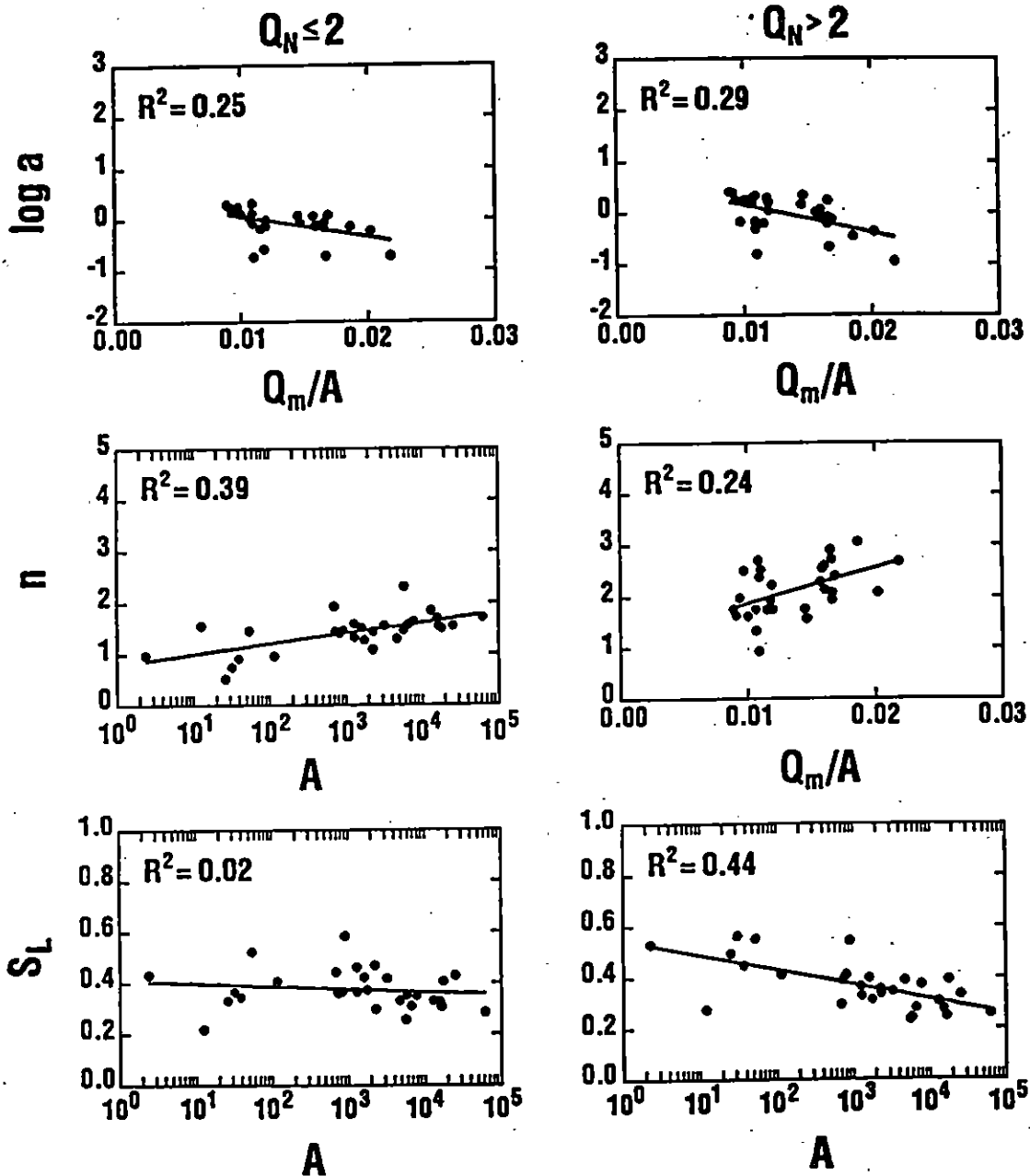
Figure A-4. Results of correlation analyses for determining log a, n and S_L values in Equation (A-4). Units of Q_m/A and A are m^3/s-km^2 and km^2, respectively.

validation of the NSL function approach to estimating sediment loads in rivers, was conducted to evaluate the accuracy of the proposed methodology with the calibration data set. Annual solids load was used as the basis of comparison. Normalized daily sediment loads, L_N, were predicted for the entire period of record for each of the twenty-nine rivers. Equation (A-3) was then used to calculate the daily sediment loads, i.e., $L_d = L_N L_m$, where L_m was determined for each river from the available data, see Table A-1. The predicted daily loads for each river were then summed on an annual basis. The resulting predicted annual sediment loads, for a total of 618 years, were next compared to measured annual loads, see Figure A-5a. These results are encouraging; the model demonstrates predictive capabilities for rivers with annual sediment loads ranging over five orders of magnitude. An error analysis was also conducted to quantify the accuracy of the NSL function. The relative error, i.e., (predicted - measured)/measured, for each of the 618 predicted annual loads was determined and the distribution of the errors is presented on Figure A-5b. The mean and median errors were 36% and -14%, respectively; 64% of the predicted annual loads were within a factor of two of the observed value.

A.3 VALIDATION OF NSL FUNCTION PREDICTIVE CAPABILITIES

The NSL function was expected to predict annual sediment loads for the rivers used to develop the model with a reasonable degree of accuracy and the above results indicate that this is the case. However, a necessary test of the model is its application to rivers not included in the calibration data set. Validation of the model was accomplished by predicting annual sediment loads for thirteen rivers from the same geographic region as the original twenty-nine rivers used to develop the model, see Figure A-2. These thirteen rivers span a wide range of drainage basin characteristics, see Table A-2, from a small stream with $A = 13$ km^2 and $Q_m = 0.43$ m^3/s to a large river with $A = 11,970$ km^2 and $Q_m = 231$ m^3/s.

Values of NSL function parameters, i.e., log a, n and S_L, for each the thirteen rivers were determined using river drainage basin characteristics, i.e., Q_m/A and A, in Equations (A-5) through (A-7). Use of the NSL function to predict sediment loads in these thirteen
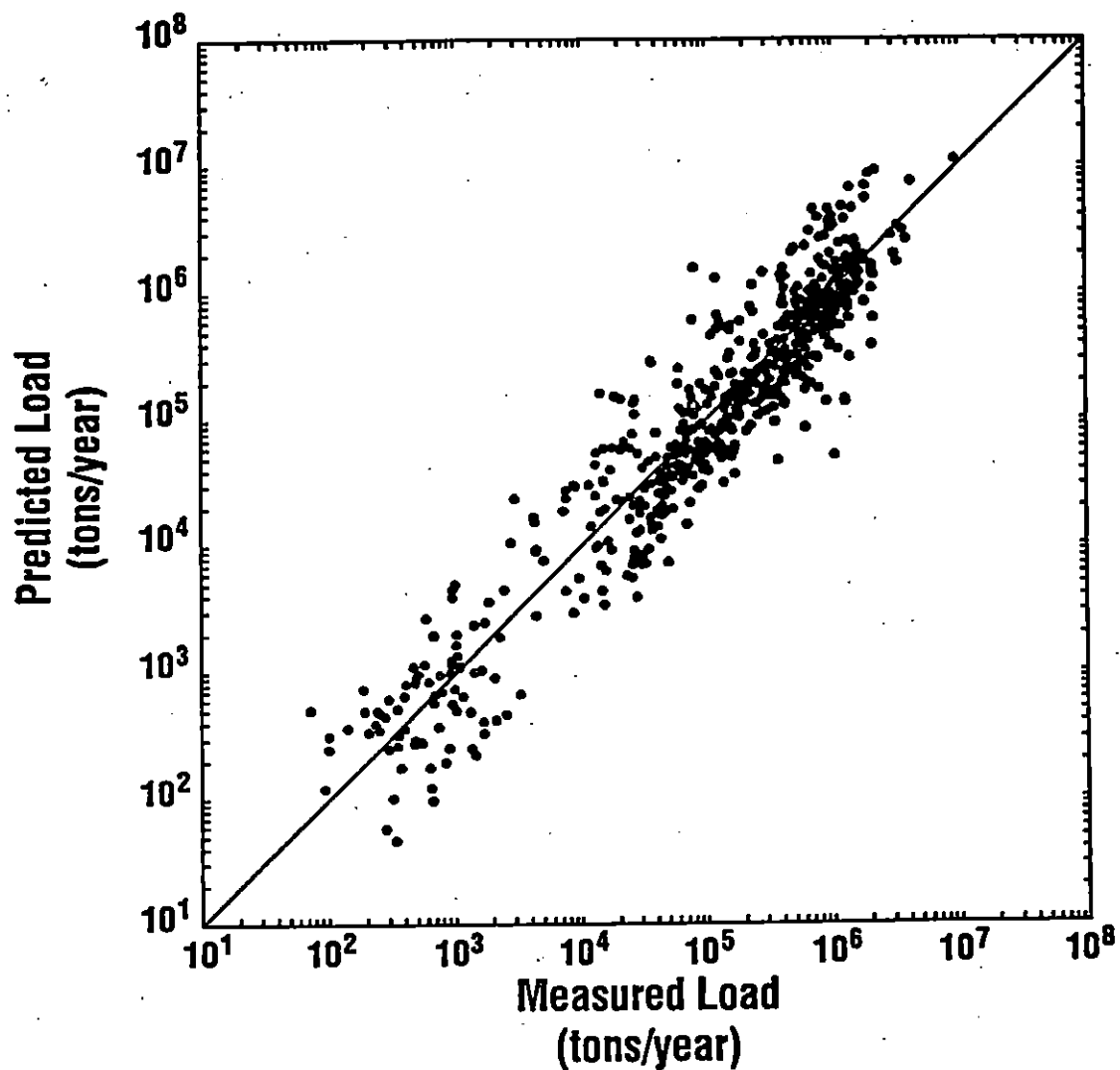
Figure A-5a. Results of NSL function application to 29 rivers used in model development: comparison of predicted and measured annual sediment loads.
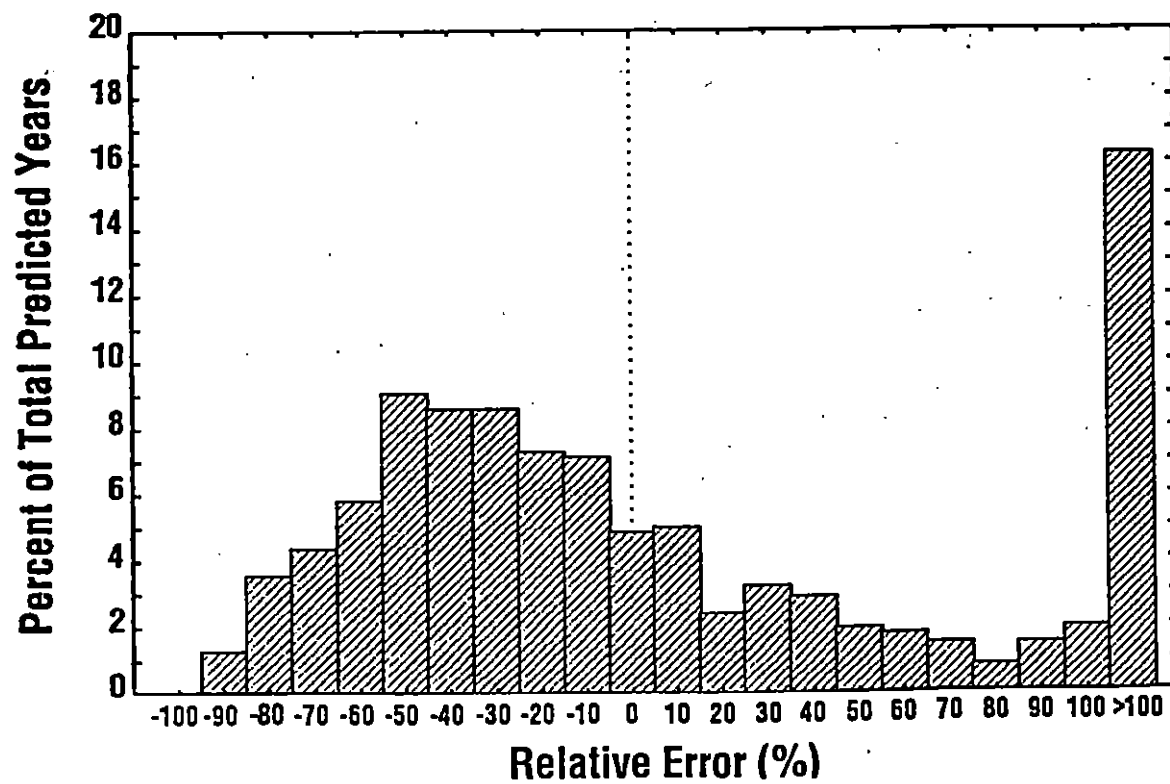
Figure A-5b. Results of NSL function application to 29 rivers used in model development: frequency distribution of relative errors.

TABLE A-2. DRAINAGE BASIN CHARACTERISTICS OF RIVERS USED IN MODEL VALIDATION					
Station Location (Figure A-2 reference number)	Record Length (years)	A (km^2)	Q_m (m^3/s)	Data-Based L_m (tons/day)	Estimated L_m (tons/day)
Juniata R. at Newport, PA (1)	40.0	8690	122	130	360
Cuyahoga R. at Independence, OH (2)	34.0	1830	23	135	63
NB Rock Cr. at Rockville, MD (3)	10.1	32	0.45	0.61	0.68
Mohawk R. at Cohoes, NY (4)	25.7	8940	165	168	360
Hudson R. at Waterford, NY (5)	8.0	11,970	231	191	520
Coginchaug R. at Middlefield, CT (6)	7.6	77	140	0.47	3.5
Hudson R. at Stillwater, NY (7)	8.5	9780	186	119	410
Tioga R. at Lindley, NY (8)	7.0	2000	23	48	70
Shavers Fork below Bowden, WV (9)	6.3	390	12	7.9	11
L. Miami R. near Oldtown, OH (10)	6.2	330	2.0	3.1	9.3
Todd F. near Roachester, OH (11)	6.1	570	6.0	23	17
Tinkers Cr. at Bedford, OH (12)	7.6	220	3.7	16	5.9
Taylor Run at Bowden, WV (13)	6.0	13	0.43	0.24	0.25

rivers also required determining L_m for each of the rivers. The mean daily sediment load under non-flood conditions, L_m, of a particular river was calculated using data from all days during which $Q_d \leq 2 Q_m$, i.e., $Q_N \leq 2$. The resulting values of L_m are presented in Table A-2 for each of the thirteen rivers in the model validation.

A total of 149 annual sediment loads were predicted in the model validation. The comparison of predicted and observed annual sediment loads, that ranged over four orders of magnitude, demonstrates that the NSL function does yield predictions, on an annual time scale, that are relatively accurate, see Figure A-6a. The model is able to properly account for variations in drainage basin characteristics, e.g., A, Q_m and L_m, indicating that the normalizations used in the NSL function, L_N and Q_N, are physically relevant. A quantitative error analysis, where the relative error was calculated for each of the 149 predicted annual loads, yielded a mean error of 3% and a median error of -18%, see Figure A-6b, with 82% of the predicted annual loads being within a factor of two of the observed value.

To demonstrate the importance of the stochastic component in the NSL function, the validation calculations were repeated with the stochastic component in Equation (A-4) set to zero, i.e., $\delta S_L = 0$. As expected, the non-stochastic calculations under-predict the annual loads (compare Figure A-7a to Figure A-6a). The non-stochastic error distribution (Figure A-7b) has significantly more negative errors (under-predictions) than the error distribution resulting from application of the complete NSL function (Figure A-6b). The mean and median relative errors were -31% and -39%, respectively, for the non-stochastic predictions, and 64% of the predicted annual loads were within a factor of two of the measured annual load.

A.4   APPLICATION OF NSL FUNCTION WHEN L_m IS UNKNOWN

The previous applications of the NSL function assumed that L_m was known for each of the rivers; L_m was determined from available data in the above calculations. Frequently, sediment loading must be determined for a river that has very limited or no sediment
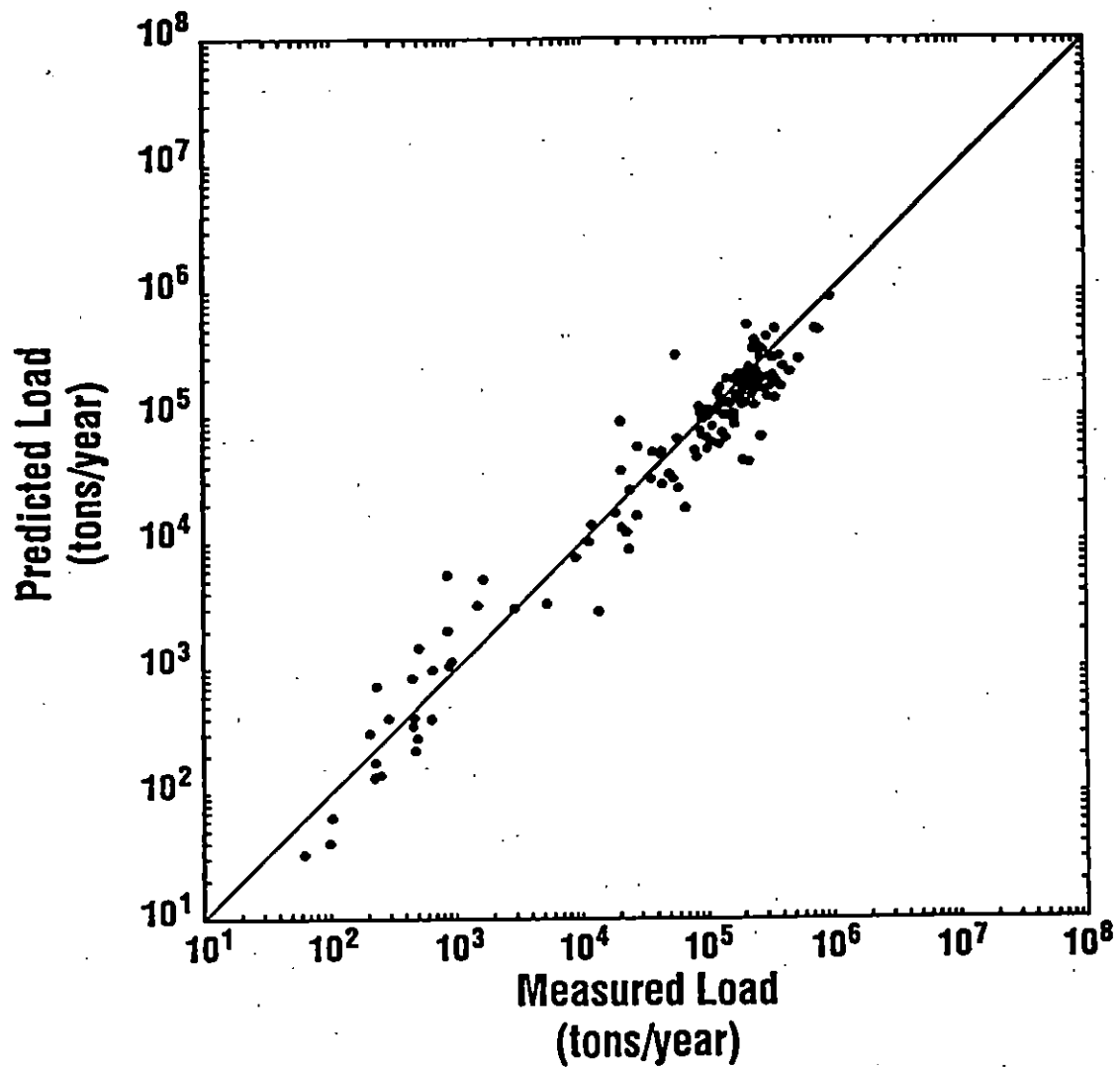
Figure A-6a. Results of NSL function application to 13 rivers used in model validation: comparison of predicted and measured annual sediment loads.
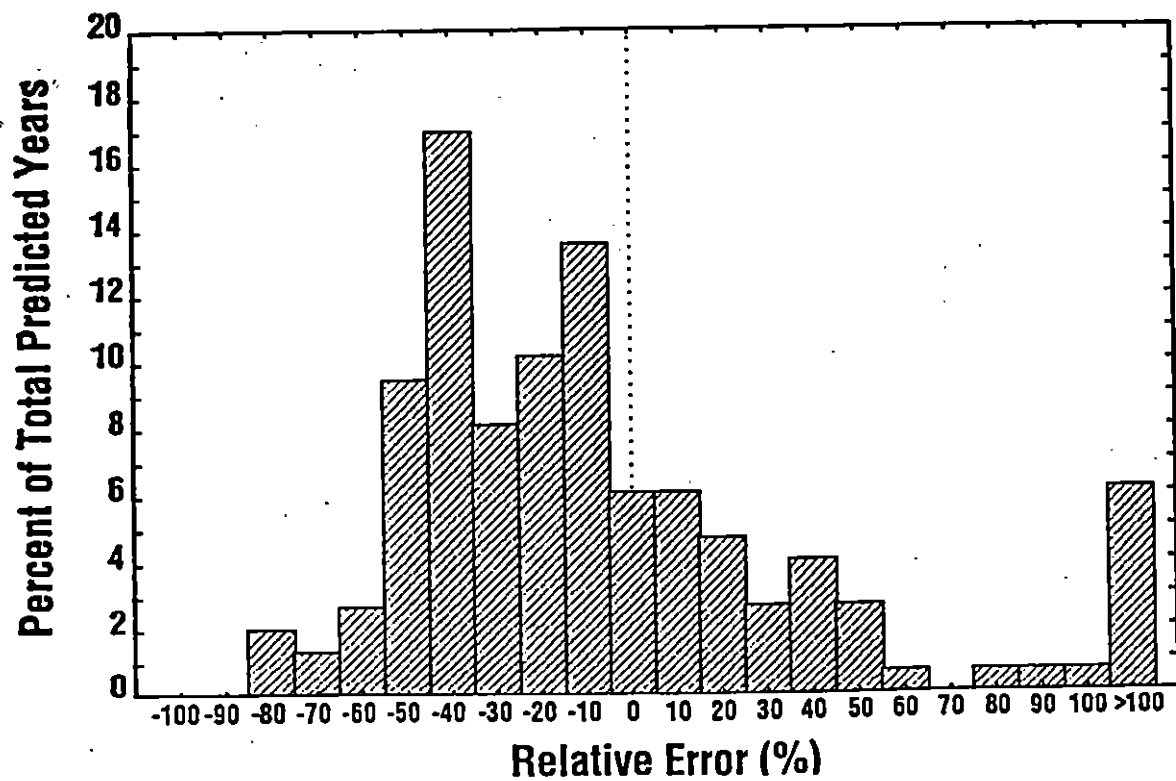
Figure A-6b. Results of NSL function application to 13 rivers used in model validation: frequency distribution of relative errors.
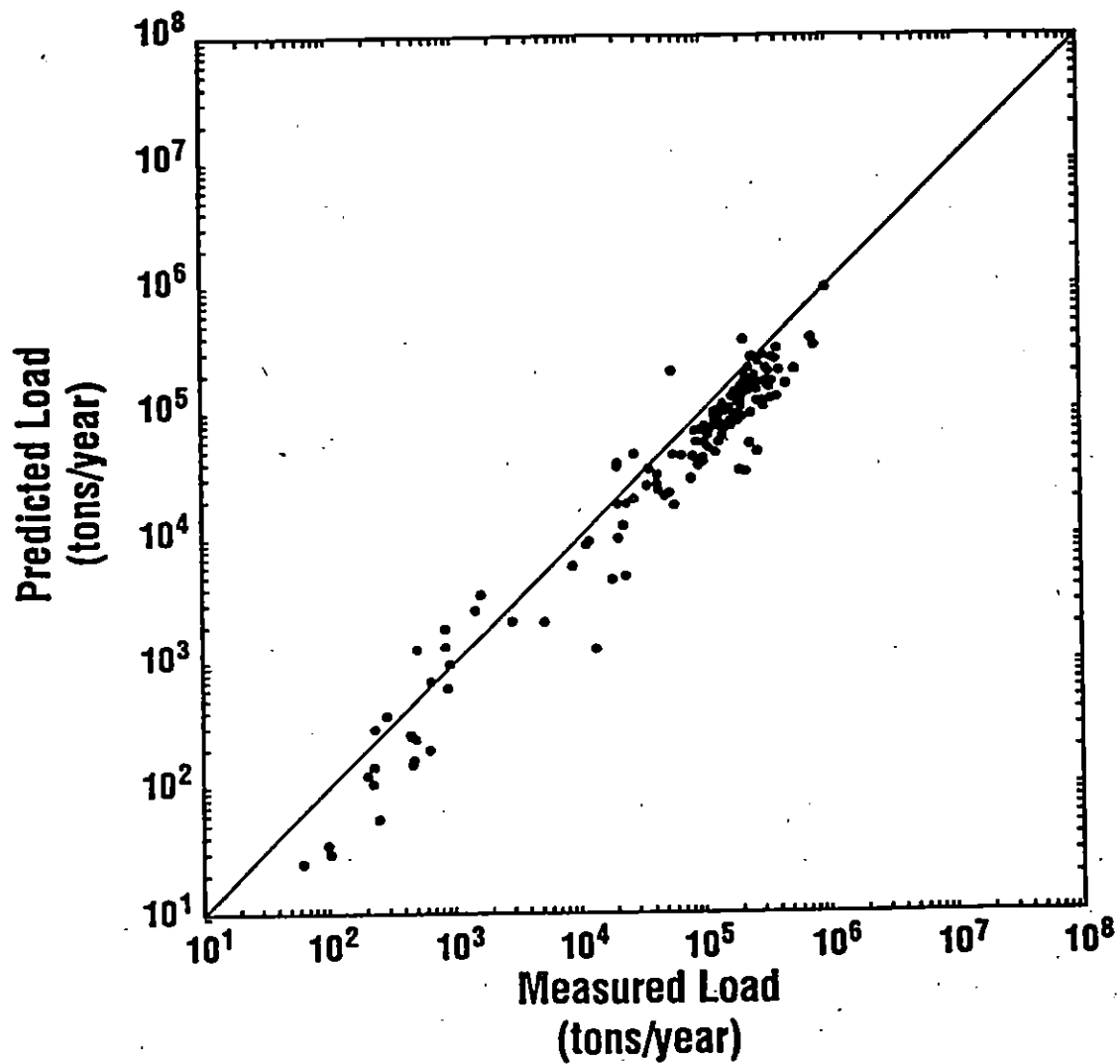
Figure A-7a. Results of NSL function application to 13 rivers used in model validation with stochastic component (δS_L) set to zero: comparison of predicted and measured annual sediment loads.
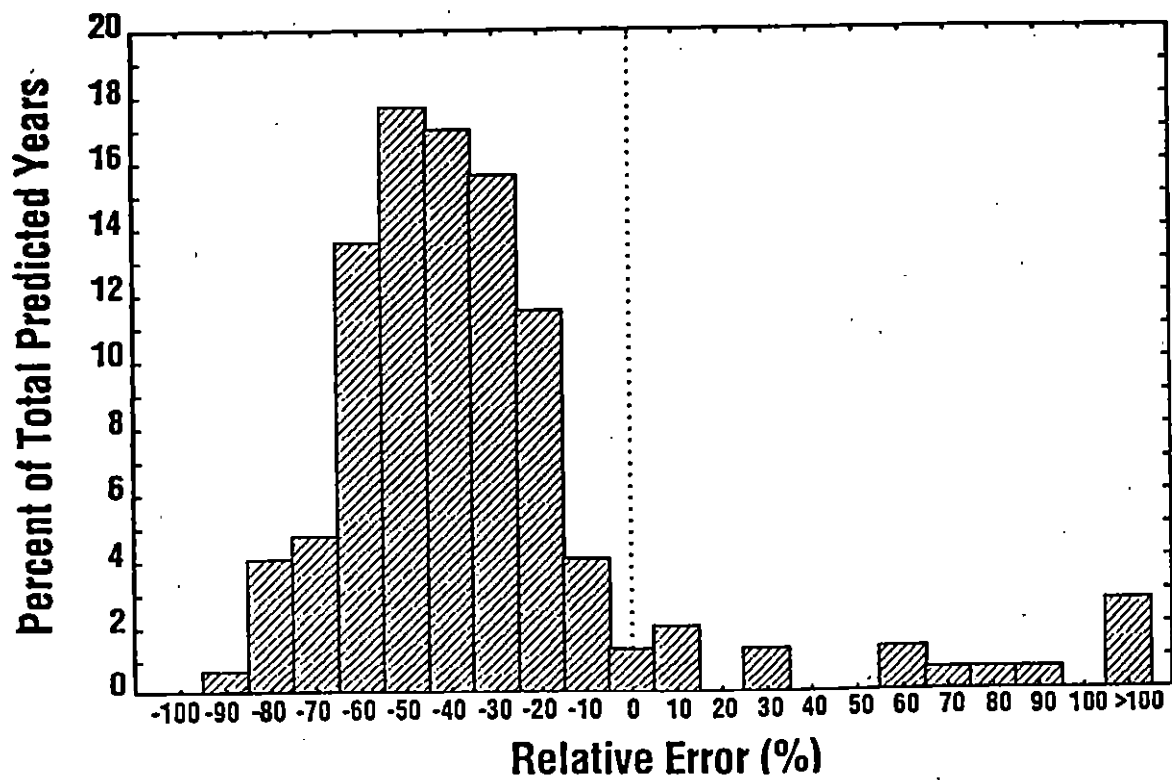
Figure A-7b. Results of NSL function application to 13 rivers used in model validation with stochastic component (δS_L) set to zero: frequency distribution of relative errors.

discharge data, making it extremely difficult to calculate L_m for that specific river. Without an estimate of L_m, the NSL function cannot be used to calculate sediment loads.

An approximate method for applying the NSL function to situations when L_m cannot be determined from data has been developed to overcome this problem. A correlation between L_m (tons/day) and drainage area, A (km^2), was found for the twenty-nine rivers used in the model development, see Figure A-8. Linear regression, in log space, of the data resulted in

$$L_m = 0.014 \, A^{1.12} \qquad\qquad\qquad (A-8)$$

with 92% of the variation of L_m explained by A, i.e., $R^2 = 0.92$.

The validation calculations were repeated using Equation (A-8) to estimate L_m for each of the thirteen rivers prior to application of the NSL function. The estimated L_m values, listed in Table A-2, are generally much different than the data-based values. The estimates of L_m are all within a factor of eight of the actual value, with five of the thirteen rivers having estimated values within a factor of two of the data-based value. Model predictions based on estimated L_m values were not as good as when the data-based L_m values were used, see Figure A-9a. However, the predicted annual loads, based on L_m estimated using Equation (A-8), were not grossly inaccurate. The relative errors were more widely distributed, see Figure A-9b, with a mean of 74% and a median of 40%. The portion of the predicted annual loads that was within a factor of two of the actual load decreased to 51%.

A.5 CONCLUDING REMARKS

Analysis of sediment discharge data from rivers in the eastern United States indicated that a similarity relationship exists for a large size range of riverine systems when the daily sediment load, L_d, and daily mean flow rate, Q_d, are properly normalized. The quantities chosen to normalize L_d and Q_d were the mean daily sediment load under non-flood conditions, L_m, and the long-term mean flow rate, Q_m, respectively. This choice of
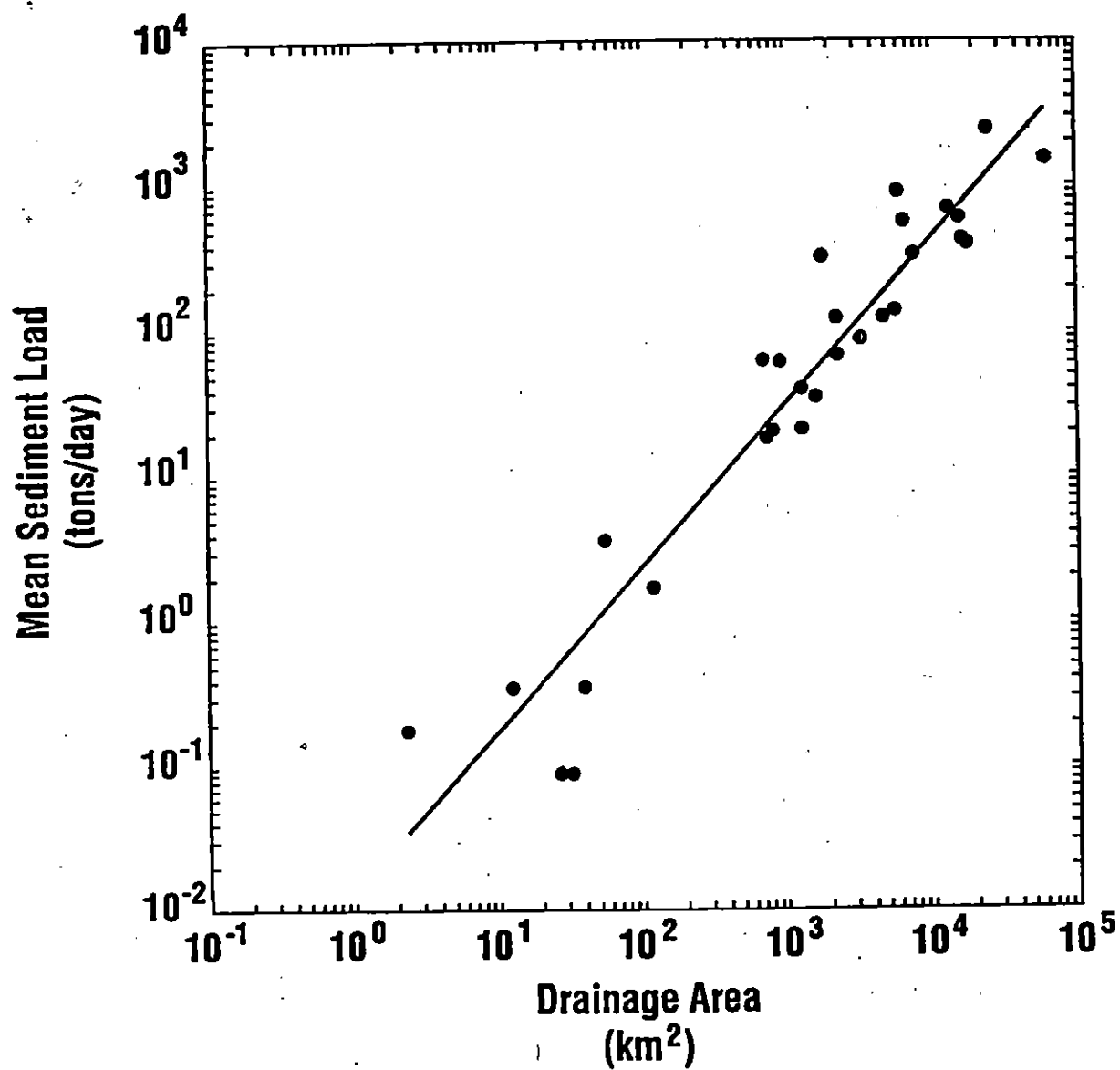
Figure A-8. Correlation between mean daily sediment load under non-flood conditions (L_m) and drainage area.
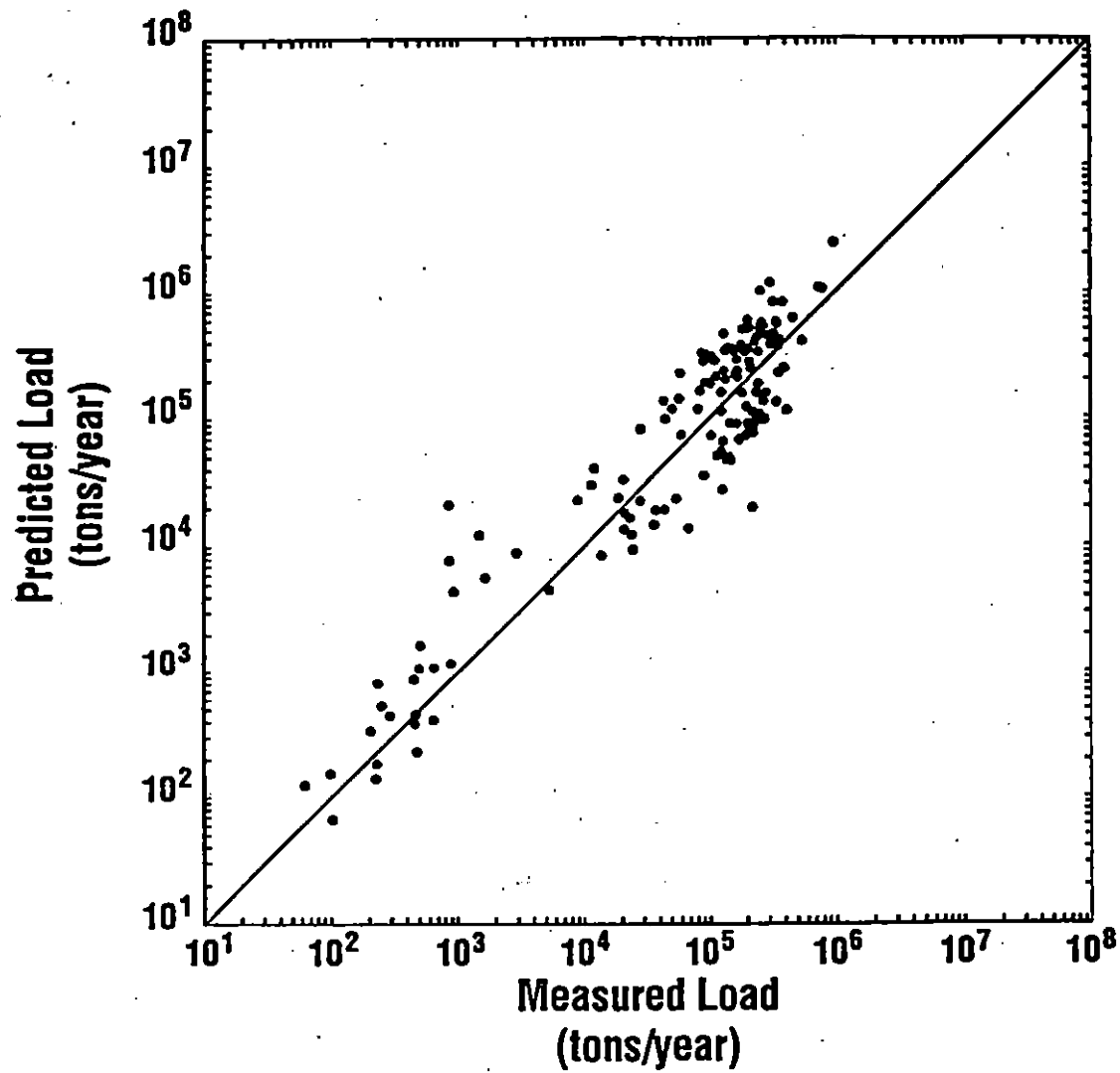
Figure 9a. Results of NSL function application to 13 rivers used in model validation with L_m predicted by Equation (A-8): comparison of predicted and measured annual sediment loads.
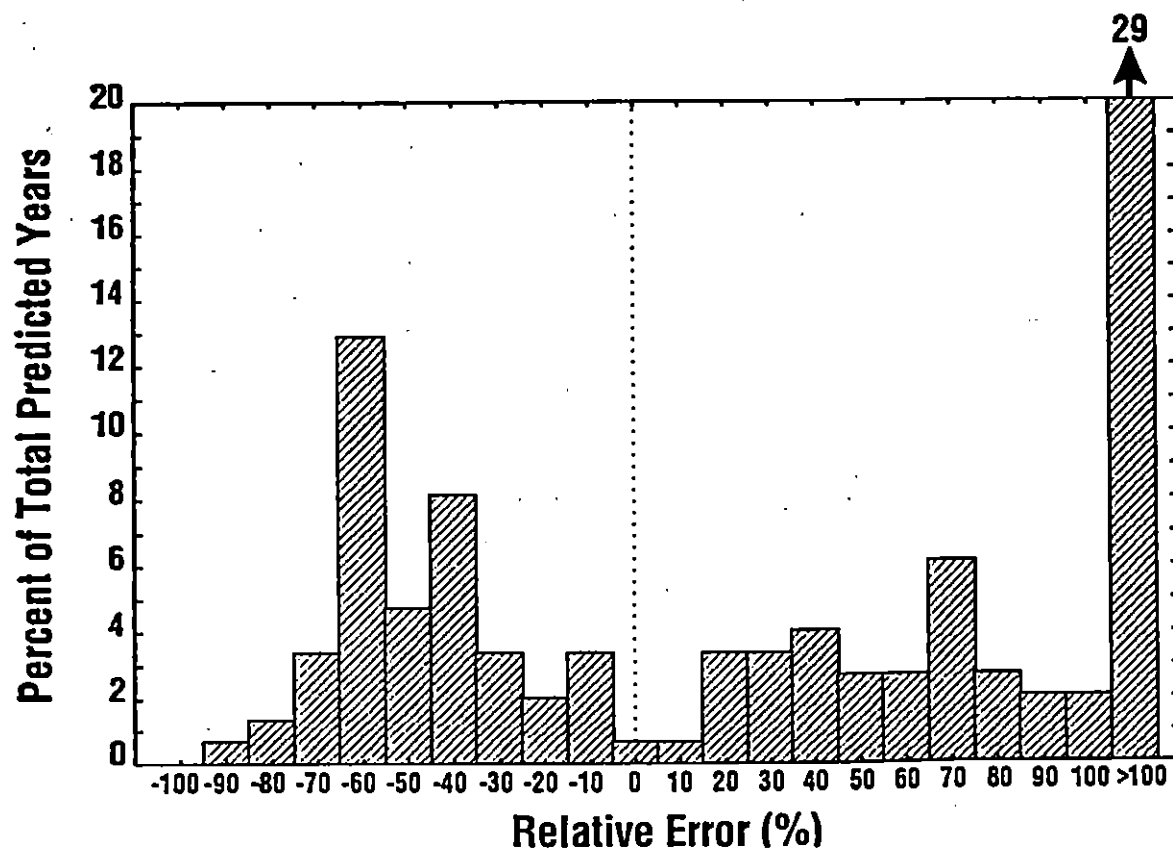
Figure 9b. Results of NSL function application to 13 rivers used in model validation with L_m predicted by Equation (A-8): frequency distribution of relative errors.

normalization, which is not unique, was chosen because L_m and Q_m can generally be determined for most riverine systems without much difficulty, either from existing data or from a relatively inexpensive field program.

This data analysis resulted in the development of a non-dimensional formulation, the NSL function, that is capable of predicting annual sediment loads in rivers located in the eastern United States with a reasonable degree of accuracy. The NSL function, as defined by Equations (A-4) through (A-7), is applicable to riverine systems, in the geographic region indicated on Figure A-2, that range over four orders of magnitude in size, with drainage areas of less than 3 km^2 to over 25,000 km^2. The proposed formulation, Equation (A-4), also includes a stochastic component that improves predictive capabilities and produces realistic variability in estimated daily sediment loads. As noted earlier, the NSL function depends upon knowledge of L_m, which may not be available for particular studies. An approximate method for estimating L_m, based upon drainage basin size, was presented that yields annual load predictions that have a higher degree of uncertainty but are still useful in situations when no sediment loading data are available for a particular river.

The NSL function, along with the parameters defined in Equations (A-5) through (A-7), has been shown to be a credible tool for predicting annual sediment loads in rivers. However, the limitations of this methodology must be acknowledged. First, the NSL function has only been shown to simulate sediment loads reasonably well on annual time scales. At the present time, this model may not be able to accurately predict riverine sediment discharge on short time scales, e.g., daily loads. Second, the NSL function parameters, Equations (A-5) through (A-7), were developed using data from rivers in the geographic region illustrated on Figure A-2. This model should not be applied to other regions because significant geographic differences in sediment discharge characteristics will require modification of the equations for log a, n and S_L. Continued work with the existing data base will hopefully result in the extension of the NSL function to other regions of the United States in the near future.

A.6 REFERENCES

Dickinson, W.T., Rudra, R.P. and Clark, D.J., 1986. A Delivery Ratio Approach for Seasonal Transport of Sediment, in: Drainage Basin Sediment Delivery, IAHS Pub. No. 159, pp. 237-252.

Ferguson, R.I., 1986. River Loads Underestimated by Rating Curves, Water Resour. Res., 22(1):74-76.

Ferguson, R.I., 1987. Accuracy and Precision of Methods for Estimating River Loads, Earth Surf. Proc. and Land., 12:95-104.

Parker, R.S. and Troutman, B.M., 1989. Frequency Distribution of Suspended Sediment Loads, Water Resour. Res., 25(7):1567-1574.

Robinson, A.R., 1977. Relationship Between Soil Erosion and Sediment Delivery, in: Erosion and Solid Matter Transport in Inland Waters, IAHS Pub. No. 122, pp. 159-167.

Thomas, R.B., 1985. Estimating Total Suspended Yield with Probability Sampling, Water Resour. Res., 21(9):1381-1388.

Walling, D.E., 1977. Assessing the Accuracy of Suspended Sediment Rating Curves for a Small Basin, Water Resour. Res., 13(3):531-538.

Walling, D.E. and Webb, B.W., 1981. The Reliability of Suspended Sediment Load Data, in: Erosion and Sediment Transport Measurement, IAHS Pub. No. 133, pp. 177-194.

Walling, D.E. and Webb, B.W., 1988. The Reliability of Rating Curve Estimates of Suspended Sediment Yield: Some Further Considerations, in: Sediment Budgets, IAHS Pub. No. 174, pp. 337-350.

Walling, D.E., Webb, B.W. and Woodward, J.C., 1992. Some Sampling Considerations in the Design of Effective Strategies for Monitoring Sediment-Associated Transport, in: Erosion and Sediment Transport Monitoring Programmes in River Basins, IAHS Pub. No. 210, pp. 183-190.

Ziegler, C.K. and Nisbet, B., 1994. Fine-Grained Sediment Transport in Pawtuxet River, Rhode Island, ASCE J. Hyd. Engr., 120(5):561-576.

APPENDIX B

WATER COLUMN AND SEDIMENT DATA PLOTS
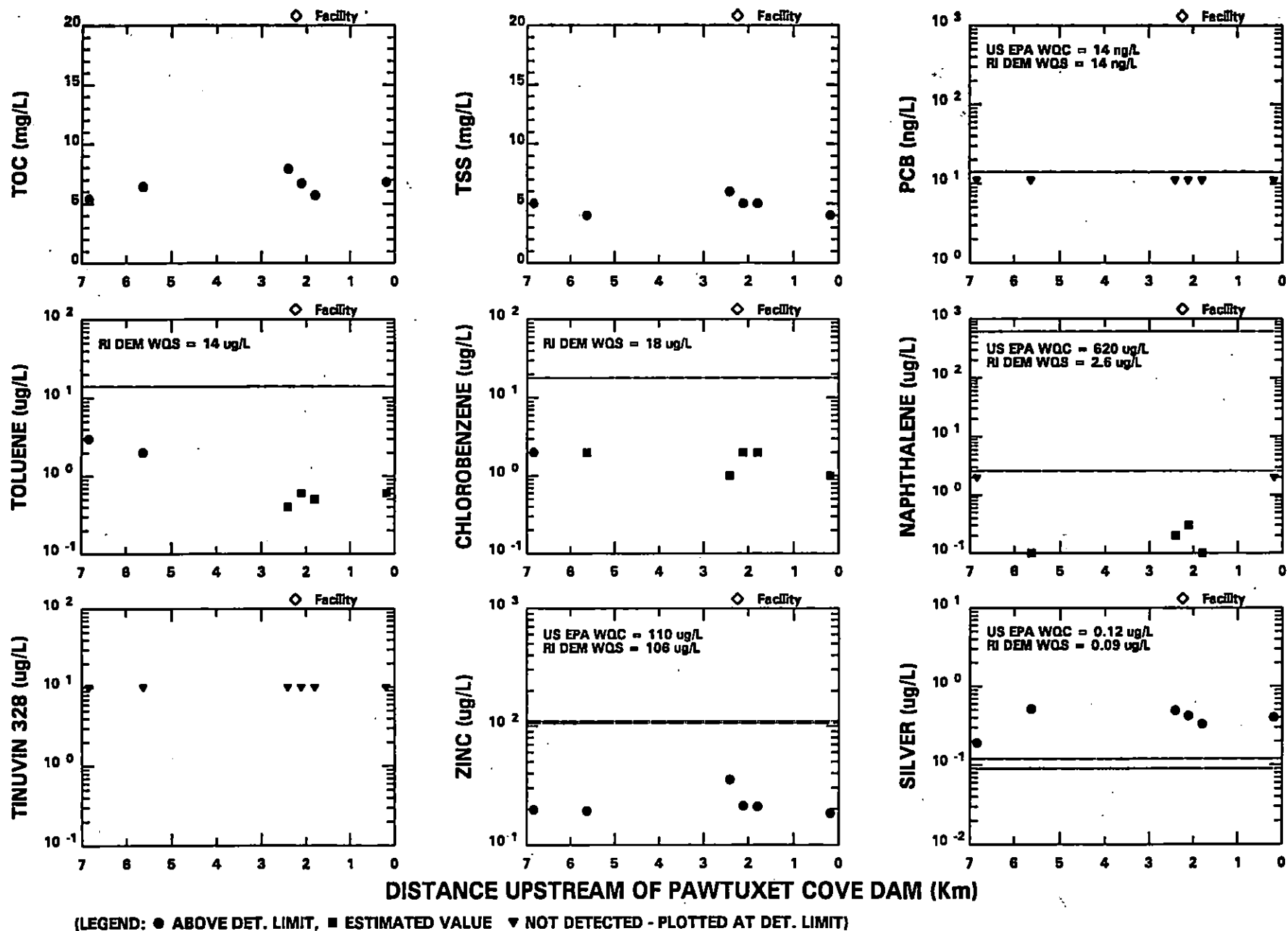
(LEGEND: ● ABOVE DET. LIMIT, ■ ESTIMATED VALUE ▼ NOT DETECTED - PLOTTED AT DET. LIMIT)

WATER COLUMN SAMPLING FOR FATE MODELING - MAY 6, 1992 DATA (RIVER FLOW = 216 cfs)

(LEGEND: ● ABOVE DET. LIMIT, ■ ESTIMATED VALUE ▼ NOT DETECTED - PLOTTED AT DET. LIMIT)
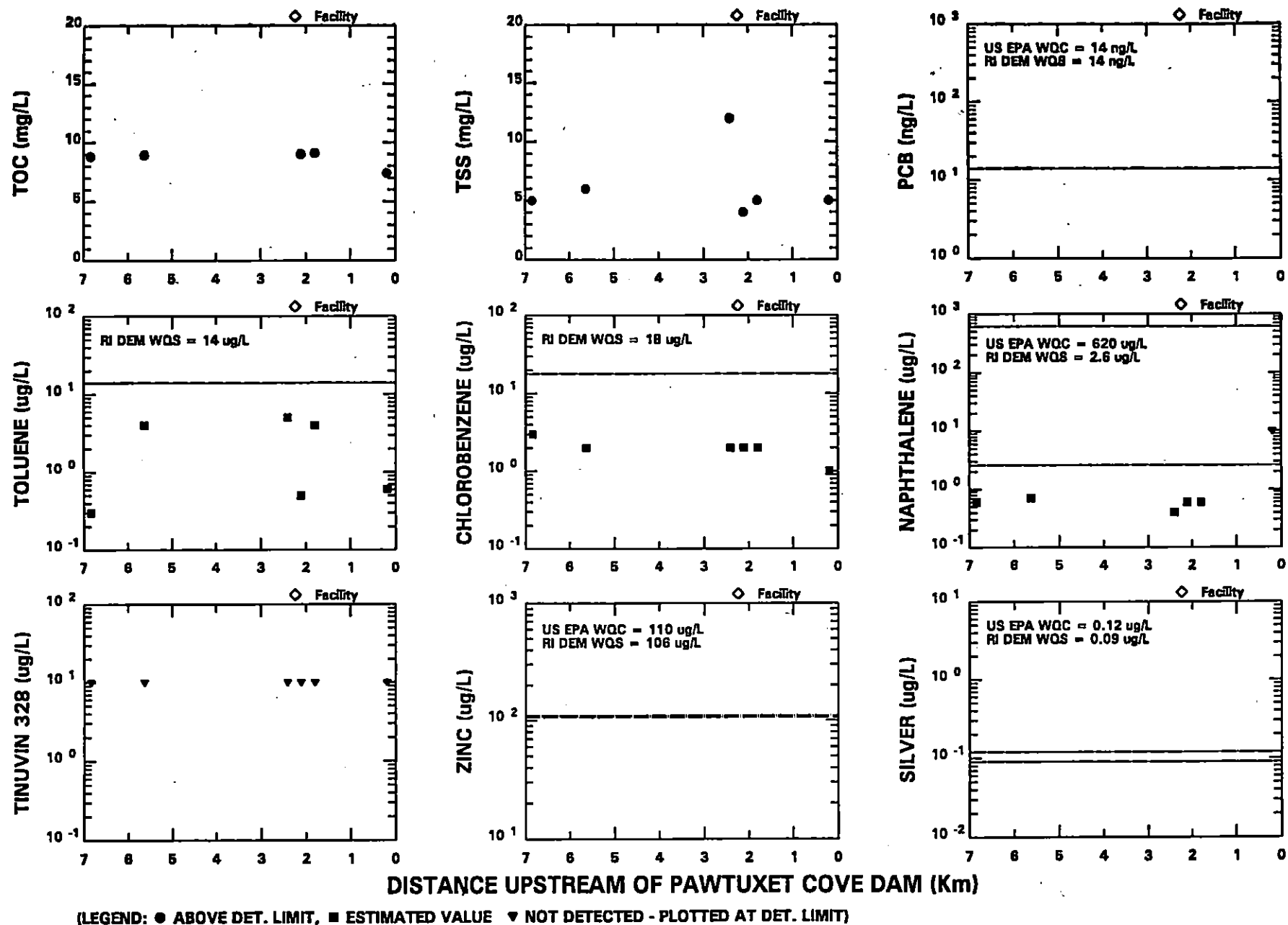
WATER COLUMN SAMPLING FOR FATE MODELING - MAY 13, 1992 DATA (RIVER FLOW = 195 cfs)

(LEGEND: ● ABOVE DET. LIMIT, ■ ESTIMATED VALUE ▼ NOT DETECTED - PLOTTED AT DET. LIMIT)
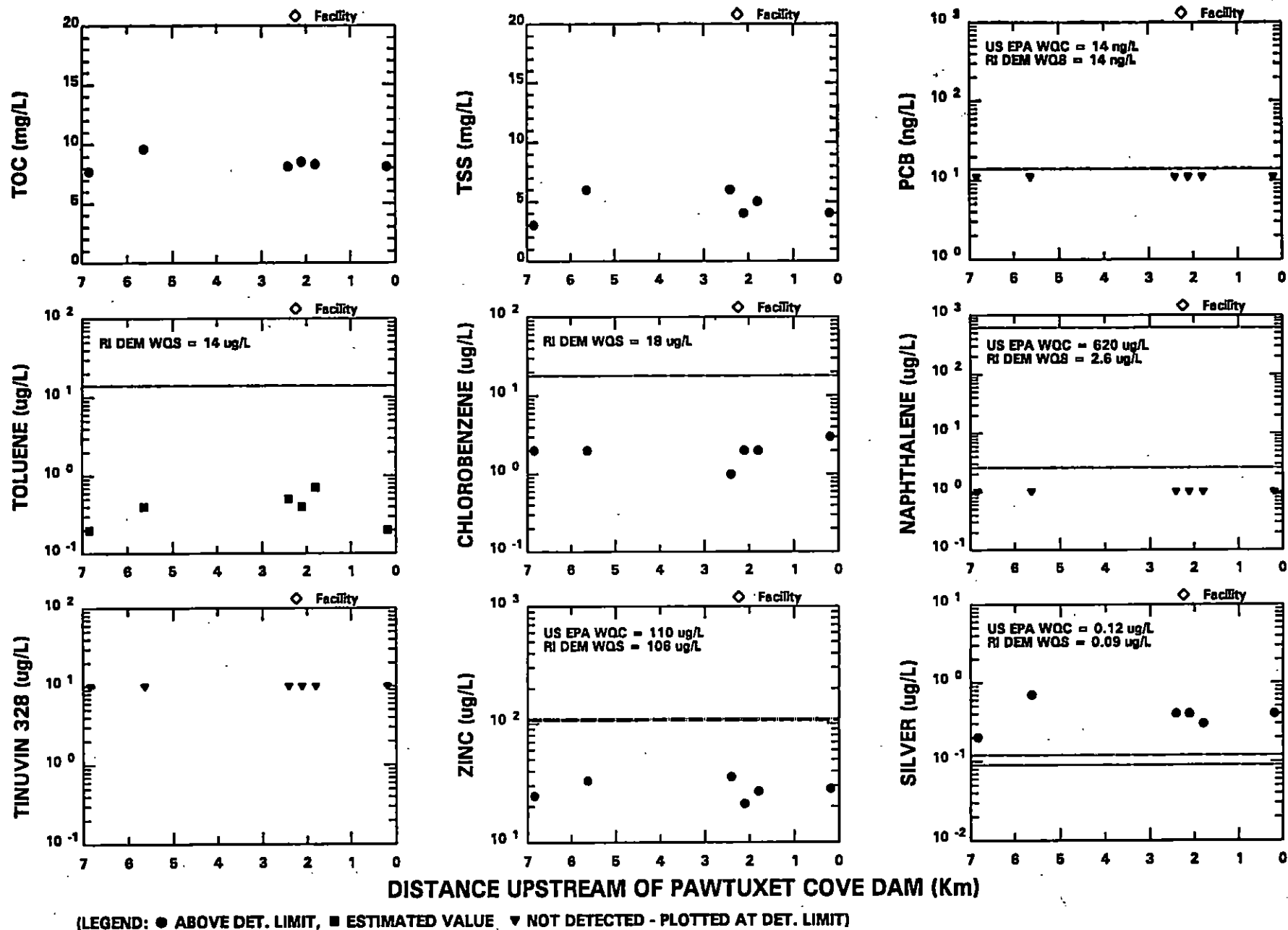
WATER COLUMN SAMPLING FOR FATE MODELING - MAY 21, 1992 DATA (RIVER FLOW = 177 cfs)
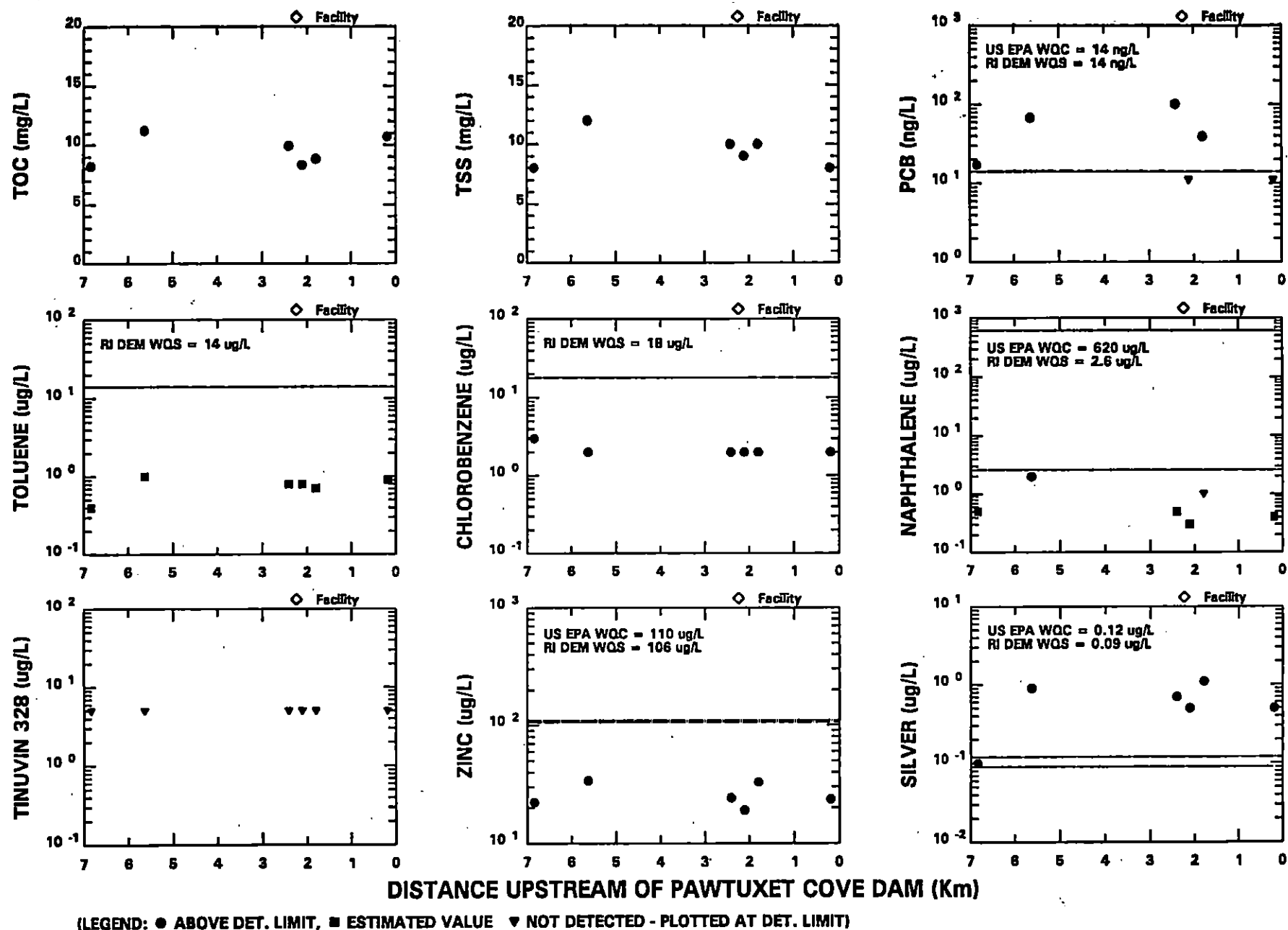
(LEGEND: ● ABOVE DET. LIMIT, ■ ESTIMATED VALUE ▼ NOT DETECTED - PLOTTED AT DET. LIMIT)

WATER COLUMN SAMPLING FOR FATE MODELING - MAY 28, 1992 DATA (RIVER FLOW = 136 cfs)

(LEGEND: ● ABOVE DET. LIMIT, ■ ESTIMATED VALUE ▼ NOT DETECTED - PLOTTED AT DET. LIMIT)
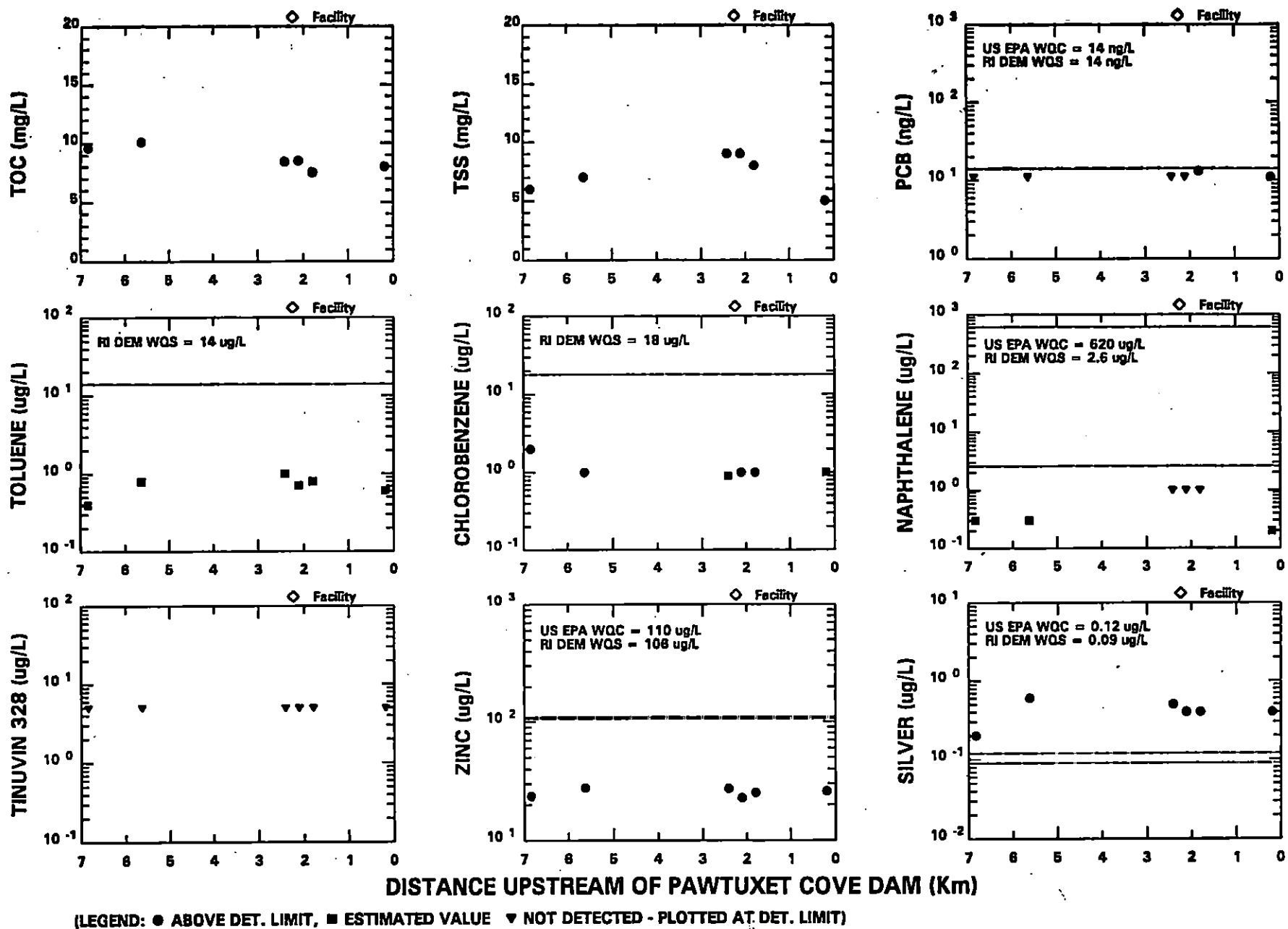
WATER COLUMN SAMPLING FOR FATE MODELING - JUNE 4, 1992 DATA   (RIVER FLOW = 189 cfs)

(LEGEND: ● ABOVE DET. LIMIT, ■ ESTIMATED VALUE ▼ NOT DETECTED - PLOTTED AT DET. LIMIT)
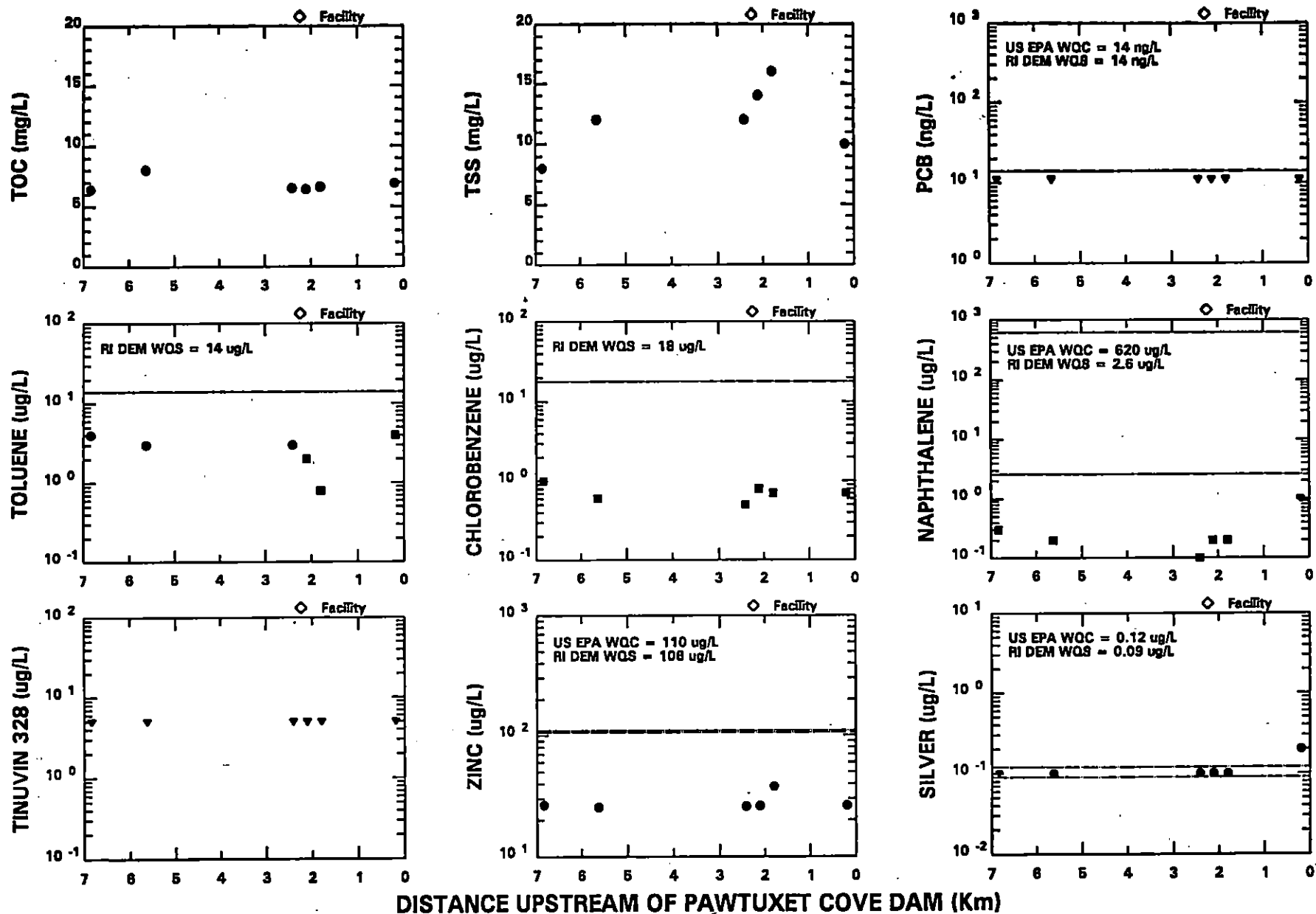
WATER COLUMN SAMPLING FOR FATE MODELING - JUNE 10, 1992 DATA (RIVER FLOW = 325 cfs)

(LEGEND: ● ABOVE DET. LIMIT, ■ ESTIMATED VALUE ▼ NOT DETECTED - PLOTTED AT DET. LIMIT)
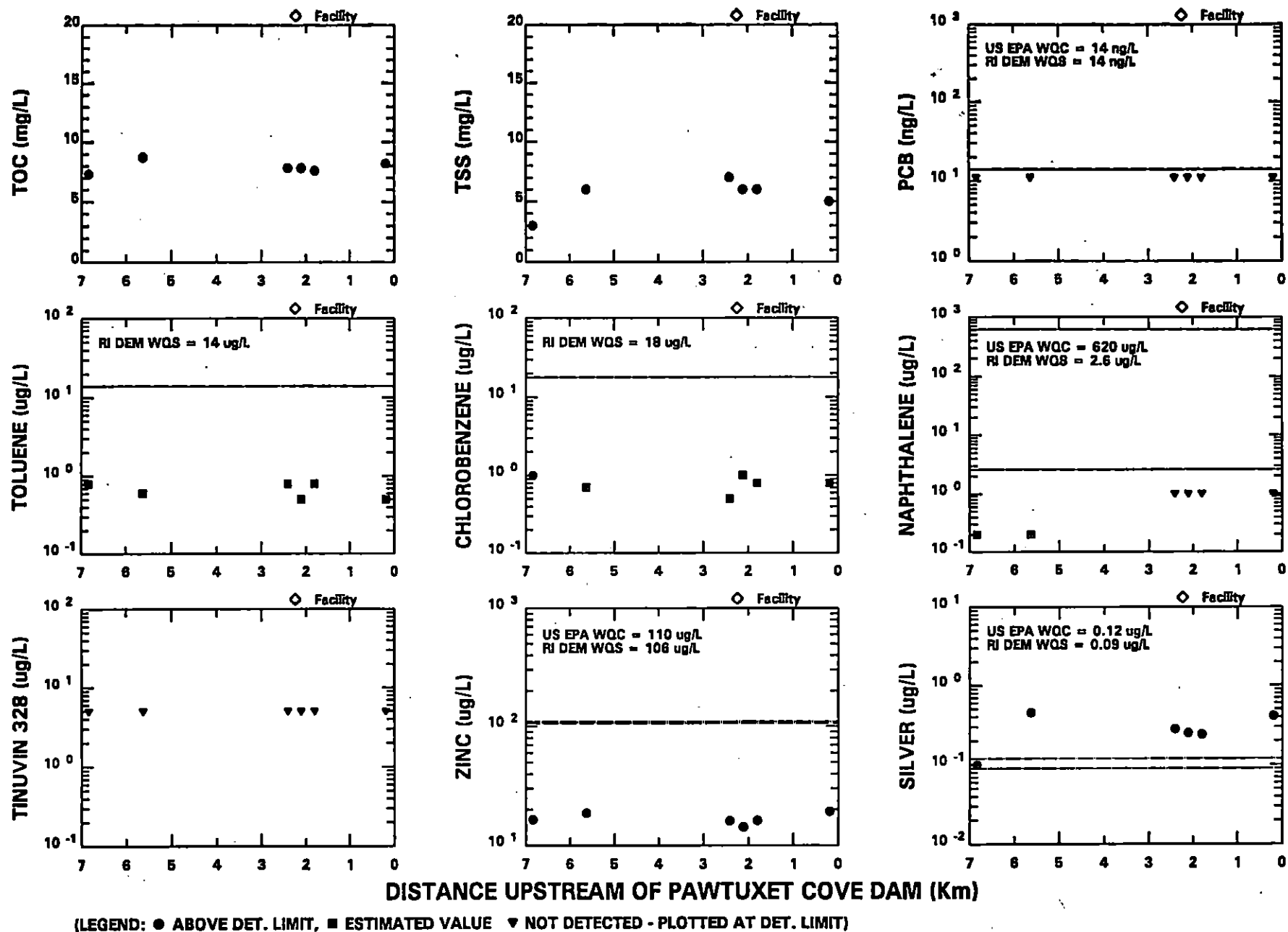
WATER COLUMN SAMPLING FOR FATE MODELING - JUNE 18, 1992 DATA (RIVER FLOW = 139 cfs)

(LEGEND: ● ABOVE DET. LIMIT, ■ ESTIMATED VALUE ▼ NOT DETECTED - PLOTTED AT DET. LIMIT)
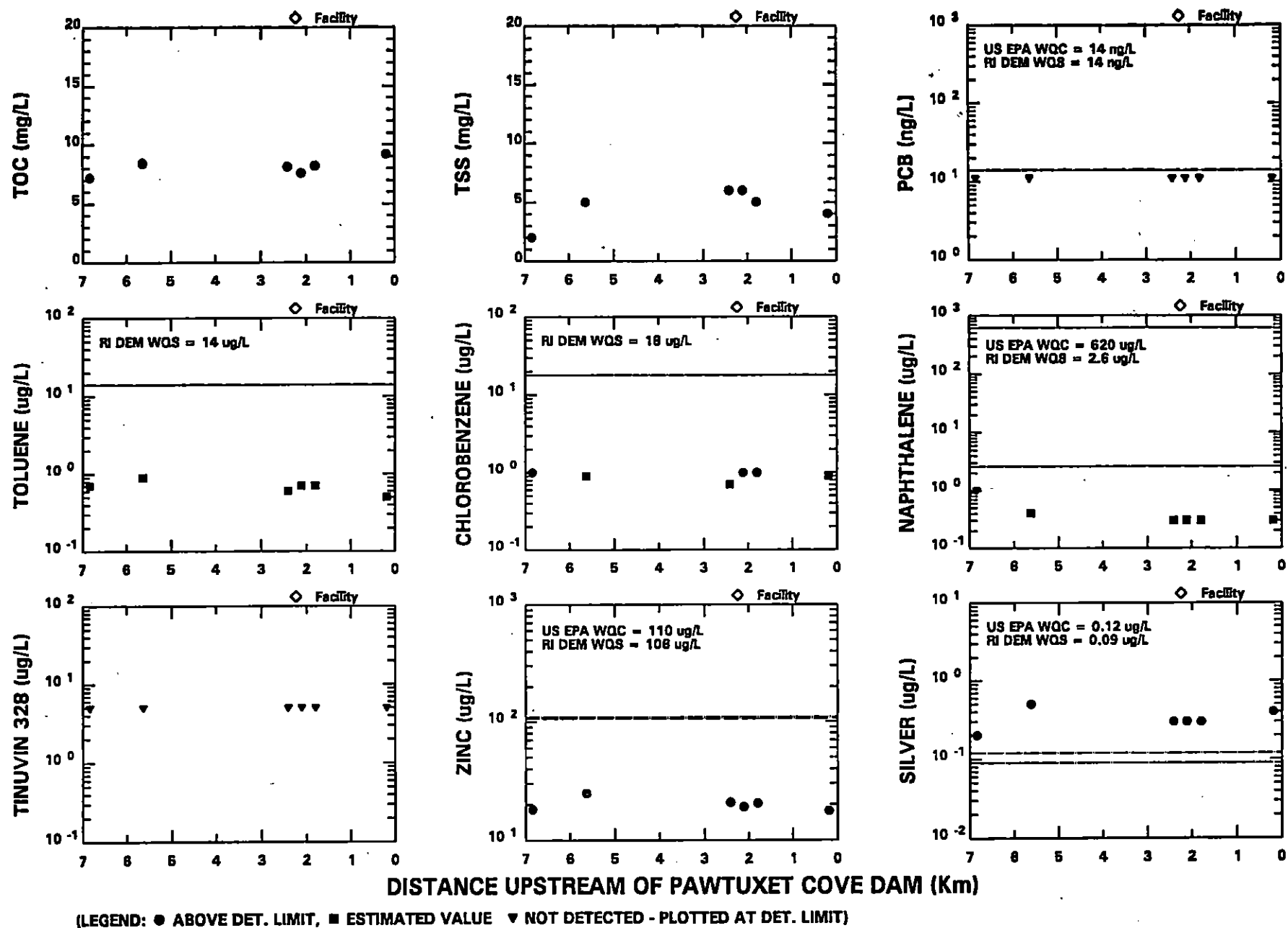
WATER COLUMN SAMPLING FOR FATE MODELING - JUNE 24, 1992 DATA (RIVER FLOW = 175 cfs)
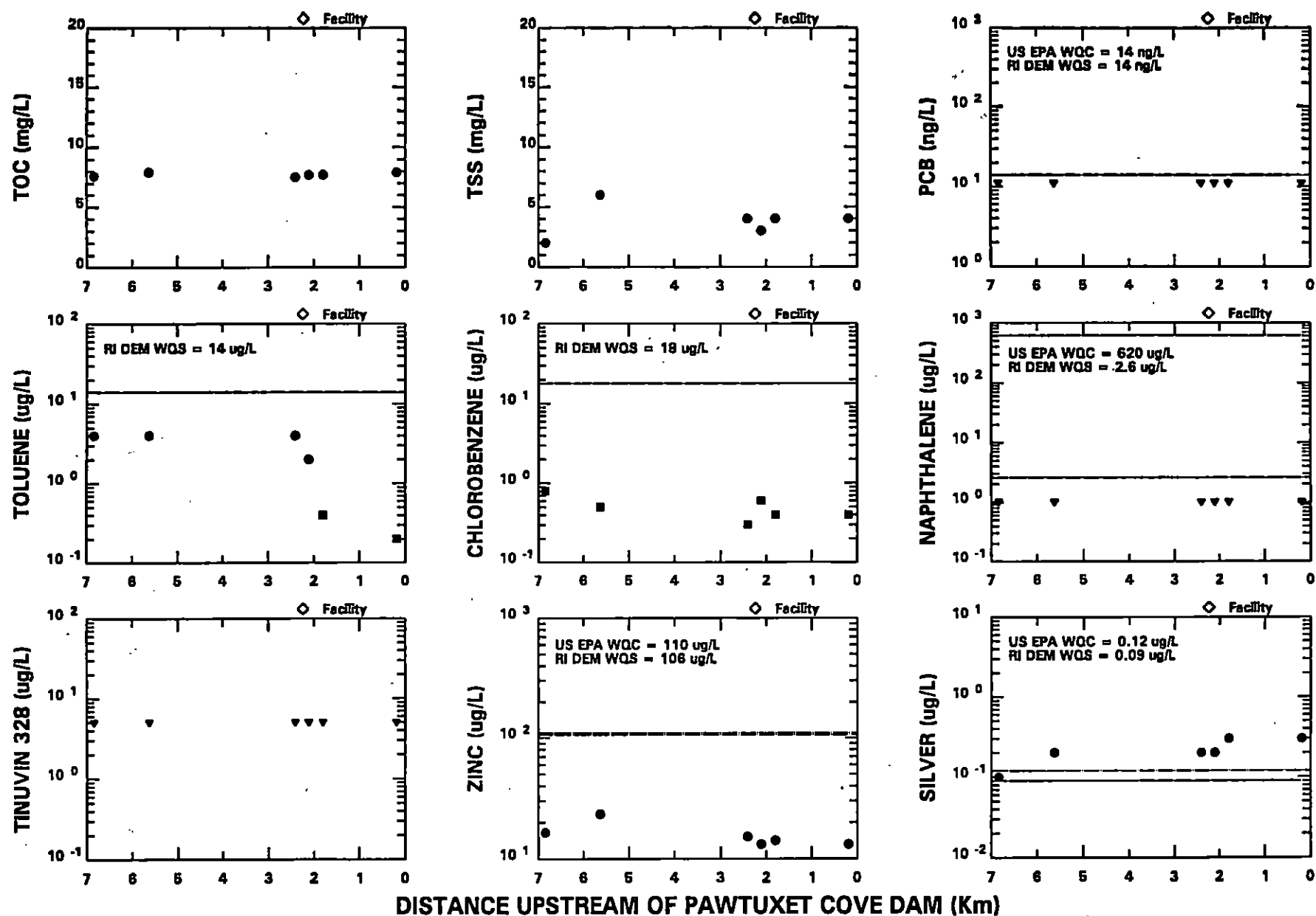
(LEGEND: ● ABOVE DET. LIMIT, ■ ESTIMATED VALUE ▼ NOT DETECTED - PLOTTED AT DET. LIMIT)

WATER COLUMN SAMPLING FOR FATE MODELING - JULY 1, 1992 DATA (RIVER FLOW = 165 cfs)
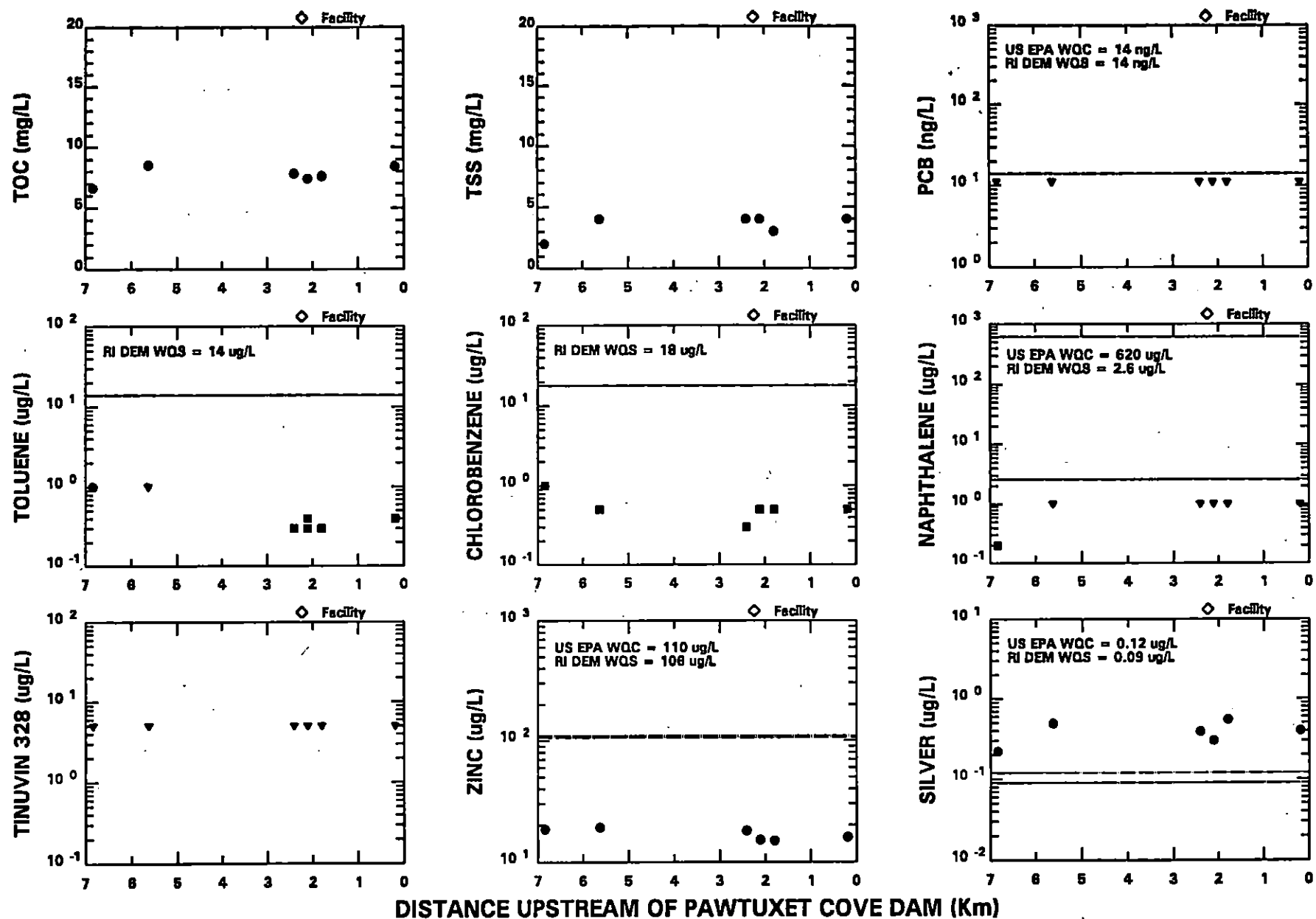
WATER COLUMN SAMPLING FOR FATE MODELING - JULY 8, 1992 DATA   (RIVER FLOW = 129 cfs)

(LEGEND: ● ABOVE DET. LIMIT, ■ ESTIMATED VALUE ▼ NOT DETECTED - PLOTTED AT DET. LIMIT)
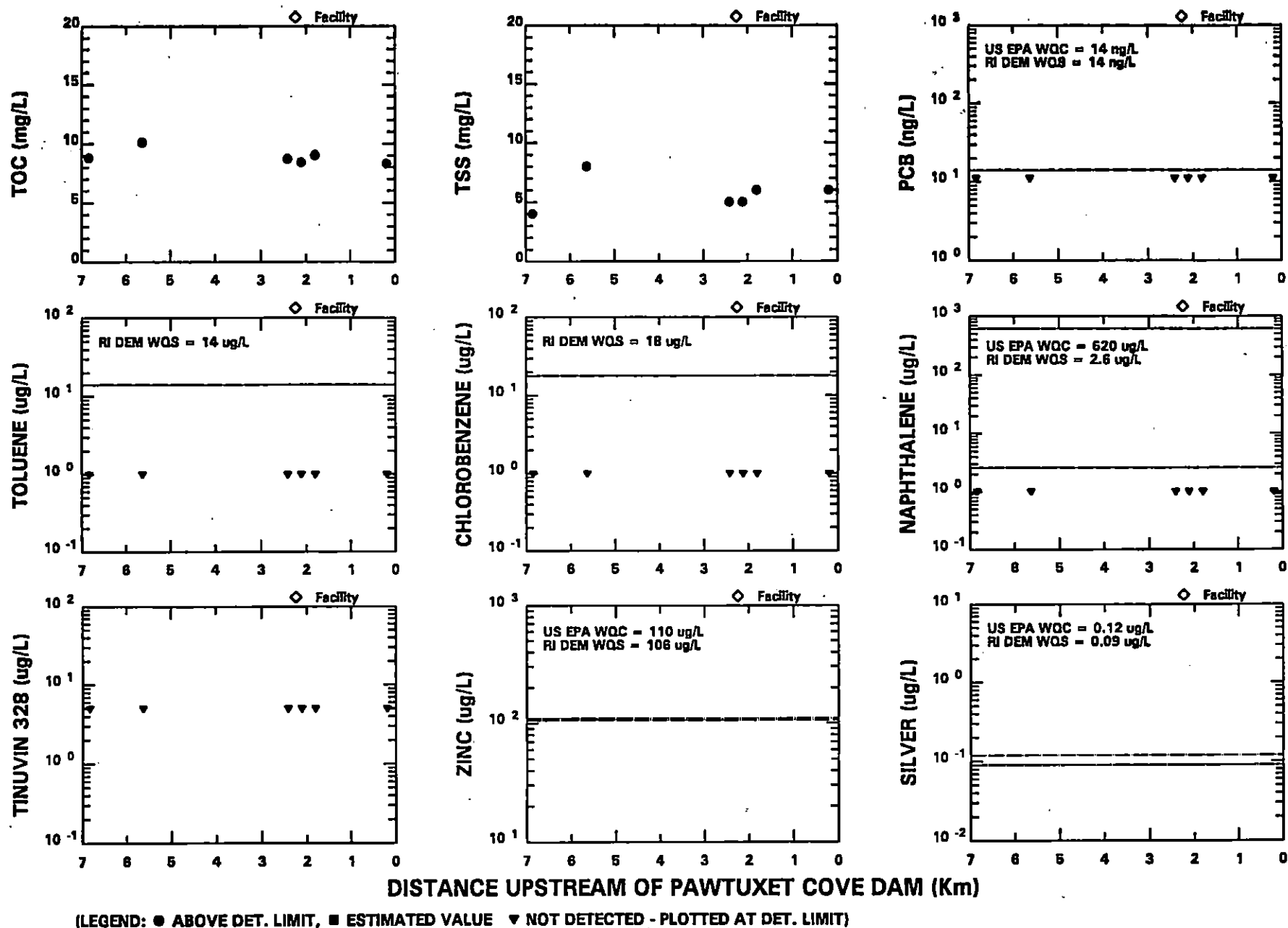
WATER COLUMN SAMPLING FOR FATE MODELING - JULY 15, 1992 DATA (RIVER FLOW = 301 cfs)

(LEGEND: ● ABOVE DET. LIMIT, ■ ESTIMATED VALUE ▼ NOT DETECTED - PLOTTED AT DET. LIMIT)
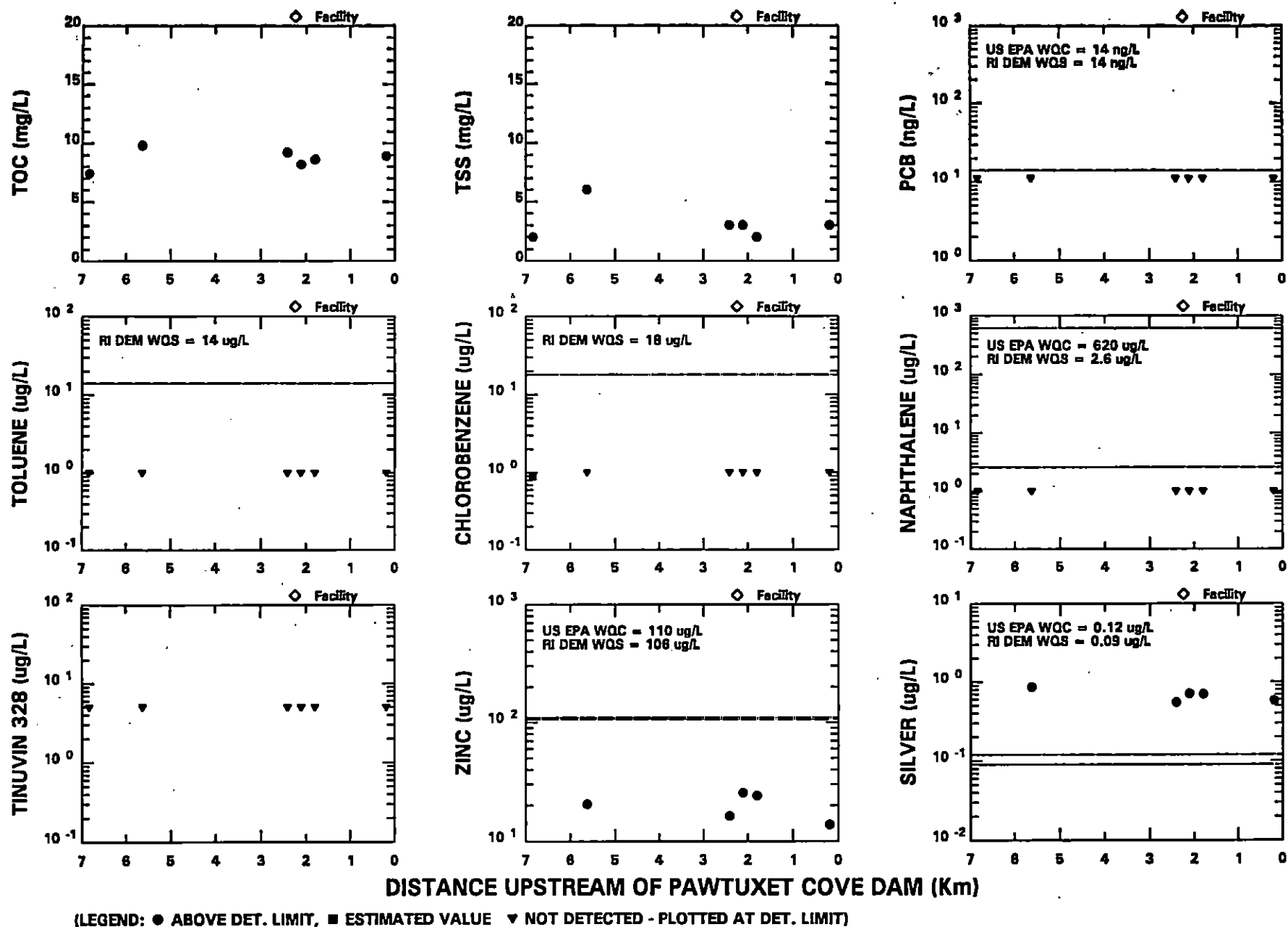
WATER COLUMN SAMPLING FOR FATE MODELING - JULY 22, 1992 DATA (RIVER FLOW = 169 cfs)

Pawtuxet River

Production Area

Wastewater Treatment Area

Warwick Ave Bridge

Warwick Area

Pawtuxet Cove Dam

Chlororbenzene (mg/Kg S) 0-5 cm

North Bank

Center Channel

South Bank

Distance Upstream of Pawtuxet Cove Dam (km)
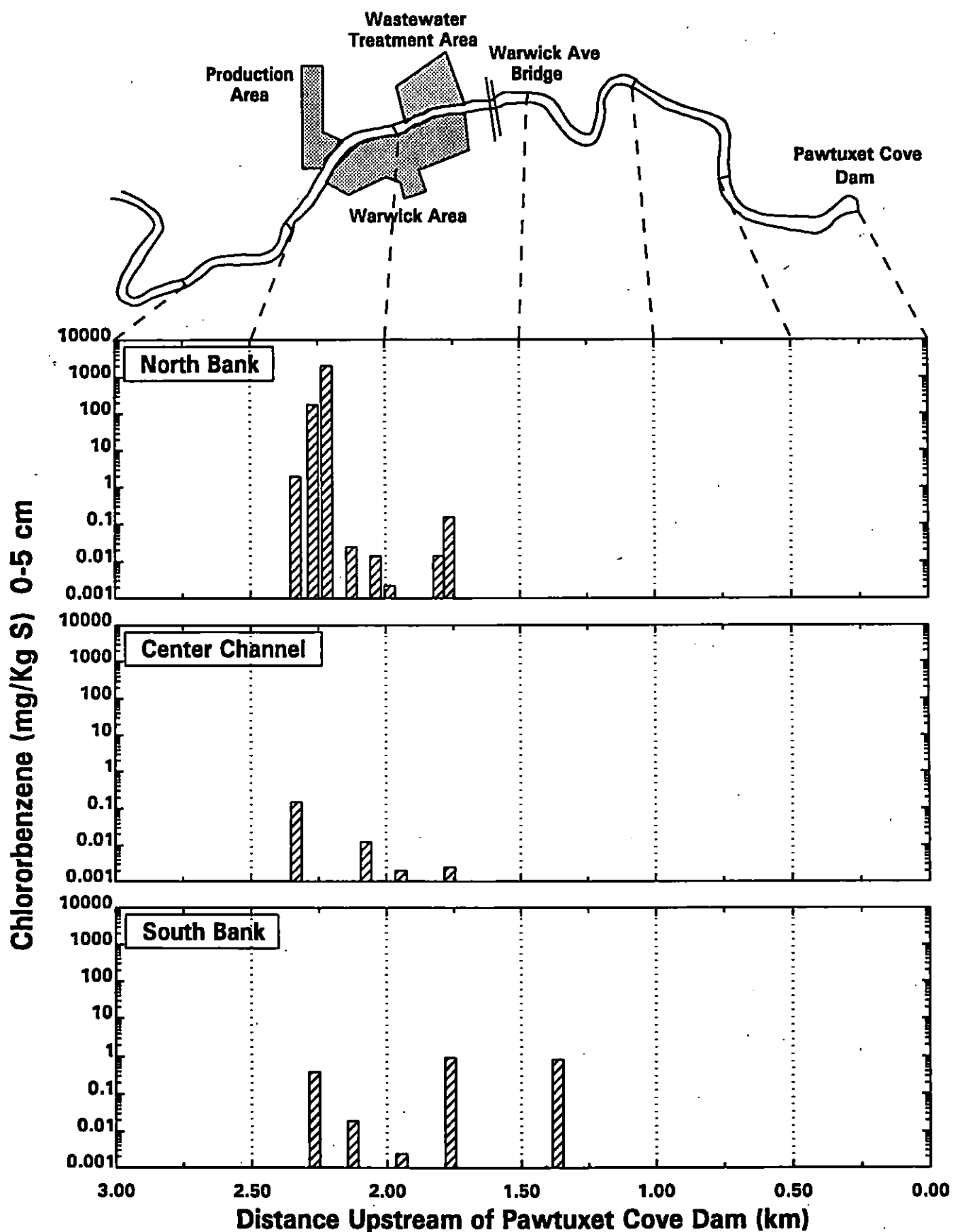
0-5 cm Sediment & Unqualified and Estimated Values (No U values)

Tue Jul 11,1995 12:05:32 sptclg3.gdp
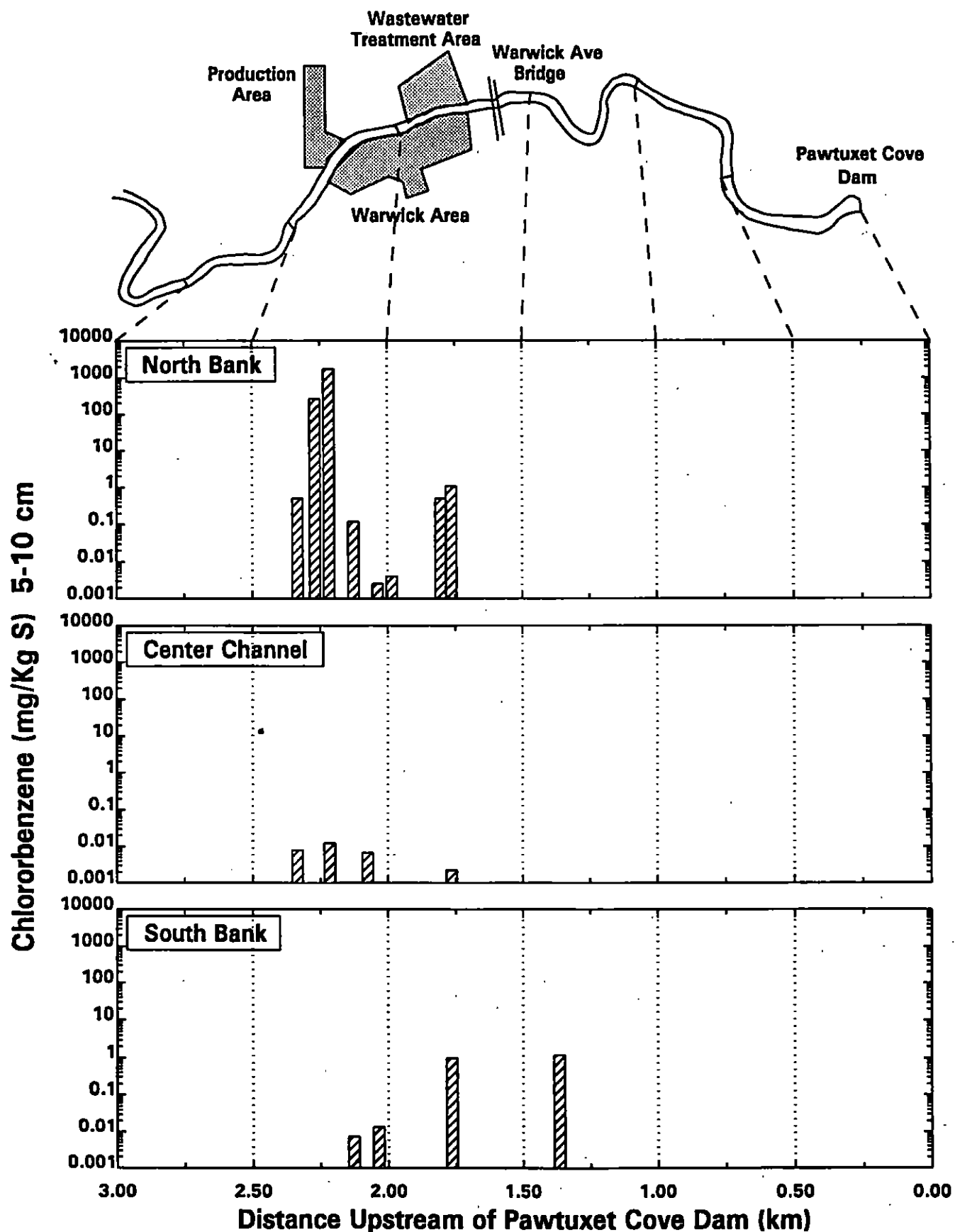
Pawtuxet River

Chlororbenzene (mg/Kg S) 5-10 cm

North Bank

Center Channel

South Bank

Distance Upstream of Pawtuxet Cove Dam (km)

5-10 cm Sediment & Unqualified and Estimated Values (No U values)

Pawtuxet River

10-20 cm Sediment & Unqualified and Estimated Values (No U values)

Pawtuxet River

Production
Area

Wastewater
Treatment Area

Warwick Ave
Bridge

Pawtuxet Cove
Dam

Warwick Area

Naphthalene (mg/Kg S) 0-5 cm

North Bank

Center Channel

South Bank

Distance Upstream of Pawtuxet Cove Dam (km)

0-5 cm Sediment & Unqualified and Estimated Values (No U values)

Tue Jul 11,1995 12:05:00 sptclg3.gdp

Pawtuxet River

North Bank

Center Channel

South Bank

Naphthalene (mg/Kg S) 5-10 cm

Distance Upstream of Pawtuxet Cove Dam (km)
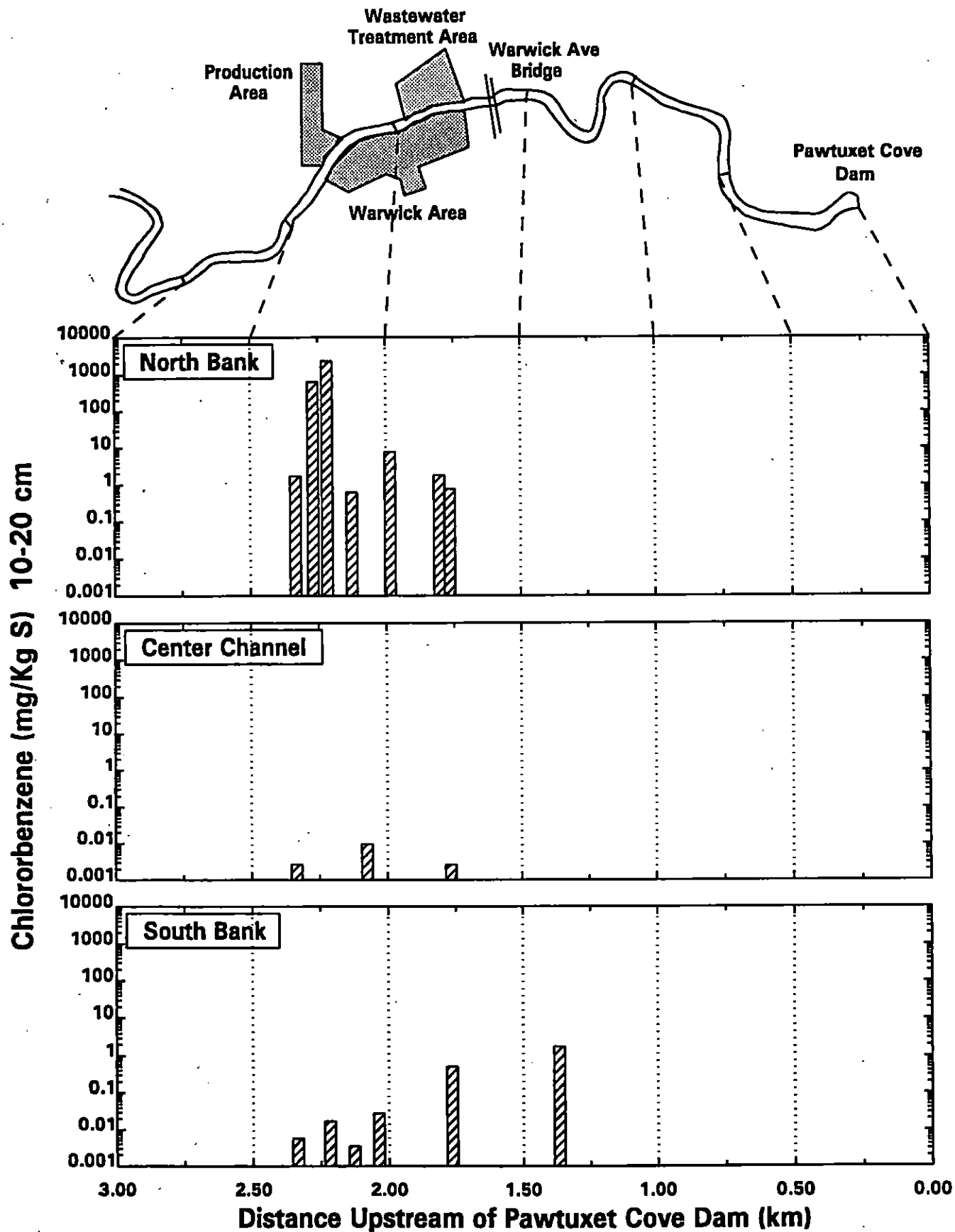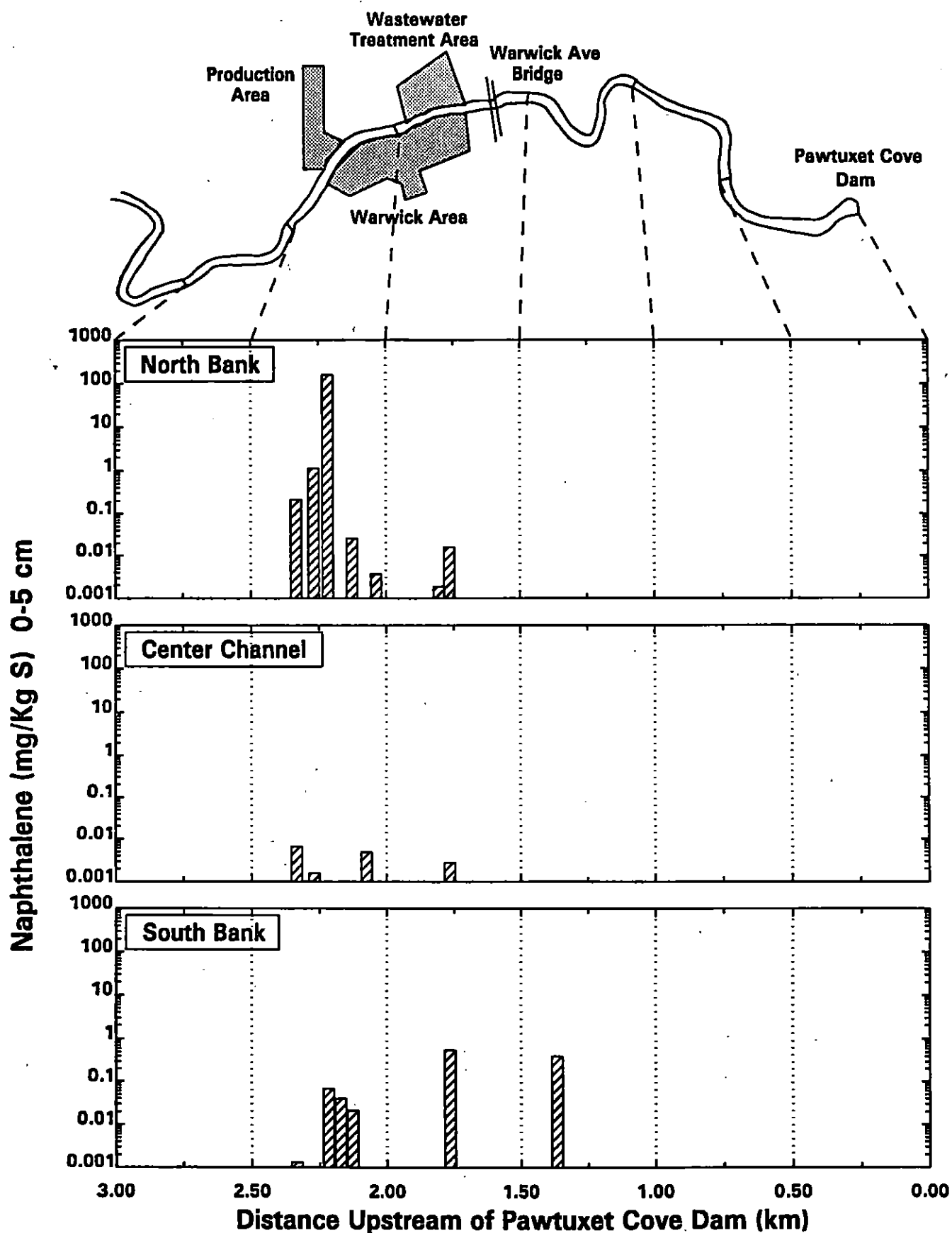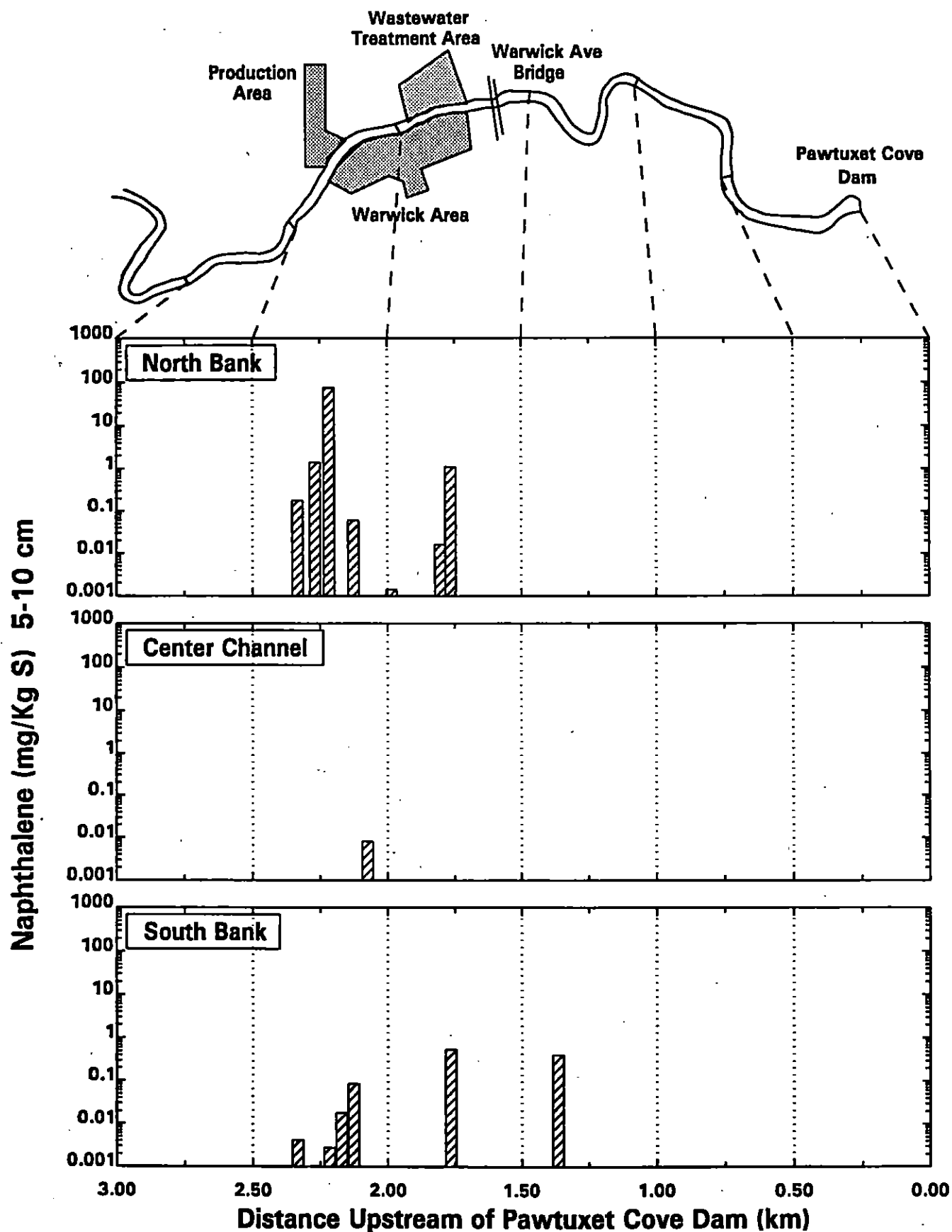
5-10 cm Sediment & Unqualified and Estimated Values (No U values)

Tue Jul 11,1995 12:05:12 sptclg3.gdp

Pawtuxet River
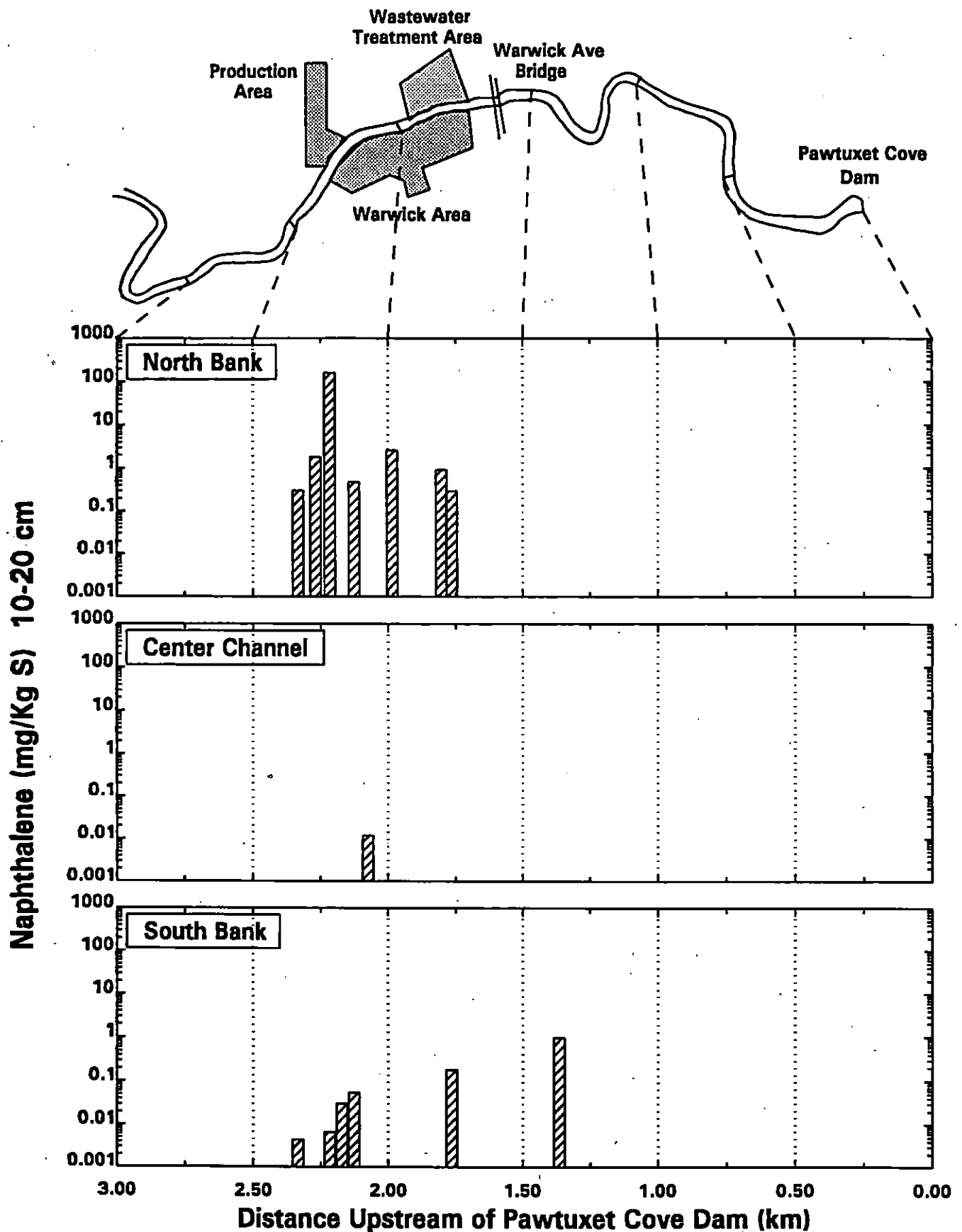
Production Area

Wastewater Treatment Area

Warwick Ave Bridge

Pawtuxet Cove Dam

Warwick Area

North Bank

Center Channel

South Bank

Naphthalene (mg/Kg S) 10-20 cm

Distance Upstream of Pawtuxet Cove Dam (km)

10-20 cm Sediment & Unqualified and Estimated Values (No U values)

Pawtuxet River

Production Area

Wastewater Treatment Area

Warwick Ave Bridge

Warwick Area

Pawtuxet Cove Dam

North Bank

Center Channel

South Bank

Total PCB (mg/Kg S) 0-5 cm

Distance Upstream of Pawtuxet Cove Dam (km)
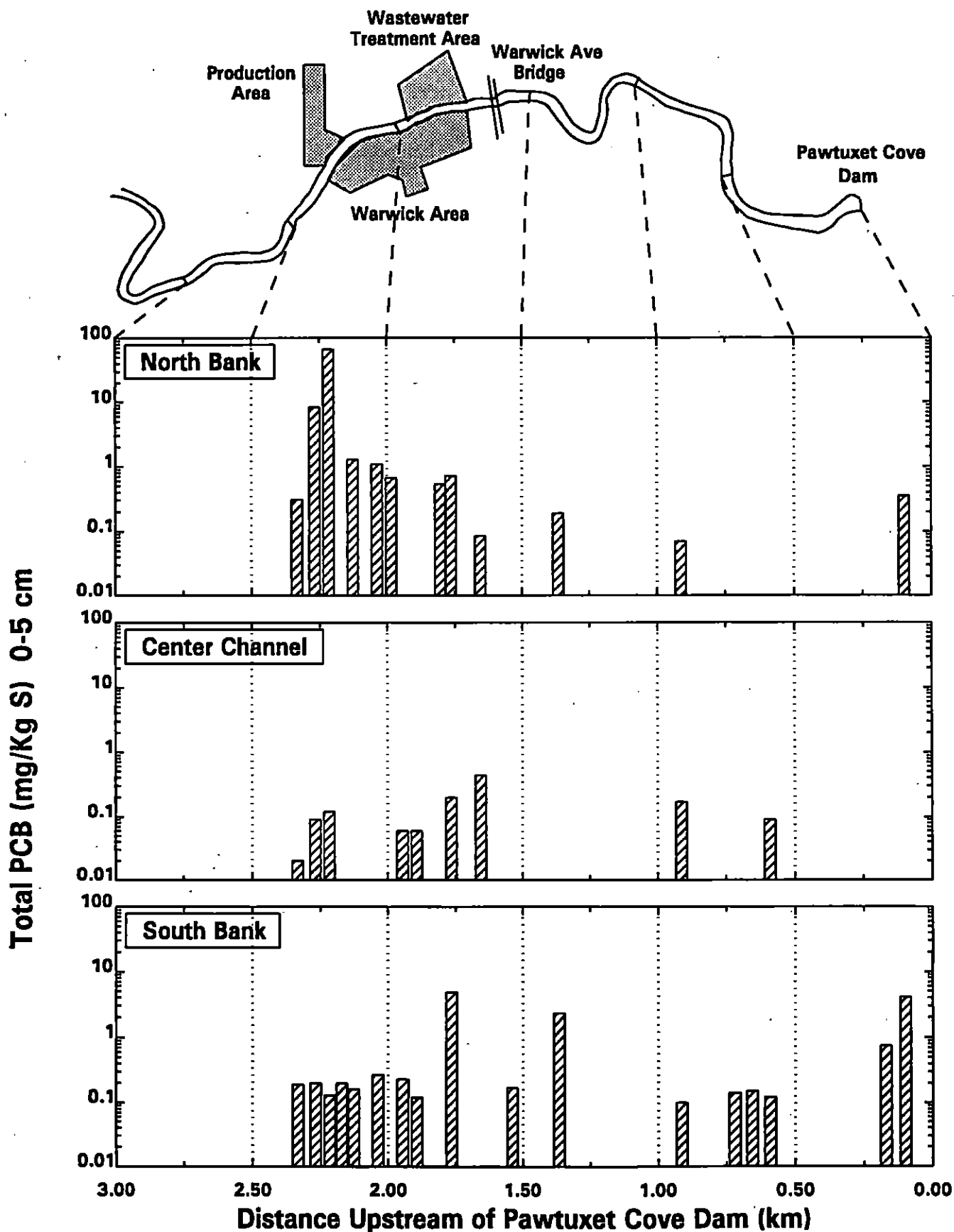
0-5 cm Sediment & Unqualified and Estimated Values (No U values)

Tue Jul 11,1995 12:06:02 sptclg3.gdp

Pawtuxet River

Production Area

Wastewater Treatment Area

Warwick Ave Bridge

Warwick Area

Pawtuxet Cove Dam

North Bank

Center Channel

South Bank

Total PCB (mg/Kg S) 5-10 cm

Distance Upstream of Pawtuxet Cove Dam (km)
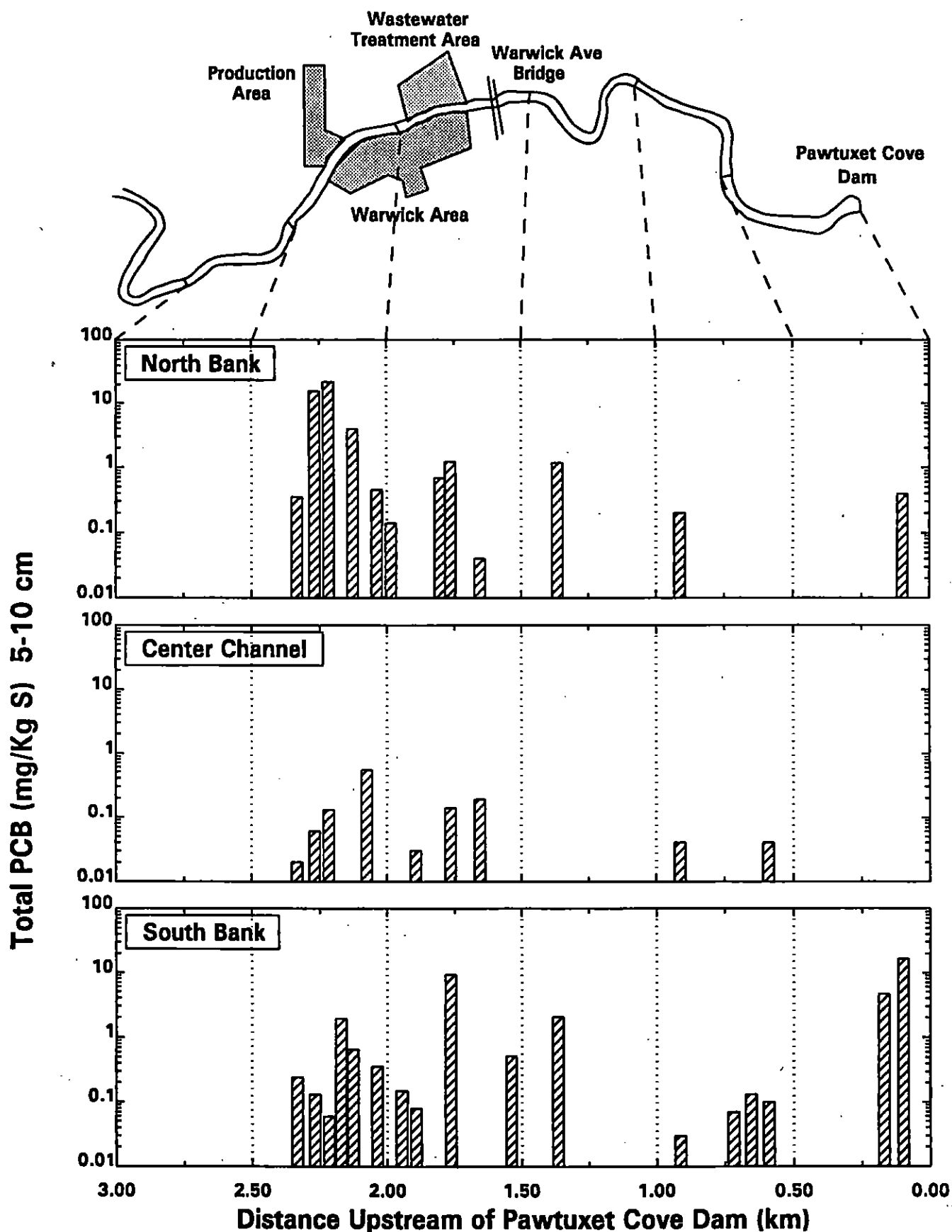
5-10 cm Sediment & Unqualified and Estimated Values (No U values)

Tue Jul 11,1995 12:06:11 sptclg3.gdp

Pawtuxet River
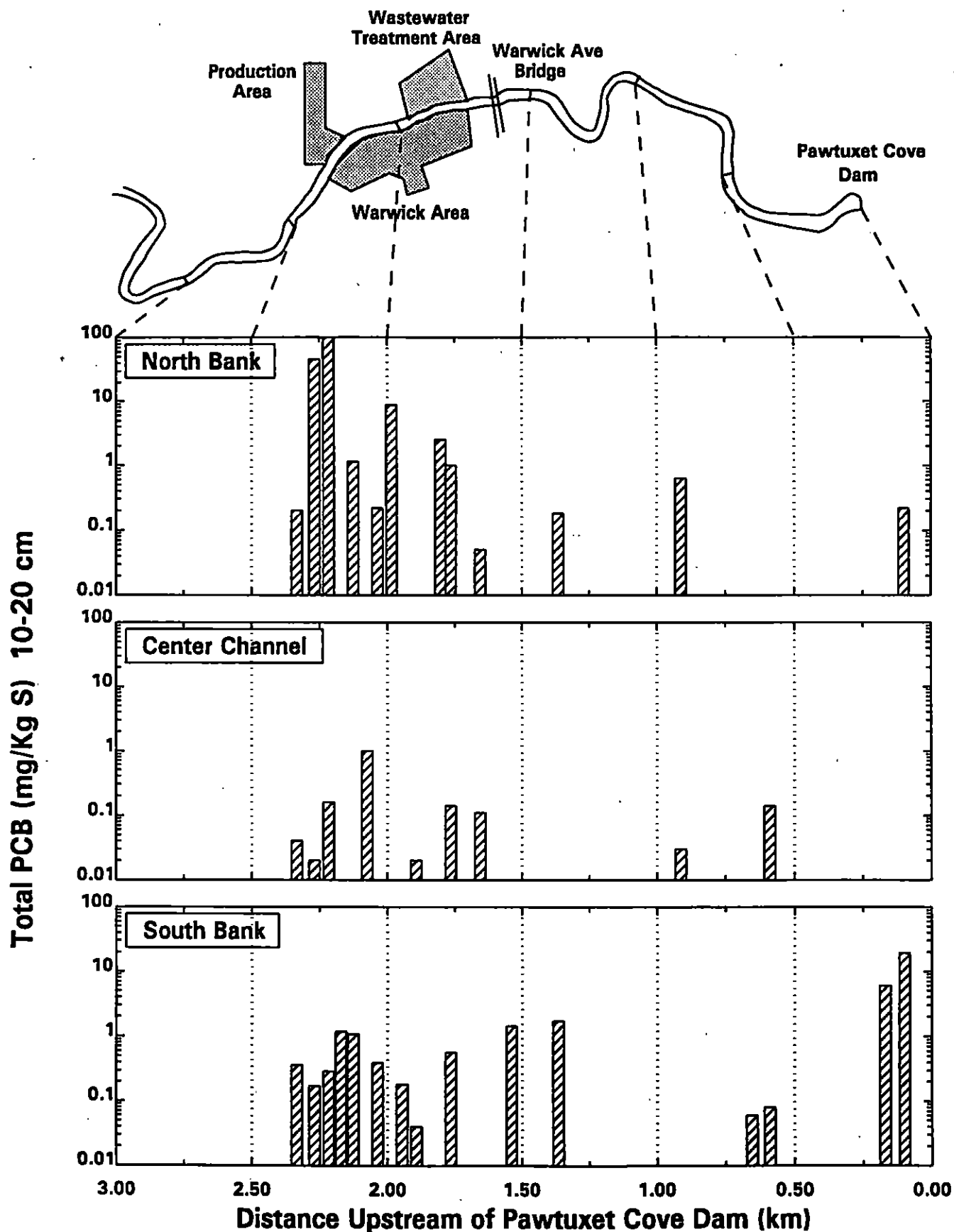
10-20 cm Sediment & Unqualified and Estimated Values (No U values)

Tue Jul 11,1995 12:06:20 sptclg3.gdp

Pawtuxet River
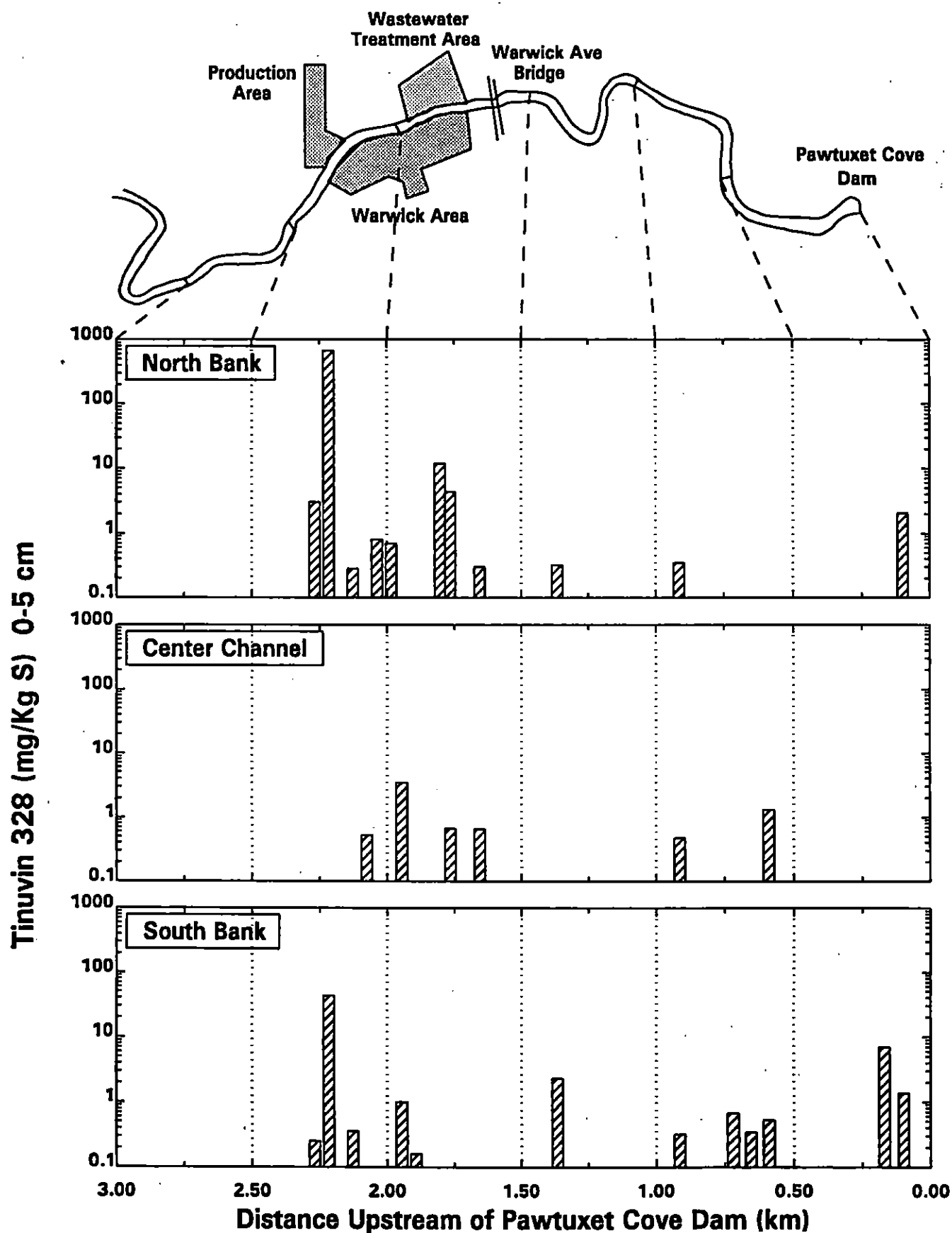
Production Area

Wastewater Treatment Area

Warwick Ave Bridge

Pawtuxet Cove Dam

Warwick Area

North Bank

Center Channel

South Bank

Tinuvin 328 (mg/Kg S) 0-5 cm

Distance Upstream of Pawtuxet Cove Dam (km)

0-5 cm Sediment & Unqualified and Estimated Values (No U values)

Tue Jul 11,1995 12:06:58 aptclg3.gdp

Pawtuxet River

Pawtuxet River

Production Area

Wastewater Treatment Area

Warwick Ave Bridge

Warwick Area

Pawtuxet Cove Dam

North Bank

Center Channel

South Bank

Tinuvin 328 (mg/Kg S) 10-20 cm

Distance Upstream of Pawtuxet Cove Dam (km)
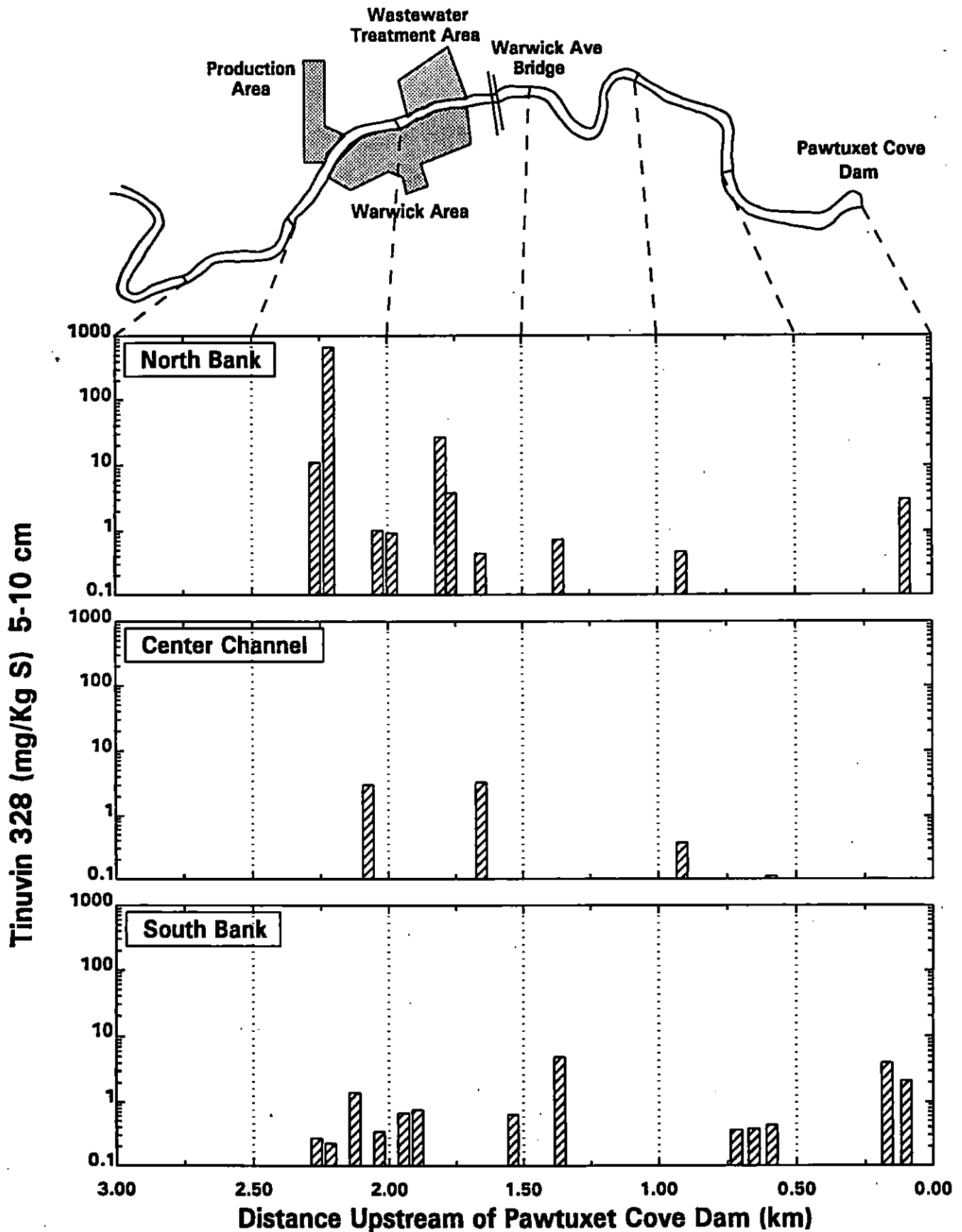
10-20 cm Sediment & Unqualified and Estimated Values (No U values)

Tue Jul 11,1995 12:07:16 sptclg3.gdp

Pawtuxet River

North Bank

Center Channel

South Bank

Zinc (mg/Kg S) 0-5 cm

Distance Upstream of Pawtuxet Cove Dam (km)
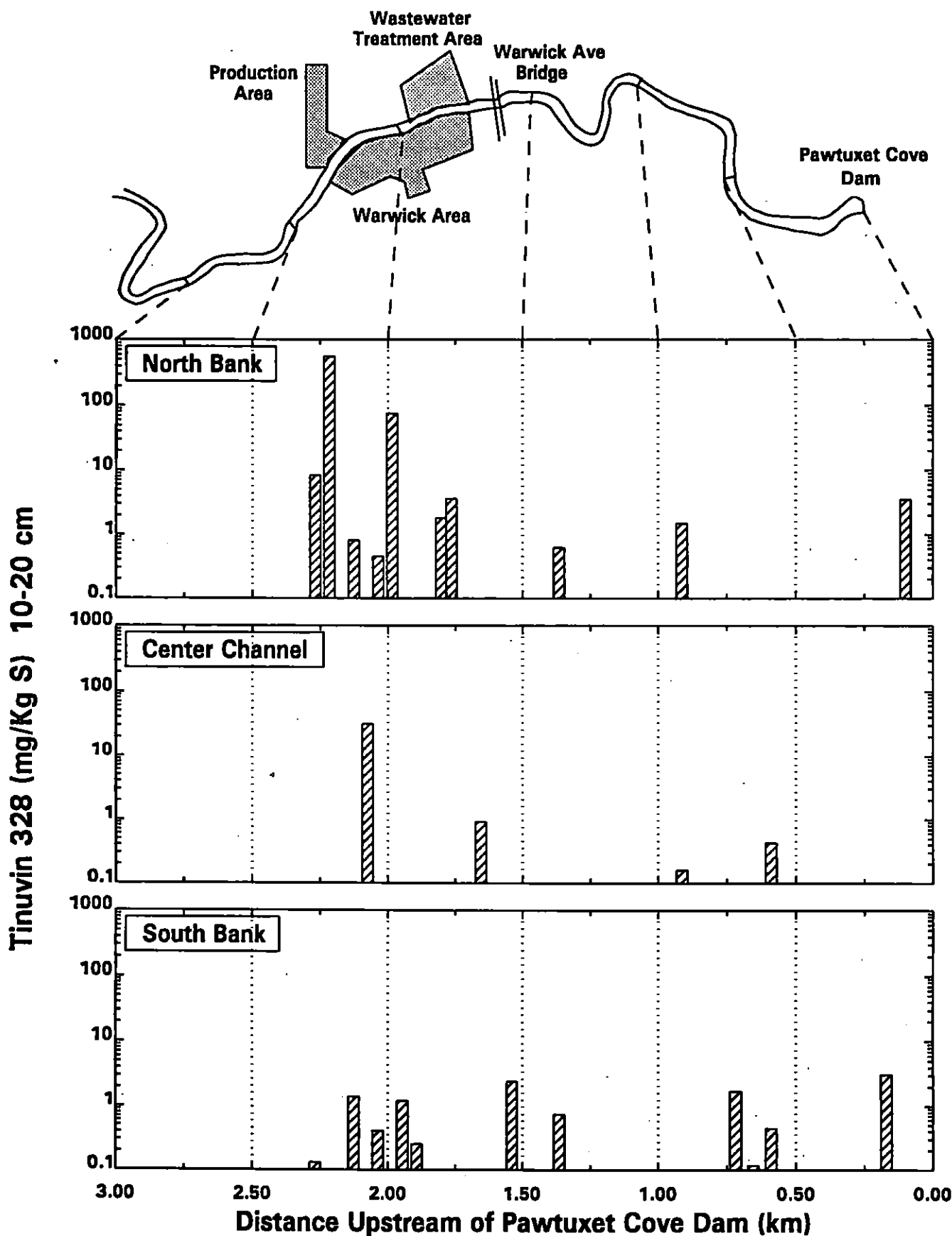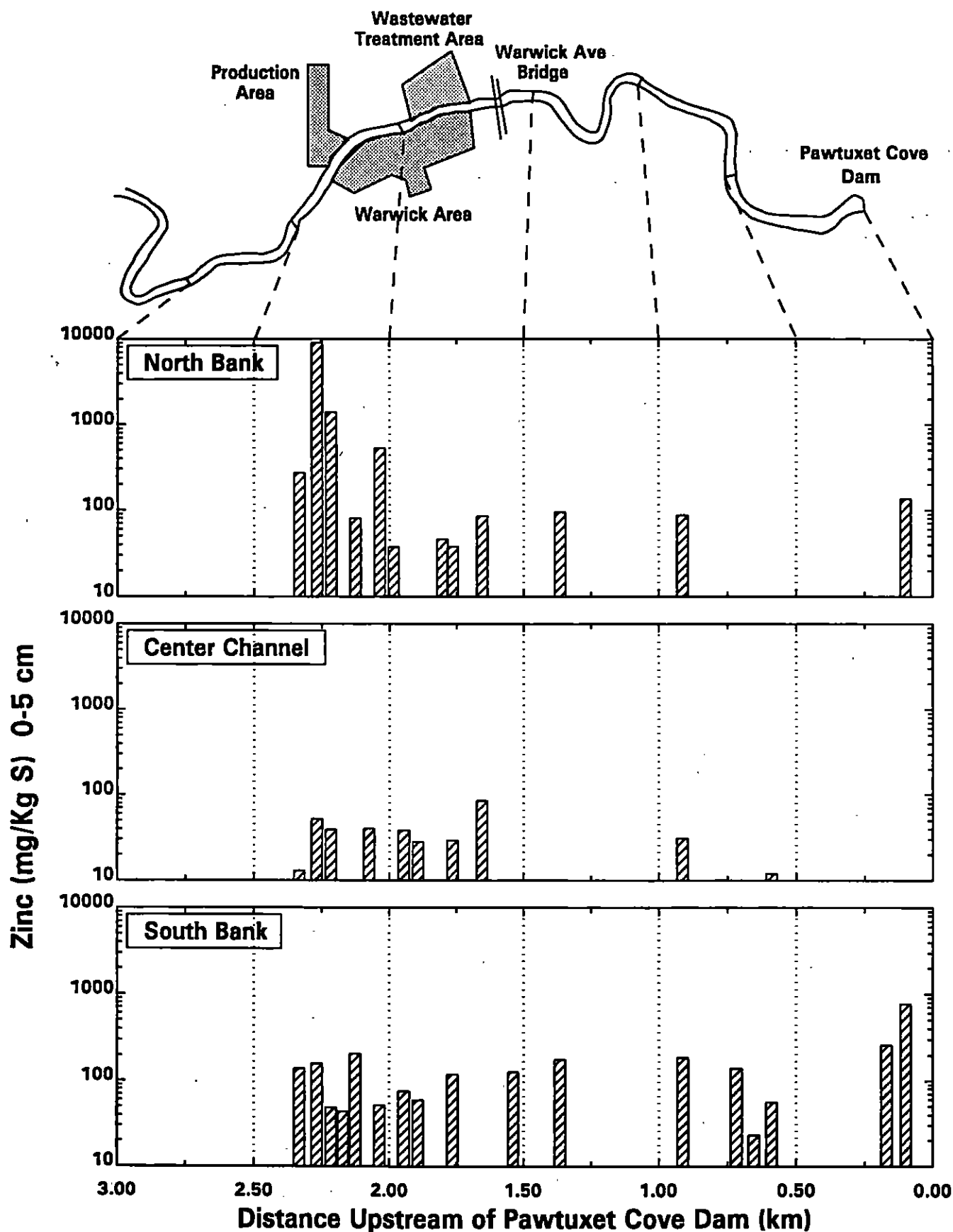
0-5 cm Sediment & Unqualified and Estimated Values (No U values)

Tue Jul 11,1995 12:06:29 sptclg3.gdp

Pawtuxet River

Figure: Zinc (mg/Kg S) 5-10 cm sediment concentrations plotted by distance upstream of Pawtuxet Cove Dam (km) for North Bank, Center Channel, and South Bank. Map shows Production Area, Wastewater Treatment Area, Warwick Area, Warwick Ave Bridge, and Pawtuxet Cove Dam.
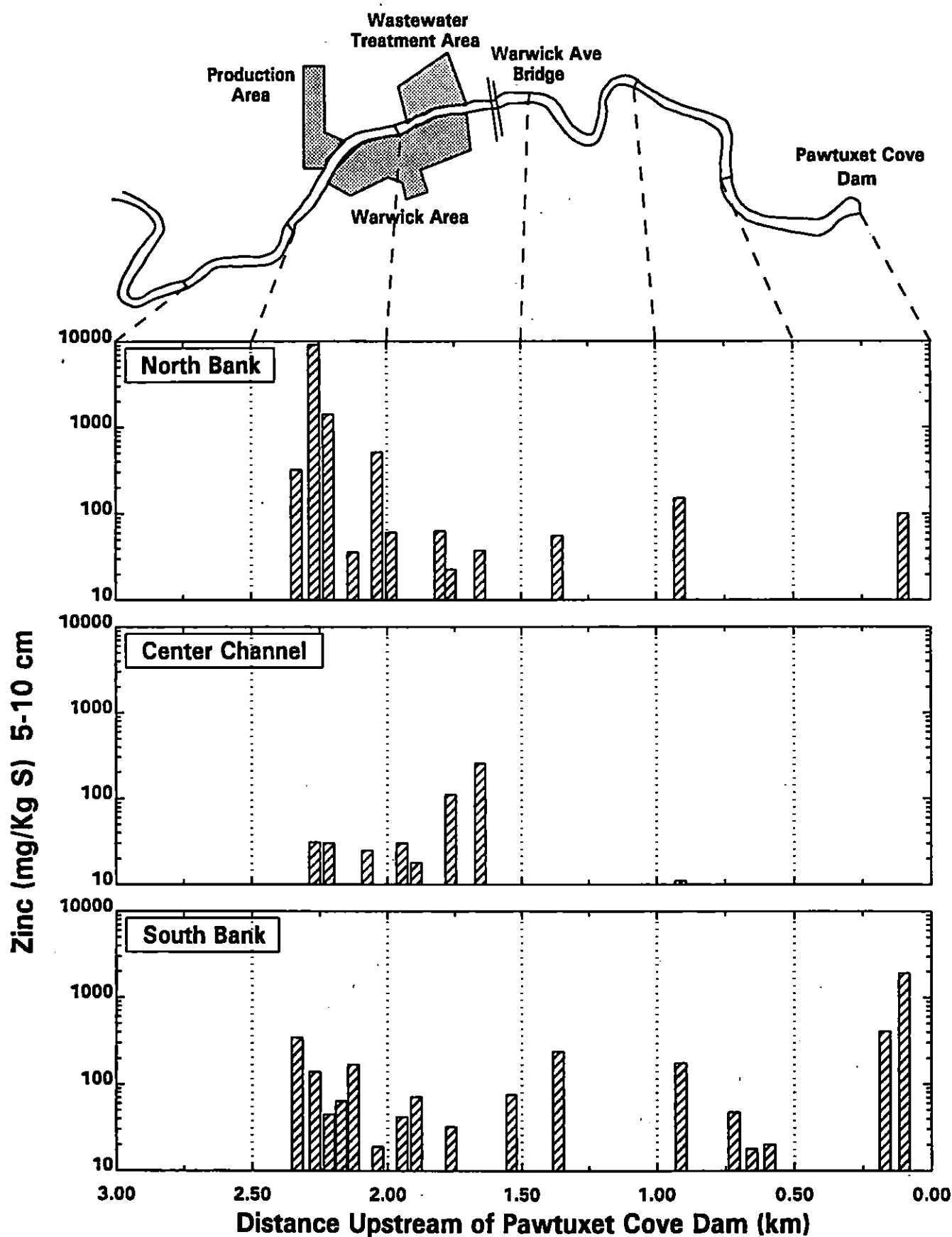
5-10 cm Sediment & Unqualified and Estimated Values (No U values)

Tue Jul 11,1998 12:06:38 sptclg3.gdp

Pawtuxet River
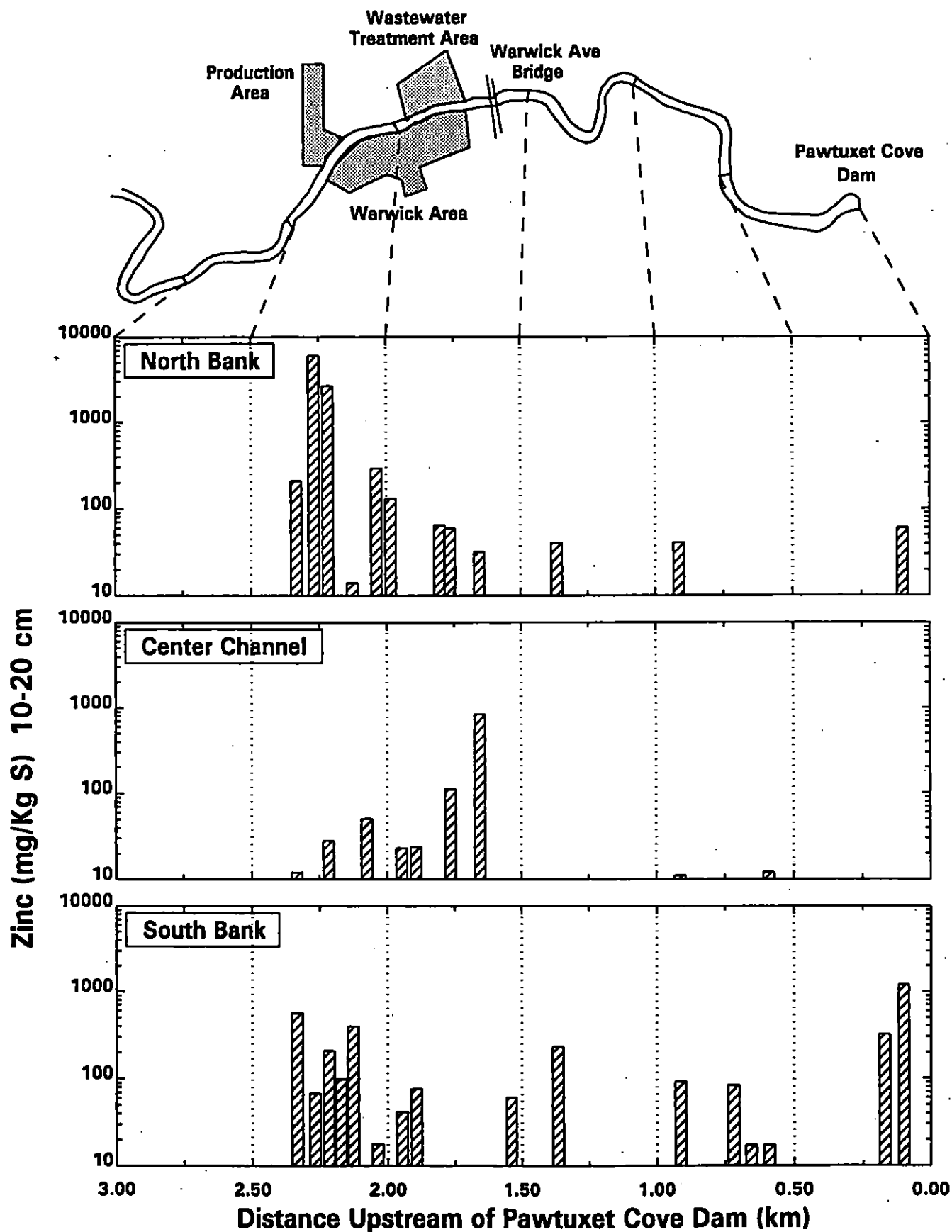
10-20 cm Sediment & Unqualified and Estimated Values (No U values)

Tue Jul 11,1995 12:06:48 sptclg3.gdp

APPENDIX C

TABULATION OF DATA

WATER COLUMN DATA

Date	Station	TOC mg/l	TSS mg/l	VSS mg/l	Tinuvin 328 ug/l	Toluene ug/l	Chlorobenzene ug/l	Naphthalene ug/l	PCB ng/l	Total Zinc ug/l	Total Silver ug/L
05/06/92	rwc-1	5.4	5		10 u	3	2	2 u	11.u	19.8	.19
05/06/92	rwc-2	6.4	4		10 u	2	2 j	0.1 j	11.u	19.3	.51
05/06/92	rwc-3	7.9	6		10 u	0.4 j	1 j	0.2 j	11.u	35.2	.49
05/06/92	rwc-4	6.7	5		10 u	0.6 bj	2 j	0.3 j	11.u	21.2	.42
05/06/92	rwc-5	5.7	5		10 u	0.5 j	2 j	0.1 j	11.u	21.0	.33
05/06/92	rwc-6	6.8	4		10 u	0.6 j	1 j	2 u	11.u	18.4	.40
05/13/92	rwc-1	8.8	5		10 u	0.3 j	3 j	0.6 j			
05/13/92	rwc-2	8.9	6		10 u	4 j	2 j	0.7 j			
05/13/92	rwc-3		12		10 u	5 j	2 j	0.4 j			
05/13/92	rwc-4	9.0	4		10 u	0.5 j	2 j	0.6 j			
05/13/92	rwc-5	9.1	5		10 u	4 j	2 j	0.6 j			
05/13/92	rwc-6	7.4	5		10 u	0.6 j	1 j	10 u			
05/21/92	rwc-1	7.7	3		10 u	0.2 j	2	1 u	11.u	24.6	.20
05/21/92	rwc-2	9.6	6		10 u	0.4 j	2	1 u	11.u	33.0	.70
05/21/92	rwc-3	8.1	6		10 u	0.5 j	1	1 u	11.u	35.5	.40
05/21/92	rwc-4	8.5	4		10 u	0.4 j	2	1 u	11.u	21.1	.40
05/21/92	rwc-5	8.3	5		10 u	0.7 j	2	1 u	11.u	26.9	.30
05/21/92	rwc-6	8.1	4		10 u	0.2 j	3	1 u	11.u	28.3	.40
05/28/92	rwc-1	8.2	8		5 u	0.4 j	3	0.5 j	17.	22.3	.10
05/28/92	rwc-2	11.2	12		5 u	1 j	2	2	68.	33.9	.90
05/28/92	rwc-3	9.9	10		5 u	0.8 j	2	0.5 j	101.	24.3	.70
05/28/92	rwc-4	8.3	9		5 u	0.8 j	2	0.3 j	11.u	19.1	.50
05/28/92	rwc-5	8.8	10		5 u	0.7 j	2	1 u	39.	33.0	1.10
05/28/92	rwc-6	10.7	8		5 u	0.9 j	2	0.4 j	11.u	23.6	.50
06/04/92	rwc-1	9.6	6		5 u	0.4 j	2	0.3 j	11.u	23.8	.20
06/04/92	rwc-2	10.1	7		5 u	0.8 j	1	0.3 j	11.u	27.8	.60
06/04/92	rwc-3	8.4	9		5 u	1 j	0.9 j	1 u	11.u	27.3	.50
06/04/92	rwc-4	8.5	9		5 u	0.7 j	1	1 u	11.u	22.8	.40
06/04/92	rwc-5	7.5	8		5 u	0.8 j	1	1 u	13.	25.2	.40
06/04/92	rwc-6	8.0	5		5 u	0.6 j	1 j	0.2 j	11.	25.9	.40
06/10/92	rwc-1	6.4	8		5 u	4	1 j	0.3 j	11.u	26.7	.10u
06/10/92	rwc-2	8.0	12		5 u	3	0.6 j	0.2 j	11.u	25.6	.10
06/10/92	rwc-3	6.5	12		5 u	3	0.5 j	0.1 j	11.u	25.9	.10
06/10/92	rwc-4	6.4	14		5 u	2 b	0.8 j	0.2 j	11.u	26.2	.10
06/10/92	rwc-5	6.6	16		5 u	0.8 j	0.7 j	0.2 j	11.u	37.9	.10
06/10/92	rwc-6	6.9	10		5 u	4 b	0.7 j	1 u	11.u	26.4	.20
06/18/92	rwc-1	7.3	3		5 u	0.8 j	1	0.2 j	11.u	16.5	.10
06/18/92	rwc-2	8.7	6		5 u	0.6 j	0.7 j	0.2 j	11.u	18.7	.45
06/18/92	rwc-3	7.8	7		5 u	0.8 j	0.5 j	1 u	11.u	16.1	.28
06/18/92	rwc-4	7.8	6		5 u	0.5 j	1 j	1 u	11.u	14.3	.25
06/18/92	rwc-5	7.6	6		5 u	0.8 j	0.8 j	1 u	11.u	16.2	.24
06/18/92	rwc-6	8.2	5		5 u	0.5 j	0.8 j	1 u	11.u	19.3	.41
06/24/92	rwc-1	7.2	2		5 u	0.7 j	1	1 u	11.u	18.2	.20
06/24/92	rwc-2	8.4	5		5 u	0.9 j	0.9 j	0.4 j	11.u	24.9	.50
06/24/92	rwc-3	8.1	6		5 u	0.6 j	0.7 j	0.3 j	11.u	20.9	.30
06/24/92	rwc-4	7.6	6		5 u	0.7 j	1	0.3 j	11.u	19.1	.30
06/24/92	rwc-5	8.2	5		5 u	0.7 j	1	0.3 j	11.u	20.5	.30
06/24/92	rwc-6	9.2	4		5 u	0.5 j	0.9 j	0.3 j	11.u	17.7	.40

Date	Station	TOC mg/l	TSS mg/l	VSS mg/l	Tinuvin 328 ug/l	Toluene ug/l	Chlorobenzene ug/l	Naphthalene ug/l	PCB ng/l	Total Zinc ug/l	Total Silver ug/L
07/01/92	rwc-1	7.6	2		5 u	4	0.8 j	1 u	11.u	16.5	.10
07/01/92	rwc-2	7.9	6		5 u	4	0.5 j	1 u	11.u	23.4	.20
07/01/92	rwc-3	7.5	4		5 u	4	0.3 j	1 u	11.u	15.2	.20
07/01/92	rwc-4	7.7	3		5 u	2	0.6 j	1 u	11.u	13.2	.20
07/01/92	rwc-5	7.7	4		5 u	0.4 j	0.4 j	1 u	11.u	14.2	.30
07/01/92	rwc-6	7.9	4		5 u	0.2 j	0.4 j	1 u	11.u	13.2	.30
07/08/92	rwc-1	6.6	2		5 u	1	1 j	0.2 j	11.u	18.6	.22
07/08/92	rwc-2	8.5	4		5 u	1 u	0.5 j	1 u	11.u	19.2	.49
07/08/92	rwc-3	7.8	4		5 u	0.3 j	0.3 j	1 u	11.u	18.1	.39
07/08/92	rwc-4	7.4	4		5 u	0.3 j	0.5 j	1 u	11.u	15.2	.30
07/08/92	rwc-5	7.6	3		5 u	0.3 j	0.5 j	1 u	11.u	15.0	.55
07/08/92	rwc-6	8.4	4		5 u	0.4 j	0.5 j	1 u	11.u	16.0	.40
07/15/92	rwc-1	8.8	4		5 u	1 u	1 u	1 u	11.u		
07/15/92	rwc-2	10.1	8		5 u	1 u	1 u	1 u	11.u		
07/15/92	rwc-3	8.7	5		5 u	1 u	1 u	1 u	11.u		
07/15/92	rwc-4	8.4	5		5 u	1 u	1 u	1 u	11.u		
07/15/92	rwc-5	9.0	6		5 u	1 u	1 u	1 u	11.u		
07/15/92	rwc-6	8.3	6		5 u	1 u	1 u	1 u	11.u		
07/22/92	rwc-1	7.4	2		5 u	1 u	0.9 j	1 u	11.u		
07/22/92	rwc-2	9.8	6		5 u	1 u	1 u	1 u	11.u	20.5	.86
07/22/92	rwc-3	9.2	3		5 u	1 u	1 u	1 u	11.u	16.3	.55
07/22/92	rwc-4	8.2	3		5 u	1 u	1 u	1 u	11.u	25.5	.71
07/22/92	rwc-5	8.6	2		5 u	1 u	1 u	1 u	11.u	24.2	.70
07/22/92	rwc-6	8.9	3		5 u	1 u	1 u	1 u	11.u	13.8	.58
05/05/94	rwc-1		5.1	2.9	1.2 u	5 u	5 u	5 u	11.1u	38.0	.15u
05/05/94	rwc-3		14.4	5.4	1.2 u	5 u	5 u	5 u	11.7u	41.0	.20
05/05/94	rwc-6		14.4	5.5	1.2 u	5 u	5 u	5 u	11.1u	42.0	.15u
05/12/94	rwc-1		2.3	1.6	1.2 u	5 u	5 u	5 u	11.3u	62.0	.15u
05/12/94	rwc-3		8.5	3.3	1.2 u	5 u	5 u	5 u	11.1u	29.0	.15u
05/12/94	rwc-6		4.3	2.3	1.2 u	5 u	5 u	5 u	11.1u	33.0	.15u
05/19/94	rwc-1		3.1	1.8	1.2 u	5 u	5 u	5 u	11.2u	25.0	.15u
05/19/94	rwc-3		9.4	4.1	1.2 u	5 u	5 u	5 u	11.5u	24.0	.15u
05/19/94	rwc-6		4.4	2.4	1.2 u	5 u	5 u	5 w	11.3u	65.0	.15u
05/26/94	rwc-1		2.0	1.4	1.2 u	5 u	5 u	5 u	11.1u	41.0	.15u
05/26/94	rwc-3		7.3	3.4	1.2 u	5 u	5 u	5 u	11.2u	44.0	.15u
05/26/94	rwc-6		3.4	2.2	1.2 u	5 u	5 u	5 w	11.2u	24.0	.15u
07/08/92	dup-4		4		5 u	0.4 j	0.5 j	1 u			

Station	Mid Depth cm	Northing ft	Easting ft	% Solids	TOC mg/Kg	AVS mg/Kg	Copper mg/Kg	Zinc mg/Kg	Tinuvin ug/Kg	Chlorobenzene ug/Kg	Toluene ug/Kg	Naphthalene ug/Kg	Page 1
SD-DS-1(0-5)*RM	2.5	247950.3	529479.4	44	56000	100	150 J	1500 J	2200				
SD-DS-1(5-10)*RM	7.5	247950.3	529479.4	48	48000	750	110 J	1900 J	2100				
SD-DS-1(10-20)*RM	15.0	247950.3	529479.4	46	62000	1200	48 J	1200 J	270 U				
SD-DS-2(0-5)*RM	2.5	248088.1	529485.9	42	29000	690	44 J	140 J	3200				
SD-DUP2(0-5)*RM	2.5	248088.1	529485.9	52	34000	430	37 J	130 J	880				
SD-DS-2(5-10)*RM	7.5	248088.1	529485.9	53	25000	450	25 J	100 J	3000				
SD-DS-2(10-20)*RM	15.0	248088.1	529485.9	63	12000	230	13 J	60 J	3500				
SD-DS-3(0-5)*RM	2.5	247889.1	529233.8	35	61000	960	70 J	260 J	7000				
SD-DS-3(5-10)*RM	7.5	247889.1	529233.8	36	67000	1200	55 J	410 J	4000				
SD-DS-3(10-20)*RM	15.0	247889.1	529233.8	49	32000	690	22 J	320 J	3100				
SD-DS-4(0-5)*RM	2.5	248700.2	528304.4	78	10000	13 U	24	56 J	530				
SD-DS-4(5-10)*RM	7.5	248700.2	528304.4	81	1600	13 U	9.2	20 J	430				
SD-DS-4(10-20)*RM	15.0	248700.2	528304.4	84	1600	11 U	9.1	17 J	440				
SD-DS-5(0-5)*RM	2.5	248701.2	528350.2	88	2100	12 U	6.6	12 J	1300				
SD-DS-5(5-10)*RM	7.5	248701.2	528350.2	89	660	11 U	5.3	10 J	110				
SD-DS-5(10-20)*RM	15.0	248701.2	528350.2	89	720	11 U	5.4	12 J	430				
SD-DS-6(0-5)*RM	2.5	248875.6	528313.5	77	3600	12 U	13	23 J	340				
SD-DUP1(0-5)*RM	2.5	248875.6	528313.5	77	4600	15	14	25 J	500				
SD-DS-6(5-10)*RM	7.5	248875.6	528313.5	85	2200	12 U	9.1	18 J	380				
SD-DS-6(10-20)*RM	15.0	248875.6	528313.5	91	1100	11 U	6.8	17 J	118				
SD-DS-7(0-5)*RM	2.5	249037.3	528264.1	49	33000	170	43	140 J	670				
SD-DS-7(5-10)*RM	7.5	249037.3	528264.1	79	8400	110	14	47 J	360				
SD-DS-7(10-20)*RM	15.0	249037.3	528264.1	77	11000	92	19	84 J	1700				
SD-DS-8(0-5)*RM	2.5	249345.2	527690.9	68	28000	85	82	190 J	320				
SD-DS-8(5-10)*RM	7.5	249345.2	527690.9	67	23000	17	63	180 J	93 U				
SD-DS-8(10-20)*RM	15.0	249345.2	527690.9	62	23000	42	24	92 J	100 U				
SD-DS-9(0-5)*RM	2.5	249318.1	527679.5	85	2300	12 U	8.3 J	31 J	470				
SD-DS-9(5-10)*RM	7.5	249318.1	527679.5	90	830	11 U	5.6 J	11 J	370				
SD-DS-9(10-20)*RM	15.0	249318.1	527679.5	91	560	11 U	5.1 J	11 J	160				
SD-DS-10(0-5)*RM	2.5	249288.4	527657.7	71	16000	16 U	28	88 J	350				
SD-DS-10(5-10)*RM	7.5	249288.4	527657.7	75	16000	15 U	40	150 J	470				
SD-DS-10(10-20)*RM	15.0	249288.4	527657.7	81	7400	39	17	41 J	1500				
SD-DS-11(0-5)*RM	2.5	248995.9	526721.3	69	18000	380	31 J	180 J	2300	850 J	490 J	400 J	
SD-DS-11(5-10)*RM	7.5	248995.9	526721.3	64	18000	170	59 J	240 J	4900	1200	1300	400 J	
SD-DS-11(10-20)*RM	15.0	248995.9	526721.3	72	18000	100	36 J	230 J	740	1800	550 J	1000	
SD-DS-12(0-5)*RM	2.5	248925.8	526673.4	68	21000	260	28 J	95 J	320				
SD-DS-12(5-10)*RM	7.5	248925.8	526673.4	78	13000	200	14 J	56 J	730				
SD-DS-12(10-20)*RM	15.0	248925.8	526673.4	78	14000	130	9 J	41 J	620				

SEDIMENT DATA

Station	Mid Depth cm	Northing ft	Easting ft	% Solids	TOC mg/Kg	AVS mg/Kg	Copper mg/Kg	Zinc mg/Kg	Tinuvin ug/Kg	Chlorobenzene ug/Kg	Toluene ug/Kg	Naphthalene ug/Kg
SD-DS-13(0-5)*RM	2.5	249319.8	526307.4	67	9500	72	:12	48 J	94 U			
SD-DS-13(5-10)*RM	7.5	249319.8	526307.4	65	10000	100	14	61 J	630			
SD-DS-13(10-20)*RM	15.0	249319.8	526307.4	62	21000	140	33	130 J	2400			
SD-DS-14(0-5)*RM	2.5	249345.2	525919.9	79	3800	34	12	38 J	650			
SD-DS-14(5-10)*RM	7.5	249345.2	525919.9	81	5000	92	10	30 J	3200			
SD-DS-14(10-20)*RM	15.0	249345.2	525919.9	87	2600	12 U	9.9	23 J	920			
SD-DS-15(0-5)*RM	2.5	249395.6	525912.9	74	4100	13 U	11	27 J	330			
SD-DS-DUP3(0-5)*RM	2.5	249395.6	525912.9	83	4000	13 U	9.1	28 J	270			
SD-DS-15(5-10)*RM	7.5	249395.6	525912.9	88	1200	12 U	7.1	18 J	440			
SD-DS-15(10-20)*RM	15.0	249395.6	525912.9	93	1000	11 U	5	24 J	68 U			
SD-F-1(0-5)*RM	2.5	249249.5	525600.6	61	21000	360	61 J	880	1000 U	950 J	540 J	560 J
SD-F-1(5-10)*RM	7.5	249249.5	525600.6	73	16000	300	54 J	790	870 U	1000	2100	550 J
SD-F-1(10-20)*RM	15.0	249249.5	525600.6	84	8000	54	21 J	110	750 U	520 J	300 J	190 J
SD-F-2(0-5)*RM	2.5	249284.7	525592.8	79	3700	19	20	52 J	660	2.5 J	6.4 U	2.8 J
SD-F-2(5-10)*RM	7.5	249284.7	525592.8	82	1300	21	13	19 J	77 U	2.2 J	6.1 U	.80 J
SD-F-2(10-20)*RM	15.0	249284.7	525592.8	87	1200	12 U	7.3	18 J	73 U	2.6 J	5.8 U	.82 J
SD-F-3(0-5)*RM	2.5	249331.9	525586.4	71	16000	130	29	170 J	4300	150	15 J	16 J
SD-F-3(5-10)*RM	7.5	249331.9	525586.4	69	16000	160	45	230 J	3800	1100	910 U	1100
SD-F-3(10-20)*RM	15.0	249331.9	525586.4	62	28000	640	63	470 J	3600	780 J	1000 U	290 J
SD-F-4(0-5)*RM	2.5	249301.2	525444.9	64	42000	600	55 J	210	12000	14	8.9	1.9 J
SD-F-4(5-10)*RM	7.5	249301.2	525444.9	48	22000	440	40 J	170	27000	510	40 J	16 J
SD-F-4(10-20)*RM	15.0	249301.2	525444.9	63	27000	210	24 J	400	1800	1800 J	680	920 J
SD-F-5(0-5)*RM	2.5	249204.1	525161.0	75	16000	210	15 J	52	160	0.5 J	6.2 U	0.8 J
SD-F-5(5-10)*RM	7.5	249204.1	525161.0	70	8500	150	9.9 J	36	750	6.8 U	6.8 U	6.8 U
SD-F-5(10-20)*RM	15.0	249204.1	525161.0	86	2600	12 U	4.7 J	14	250	5.3 U	5.3 U	5.3 U
SD-F-6(0-5)*RM	2.5	249186.3	525156.4	87	2300	13 U	7.6 J	18	73 U	5.8 U	5.8 U	5.8 U
SD-F-6(5-10)*RM	7.5	249186.3	525156.4	91	690	11 U	3.5 J	8.2	70 U	5.7 U	5.7 U	5.7 U
SD-F-6(10-20)*RM	15.0	249186.3	525156.4	89	440	11 U	1.6 J	3.6	71 U	5.8 U	5.8 U	5.8 U
SD-F-7(0-5)*RM	2.5	249148.3	525003.4	57	22000	270	37 J	110	1000	2.4 J	8.3 J	8.4 U
SD-F-7(5-10)*RM	7.5	249148.3	525003.4	78	9800	32	17 J	68	670	6.2 U	1.3 J	6.2 U
SD-F-7(10-20)*RM	15.0	249148.3	525003.4	80	13000	19	18 J	69	1200	6.1 U	0.85 J	6.1 U
SD-F-8(0-5)*RM	2.5	249129.7	525010.9	85	5200	13 U	7.8 J	20 J	3400	2 J	6 U	6 U
SD-F-8(5-10)*RM	7.5	249129.7	525010.9	89	1000	11 U	2.6 J	6.4 J	71 U	5.9 U	5.9 U	5.9 U
SD-F-8(10-20)*RM	15.0	249129.7	525010.9	90	450	11 U	0.84 J	2.5 J	70 U	5.8 U	5.8 U	5.8 U
SD-F-9(0-5)*RM	2.5	249134.1	524842.6	53	28000	410	22 J	97	700	2.2 J	6.4 J	8.6 U
SD-DUP4(0-5)*RM	2.5	249134.1	524842.6	39	20000	16	18 J	76	3400	12 U	8.1 J	12 U
SD-F-9(5-10)*RM	7.5	249134.1	524842.6	81	4100	13 U	9.1 J	34	920	4 J	13	1.4 J
SD-F-9(10-20)*RM	15.0	249134.1	524842.6	75	12000	85	6.7 J	48	76000	7900	1500	2600

SEDIMENT DATA

Station	Mid Depth cm	Northing ft	Easting ft	% Solids	TOC mg/Kg	AVS mg/Kg	Copper mg/Kg	Zinc mg/Kg	Tinuvin ug/Kg	Chlorobenzene ug/Kg	Toluene ug/Kg	Naphthalene ug/Kg
SD-P-10(0-5)*RM	2.5	248993.6	524735.5	53	32000	22 U	45 J	210 J	120 U	9.3 U	9.3 U	9.3 U
SD-P-10(5-10)*RM	7.5	248993.6	524735.5	61	17000	800	14 J	92 J	340	13	21	8 U
SD-P-10(10-20)*RM	15.0	248993.6	524735.5	60	26000	490	38 J	320 J	410	28	6.6 J	8.6 U
SD-P-11(0-5)*RM	2.5	249082.2	524713.1	22	120000	1000	130 J	420 J	1200	24	130	3.7 J
SD-P-11(5-10)*RM	7.5	249082.2	524713.1	79	8000	130	8.8 J	54 J	340	0.96 J	2.1 J	6 U
SD-P-11(10-20)*RM	15.0	249082.2	524713.1	87	3600	44	5.8 J	42 J	210	5.5 U	5.5 U	5.5 U
SD-P-12(0-5)*RM	2.5	249068.2	524714.6	71	51000	840	64 J	190 J	420	4.1 J	78	6.5 U
SD-P-12(5-10)*RM	7.5	249068.2	524714.6	59	21000	410	27 J	110 J	1700	4.1 J	20	7.9 U
SD-P-12(10-20)*RM	15.0	249068.2	524714.6	82	4200	54	8.8 J	35 J	690	5.8 U	0.54 J	5.8 U
SD-P-13(0-5)*RM	2.5	248996.0	524569.5	79	4900	46	10	40	520	12 J	4.1 J	4.8 J
SD-P-13(5-10)*RM	7.5	248996.0	524569.5	85	2900	24	9.3	25	3000	6.6 J	21 J	8 J
SD-P-13(10-20)*RM	15.0	248996.0	524569.5	90	2300	11 U	7.8	51	31000	9.7 J	7.9 J	12 J
SD-P-14(0-5)*RM	2.5	248939.3	524426.8	74	11000	150	16 J	63 J	360	19	2 J	21
SD-P-14(5-10)*RM	7.5	248939.3	524426.8	59	20000	74	13 J	150 J	1400	7.2 J	1.1 J	85
SD-P-14(10-20)*RM	15.0	248939.3	524426.8	73	23000	270	47 J	300 J	1400	3.5 J	1.5 J	55
SD-P-15(0-5)*RM	2.5	249015.3	524409.9	44	52000	960	57 J	430 J	280 J	23	11 U	8.1 J
SD-DUP5*RM	2.5	249015.3	524409.9	36	94000	2200	98 J	530 J	2400 U	26 J	80 J	43 J
SD-P-15(5-10)*RM	7.5	249015.3	524409.9	53	26000	900	14 J	220 J	1200 U	120	26 J	60 J
SD-P-15(10-20)*RM	15.0	249015.3	524409.9	67	40000	670	36 J	300 J	800 J	630	16 J	470
SD-P-16(0-5)*RM	2.5	248895.2	524291.8	77	11000	19	15	44	2200 U	6.9 U	6.9 U	40
SD-P-16(5-10)*RM	7.5	248895.2	524291.8	64	15000	55	27	64	2700 U	8.4 U	8.4 U	18
SD-P-16(10-20)*RM	15.0	248895.2	524291.8	64	19000	39	19	100	2700 U	8.3 U	1.7 J	31
SD-P-17(0-5)*RM	2.5	248823.9	524173.2	50	13000	360	18	40	43000	6.5 U	6.5 U	6.5 U
SD-DUP6*RM	2.5	248823.9	524173.2	80	12000	130	18	58	540 U	49 U	10 J	68
SD-P-17(5-10)*RM	7.5	248823.9	524173.2	85	5300	38	13	45	220	39 U	39 U	2.7 J
SD-P-17(10-20)*RM	15.0	248823.9	524173.2	74	13000	18	39	210	1200 U	17 J	3.8 J	6.4 J
SD-P-18(0-5)*RM	2.5	248856.6	524151.5	5500	85	13	39					
SD-P-18(5-10)*RM	7.5	248856.6	524151.5	84	2900	130	7.6	30	75	12	6.5 U	6.5 U
SD-P-18(10-20)*RM	15.0	248856.6	524151.5	88	1800	13	5.3	28	72 U	6 U	6 U	6 U
SD-P-19(0-5)*RM	2.5	248902.1	524115.0	81	2200	18	9.7	51	2100	160	34 U	34 U
SD-P-19(5-10)*RM	7.5	248902.1	524115.0	87	1100	12 U	6.1	26	200 U	6400	890	220
SD-P-19(10-20)*RM	15.0	248902.1	524115.0	90	770	11 U	6.4	22	1100	200	30 J	48 U
SD-P-20(0-5)*RM	2.5	248885.7	524124.0	63	63000	190	48	2300	960000	3900000	4000000	185000
SD-P-20(5-10)*RM	7.5	248885.7	524124.0	74	49000	410	35	2800	660000	3400000	3600000	148000
SD-P-20(10-20)*RM	15.0	248885.7	524124.0	59	85000	160	67	5300	1100000	4600000	4200000	159000
SD-P-21(0-5)*RM	2.5	248768.2	523988.1	50	42000	1800	34	170 B	250	12 J	13 U	13 U
SD-DUP7*RM	2.5	248768.2	523988.1	42	39000	1000	30	150 B	150 U	770	270	44 U
SD-P-21(5-10)*RM	7.5	248768.2	523988.1	50	23000	1200	22	140 B	270	13 U	13 U	13 U

Station	Mid Depth cm	Northing ft	Easting ft	% Solids	TOC mg/Kg	AVS mg/Kg	Copper mg/Kg	Zinc mg/Kg	Tinuvin ug/Kg	Chlorobenzene ug/Kg	Toluene ug/Kg	Naphthalene ug/Kg	Page 4
SD-F-21(10-20)*RM	15.0	248768.2	523988.1	76	8900	170	23	68 B	130	6.4 U	6.4 U	6.4 U	
SD-F-22(0-5)*RM	2.5	248737.3	524031.4	75	9500	230	17	52 B	84 U	7.8 U	3 J	1.6 J	
SD-F-22(5-10)*RM	7.5	248737.3	524031.4	78	7300	200	8.8	31 B	81 U	8 U	1.6 J	8 U	
SD-F-22(10-20)*RM	15.0	248737.3	524031.4	88	840	11 U	6.4	9.5 B	72 U	5.7 U	5.7 U	5.7 U	
SD-F-23(0-5)*RM	2.5	248758.6	524000.9	41	38000	1000	140	11000 B	3000	17000	130	890	
SD-F-23(5-10)*RM	7.5	248758.6	524000.9	46	55000	1700	140	15000 B	1900 U	39000	500	2400	
SD-F-23(10-20)*RM	15.0	248758.6	524000.9	56	43000	580	59	5400 B	1400 J	54000	210	1400	
SD-F-24(0-5)*RM	2.5	248700.2	524061.1	45	41000	1000	130	7100 B	1400 U	330000	7100	1385	
SD-F-24(5-10)*RM	7.5	248700.2	524061.1	51	45000	230	95	3300 B	11000	480000	15000	420	
SD-F-24(10-20)*RM	15.0	248700.2	524061.1	51	54000	670	230	6600 B	15000	1200000	33000	2200	
SD-F-25(0-5)*RM	2.5	248507.5	523940.9	60	20000	210	44	140 B	110 U	0.75 J	8.3 U	1.3 J	
SD-F-25(5-10)*RM	7.5	248507.5	523940.9	65	37000	350	110	350 B	190 U	0.61 J	0.33 J	4.1 J	
SD-F-25(10-20)*RM	15.0	248507.5	523940.9	59	31000	260	100	570 B	210 U	5.6 J	8.4 U	4.4 J	
SD-F-26(0-5)*RM	2.5	248541.7	523906.0	87	1700	12 U	9	13 B	73 U	150	1.4 J	6.4 J	
SD-F-26(5-10)*RM	7.5	248541.7	523906.0	87	550	11 U	6.9	8.2 B	73 U	8	5.4 U	0.66 J	
SD-F-26(10-20)*RM	15.0	248541.7	523906.0	88	1000	23	11	12 B	65 J	2.7 J	0.97 J	5 U	
SD-F-27(0-5)*RM	2.5	248568.8	523863.9	56	21000	130	130	300 B	1100 U	3000	170	300	
SD-DUP8*RM	2.5	248568.8	523863.9	61	31000	560	95	240	1400 U	930	360	130	
SD-F-27(5-10)*RM	7.5	248568.8	523863.9	66	24000	670	98	320	960 U	510	99	180	
SD-F-27(10-20)*RM	15.0	248568.8	523863.9	63	19000	340	44	210	100 U	1700	520	300	
SD-US-1(0-5)*RM	2.5	247217.1	522075.3	52	34000	390	53	130	130 J				
SD-US-1(5-10)*RM	7.5	247217.1	522075.3	54	20000	53	48	76	230				
SD-US-1(10-20)*RM	15.0	247217.1	522075.3	75	13000	13 U	21	61	190				
SD-US-2(0-5)*RM	2.5	247252.8	522061.9	67	21000	210	32	98	61 J				
SD-US-2(5-10)*RM	7.5	247252.8	522061.9	78	7000	18	16	38	110				
SD-US-2(10-20)*RM	15.0	247252.8	522061.9	87	2100	11 U	7.2	32	99 U				
SD-US-3(0-5)*RM	2.5	243098.9	515135.3	85	13000	220	20	74	160				
SD-US-3(5-10)*RM	7.5	243098.9	515135.3	75	19000	37	45	250	670				
SD-US-3(10-20)*RM	15.0	243098.9	515135.3	61	32000	360	30	840	130 J				
SD-US-4(0-5)*RM	2.5	244613.2	515974.5	84	3300	12 U	17	29	76 J				
SD-US-4(5-10)*RM	7.5	244613.2	515974.5	82	2100	12 U	14	23	78 U				
SD-US-4(10-20)*RM	15.0	244613.2	515974.5	80	5000	51	59	60	80 U				
SD-US-5(0-5)*RM	2.5	245834.3	516187.5	70	13000	330	31	86	62 J				
SD-US-5(5-10)*RM	7.5	245834.3	516187.5	73	23000	200	31	110	860 U				
SD-US-5(10-20)*RM	15.0	245834.3	516187.5	65	13000	20	16	110	970				
SD-US-6(0-5)*RM	2.5	245803.8	516212.1	81	17000	16	250	38	78 U				
SD-US-6(5-10)*RM	7.5	245803.8	516212.1	87	5000	12 U	1100	32	75 U				
SD-US-6(10-20)*RM	15.0	245803.8	516212.1	84	5000	12 U	150	9.3	75 U				

SEDIMENT DATA

Station	Mid Depth cm	Northing ft	Easting ft	% Solids	TOC mg/Kg	AVS mg/Kg	Copper mg/Kg	Zinc mg/Kg	Tinuvin ug/Kg	Chlorobenzene ug/Kg	Toluene ug/Kg	Naphthalene ug/Kg	Page 5
SD-US-7(0-5)*RM	2.5	247233.1	519983.5	52	42000	640	38	120	190				
SD-DUP9*RM	2.5	247233.1	519983.5	63	13000	15 U	15	46	140 U				
SD-US-7(5-10)*RM	7.5	247233.1	519983.5	69	20000	250	20	63	190				
SD-US-7(10-20)*RM	15.0	247233.1	519983.5	73	26000	52	23	65	290				
SD-US-8(0-5)*RM	2.5	244460.0	516120.0	71	9900	230	20	59	120 U				
SD-US-8(5-10)*RM	7.5	244460.0	516120.0	74	12000	75	25	71	260				
SD-US-8(10-20)*RM	15.0	244460.0	516120.0	74	15000	160	21	77	120 U				
SD-US-9(0-5)*RM	2.5	243150.0	515450.0	61	17000	240	28	76	140 U				
SD-US-9(5-10)*RM	7.5	243150.0	515450.0	78	9800	120	18	42	110 U				
SD-US-9(10-20)*RM	15.0	243150.0	515450.0	78	4600	13 U	20	42	110 U				

SEDIMENT PCB DATA

Depth	Station ID	Total PCBs mg/kg	Mono wt %	Di wt %	Tri wt %	Tetra wt %	Penta wt %	Hexa wt %	Hepta wt %	Octa wt %	Nona wt %	Deca wt %
2.5	SD-DS-1(0-5)*RM	8.20	0.00	3.10	19.47	47.05	17.72	8.97	3.05	0.64	0.00	0.00
7.5	SD-DS-1(5-10)*RM	16.50	0.00	2.18	20.42	49.44	17.52	7.92	2.05	0.47	0.00	0.00
15.0	SD-DS-1(10-20)*RM	19.22	0.00	1.54	20.05	46.99	18.55	9.03	2.93	0.91	0.00	0.00
2.5	SD-DS-2(0-5)*RM	0.41	0.00	3.62	21.94	31.64	20.74	12.44	7.39	2.23	0.00	0.00
2.5	SD-DUP2(0-5)*RM	0.29	0.00	4.03	17.55	35.81	19.03	13.38	8.86	1.34	0.00	0.00
7.5	SD-DS-2(5-10)*RM	0.39	0.00	6.15	18.84	30.57	17.58	14.45	9.37	3.04	0.00	0.00
15.0	SD-DS-2(10-20)*RM	0.22	0.00	7.78	21.96	33.47	18.62	12.60	4.41	1.15	0.00	0.00
2.5	SD-DS-3(0-5)*RM	0.75	0.00	10.50	18.25	28.39	18.29	15.11	7.77	1.69	0.00	0.00
7.5	SD-DS-3(5-10)*RM	4.64	0.00	4.20	23.59	40.95	18.29	9.03	3.30	0.63	0.00	0.00
15.0	SD-DS-3(10-20)*RM	6.03	0.00	2.04	19.86	46.91	18.44	8.87	2.94	0.93	0.00	0.00
2.5	SD-DS-4(0-5)*RM	0.18	0.00	3.54	15.06	27.87	24.69	19.71	6.95	2.17	0.00	0.00
7.5	SD-DS-4(5-10)*RM	0.12	0.00	5.27	18.88	34.32	18.82	13.55	6.26	2.90	0.00	0.00
15.0	SD-DS-4(10-20)*RM	0.04	0.00	7.01	17.30	32.57	21.35	14.82	4.94	2.01	0.00	0.00
2.5	SD-DS-5(0-5)*RM	0.08	0.00	11.63	15.46	32.88	19.64	11.75	6.60	2.04	0.00	0.00
7.5	SD-DS-5(5-10)*RM	0.05	0.00	11.84	29.52	29.90	14.30	8.92	3.76	1.76	0.00	0.00
15.0	SD-DS-5(10-20)*RM	0.10	0.00	4.21	7.99	23.85	34.70	23.00	4.96	1.29	0.00	0.00
2.5	SD-DS-6(0-5)*RM	0.13	0.00	6.92	13.59	31.94	21.58	17.95	5.98	2.04	0.00	0.00
2.5	SD-DUP1(0-5)*RM	0.36	0.00	2.62	28.78	41.93	12.79	7.79	4.47	1.62	0.00	0.00
7.5	SD-DS-6(5-10)*RM	0.15	0.00	3.14	7.85	21.91	33.59	27.32	5.22	0.97	0.00	0.00
15.0	SD-DS-6(10-20)*RM	0.06	0.00	7.02	16.17	33.44	22.13	14.72	4.62	1.91	0.00	0.00
2.5	SD-DS-7(0-5)*RM	0.41	0.00	1.83	10.71	32.97	21.85	18.55	10.81	3.28	0.00	0.00
7.5	SD-DS-7(5-10)*RM	0.17	0.00	3.08	13.37	26.36	21.15	18.36	13.61	4.08	0.00	0.00
15.0	SD-DS-7(10-20)*RM	0.64	0.00	2.79	19.93	34.07	15.99	17.41	7.90	1.90	0.00	0.00
2.5	SD-DS-8(0-5)*RM	0.66	0.00	2.98	15.93	32.84	22.07	16.77	7.07	2.33	0.00	0.00
7.5	SD-DS-8(5-10)*RM	0.59	0.00	2.20	13.08	27.96	25.14	21.59	7.20	2.82	0.00	0.00
15.0	SD-DS-8(10-20)*RM	0.08	0.00	4.98	16.12	34.66	22.34	12.06	2.25	7.60	0.00	0.00
2.5	SD-DS-9(0-5)*RM	0.17	0.00	4.99	21.03	36.52	19.15	11.42	5.26	1.63	0.00	0.00
7.5	SD-DS-9(5-10)*RM	0.04	0.00	7.85	23.72	34.14	19.53	11.23	3.53	0.00	0.00	0.00
15.0	SD-DS-9(10-20)*RM	0.03	0.00	6.77	26.73	40.31	16.26	8.73	1.20	0.00	0.00	0.00
2.5	SD-DS-10(0-5)*RM	0.15	0.00	3.57	13.77	38.15	23.94	11.81	5.32	3.44	0.00	0.00
7.5	SD-DS-10(5-10)*RM	0.21	0.00	3.22	13.15	29.40	27.63	14.55	8.44	3.62	0.00	0.00
15.0	SD-DS-10(10-20)*RM	0.17	0.00	6.61	19.86	27.15	22.70	14.17	6.38	3.12	0.00	0.00
2.5	SD-DS-11(0-5)*RM	2.33	0.00	1.97	20.09	45.86	17.90	9.53	3.55	1.10	0.00	0.00
7.5	SD-DS-11(5-10)*RM	2.06	0.00	4.94	19.49	35.08	18.66	13.11	6.55	2.15	0.00	0.00
15.0	SD-DS-11(10-20)*RM	1.71	0.00	2.25	18.38	34.59	19.05	14.27	7.71	3.76	0.00	0.00
2.5	SD-DS-12(0-5)*RM	0.19	0.00	1.99	16.26	33.90	20.02	13.99	10.53	3.30	0.00	0.00
7.5	SD-DS-12(5-10)*RM	1.18	0.00	0.26	2.64	21.99	38.77	28.91	6.64	0.79	0.00	0.00

Depth	Station ID	Total PCBn mg/kg	Mono wt %	Di wt %	Tri wt %	Tetra wt %	Penta wt %	Hexa wt %	Hepta wt %	Octa wt %	Nona wt %	Deca wt % Page 2
15.0	SD-DS-12(10-20)*RM	0.18	0.00	3.87	13.71	31.61	23.55	19.82	6.15	1.30	0.00	0.00
2.5	SD-DS-13(0-5)*RM	0.17	0.00	2.22	13.72	28.72	24.99	21.38	7.39	1.59	0.00	0.00
7.5	SD-DS-13(5-10)*RM	0.52	0.00	2.32	12.33	26.55	22.93	20.31	12.63	2.93	0.00	0.00
15.0	SD-DS-13(10-20)*RM	1.44	0.00	1.41	11.13	34.42	20.76	17.21	11.55	2.87	0.64	0.00
2.5	SD-DS-14(0-5)*RM	0.43	0.00	4.48	20.68	43.47	19.27	9.01	2.34	0.74	0.00	0.00
7.5	SD-DS-14(5-10)*RM	0.19	0.00	2.73	13.75	40.04	22.62	14.55	4.84	1.46	0.00	0.00
15.0	SD-DS-14(10-20)*RM	0.11	0.00	4.87	16.81	35.09	20.88	14.70	5.80	1.86	0.00	0.00
2.5	SD-DS-15(0-5)*RM	0.08	0.00	5.16	15.69	33.70	19.42	16.29	7.39	2.35	0.00	0.00
2.5	SD-DS-DUP3(0-5)*RM	0.09	0.00	6.98	18.23	34.31	20.14	12.89	5.43	2.02	0.00	0.00
7.5	SD-DS-15(5-10)*RM	0.04	0.00	6.06	19.27	35.65	20.88	12.20	3.35	2.60	0.00	0.00
15.0	SD-DS-15(10-20)*RM	0.05	0.00	12.48	21.82	32.40	15.73	8.87	2.89	5.81	0.00	0.00
2.5	SD-P-1(0-5)*RM	4.90	1.97	2.22	21.31	43.71	16.65	9.19	3.68	1.22	0.04	0.00
7.5	SD-P-1(5-10)*RM	9.27	0.73	1.83	21.15	50.31	15.93	7.23	2.16	0.67	0.00	0.00
15.0	SD-P-1(10-20)*RM	0.57	7.11	2.14	12.72	29.71	20.65	16.06	8.75	2.87	0.00	0.00
2.5	SD-P-2(0-5)*RM	0.20	0.00	10.46	17.97	32.41	14.74	11.41	7.39	5.61	0.00	0.00
7.5	SD-P-2(5-10)*RM	0.14	0.00	4.72	16.29	32.77	19.99	14.01	7.49	4.73	0.00	0.00
15.0	SD-P-2(10-20)*RM	0.14	0.00	4.68	18.33	30.29	13.92	11.25	13.41	8.13	0.00	0.00
2.5	SD-P-3(0-5)*RM	0.71	0.00	4.94	16.33	31.09	22.20	16.22	7.76	1.46	0.00	0.00
7.5	SD-P-3(5-10)*RM	1.22	0.00	2.95	19.65	34.66	18.23	14.76	7.87	1.87	0.00	0.00
15.0	SD-P-3(10-20)*RM	1.00	0.00	2.58	18.40	34.56	19.03	15.84	7.44	2.14	0.00	0.00
2.5	SD-P-4(0-5)*RM	0.53	3.62	5.27	17.83	28.03	20.47	14.07	8.14	2.57	0.00	0.00
7.5	SD-P-4(5-10)*RM	0.68	3.72	3.27	19.65	34.72	19.69	12.03	5.32	1.62	0.00	0.00
15.0	SD-P-4(10-20)*RM	2.52	7.26	3.61	20.91	34.37	14.77	11.11	6.08	1.91	0.00	0.00
2.5	SD-P-5(0-5)*RM	0.12	0.00	2.36	16.31	26.04	21.90	19.02	10.90	3.46	0.00	0.00
7.5	SD-P-5(5-10)*RM	0.08	0.00	2.81	19.61	26.14	21.93	18.66	8.48	2.37	0.00	0.00
15.0	SD-P-5(10-20)*RM	0.04	0.00	3.50	22.57	26.85	21.07	16.16	6.23	3.61	0.00	0.00
2.5	SD-P-6(0-5)*RM	0.06	0.00	8.07	20.09	29.85	18.77	15.32	6.02	1.88	0.00	0.00
7.5	SD-P-6(5-10)*RM	0.03	0.00	16.69	31.88	27.61	13.75	8.27	1.80	0.00	0.00	0.00
15.0	SD-P-6(10-20)*RM	0.02	0.00	12.65	21.56	31.91	19.36	12.36	2.16	0.00	0.00	0.00
2.5	SD-P-7(0-5)*RM	0.23	0.00	1.66	13.45	20.81	21.56	22.84	14.96	4.71	0.00	0.00
7.5	SD-P-7(5-10)*RM	0.15	0.00	5.17	15.15	21.80	25.16	20.88	8.70	3.14	0.00	0.00
15.0	SD-P-7(10-20)*RM	0.18	0.00	3.70	21.51	25.33	21.00	17.62	7.67	3.17	0.00	0.00
2.5	SD-P-8(0-5)*RM	0.06	0.00	2.86	9.04	23.52	21.51	22.71	8.05	12.30	0.00	0.00
7.5	SD-P-8(5-10)*RM	0.01	0.00	0.00	10.04	30.37	29.70	16.44	2.45	11.01	0.00	0.00
15.0	SD-P-8(10-20)*RM	0.01	0.00	0.00	51.27	29.75	16.13	2.86	0.00	0.00	0.00	0.00
2.5	SD-P-9(0-5)*RM	0.67	2.49	3.58	7.09	19.96	26.71	29.94	8.90	1.34	0.00	0.00
-99.0	SD-DUP4*RM	0.55	3.24	6.36	19.89	32.11	18.96	12.18	5.63	1.62	0.00	0.00

SEDIMENT PCB DATA

Depth	Station ID	Total PCBo mg/kg	Mono wt %	Di wt %	Tri wt %	Tetra wt %	Penta wt %	Hexa wt %	Hepta wt %	Octa wt %	Nona wt %	Deca wt % Page 3
7.5	SD-P-9(5-10)*RM	0.14	6.50	8.75	14.17	29.01	19.26	14.25	6.39	1.68	0.00	0.00
15.0	SD-P-9(10-20)*RM	8.71	39.41	37.37	8.08	7.22	4.51	2.51	0.71	0.19	0.00	0.00
2.5	SD-P-10(0-5)*RM	0.27	0.00	2.19	13.89	25.15	25.00	17.27	11.70	4.79	0.00	0.00
7.5	SD-P-10(5-10)*RM	0.36	0.00	1.46	9.58	21.36	24.32	23.15	8.78	11.35	0.00	0.00
15.0	SD-P-10(10-20)*RM	0.39	0.00	1.41	9.11	15.68	19.16	18.16	9.11	27.38	0.00	0.00
2.5	SD-P-11(0-5)*RM	0.93	0.93	2.20	11.38	30.65	24.09	17.84	9.74	3.17	0.00	0.00
7.5	SD-P-11-(5-10)*RM	0.16	0.87	5.28	17.97	32.78	19.52	13.83	7.50	2.25	0.00	0.00
15.0	SD-P-11(10-20)*RM	0.20	0.65	2.61	10.24	27.89	26.90	23.07	7.18	1.46	0.00	0.00
2.5	SD-P-12(0-5)*RM	1.24	0.52	1.52	11.54	29.84	25.16	21.87	7.48	2.07	0.00	0.00
7.5	SD-P-12(5-10)*RM	0.45	0.53	2.14	15.29	38.07	20.17	14.10	6.21	3.49	0.00	0.00
15.0	SD-P-12(10-20)*RM	0.24	1.59	4.01	13.36	32.65	22.42	16.82	6.29	2.86	0.00	0.00
2.5	SD-P-13(0-5)*RM	46.07	0.00	0.00	0.10	1.36	6.31	27.93	45.82	17.06	1.36	0.05
7.5	SD-P-13(5-10)*RM	0.53	5.45	7.59	13.37	27.73	17.27	13.64	9.95	3.91	0.80	0.29
15.0	SD-P-13(10-20)*RM	1.01	13.85	14.72	13.91	27.53	15.91	10.17	2.87	0.82	0.11	0.11
2.5	SD-P-14(0-5)*RM	0.16	2.21	7.11	13.13	21.46	24.01	18.02	7.39	6.67	0.00	0.00
7.5	SD-P-14(5-10)*RM	0.66	0.27	1.13	5.02	19.85	32.48	25.40	8.60	7.25	0.00	0.00
15.0	SD-P-14(10-20)*RM	1.09	0.16	0.40	2.41	16.80	36.89	31.86	8.78	2.70	0.00	0.00
2.5	SD-P-15(0-5)*RM	1.28	9.89	2.19	16.55	29.40	16.79	14.87	7.89	2.44	0.00	0.00
-99.0	SD-DUP5-*RM	4.61	5.89	1.79	20.22	41.82	14.27	9.87	4.75	1.40	0.00	0.00
7.5	SD-P-15(5-10)*RM	3.94	5.26	1.44	14.81	34.61	21.22	14.62	6.32	1.72	0.00	0.00
15.0	SD-P-15(10-20)*RM	1.14	16.03	2.31	12.68	29.16	19.49	12.30	6.16	1.88	0.00	0.00
2.5	SD-P-16(0-5)*RM	0.20	0.00	5.70	20.84	20.58	24.67	20.97	5.44	1.81	0.00	0.00
7.5	SD-P-16(5-10)*RM	1.93	0.00	0.35	1.40	19.70	39.02	31.58	6.64	0.81	0.49	0.00
15.0	SD-P-16(10-20)*RM	1.17	0.00	0.42	1.86	20.80	38.31	30.26	7.12	1.25	0.00	0.00
2.5	SD-P-17(0-5)*RM	0.13	0.00	3.81	10.32	19.41	24.37	25.17	11.93	5.00	0.00	0.00
-99.0	SD-DUP6*RM	0.27	0.00	3.76	12.53	33.17	27.08	14.79	6.47	2.20	0.00	0.00
7.5	SD-P-17(5-10)*RM	0.06	0.00	3.96	10.63	21.03	25.82	21.78	9.13	7.65	0.00	0.00
15.0	SD-P-17(10-20)*RM	0.29	0.00	1.93	7.35	15.71	22.69	25.92	9.36	17.04	0.00	0.00
2.5	SD-P-18(0-5)*RM	0.12	0.00	2.75	17.70	30.24	28.87	13.46	5.07	1.92	0.00	0.00
7.5	SD-P-18(5-10)*RM	0.13	0.00	3.16	28.00	32.16	19.42	11.51	4.25	1.50	0.00	0.00
15.0	SD-P-18(10-20)*RM	0.16	0.00	3.64	21.38	38.66	20.63	11.55	3.21	0.92	0.00	0.00
2.5	SD-P-19(0-5)*RM	0.15	0.00	6.01	29.32	35.65	16.19	7.43	3.97	1.44	0.00	0.00
7.5	SD-P-19(5-10)*RM	0.29	0.00	4.97	45.71	39.28	6.26	2.52	1.04	0.22	0.00	0.00
15.0	SD-P-19(10-20)*RM	0.05	0.00	5.14	10.51	27.07	17.95	20.81	14.69	3.84	0.00	0.00
2.5	SD-P-20(0-5)*RM	122.19	18.42	16.20	14.83	25.49	13.34	8.11	2.80	0.81	0.00	0.00
7.5	SD-P-20(5-10)*RM	43.70	18.65	15.38	15.25	26.17	13.77	7.92	2.25	0.59	0.00	0.00
15.0	SD-P-20(10-20)*RM	281.16	6.29	7.57	22.14	40.81	14.39	6.03	2.11	0.66	0.00	0.00

SEDIMENT PCB DATA

Depth	Station ID	Total PCBo mg/kg	Mono wt %	Di wt %	Tri wt %	Tetra wt %	Penta wt %	Hexa wt %	Hepta wt %	Octa wt %	Nona wt %	Deca wt %
2.5	SD-F-21(0-5)*RM	0.20	0.00	2.59	12.51	14.59	17.95	22.27	18.29	11.79	0.00	0.00
-99.0	SD-DUP7*RM	0.17	0.00	2.59	13.56	16.01	19.29	25.47	18.16	4.93	0.00	0.00
7.5	SD-F-21(5-10)*RM	0.13	0.00	3.13	14.07	17.39	20.56	23.49	14.45	6.92	0.00	0.00
15.0	SD-F-21(10-20)*RM	0.17	0.00	3.96	13.85	14.16	13.57	14.43	9.43	30.60	0.00	0.00
2.5	SD-F-22(0-5)*RM	0.09	0.00	3.83	16.82	24.86	18.11	19.76	11.71	4.90	0.00	0.00
7.5	SD-F-22(5-10)*RM	0.06	0.00	5.51	18.33	23.19	19.19	17.93	10.69	5.16	0.00	0.00
15.0	SD-F-22(10-20)*RM	0.02	0.00	3.21	17.36	28.67	20.71	18.14	6.66	5.26	0.00	0.00
2.5	SD-F-23(0-5)*RM	8.74	0.54	4.00	24.35	45.17	15.77	.7.29	2.20	0.67	0.00	0.00
7.5	SD-F-23(5-10)*RM	21.89	1.32	3.16	23.08	48.19	15.12	6.53	1.98	0.62	0.00	0.00
15.0	SD-F-23(10-20)*RM	35.41	0.33	2.10	23.00	49.12	15.73	7.01	2.16	0.55	0.00	0.00
2.5	SD-F-24(0-5)*RM	7.89	0.68	3.31	20.46	44.72	17.87	9.38	2.86	0.72	0.00	0.00
7.5	SD-F-24(5-10)*RM	9.53	0.84	2.71	16.93	39.82	22.78	12.53	3.61	0.78	0.00	0.00
15.0	SD-F-24(10-20)*RM	55.01	0.35	4.32	22.36	46.34	16.65	7.55	1.95	0.48	0.00	0.00
2.5	SD-F-25(0-5)*RM	0.19	0.00	3.01	10.47	14.03	19.29	21.34	12.78	19.08	0.00	0.00
7.5	SD-F-25(5-10)*RM	0.24	0.00	2.50	7.85	15.76	20.93	18.63	9.79	24.53	0.00	0.00
15.0	SD-F-25(10-20)*RM	0.36	0.00	1.51	5.32	15.67	19.02	18.04	9.05	31.39	0.00	0.00
2.5	SD-F-26(0-5)*RM	0.02	0.00	0.00	15.06	26.88	21.78	23.22	7.28	5.77	0.00	0.00
7.5	SD-F-26(5-10)*RM	0.02	0.00	0.29	29.95	27.65	20.55	15.71	2.80	3.05	0.00	0.00
15.0	SD-F-26(10-20)*RM	0.04	0.00	4.46	21.99	24.13	18.77	19.22	8.03	3.39	0.00	0.00
2.5	SD-F-27(0-5)*RM	0.31	0.00	4.03	7.50	25.07	22.96	18.80	9.75	11.90	0.00	0.00
-99.0	SD-DUP8*RM	0.65	0.00	2.01	16.33	37.80	17.29	15.21	6.84	4.52	0.00	0.00
7.5	SD-F-27(5-10)*RM	0.35	0.00	0.83	4.83	12.72	13.61	15.23	24.28	28.50	0.00	0.00
15.0	SD-F-27(10-20)*RM	0.20	0.00	2.02	15.78	32.70	16.13	13.22	9.18	10.96	0.00	0.00
2.5	SD-US-1(0-5)*RM	0.12	0.00	1.65	12.72	15.32	19.94	25.71	18.14	6.51	0.00	0.00
7.5	SD-US-1(5-10)*RM	0.10	0.00	2.68	13.73	15.12	22.26	22.94	16.54	6.72	0.00	0.00
15.0	SD-US-1(10-20)*RM	0.08	0.00	2.74	6.10	8.75	12.27	15.10	11.43	43.60	0.00	0.00
2.5	SD-US-2(0-5)*RM	0.10	0.00	2.26	19.73	11.61	16.81	16.66	15.87	17.05	0.00	0.00
7.5	SD-US-2(5-10)*RM	0.03	0.00	6.44	20.82	15.23	16.52	18.12	12.77	10.11	0.00	0.00
15.0	SD-US-2(10-20)*RM	0.01	0.00	9.62	27.97	10.98	7.75	8.84	5.03	29.82	0.00	0.00
2.5	SD-US-3(0-5)*RM	0.07	0.00	4.59	22.73	16.67	16.84	20.86	13.56	4.76	0.00	0.00
7.5	SD-US-3(5-10)*RM	0.20	0.00	3.64	14.54	21.51	25.02	22.38	9.16	3.76	0.00	0.00
15.0	SD-US-3(10-20)*RM	0.63	0.00	1.67	6.36	15.38	24.50	17.64	8.76	25.69	0.00	0.00
2.5	SD-US-4(0-5)*RM	0.02	0.00	0.26	23.11	17.15	22.38	22.06	9.23	5.82	0.00	0.00
7.5	SD-US-4(5-10)*RM	0.04	0.00	2.78	17.12	20.77	24.55	21.72	8.65	4.42	0.00	0.00
15.0	SD-US-4(10-20)*RM	0.14	0.00	2.16	18.51	25.16	24.79	14.66	9.28	5.43	0.00	0.00
2.5	SD-US-5(0-5)*RM	0.15	0.00	1.81	9.15	10.83	12.55	19.74	30.36	15.54	0.00	0.00
7.5	SD-US-5(5-10)*RM	0.13	0.00	9.91	22.33	16.30	14.21	16.93	13.40	6.92	0.00	0.00

SEDIMENT PCB DATA

Depth	Station ID	Total PCBs mg/kg	Mono wt %	Di wt %	Tri wt %	Tetra wt %	Penta wt %	Hexa wt %	Hepta wt %	Octa wt %	Nona wt %	Deca wt %
15.0	SD-US-5(10-20)*RM	0.06	0.00	3.86	16.06	18.02	19.43	23.12	13.89	5.62	0.00	0.00
2.5	SD-US-6(0-5)*RM	0.14	0.00	2.37	20.77	24.50	10.87	19.10	17.39	5.01	0.00	0.00
7.5	SD-US-6(5-10)*RM	0.07	0.00	2.92	30.92	20.10	12.53	16.98	12.47	4.08	0.00	0.00
15.0	SD-US-6(10-20)*RM	0.01	0.00	0.00	35.99	25.78	14.01	16.71	3.43	4.09	0.00	0.00
2.5	SD-US-7(0-5)*RM	0.09	0.00	2.58	17.16	21.10	19.02	20.36	15.25	4.53	0.00	0.00
-99.0	SD-DUP9*RM	0.06	0.00	3.59	21.99	25.75	13.02	16.60	11.34	7.71	0.00	0.00
7.5	SD-US-7(5-10)*RM	0.08	0.00	0.13	14.56	17.55	15.62	27.62	18.88	5.64	0.00	0.00
15.0	SD-US-7(10-20)*RM	0.05	0.00	2.91	24.81	27.85	16.59	16.83	7.53	3.48	0.00	0.00
2.5	SD-US-8(0-5)*RM	0.07	0.00	1.59	12.62	19.88	17.52	21.13	19.14	8.12	0.00	0.00
7.5	SD-US-8(5-10)*RM	0.06	0.00	2.44	16.55	20.49	19.49	20.98	11.44	8.61	0.00	0.00
15.0	SD-US-8(10-20)*RM	0.09	0.00	1.34	12.99	22.03	21.37	19.01	12.40	10.85	0.00	0.00
2.5	SD-US-9(0-5)*RM	0.05	0.00	3.24	12.57	24.42	17.48	25.28	10.60	6.41	0.00	0.00
7.5	SD-US-9(5-10)*RM	0.05	0.00	1.40	13.47	17.84	24.00	29.62	9.12	4.55	0.00	0.00
15.0	SD-US-9(10-20)*RM	0.04	0.00	1.61	17.71	18.05	17.33	25.08	7.88	12.34	0.00	0.00